CONTRIBUTIONS TO THE DEVELOPMENT OF A POWER-SPECTRAL GUST DESIGN PROCEDURE FOR CIVIL AIRCRAFT

TECHNICAL REPORT

JANUARY 196[illegible]

by

J.R. Fuller, L.D. Richmond, C.D. Larkins, and S.W. Russell
(of The Boeing Company, Renton, Washington)

Lockheed-California Company
Burbank, California
Under Contract FA-WA-4768

for

Federal Aviation Agency
Aircraft Development Service

CONTRIBUTIONS TO THE DEVELOPMENT OF A POWER SPECTRAL GUST DESIGN PROCEDURE FOR CIVIL AIRCRAFT

TECHNICAL REPORT

ADS-54

Contract FA-WA-4768

by

J. R. Fuller, L. D. Richmond, C. D. Larkins, and S. W. Russell
(of The Boeing Company, Renton, Washington)

January 1966

Prepared For
THE FEDERAL AVIATION AGENCY
Under Contract FA-WA-4768

by

Lockheed-California Company
Burbank, California

PAGES ______

ARE

MISSING

IN

ORIGINAL

DOCUMENT

SUMMARY

This report presents a dynamic gust analysis of the Boeing Model 720B airplane and outlines two procedures for assessing gust design strength for future civil transports. This work was conducted under subcontract for the Lockheed-California Company in support of their study contract with the Federal Aviation Agency (FAA) to develop a power spectral gust design procedure for civil aircraft.

The procedures outlined are based on two approaches. The first is the design envelope approach, the second is the flight profile approach. In the design envelope approach, certain flight conditions are established by successive analyses to determine the most critical flight condition for a given portion or component of the airplane for either vertical or lateral gust loads. The one-factor level flight load added to the rms load times a particular constant will just equal the limit design strength of the component. This constant, $\sigma_w \eta_d$, represents an effective gust intensity which would just stress the structure to its limit design strength.

The object of the flight profile approach is to determine the expected number of flight hours that the airplane could be operated before the limit design strength of any of its major components would be exceeded. The flight profile approach requires a description of airplane operation in terms of flight profiles that best typify the airplane usage. A separate power spectral analysis is conducted for each of the profile conditions. In addition, a description of the atmosphere applicable to the condition altitude is determined. From this information, the expected number of hours required to exceed the limit strength is computed.

The 720B airplane was studied for both concepts, first, by using the bending moment on the wing, fuselage, and vertical tail as indicies of their strengths. This procedure was used to locate critical flight conditions, critical portions of the structure, and to obtain preliminary values of $\sigma_w \eta_d$ by the design envelope approach, and expected hours to fly to exceed limit design strength by the flight profile approach.

The second step was to study the more critical structural areas using a joint probability stress analysis approach developed by Boeing. The critical values of $\sigma_w \eta_d$ and hours to fly to exceed limit design strength of each structural element in the critical area were determined. The results of these analyses indicate that the design envelope and flight profile approaches give results that are in general agreement.

TABLE OF CONTENTS

REFERENCES

1. Press, Harry; Steiner, Roy: An Approach to the Problem of Estimating Severe and Repeated Gust Loads for Missile Operations, NACA TN 4332, September 1958.

2. Houbolt, J. C., Steiner, Roy, and Pratt, K. G.: Dynamic Response of Airplanes to Atmospheric Turbulence Including Flight Data on Input and Response, NASA TR R-199, June 1964.

3. VGH Data Samples for L-749, L-188, and B-707-300 Commercial Transport Airplanes, Letter to Herbert C. Spicer, Jr., Aircraft Development Service, DS-41, Federal Aviation Agency, 800 Independence Avenue, Washington, D.C. (20553), from Floyd L. Thompson, Director, Langley Research Center, Langley Station, Hampton, Virginia, Letter No. 23365, April 9, 1964.

4. Neuls, G. S., Maier, H. G., Lerivick, T. R., Robb, E. A., Webster, I.J.: Optimum Fatigue Spectra, Technical Report ASD-TR-61-235, Flight Dynamics Laboratory, Aeronautical Systems Division, Air Force Systems Command, Wright-Patterson Air Force Base, Ohio, April 1962.

5. Harris, C. E.: Boeing Document D6-1978, Design Loads Criteria for 720/720B Airplanes, Vol. I - Flight Loads, Released January 27, 1960, Last Revision September 29, 1964.

6. Lomax, T. L.: Boeing Technical Note D6-7500 TN, Computer Programs for Airplane Structural Design Load Analyses, Released October 17, 1960.

7. Gray, W. L., Schenk, K. M.: Å Method for Calculating the Subsonic Steady-State Loading on an Airplane with a Wing of Arbitrary Plan Form and Stiffness, NACA TN 3030, December 1953.

8. Richmond, L. D.: Boeing Document D6-7401, A Rational Method of Obtaining Three-Dimensional Unsteady Aerodynamic Derivatives of Intersecting Airfoils in Subsonic Flow, Released April 2, 1962, Last Revision May 1, 1964.

9. Theodorsen, T.: General Theory of Aerodynamic Instability and the Mechanism of Flutter, NACA Report 496, 1935.

10. Küssner, H. G., Schwarz, I.: The Oscillating Wing with Aerodynamically Balanced Elevator, NACA TM 991, 1941.

11. Bott, R. F.: Boeing Document D6-3214, Fuselage Stress Analysis for 720 Airplane, Vols. I and II, Vol. I, Released February 9, 1960, Last Revision August 30, 1962; Vol. II, Released February 9, 1960, Last Revision June 26, 1961.

12. Hansen, W., Rowniak, R.: Boeing Document D6-3408, Wing Stress Analysis - Model 720B, Vols. I and II; Vol. I Released January 27, 1960, Last Revision April 17, 1961; Vol. II Released October 14, 1960, Last Revision May 9, 1961.

13. Smith, J. E., Watanabe, M.: Boeing Document D6-5228, Vertical Tail Stress Analysis, Model 720; Released February 20, 1960, Last Revision January 24, 1963.

14. Rice, S. O.: Mathematical Analysis of Random Noise, Bell System Technical Journal, Vol. 23, pp. 282-332, July 1944, Vol. 24, pp. 46-156, January 1945.

15. Von Karman, T., Howarth, L.: On the Theory of Isotropic Turbulence, Proceedings, Royal Society of London, pp. 193-194, 1938.

16. Fung, Y. C.: Statistical Aspects of Dynamic Loads, Journal of the Aeronautical Sciences, May 1953.

17. Ross, Alan S.: Boeing Document T6-1718, Ground Vibration Tests, 720-020 Series Airplane, June 1960.

18. Hoblit, F. M., Paul, N., Shelton, J. D., and Ashford, F. E.: Development of a Power-Spectral Gust Design Procedure for Civil Aircraft. FAA-ADS-53, 1966.

INTRODUCTION

Background

Gust load formulas embodying a number of simplifying assumptions have been used in the United States for over 30 years to calculate gust loads for airplanes. The underlying concept in the use of a gust formula is that measured airplane center of gravity accelerations due to continuous turbulence can be used to derive effective or derived gust velocities for specified gust shapes. These derived gust velocities for a specified gust shape, in turn, can be used to calculate the accelerations on other airplanes by reversing the process. Therefore, a gust load formula relates the peak gust induced accelerations on a given airplane to the peak accelerations expected on other more or less similar airplanes for flight through the same continuous rough air. It is clear that when newer airplanes differ significantly from past or present successful airplanes on which acceleration measurements have been made, the simple gust formula approach may not be adequate.

When a proposed airplane design or mode of operation does differ significantly from past practice, the aircraft manufacturer and the certifying agency must cope with the problem of providing adequate strength for gust loading. Ideally, the risk of exceeding the limit design gust loads per flight hour for the new airplane should be just equal to the risk of exceeding the limit design gust loads per flight hour for the older proven airplanes.

An evaluation to establish gust loads for new airplane designs should rely on rather detailed theoretical dynamic analyses that can adequately describe the behavior of the new airplanes relative to the older proven models. A generally accepted analysis technique that is used to account for differences in airplane dynamic responses and in modes of operation is power spectral analysis. The theoretical technique for using generalized harmonic analysis or power spectral analysis methods in the airplane gust loads problem have been developed and summarized by the National Aeronautics and Space Administration, (NASA). [1,2]*

The contracting agency, Federal Aviation Agency, (FAA), has assumed that the manufacturers of given airplanes can best analyze their own designs, since they are most familiar with the developmental wind tunnel and structural testing, the detailed construction, and the manner in which the airplanes have been used in day by day service. After an evaluation

*Numbers in parentheses refer to items in the list of references.

of detailed proposals submitted for this study, the FAA contracted with the Lockheed-California Company, Burbank, California, to study the Lockheed Electra, Model 188, a medium weight, straight wing, 4-engine, turboprop airplane and the Lockheed Constellation, Model 749, a medium weight, straight-wing, 4-engine, reciprocating engine airplane. In addition, the FAA arranged to have The Boeing Company, Airplane Division, participate in the study under a subcontract with Lockheed to conduct a study of the Boeing Model 720B, a medium range, swept wing, 4-engine, jet transport airplane. A view of the 720B airplane in flight is shown in Fig. 1.

Approach

Even though the basic power spectral technique is well defined, the problem of establishing specific gust design levels for new airplanes requires that a concerted effort be made to establish the relationship between the stresses induced in critical structural elements of existing successful airplanes and the design strength of these elements. In this manner, an estimate can be made of the expected number of flight hours that proven airplanes can be expected to operate before the limit design strengths of their various structural elements are exceeded. This approach requires an intimate knowledge of the airplane usage, and is commonly referred to as the flight profile approach. A second approach involves computation of the statistical probability of exceeding the limit strengths of critical structural elements when the airplane is being flown in a manner to most highly stress that portion of the airplane containing the critical elements. The level of gust intensity at a given altitude that would just stress the structural element in question to its limit strength provides a measure of gust intensity that might logically be used on a new design for the same altitude. This second approach is referred to herein as the design envelope approach. Both of these approaches are exercised in the analyses that follow.

The approach of establishing gust design levels for new airplanes by strength analyses of older successful airplanes raises the question of sensitivity of the analysis procedure to the various parameters used in the analyses. Therefore, the results are studied to determine the sensitivity of the analyses to variations in aerodynamic parameters, the mathematical model, and in assumed airplane usage.

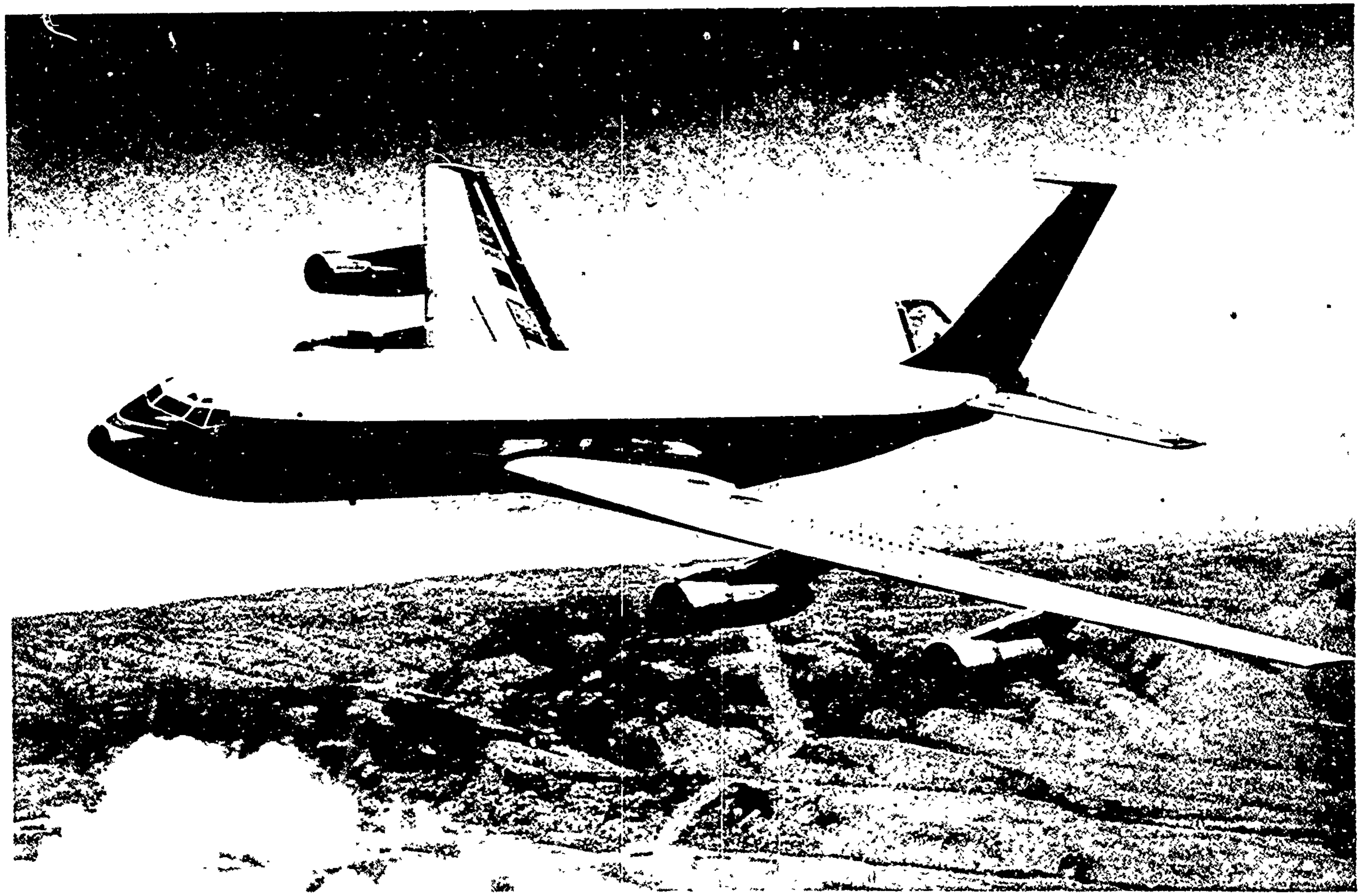

FIGURE 1. 720B AIRPLANE

NOMENCLATURE

x, ξ	Shear stress, psi
y, f	Axial stress, psi
x_o, ξ_o, y_o, f_o	Steady stress values, shear and axial stress, respectively, psi
F_ξ	Allowable shear stress, psi
F_t	Allowable axial stress, psi
$\overline{Z}$	Stress vector,
$\overline{\dot{Z}}$	Stress velocity vector,
$\sigma_x, \sigma_y, \sigma_\alpha, \sigma_\beta$	Root mean square values (standard deviations) for x, y, α, and β, respectively
$\Phi_x(\omega), \Phi_y(\omega)$	Power spectral density functions for random process x(t) and y(t), respectively
$\Phi_{xy}(\omega)$	Cross power spectral density function for x(t) and y(t)
ω	Circular frequency, rad. per sec.
ρ	Correlation coefficient for x(t) and y(t)
α, β	Time rate of change of x and y, respectively
$p(x), p(y)$	Probability densities of x and y
$p(x,y)$	Joint probability density of x and y
$f(x, \alpha, y, \beta)$	Probability density of x, α, y, β
MS	Margin of safety
$p(MS < 0)$	Probability that MS is less than zero or percent time that MS is less than zero

$P(MS \geq 0)$	Probability that MS is greater than or equal to zero
C	A curve on xy-plane
$\bar{N}$	Unit vector normal on C
[ ]	Column matrix
⌊ ⌋	Row matrix
N_c	Total number of passages across an arbitrary curve per second or per foot traveled
σ_w, σ_v	Root mean square gust velocity, ft. per sec.
$\hat{f}(\sigma_w)$	Probability density distribution of σ_w
V	Velocity, ft. per sec.
$\bar{G}$	Expected exceedances of limit design strength per hour
$\bar{A}_f$, $\bar{A}_\xi$	Root mean square stress response for σ_w of unity, psi per ft. per sec.
N_o	Number of times per unit time or distance that a time-history crosses its mean value with positive slope; or negative slope

DESCRIPTION OF THE ATMOSPHERE

Gust Power Spectrum

Certain statistical estimates for loads, accelerations or stresses for flight vehicles can be obtained by generalized harmonic analysis techniques if sufficient statistical information is available for the random forcing environment. If it can be assumed, as has been done for the current study, that (1) the turbulence is essentially frozen and the airplane penetrates or passes over the turbulence much as an automobile would travel a rough road, and (2) if it is assumed that the spanwise effects of the turbulence are not of major importance, then a one-dimensional power spectral approach is adequate.

If it is further assumed that the turbulence is isotropic; that is, statistically invariant for any rotation of translation of the coordinate axis system; then, a single power spectral density function can be used for separate vertical and lateral analyses for a given flight condition. The assumption that there is no significant aerodynamic or inertia coupling between vertical and lateral airplane degrees of freedom is made when it is assumed that separate or uncoupled vertical and lateral dynamic analyses will suffice. All of these rather restrictive assumptions have been made for the analyses discussed herein; and a constant parameter normalized power spectral density function was chosen to represent atmospheric turbulence for all altitudes.

A meeting was held with NASA and FAA personnel at Langley Field on March 10, 1964, to discuss the atmospheric turbulence description to be used in this program.[3] These discussions resulted in the choice of an isotropic turbulence power spectral density function and NASA's consent to provide operational VGH data for the three airplane types being studied. The VGH data was provided to aid Lockheed in determining a probability distribution for root-mean-square (rms) gust velocity to be used with the selected spectrum shape. These two functions provided a sufficient atmospheric turbulence model for the overall study.

The atmospheric turbulence of spectrum chosen was as follows:

$$\phi_w(\Omega) = \frac{\sigma_w^2 L}{\pi} \frac{1 + \frac{8}{3}(1.339\ L\Omega)^2}{\left[1 + (1.339\ L\Omega)^2\right]^{11/6}} \qquad (1)$$

A scale of turbulence, L, of 2,500 feet was selected. This spectrum shape, designated as the "isotropic turbulence," Case I spectrum, has been extensively evaluated by NASA and appears to provide a good fit to their experimentally determined gust spectra.[2] The 2,500 ft. scale of turbulence is most probably low, and would be expected to give a somewhat conservative or high number of load or stress exceedance counts per unit time. NASA's experience indicates a scale of turbulence for the above power spectrum in the order of 3,000 to 6,000 ft. A comparison of the Case I spectrum shape chosen for this study, and the commonly used Case II isotropic turbulence spectrum with a scale of turbulence of 1,000 ft. is shown in Fig. 2.

Distribution of RMS Gust Velocities

The power spectral analysis approach used herein is applicable only to stationary Gaussian continuous turbulence, but atmospheric turbulence is not statistically stationary or Gaussian over long distances. The statistical quantities used to describe turbulence vary with altitude, wind condition, terrain roughness, temperature gradient, season of the year, and a host of other variables. However, it has been observed that the power spectrum shape from 1,000 to 40,000 ft. above the terrain is reasonably invariant. As a result, NASA has proposed that atmospheric turbulence be considered locally Gaussian and stationary and that the total experience of flying through rough air be considered to be made up of a range of exposures to turbulence of various intensities all using the same shape power spectrum. Thus, they have proposed that a statistical distribution of rms gust intensities be considered.[1] The proposed probability density function for rms gust velocity is,

$$\hat{f}(\sigma_w) = \frac{P_1}{b_1}\sqrt{\frac{2}{\pi}}\, e^{-\sigma_w^2/2b_1^2} + \frac{P_2}{b_2}\sqrt{\frac{2}{\pi}}\, e^{-\sigma_w^2/2b_2^2} \qquad (2)$$

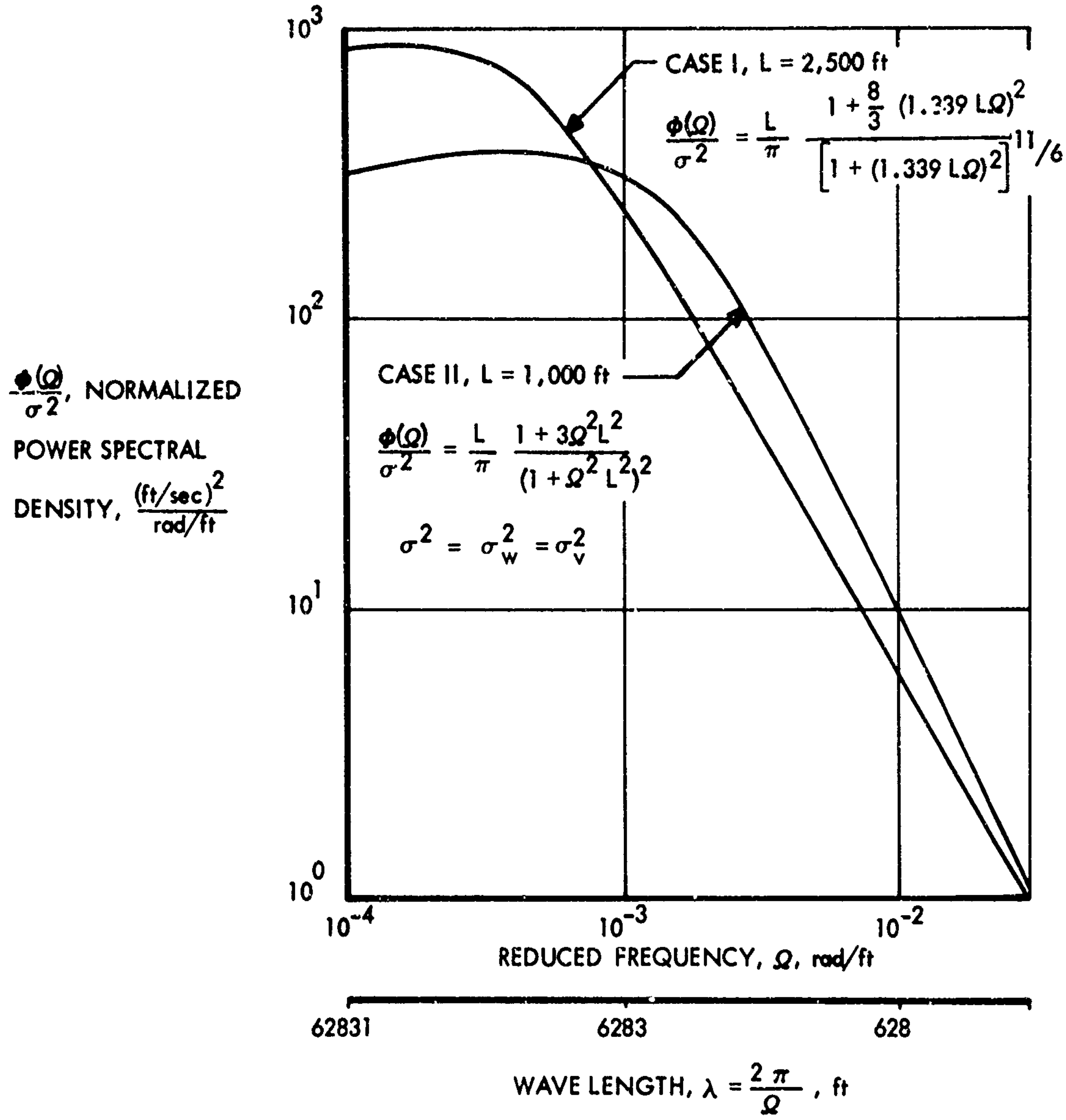

FIGURE 2. NORMALIZED ISOTROPIC TURBULENCE POWER SPECTRA

Eq. (2) leads to an expression for the number of times per unit time that a given load level, y, is exceeded,

$$\bar{G}(y) = P_1 N_o e^{-y/b_1 \bar{A}} + P_2 N_o e^{-y/b_2 \bar{A}} \qquad (3)$$

where,

N_o	number of times per unit time that the y-time history crosses its mean value with positive (or negative) slope
P_1, P_2	fraction of time or distance flown in nonstorm (light) turbulence, and fraction of time or distance flown in storm (heavy) turbulence, respectively
b_1, b_2	turbulence scale parameters for nonstorm and storm turbulence, respectively
$\bar{A}$	rms value for the load quantity, y, per unit rms gust velocity

The zero crossings per unit time, N_o, is a function of the shape of the gust power spectral density function. As a result, when a new spectrum shape is chosen, the values for P_1, P_2, b_1, and b_2 must be re-evaluated to provide load results which agree with flight data

Lockheed investigated the turbulence parameters P_1, P_2, b_1, b_2 and arrived at the relationships shown in Figs. 3 and 4. These turbulence parameters were determined not only from a substantial sample of airline VGH data, but also from data obtained from military operations at higher altitudes. Most of the basic data was obtained from a summary report prepared by the Douglas Aircraft Company, Inc., Long Beach, California, under contract with the Flight Dynamics Laboratory, Wright-Patterson Air Force Base, Ohio.[4]

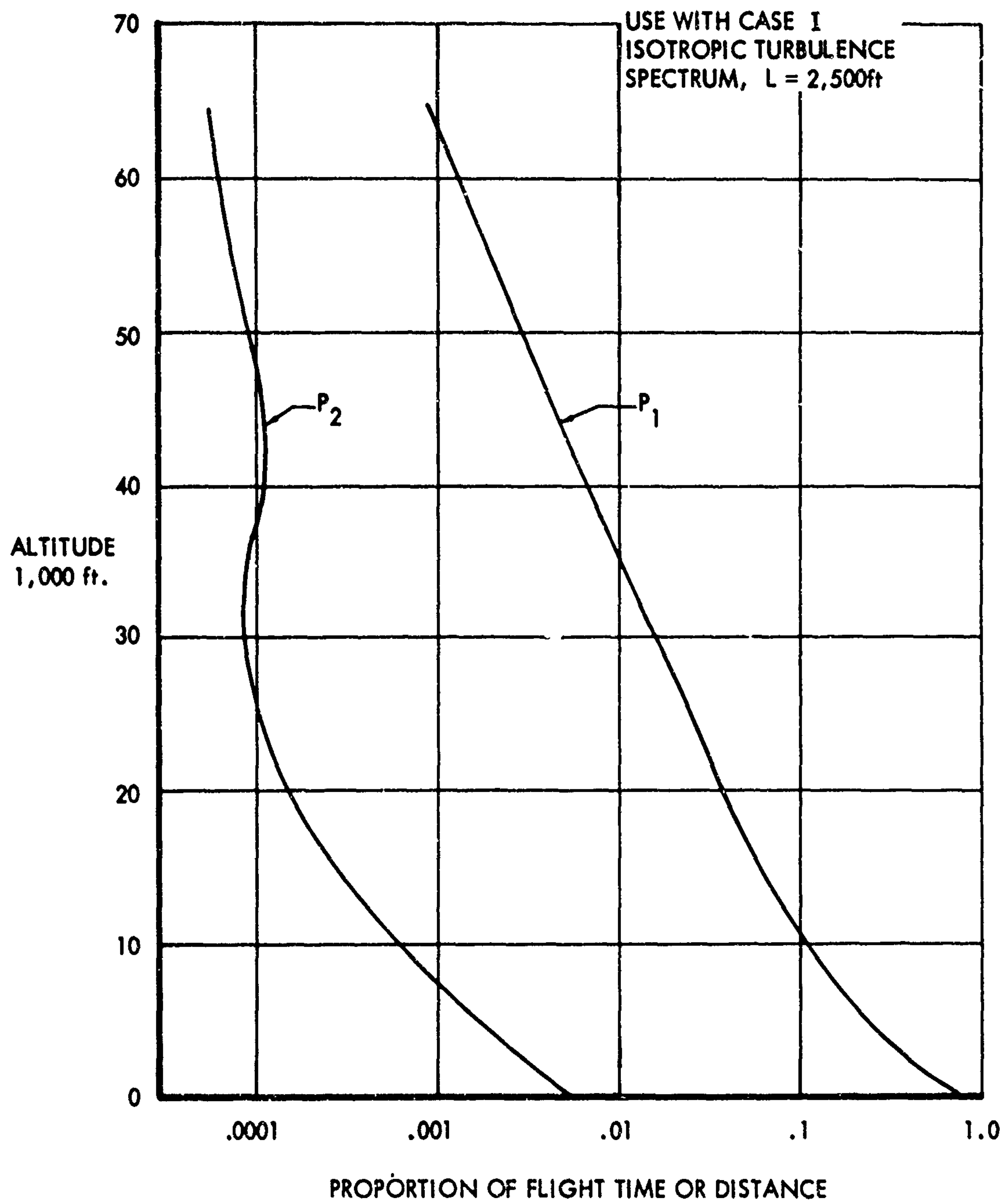

FIGURE 3. PROPORTION OF FLIGHT TIME OR DISTANCE IN STORM AND NONSTORM TURBULENCE

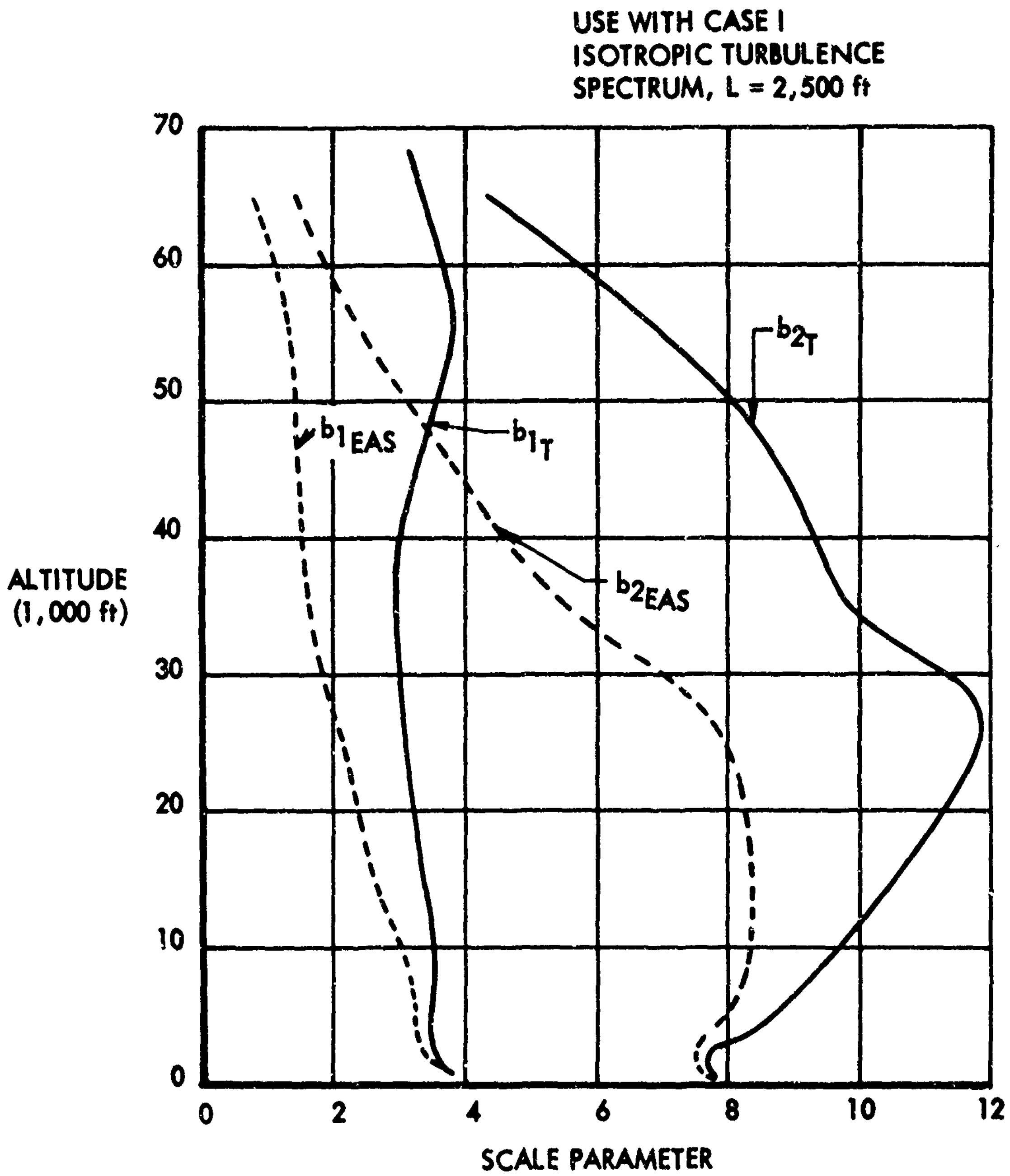

FIGURE 4. TURBULENCE SCALE PARAMETERS

ANALYSIS CONDITIONS

Estimated Airline Usage of 720B Airplane

The airplane configurations analyzed during this study were selected to provide statistical loads and stress information for use with two different design approaches. One approach, flight profile analysis, requires information based on actual airplane usage and reflects the speeds, altitudes, and gross weights experienced during routine airline operation. The second approach, design envelope analysis, requires the generation of statistical loads estimates for critical design points on or within the speed-altitude design envelope.

A survey of the airline usage of 720 and 720B airplanes was made to determine the airplane usage most appropriate for flight profile analysis. Three airlines, whose route structures were representative of the fleet usage, were chosen for the survey. These airlines operate a total of thirty-seven 720/720B airplanes or 30 percent of the entire 720/720B fleet. The survey consisted of compiling the usage of these airplanes in terms of the total profiles flown for particular profile lengths. The profile intervals chosen varied from 100 to 2,600 n. miles in 100 n. mile intervals. One flight profile or segment is comprised of a single takeoff, climb-out, cruise, and descent. The results of this survey are presented in Fig. 5(a) in terms of profile length as percent of the total profiles flown. A comparison of these results with the results of the NASA VGH data for 707-300 airplanes [3] is shown in Fig. 5(b). The comparison is made in terms of the percent of total profiles flown versus profile duration in minutes. It can be seen that there is a definite similarity between the operation of 707-300 airplanes and 720/720B airplanes for the shorter flights. As would be expected, the longer range 707-300 shows a greater usage over longer segments than 720/720B airplanes.

The selection of representative analysis profiles was based on a distribution of time spent on the various flights.. This distribution, shown in Fig. 5(c), differs from the percent of segments flown, Fig. 5(a), because each segment was weighted by the segment flight time. The flight segment duration information in Fig. 5(c) was used to establish the representative flight profiles for the analysis of the 720B airplane.

Values of indicated airspeed versus altitude based on the NASA VGH data [3] were used for the flight profile studies. A comparison of the recommended airspeeds with the average operational speeds is presented in Fig. 6. This comparison shows that the actual operating airspeeds are less than the recommended speeds at the lower altitudes, while at the

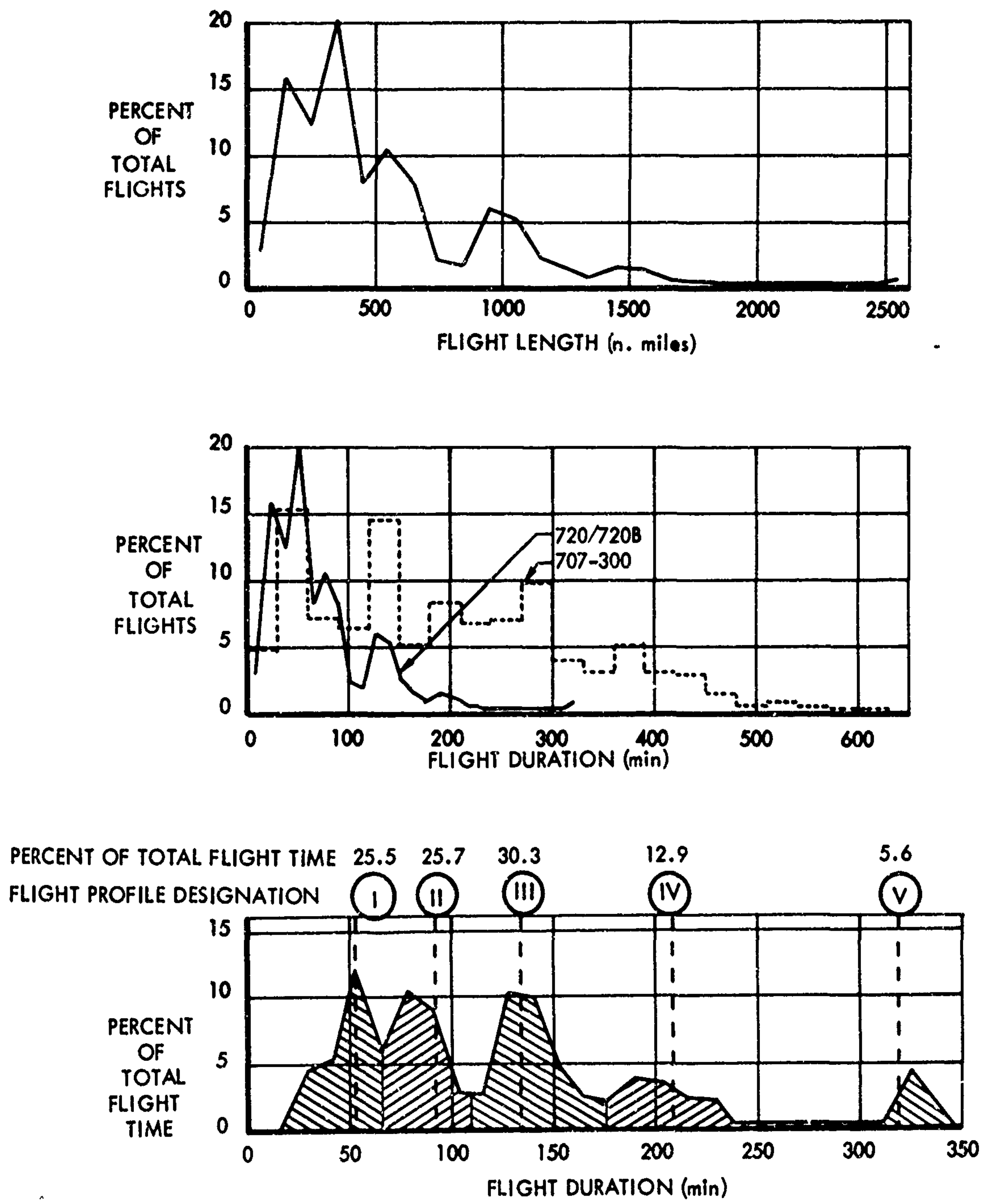

FIGURE 5. FLIGHT SEGMENT UTILIZATION, 707-300 AND 720B

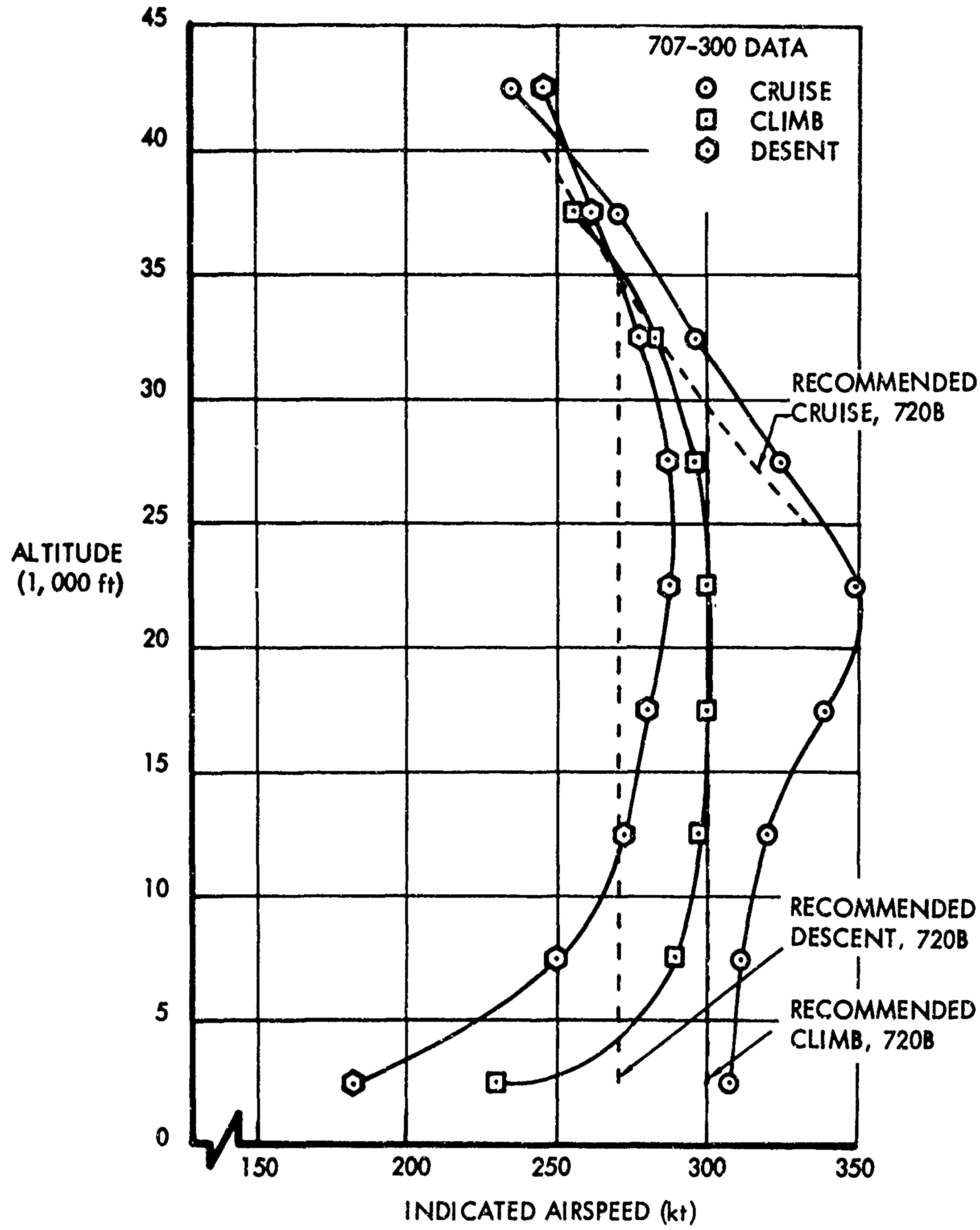

FIGURE 6. RECOMMENDED AND AVERAGE OPERATIONAL AIRSPEEDS

higher altitudes there is better agreement between the recommended and operational speeds. The statistical values for indicated airspeed were used in the flight profile analyses in order to be as consistent as possible with the operational experience.

Flight Profiles for 720B Analyses

Five profiles were chosen from Fig. 5(c) for the dynamic analyses. The five basic and alternate profiles are shown in Figs. 7 through 11. Profiles I through V have ranges of 350, 600, 1000, 1600, and 2500 n. miles for flight durations of 55, 85, 135, 205 and 325 minutes, respectively. The variations of gross weight and speed are also given in Figs. 7 through 11. The gross weight at the beginning of each flight profile is based on the prescribed fuel loading necessary to accomplish the flight plus 10,000 lb. of reserve fuel for holding or alternate field requirements. The cargo compartments were considered to be fully loaded on a space limited basis, and the passenger load factor was assumed to be 55 percent. This load factor was the 1963 average for 720 and 720B operations by United States airlines.

Flight Profile Analysis Conditions

A summary of the flight profile analysis conditions is given in Tables 1 and 2. Conditions 1, 2, and 3 were selected to represent the climb portion of Profile III, Fig. 9. Results from analysis for these conditions allowed a study to be made of the variations of load and stress exceedance data for climb at an average climb gross weight. Parametric variations in gross weight at the 15,000 ft. altitude, Conditions 4, 5, and 6, provided information to account for the climb portions of other profiles. Three cruise conditions, Conditions 7, 8, and 9, were selected to examine the variations in loads with cruise altitude at a constant gross weight. These points are indicated on Profile II, Fig. 8, as Options A and B, and on Profile V, Fig. 11. Two additional conditions, Conditions 10 and 11, were studied for the same 35,000 ft. altitude at different gross weights to account for the fuel burn-off during cruise. Conditions 12 and 13, for altitudes of 10,000 and 20,000 ft., respectively, were chosen to evaluate the descent. The descent portions of all the profiles are the same; therefore, the results obtained for one descent were applied to all profiles.

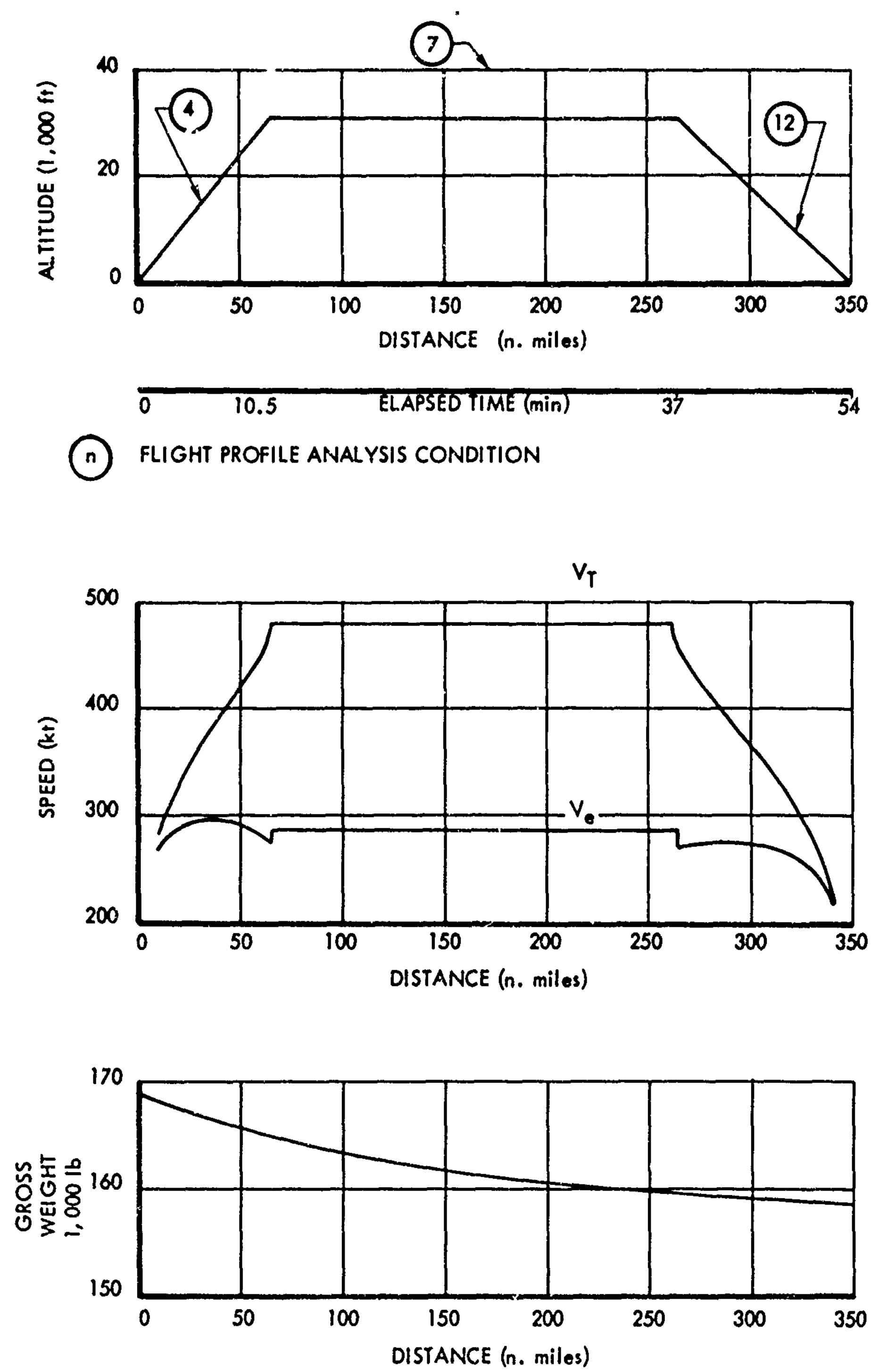

FIGURE 7. FLIGHT PROFILE I

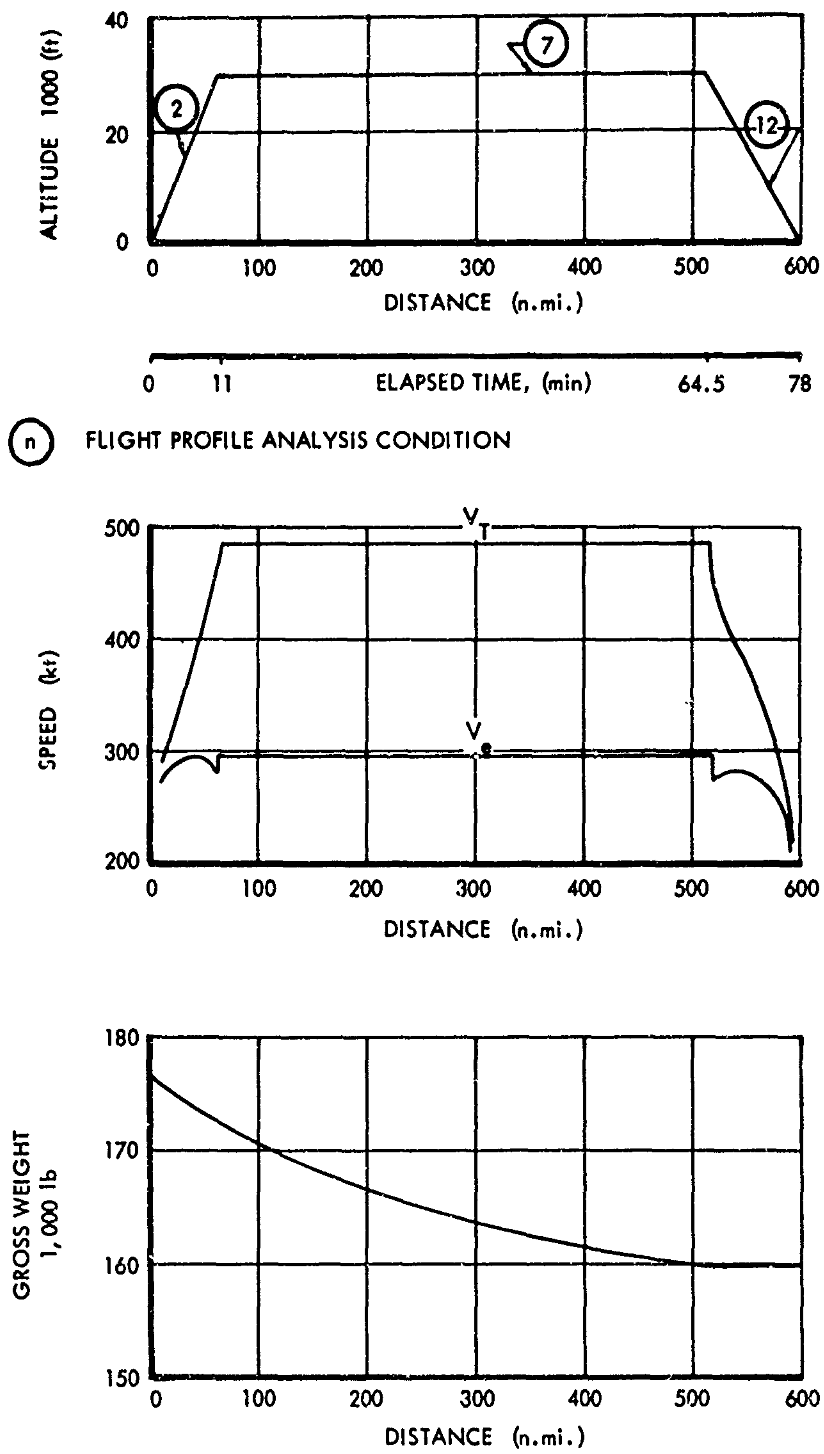

FIGURE 8a. FLIGHT PROFILE IIA

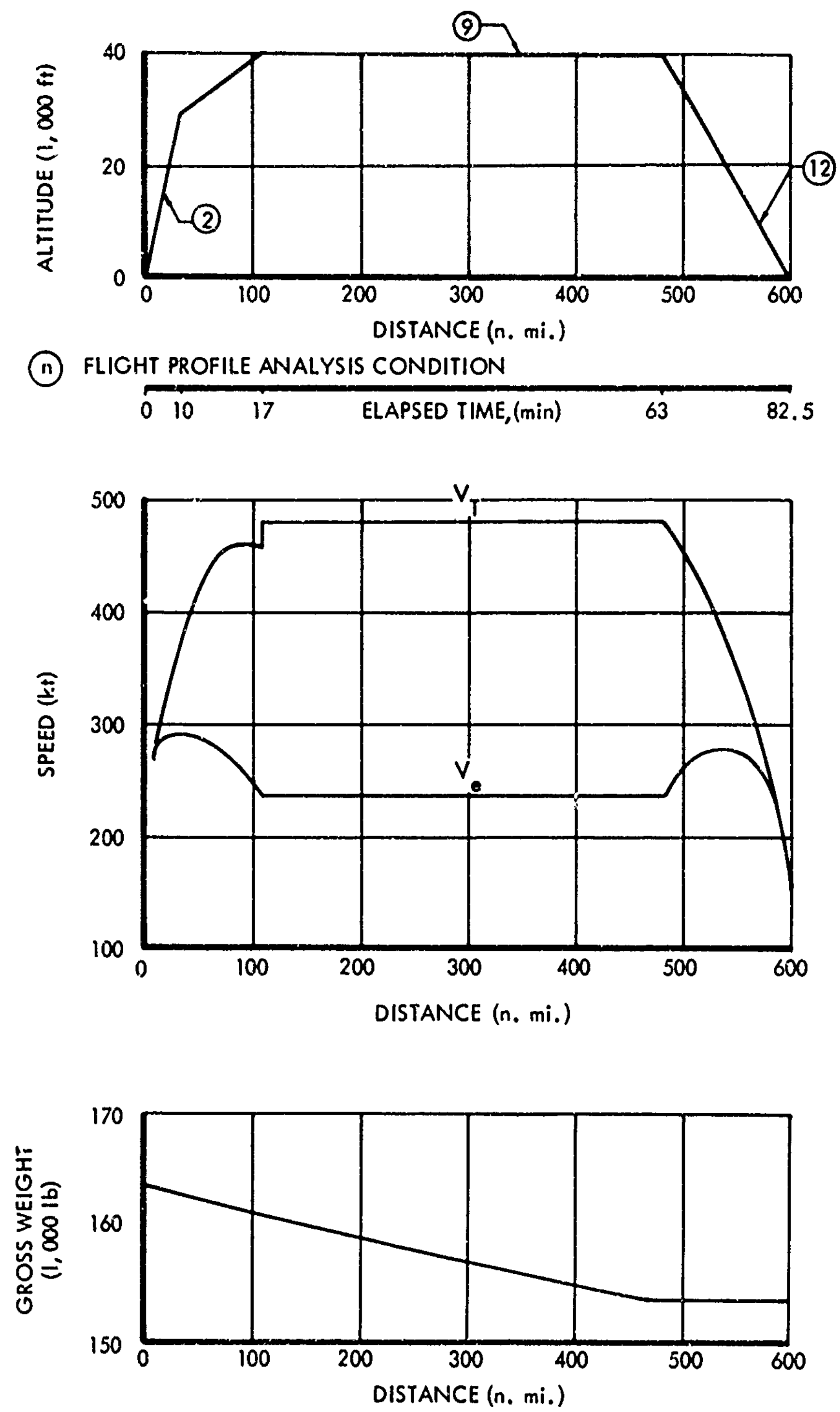

FIGURE 8b. FLIGHT PROFILE IIB

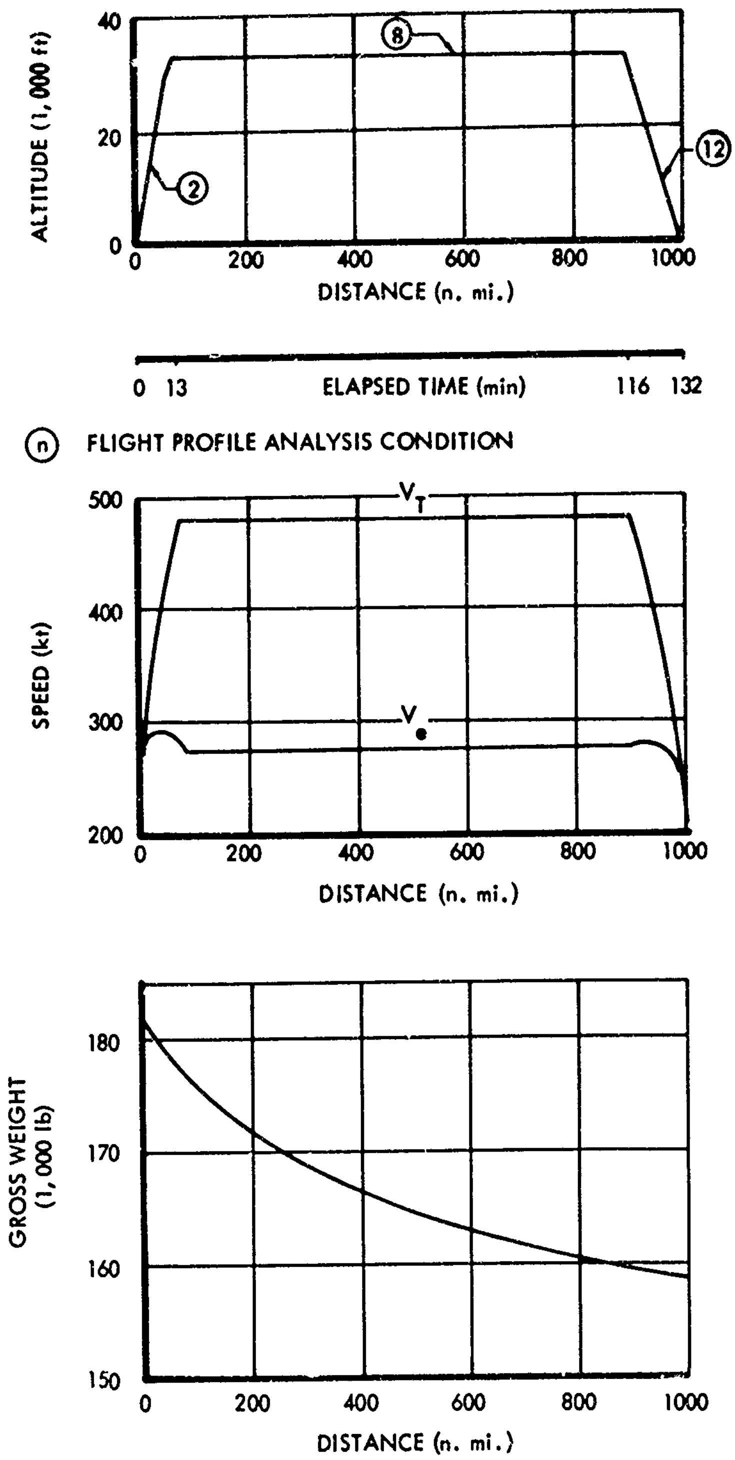

FIGURE 9. FLIGHT PROFILE III

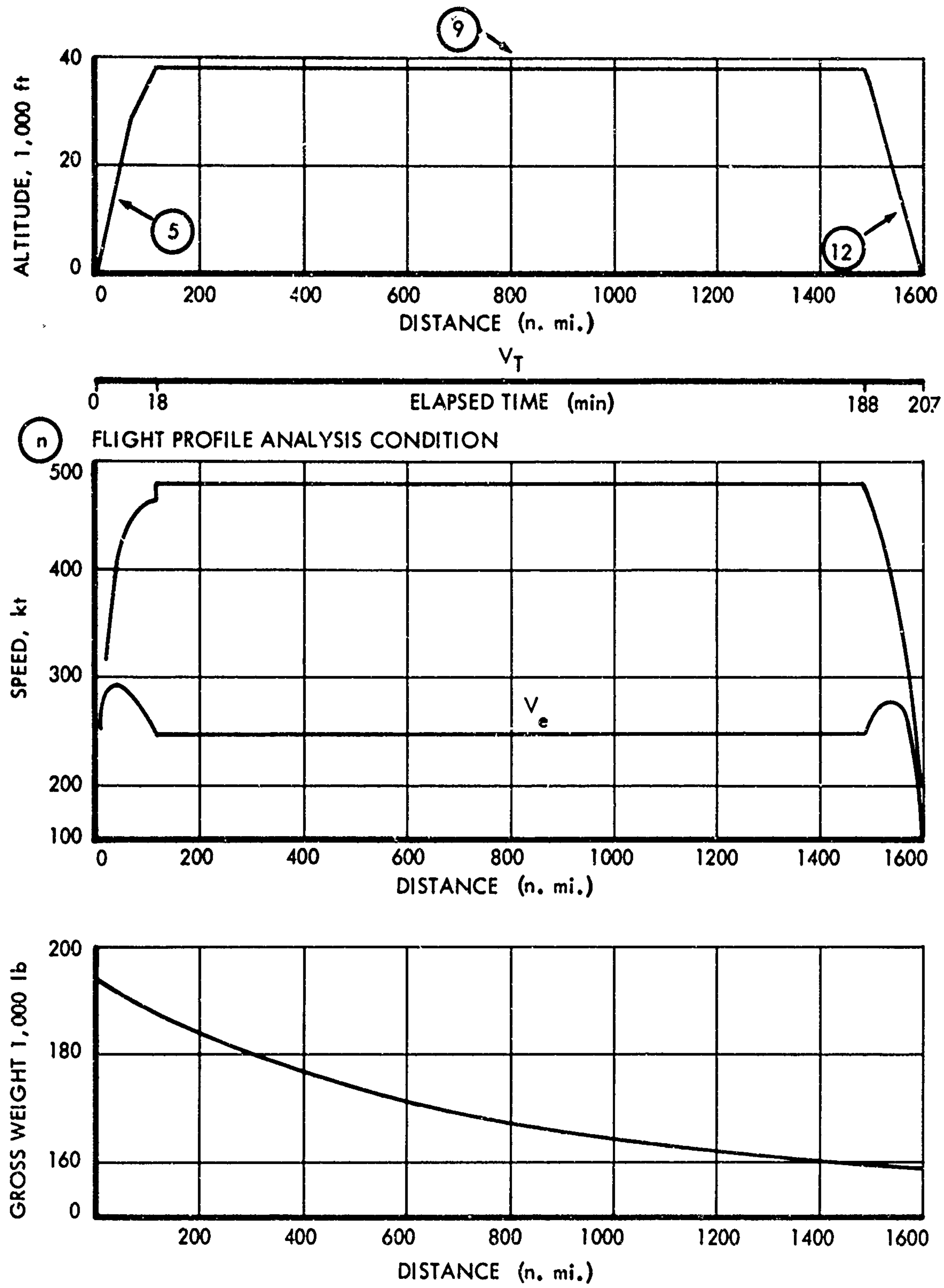

FIGURE 10. FLIGHT PROFILE IV

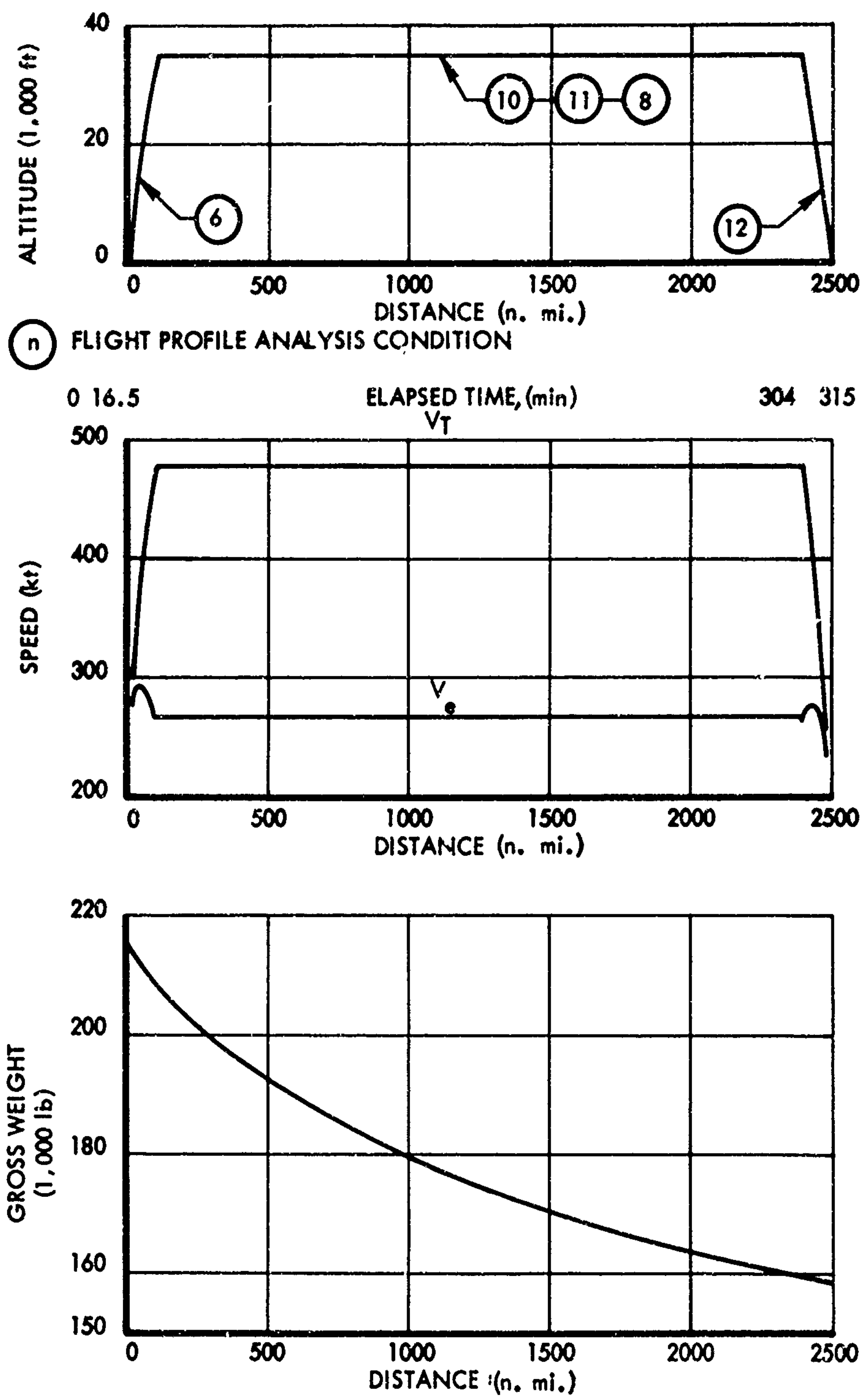

FIGURE 11. FLIGHT PROFILE V

TABLE 1. FLIGHT PROFILE ANALYSES

Flight Profile	Percent of Total Flight Time	Profile Length, N.Miles	Flight Duration, Min.	Phase	Analysis Condition No.	Condition Time, Min.	Condition Length, N.Miles
I	25.5	350.	52.	Climb	4	11.	65.
				Cruise	7	26.	198.
				Descent	12	15.	87.
					Total	52.	350.
IIA	12.8	600.	79.	Climb	2	11.	65.
				Cruise	7	53.5	452.
				Descent	12	14.5	83.
					Total	79.0	600.
IIB	12.9	600.	82.5	Climb	2	17.	110.
				Cruise	9	46.	370.
				Descent	12	19.5	120.
					Total	82.5	600.
III	30.3	1000.	131.5	Climb	2	12.5	80.
				Cruise	8	103.	826.
				Descent	12	16.	94.
					Total	131.5	1000.
IV	12.9	1600.	206.5	Climb	5	18.	119.
				Cruise	9	170.	1368.
				Descent	12	18.5	113.
					Total	206.5	1600.
V	5.6	2500.	315.0	Climb	6	17.	115.
				Cruise	10	95.3	761.3
				Cruise	11	95.3	761.3
				Cruise	8	95.4	761.4
				Descent	12	12.	101.0
Total	100.0					315.0	2500.

Note: These profiles are used for both vertical and lateral analyses

TABLE 2

FLIGHT PROFILE ANALYSIS CONDITIONS

Analysis Condition No.	Gross Weight, Lb.	Altitude, Ft.	True Airspeed, Kt.	Indicated Airspeed, Kt.	Mach No.	Payload, Lb.	Fuel, Lb.	cg, Percent MAC
1	181,600	5,000	290	270	.45	29,100	32,800	18.6
2	178,800	15,000	370	300	.59	29,100	30,000	17.0
3	178,800	25,000	432	300	.72	29,100	30,000	17.0
4	166,600	15,000	370	300	.59	29,100	17,800	18.1
5	191,800	15,000	370	300	.59	29,100	43,000	19.6
6	211,600	15,000	370	300	.59	29,100	62,800	20.6
7	163,800	30,000	480	310	.82	29,100	15,000	16.4
8	163,800	35,000	475	280	.82	29,100	15,000	16.4
9	163,800	40,000	475	250	.82	29,100	15,000	16.4
10	204,200	35,000	475	280	.82	29,100	55,400	21.5
11	183,000	35,000	475	280	.82	29,100	34,200	19.4
12	159,000	10,000	310	266	.48	29,100	10,200	17.0
13	159,000	20,000	380	284	.62	29,100	10,200	17.0

Note: These flight profile analysis conditions are used for both vertical and lateral analyses

Design Envelope Analysis Conditions

The design envelope analyses conditions selected initially were based on conditions used in the airplane design loads analysis [5]. A summary of all design envelope conditions analyzed for the vertical and lateral analyses are given in Tables 3 and 4, respectively. The first design envelope vertical analyses were conducted for the airplane cruise speed, V_C, of 375 kt. equivalent, Mach .873, at an altitude of 22,000 ft. Four gross weight configurations were analyzed for this speed and altitude to determine the most critical condition. The conditions were operating weight empty, 119,700 lb.: maximum zero fuel weight, 156,000 lb.; fuel transfer weight, 186,000 lb.; and maximum flight weight, 221,600 lb. The conditions that were most critical were then examined at V_C speed, 375 kt. at 5,000 and 15,000 ft. and at M_C speed, Mach No. .90 at 30,000 and 40,000 ft. to obtain the load and stress variations with changes in altitude. At the critical altitudes determined from the foregoing results, three speed variations were conducted. The speeds chosen for the variations were V_B, 253 kt. EAS; 300 kt. EAS and V_D, 445 kt. EAS to Mach .95. Combining the results from the speed, altitude and weight configuration variations, the boundary of minimum margins was determined. A tabulation of the design envelope analyses conditions for the vertical analysis is given in Table 3. These conditions are also indicated on the speed altitude diagram in Fig. 12.

The design envelope conditions selected to isolate the most critical point for the lateral analyses were slightly different from those for the vertical analyses because the lateral response is not sensitive to the specific details of fuel loading. A high gross weight, which tends to give lower Dutch roll stability, was selected and six solutions were obtained at V_e for altitudes ranging from 15,000 to 43,000 ft.

Additional conditions were analyzed to evaluate the effects of other parameter variations such as wing bending and torsional stiffness, fuel loading, number and limits of discrete frequencies used in the analysis, yaw damper operation and lateral aerodynamic stability parameters. A summary to the parametric variation conditions is given in Table 5.

TABLE 3

DESIGN ENVELOPE CONDITIONS - VERTICAL ANALYSES

Analysis Condition No.	Gross Weight, Lb.	Altitude, Ft.	True Airspeed, Kt.	Equivalent Airspeed, Kt.	Mach No.	Payload Lb.	Fuel Lb.	cg, Percent MAC
14	119,700	22,000	532	375	.87	0	0	20.5
15	156,000	22,000	532	375	.87	36,300	0	15.6
16	186,000	22,000	532	375	.87	36,300	30,000	16.3
17	221,600	22,000	532	375	.87	36,300	65,600	21.2
18	186,000	5,000	403	375	.62	36,300	30,000	16.3
19	186,000	15,000	472	375	.76	36,300	30,000	16.3
20	186,000	30,000	530	327	.90	36,300	30,000	16.3
21	186,000	40,000	516	260	.90	36,300	30,000	16.3
22	186,000	22,000	359	253	.59	36,300	30,000	16.3
23	186,000	22,000	425	300	.70	36,300	30,000	16.3
24	186,000	22,000	480	340	.79	36,300	30,000	16.3
25	186,000	22,000	576	406	.95	36,300	30,000	16.3
26	221,600	5,000	403	375	.62	36,300	65,600	21.2
27	221,600	15,000	472	375	.76	36,300	65,600	21.2
28	221,600	30,000	530	327	.90	36,300	65,600	21.2
29	221,600	40,000	516	260	.90	36,300	65,600	21.2
30	221,600	15,000	319	253	.51	36,300	65,600	21.2
31	221,600	15,000	378	300	.60	36,300	65,600	21.2
32	221,600	15,000	561	445	.90	36,300	65,600	21.2

TABLE 4

DESIGN ENVELOPE CONDITIONS - LATERAL ANALYSES

Analysis Condition No.	Weight, Lb.	Altitude, Ft.	Airspeed, Kt.	Equivalent Airspeed, Kt.	Mach No.	Payload Lb.	Fuel Lb.	cg, Percent MAC
1B	214,400	42,000	505	239	.90	29,100	65,600	21.4
2B	214,400	35,000	519	289	.90	29,100	65,600	21.4
3B	214,400	30,500	528	320	.90	29,100	65,600	21.4
4B	214,400	23,500	544	374	.90	29,100	65,600	21.4
5B	214,400	18,000	495	374	.80	29,100	65,600	21.4
6B	214,400	15,000	473	375	.75	29,100	65,600	21.4

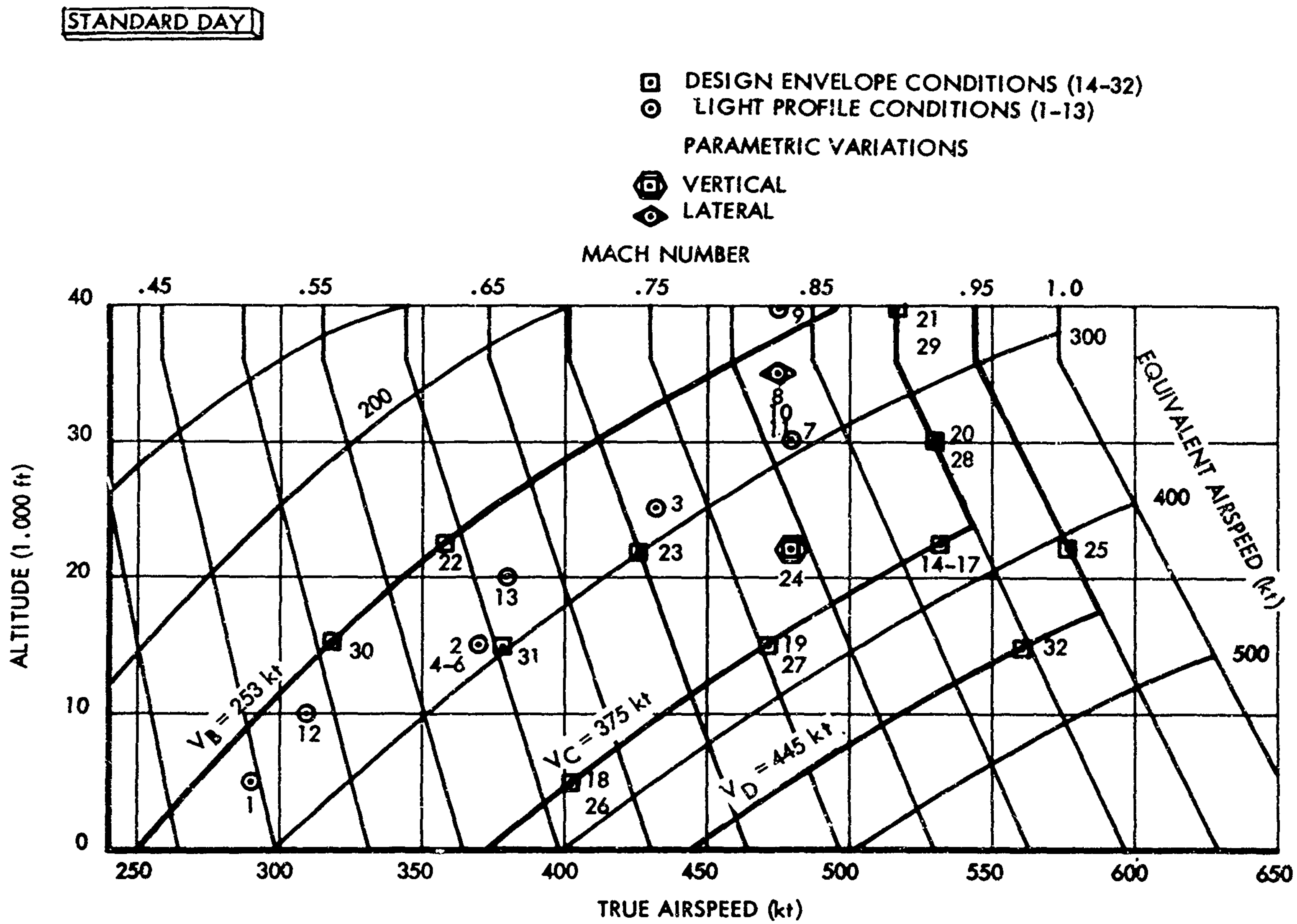

FIGURE 12. SPEED - ALTITUDE DIAGRAM

TABLE 5

PARAMETRIC VARIATION CONDITIONS

Gross Weight, Lb.	Altitude Ft.	True Airspeed, Kt.	Equivalent Airspeed, Kt.	Mach No.	Payload, Lb.	Fuel Lb.	cg, Percent MAC
Vertical Analyses - Design Envelope Condition No. 24							
186,000	22,000	480	340	.78	36,300	30,000	16.3

Variation
- 24A 80 Percent of Nominal Bending Stiffness
- 24B 80 Percent of Nominal Torsional Stiffness
- 24C Most Aft cg Location, Changed from 16.3 to 25.0
- 24D No Structural Damping
- 24E No Gradual Penetration of Gust Front, Instantaneous Penetration

Gross Weight, Lb.	Altitude Ft.	True Airspeed, Kt.	Equivalent Airspeed, Kt.	Mach No.	Payload, Lb.	Fuel Lb.	cg, Percent MAC
Lateral Analyses - Flight Profile Condition No. 10							
204,200	35,000	475	263	.82	29,100	55,400	21.5

Variation
- 10A Airplane Product of Inertia Changed from Nominal $7.75(10)^5$ to $-7.75(10)^5$ in. lb. sec.^{2}
- 10B Airplane Product of Inertia, Twice Nominal Value
- 10C Airplane Product of Inertia, 1.5 times Nominal Value
- 10D Yawing Moment Due to Roll Rate Derivative, $C_{n_{\frac{b\dot{\Phi}}{2V}}}$, Changed from Nominal .0065 to -.013.
- 10E Yawing Moment Due to Roll Rate Derivative -.0189
- 10F Yawing Moment Due to Roll Rate Derivative -.0378
- 10G Yawing Moment Due to Yaw Rate Derivative, $C_{n_{\frac{b\dot{\psi}}{2V}}}$, Changed from Nominal -.180 to -.144
- 10H Yaw Moment Due to Roll Rate Derivative, -.126.

ANALYSIS

General Remarks

The Boeing Model 720B airplane was used to idealize the basic mathematical models for all analyses. Fig. 1 shows the airplane in flight. This airplane requires a crew of three, pilot, copilot and flight engineer, and has a maximum range of 3,300 miles. The airplane normally cruises from 15,000 to 40,000 ft. at gross weights in excess of 200,000 lb. and at speeds up to 615 miles per hour. The airplane has a wing span of approximately 131 ft., and an overall length of approximately 137 ft. A more detailed 3-view diagram of the airplane is shown in Fig. 13.

All major parts of the airplane except the horizontal stabilizer were considered to be elastic in the analyses. Therefore, a rather comprehensive mass and stiffness description of the airplane was required. Simple beam bending theory was used to represent the stiffness characteristics of the major components such as the wing, forward and aft fuselage, and the vertical tail. The elastic axes were generally located on the locus of shear centers along each component, but were adjusted to agree with information obtained in previous airplane static testing.

Structural damping for the various airplane flexible modes of vibration was taken directly from whole airplane shake test results[(17)].

Considerable airplane test data was available to formulate the mathematical models that were used in the analyses of the 720B. The method used to represent the detailed aerodynamics, mass, and stiffness characteristics are not complex, but they do provide a solid basis for understanding the airplane's dynamic response characteristics. The airplane responses obtained herein by analysis show good agreement with static aeroelastic results for slow maneuvers and with flutter analyses for the higher frequency elastic responses.

Airplane Mass Data

The weight and inertia data for the analyses were originally calculated from released detailed drawings and have been updated as drawing changes or actual weights became available. The airplane fuselage was divided into eighteen panels and the mass properties in the form of weight, center of gravity, and mass moments of inertia for pitch, roll and yaw were determined for each section. Mass data for the operating weight empty (OWE) configuration and for full and partial payloads were calculated to facilitate selection of partial payload conditions.

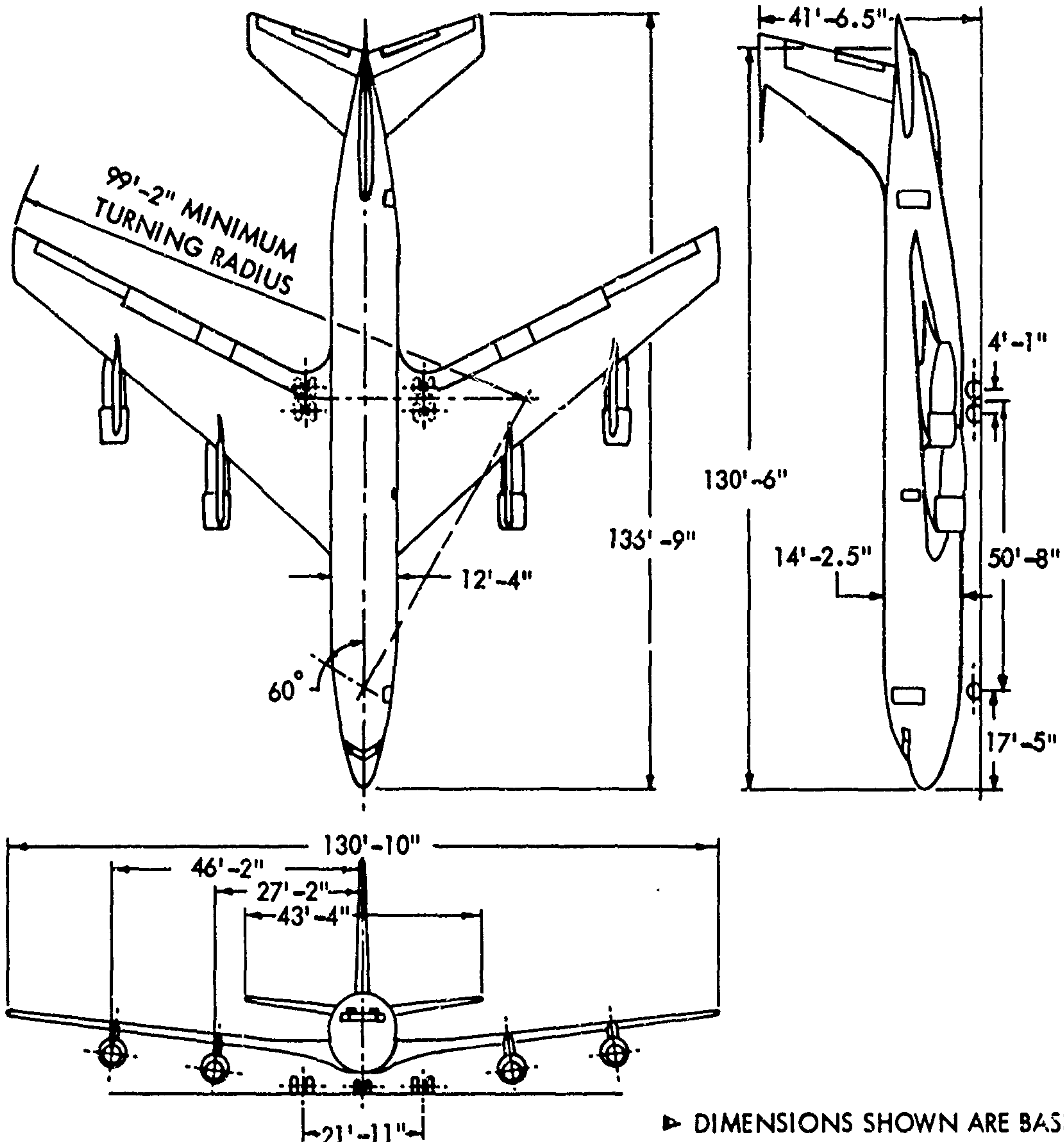

► DIMENSIONS SHOWN ARE BASED UPON GROSS WEIGHT OF 110,000 POUNDS AND CENTER OF GRAVITY AT 15% OF MAC

FIGURE 13. 3 - VIEW DIAGRAM OF 720B

The wing structure and contents with the exception of fuel were divided into ten spanwise panels. Each of these panels was further divided into five zones: the leading edge, front spar, inner spar, rear spar and trailing edge. The weight and center of gravity were calculated for each zone and summed to give the total panel weight and center of gravity. The total panel mass moments of inertia were computed by rotation and transfer of zone results into axes parallel and perpendicular to the wing elastic axis.

The vertical tail structure and contents were divided into seven spanwise panels and the section mass properties were calculated in the same manner as the wing. The horizontal stabilizer was considered as a single panel for these analyses. The lumped mass properties for the horizontal stabilizer were obtained by combining previously panelled data which were obtained in the same manner as the wing and vertical tail data.

The mass properties for each JT3D-1 engine, nacelle, and nacelle strut were combined, and a lumped center of gravity location determined. Then, the nacelle mass moments of inertia were determined for axes perpendicular and parallel to the airplane reference axes.

The fuel mass properties were obtained for conditions representing fuel loadings of 25, 50, 75 and 100 percent of full fuel. The particular percentage used was determined by the flight condition being analyzed. Fuel weights and cg positions were calculated by a computer program which accounted for the geometry of each tank.

The accuracy of the mass properties used in these analyses is estimated to be within 1.0 percent for the total airplane weight, 2.0 in. for total airplane center of gravity location, and 3.0 percent for the total airplane mass moments of inertia. Also, it is estimated that the panelled mass data and the major airplane component mass data are accurate to similar limit.

Component Stiffnesses

The stiffness characteristics of each major component of the airplane was described by a distribution of bending stiffness, EI, and torsional stiffness, GJ, along the elastic axis. The wing section properties were computed using front and rear spar areas and all inspar skin for both the upper and lower surfaces. Values for the modulus and shear modulus of elasticity, E and G, were $10.3(10)^6$ and $3.8(10)^6$ psi, respectively. The body section properties were computed using stiffeners with full skin effective in tension and 2W widths of skin effective in compression. The body cutout sections were handled on an individual basis by special analysis.

The section properties for determining the bending stiffness of the vertical tail were computed using front and rear spar chord area with 2W widths of skin assumed effective on the compression side of the rear spar chord in trailing edge beam areas. Fully effective tension skin was assumed between the front and rear spars and for balance panel covers. Near the body intersection, the inspar skin and front spar areas are assumed to be partially effective because of shear lag. The section properties for the determination of the torsional stiffness of the vertical tail were computed using front and rear spar areas and all inspar skin for both surfaces.

Aerodynamics - Vertical Analyses

The stresses induced into the airplane structure for unaccelerated flight in turbulent air result from the sum of the one factor aerodynamic and inertia forces on the airplane, the gust forces, and the dynamic response forces. The one factor flight loads and stresses were added to the respective incremental dynamic loads and stresses to assess the strength capabilities of the 720B airplane for flight in turbulent air.

The one factor level flight loads, that is bending moments, shears, and torsions, were determined by aeroelastic analyses.[6,7] All of the basic aerodynamic data required for these analyses were obtained from a series of wind tunnel tests performed for the entire Mach number range. Wind tunnel pressure model test results were used to establish wing, fuselage, and vertical tail airload distributions. The section lift and moment coefficients were corrected for model flexibility before they were used for full scale airplane analysis, and were later refined to obtain final agreement between the aeroelastic analyses and actual airplane flight load survey measurements.

The rigid airplane aerodynamic section coefficients, corrected to provide agreement with flight measurements, can be used to obtain an aeroelastic solution for any longitudinal maneuvered flight condition. Simultaneous equations are solved to obtain an aeroelastic solution. These equations define the following: (1) wing lift distribution on 10 aerodynamic sections on the wing semi-span, (2) airplane lift balance, and (3) the airplane pitching moment balance. Specifically, the solution gives the elastic wing lift distribution, the airplane wing root angle of attack, and the balancing tail load.

The unsteady aerodynamics used in the vertical dynamic analyses are based on modified two-dimensional strip theory.[8] The strip theory, originally developed by Theodorsen[9] and Küssner,[10] has been modified to include aerodynamic induction effects[8]. These induction effects account for the aerodynamic pressure carry-over between wing panels and between the wing and horizontal tail. This is accomplished by using a downwash matrix based on lifting line theory. The dynamic downwash matrix includes pressure carry-over and pressure transmittal functions to provide the proper magnitude and phasing of the carry-over pressures. The section (strip) aerodynamics for zero frequency are made to agree with the comparable aeroelastic solution. The results of this modification have been compared to experimental results and to theoretical results based on lifting surface theories; satisfactory correlation was obtained.(8)

The unsteady aerodynamic expressions for the vertical analyses were calculated for a range of reduced frequencies to adequately define the airplane dynamic responses. The gust or excitation airforces for a sinusoidal gust field were also expressed in a modified two-dimensional form for the same reduced frequency values. The aerodynamic forces acting on the fuselage were obtained using simple quasi-steady aerodynamic expressions. The fuselage was first divided into thirteen streamwise panels, seven on the forebody and six on the aftbody. A static pressure distribution was then used to determine the individual panel lift and moment coefficients. The panel angles of attack were assumed to arise from the deflection slopes and displacement velocities of the fuselage.

Aerodynamics - Lateral Analyses

The lateral dynamic response of large swept wing subsonic jet transports is generally dominated by the low damped Dutch roll mode. The damping of this mode, as determined by dynamic analysis, is very sensitive to the estimated ro...ry stability derivatives used in the equations of motion. Large changes in the lateral gust loads result from small changes in particular rotary derivatives for flight conditions in which the Dutch roll damping is low.

All of the airforces and inertia forces were referenced to the airplane stability axes. The stability axes were determined as the orthogonal set attached to the airplane with the initial orientation of the x-axis in the wind direction for undisturbed and unaccelerated flight. The airplane angle of attack for one factor level flight was determined by a separate aeroelastic analysis for each condition.

The lateral stability derivatives were decomposed into wing, fuselage, and vertical tail components. The pressure distributions for the fuselage and the vertical tail were determined from wind tunnel pressure model test data. The aerodynamic side force and moment from the wing were accounted for by a concentrated side force and a moment applied to the airplane center of gravity. The integrated force and moment resulting from the aerodynamic pressures on the fuselage and vertical tail together with the concentrated force and moment from the wing were made to agree with the lateral whole airplane derivatives.

Generalized Coordinates

Each dynamic analysis was conducted for a mathematical model which was in equilibrium at one factor level flight. When such a system is subjected to an external sinusoidal gust field, it responds about its static equilibrium configuration. This gives rise to displacements, velocities and accelerations necessary to preserve the energy balance with the external gust loading. The structural deformation of the airplane can be described as a sum of incremental displacements in the system's natural modes of vibration. These deflected shapes and whole airplane rigid body displacements are used as the so-called generalized coordinates to describe the airplane motions. The development of the equations of motion by the Lagrangian approach using these generalized coordinates is discussed in Appendix A.

The natural modes of vibration of a flexible system can take various forms depending upon the manner in which the system is restrained. When the airplane is in flight there are no external restraints, and the airplane can displace with complete freedom. There are several methods by which this so-called free-free state can be described. One method is to define the cantilevered vibration modes of each major component, such as the wing, body, and nacelles by separate orthogonal mode sets. A limited number of these cantilevered modes along with the rigid airplane freedoms are used as the generalized coordinates to describe the overall airplane response.

A better set of generalized coordinates is obtained when a large number of cantilevered modes are coupled with the rigid airplane freedoms to produce a set of unrestrained free-free airplane normal modes. The advantages of this approach is that the overall airplane response can be more accurately described by fewer degrees of freedom or generalized coordinates than in the cantilevered mode approach. The free-free normal mode approach was used for the 720B vertical analyses, and the cantilevered mode approach was used for the lateral analyses. A representative summary of cantilevered modes which were coupled with airplane vertical translation and pitch freedoms for the vertical analyses is given in Table 6. Corresponding representative airplane free-free modal data is given in Table 7. A summary of cantilevered modes used in the lateral analyses is given in Table 8.

TABLE 6

REPRESENTATIVE CANTILEVERED MODES
VERTICAL ANALYSES

Airplane Component	No. of Discrete Masses**	Cantilevered Mode Description	Modal Frequency, cps OWE	Half Fuel	Full Fuel
Wing	10	1st Bending	1.31	1.27	.93
		2nd Bending	3.77	3.51	2.81
		3rd Bending	7.75	6.59	5.83
		4th Bending	10.67	10.62	9.28
		1st Torsion	2.52	2.52	2.52
		2nd Torsion	5.19	5.18	5.19
		3rd Torsion	19.79	19.28	18.42
Forward Fuselage	7	1st Bending	3.99	3.71	3.71
Aft Fuselage	13*	1st Bending	2.57	2.46	2.46
		2nd Bending	9.87	8.62	8.62
Inboard Nacelle	1	Vertical Bending	4.31	4.31	4.31
		Coupled Side Bending & Torsion	2.07	2.07	2.07
Outboard Nacelle	1	Vertical Bending	4.28	4.28	4.28
		Coupled Side Bending & Torsion	2.24	2.24	2.24

*Includes horizontal and vertical tail masses.
**See Fig. 23

TABLE 7

REPRESENTATIVE FREE-FREE NORMAL MODES VERTICAL ANALYSES

Mode No.	Responding Component	Modal Frequency, cps				Structural Damping, g**
		OWE	Half Fuel	Full Fuel	Ground Vibration Test*	
1	Wing Bending	1.40	1.35	1.08	1.44	.040
2	Nacelle	2.07	2.07	2.05	2.07	.027
3	Nacelle	2.22	2.20	2.14	--	.037
4	Wing Torsion	2.46	2.44	2.25	2.96	.022
5	Forward Fuselage	3.32	3.26	3.19	3.75	.030
6	Fuselage	4.07	3.65	3.40	5.40	.030
7	Wing Bending	6.07	5.30	4.55	6.50	.030

*The ground vibration test was conducted for the 720 airplane with the main gear and nose gear restrained. (Ref. 17)

**Damping coefficient, g, is equal to twice the actual damping divided by the critical damping.

TABLE 8

CANTILEVERED MODES LATERAL ANALYSES

Airplane Component	No. of Discrete Masses*	Cantilevered Mode Description	Modal Frequency, cps
Aft Fuselage	12	1st Side Bending	2.41
Aft Fuselage	12	2nd Side Bending	7.22
Aft Fuselage	12	1st Torsion	5.83
Forward Fuselage	7	1st Side Bending	3.66
Fin	13	1st Bending	4.34
Fin	13	1st Torsion	14.62

*See Fig. 24

Equations of Motion

The equations of motion for the 720B gust analyses were developed by Lagrange's energy approach. The derivation of vertical and lateral equations of motion is discussed in Appendix A. The equations for both analyses are a set of simultaneous second-order differential equation in the generalized coordinates described previously. These equations can be expressed in matrix form as follows:

$$\left[M_{ij}\right] \left\{\ddot{q}_i\right\} + \left[D_{ij}\right] \left\{\dot{q}_i\right\} + \left[K_{ij}\right] \left\{q_i\right\} = \left\{C_i\right\} \alpha_g \tag{4}$$

The coefficient matrices of $\ddot{q}_i$, $\dot{q}_i$, and q_i are the generalized mass, $[M_{ij}]$, the structural and aerodynamic damping, $[D_{ij}]$, and the structural and aerodynamic stiffness, $[K_{ij}]$, respectively. The right hand side of the equation represents the generalized forces in the degrees of freedom due to the gust excitation, $\left\{C_i\right\}$.

The generation of the generalized mass coefficient matrix began with the lumped mass representation of the airplane in terms of discrete masses and mass moments of inertia about the discrete mass center of gravity for each mass panel. Then, the center of gravity mass properties were transferred to their respective elastic axis reference stations. The total kinetic energy of the system was written in terms of generalized coordinate velocities. Differentiation of the kinetic energy expression, first with respect to the generalized coordinate velocities, and then with respect to time, resulted in the generalized mass matrix, $[M_{ij}]$.

The damping coefficients arise partly from the aerodynamic response forces and partly from structural damping. The aerodynamic damping results from that portion of the total aerodynamic force which is in phase with the particular generalized coordinate velocities. The structural damping is represented as forces that are proportional to the structural stiffnesses but are in phase with the response velocities. The values for structural damping used in the vertical analyses were obtained from ground vibration tests of the 720 airplane. The damping coefficient for each mode for the vertical analyses is listed in Table 7. The energy or work expression for these damping forces was differentiated with respect to each coordinate to arrive at the generalized damping matrix, $[D_{ij}]$.

The stiffness matrix also results from structural and aerodynamic sources. The stiffness of the primary airplane structure is represented in the equations of motion by the elastic potential energy stored in the structure when it is deformed in a linear combination of the selected vibration mode shapes. The aerodynamic work resulting from the response displacements of the primary components of the airplane is added to the internal elastic energy and the entire expression is differentiated with respect to each generalized coordinate to form the stiffness matrix, $[K_{ij}]$.

The yaw damper effects in the lateral equations of motion are handled by including a generalized force specifically for the yaw damper. This generalized force is a function of both the gust excitation frequency and the resulting airplane yawing velocity. The yaw damper system consists of a yaw rate sensor, a yaw axis amplifier, a servo system with rudder position and rudder angular rate feedback loops, and an hydraulic rudder actuator unit.

In the airplane, the signal from the yaw rate sensor is filtered to remove the effects of both slow maneuvers and higher frequency fuselage vibrations. The filtered signal is amplified and applied to an electronic servo which, in turn, drives the hydraulic rudder actuator.

The yaw damper system is simulated in the lateral analyses by incorporating a transfer function due to yawing velocity. This transfer function is a composite of the transfer functions for all of the sub-parts of the yaw damper system. The generalized force associated with the rudder deflection varies with frequency, but it is a function of yaw rate only at any given frequency. The generalized force coefficients were added to the coefficients in the rudder-fixed equations of motion to account for the yaw damper effects. A more complete description of the mathematical model for the yaw damper is given in Appendix A, Equations of Motion.

Both the vertical and lateral equations of motion were solved to obtain the real and imaginary parts of the steady-state complex responses of the generalized coordinates due to a 1.0 ft. per sec. continuous sinusoidal gust velocity excitation. Consequently, the accelerations, $\ddot{q}_i$, could be replaced by $-\omega^2 q_i$ and the velocity, $\dot{q}_i$, by $i\omega q_i$, where ω is the excitation frequency. When these assumptions were incorporated into the equations of motion, the matrix coefficients $\omega^2[M_{ij}]$, $i\omega[D_{ij}]$ and $[K_{ij}]$ could be combined into a single complex set of matrix coefficients $[A_{ij} + iB_{ij}]$ of the generalized coordinates for each frequency. The generalized coordinate responses were obtained by premultiplying the generalized gust forces, $\{C_i\}$, by the inverse of this matrix for each of the selected frequencies.

Solutions were obtained in the vertical analyses to define the complex frequency response functions over the range from $0.5(10)^{-5}$ to 0.6 rad. per ft. The sensitivity of the rms values, $\bar{A}$, and the number of zero crossings, N_0, to the upper and lower limits of the frequency range and to the overall number of frequencies was examined. The lower end of the frequency range was taken at $0.5(10)^{-5}$ rad. per ft which was well below the short period mode response frequency. The maximum frequency, 0.6 rad. per ft., was sufficiently high such that the number of zero crossings had converged. A total of 95 frequencies between the above limits were used in the vertical analysis. The major contribution to the rms values is in the lower end of the frequency range; therefore, the solution frequencies were selected at closer intervals in the lower frequency range.

Load Equations

The detailed loads for the aircraft structure were obtained from the complex frequency responses of the generalized coordinates. This was accomplished by transforming the generalized inertia, damping and stiffness forces used in the equations of motion into shears, bending moments, and torsions referenced to given stations on the elastic axes. The shear, moment, and torsion coefficients were calculated for unit deflections in the generalized coordinates. Then, these coefficients were multiplied by the complex frequency responses of the generalized coordinates to obtain load complex frequency responses for all elastic axis reference stations.

Complex frequency response functions for stresses were obtained by incorporating unit load solution stress coefficients from the airplane stress analyses[11,12,13] into the load equations.

Spectral Analysis

The complex frequency response functions for the incremental shears, moments, and torsions were used to define complex frequency response functions for incremental axial and shear stresses in the detailed airplane structure. The output power spectra for the loads and stresses were obtained as follows:

$$\Phi_o(\Omega) = \Phi_w(\Omega) \left| T(i\Omega) \right|^2 \qquad (5)$$

where,

$\Phi_o(\Omega)$	output, load or stress power spectral density function
$\Phi_w(\Omega)$	input, normalized vertical or lateral gust power spectral density function
$T(i\Omega)$	complex frequency response function for load or stress at a given station in the airplane

The rms values for the loads and stresses for a rms gust velocity of unity, $\bar{A}$, were determined by integrating the appropriate output power spectrum.

$$\bar{A} = \left[\int_0^\infty \phi_o(\Omega) d\Omega \right]^{1/2} \tag{6}$$

The zero crossings per ft. for all loads and stresses were determined by Rice's expression[14].

$$N_o = \frac{1}{2\pi} \left[\frac{\int_0^\infty \Omega^2 \phi_o(\Omega) d\Omega}{\int_0^\infty \phi_o(\Omega) d\Omega} \right]^{1/2} \tag{7}$$

Since the actual strength of a detailed structural element is in general governed by the combined stresses, stress interaction functions and one factor level flight stresses must be incorporated into the statistical analysis. The problem was to determine the probability of exceeding the limit strength for a given flight condition (Design Envelope Approach) and to determine the number of times the limit strength is exceeded per unit time (Flight Profile Approach). The joint probability density function for two components of stress on a structural element, say, axial stress and shear stress is,

$$P(f,\xi) = \frac{1}{2\pi} \frac{1}{\sigma_f \sigma_\xi (1-\rho^2)^{1/2}} \exp \left\{ \frac{-1}{2(1-\rho^2)} \left[\frac{(f-f_o)^2}{\sigma_f^2} - \frac{2\rho(f-f_o)(\xi-\xi_o)}{\sigma_f \sigma_\xi} + \frac{(\xi-\xi_o)^2}{\sigma_\xi^2} \right] \right\} \tag{8}$$

where,

f axial stress, psi

ξ shear stress, psi

f_o, ξ_o	one factor axial and shear stresses, respectively, psi
σ_f, σ_ξ	rms axial and shear stresses, respectively, psi
ρ	correlation coefficient

Statistical Analysis - Design Envelope Approach

The volume under the probability density functionshown in Fig. 14 bounded by the interaction limit strength envelope is equal to the probability that the limit strength will not be exceeded, that is, that the margin of safety is greater than zero. The probability that the limit strength will be exceeded is 1.0 minus the probability that the limit strength will not be exceeded. Therefore,

$$P(MS < 0) = 1 - P(MS \geq 0) \tag{9}$$

Since the input or gust power spectral density varies directly with the mean squared gust velocity, σ_W^2 or σ_V^2 , the probability of exceeding the limit design strength is a function of σ_W or σ_V. That is,

$$\sigma_f = \bar{A}_f \sigma_W \tag{10}$$

and

$$\sigma_\xi = \bar{A}_\xi \sigma_W \tag{11}$$

Consider a stiffened skin-stringer segment typical of those used in wing panel construction of subsonic jet transport airplanes. A cross section through the segment normal to the stringer is shown in Fig. 15. It was assumed that the airplane, of which this structural element is a part, was flying in turbulent air. It was of interest to determine (1) the probability of exceeding the limit design strength of the segment and (2) the expected number of times per hour that the limit strength would be exceeded for various root mean square (rms) gust velocities, σ_W.

Numerical information pertinent to this example is given in Table 9. The appropriate limit strength interaction diagram is shown with a sketch of the structural segment in Fig. 15. It will be noted that two level-flight stress points, skin stress and segment stress, are shown in

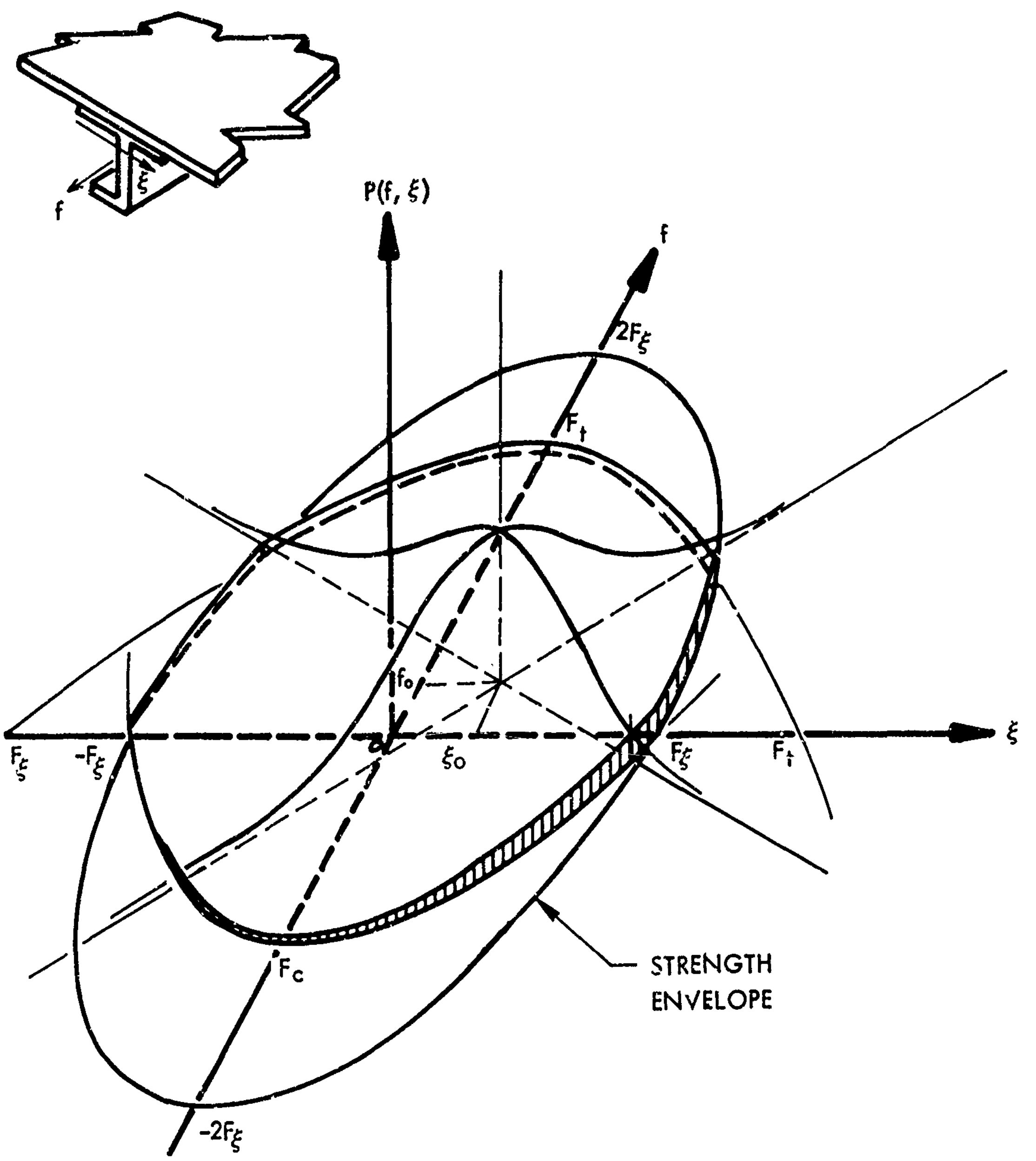

FIGURE 14. JOINT GAUSSIAN PROBABILITY DENSITY FUNCTION

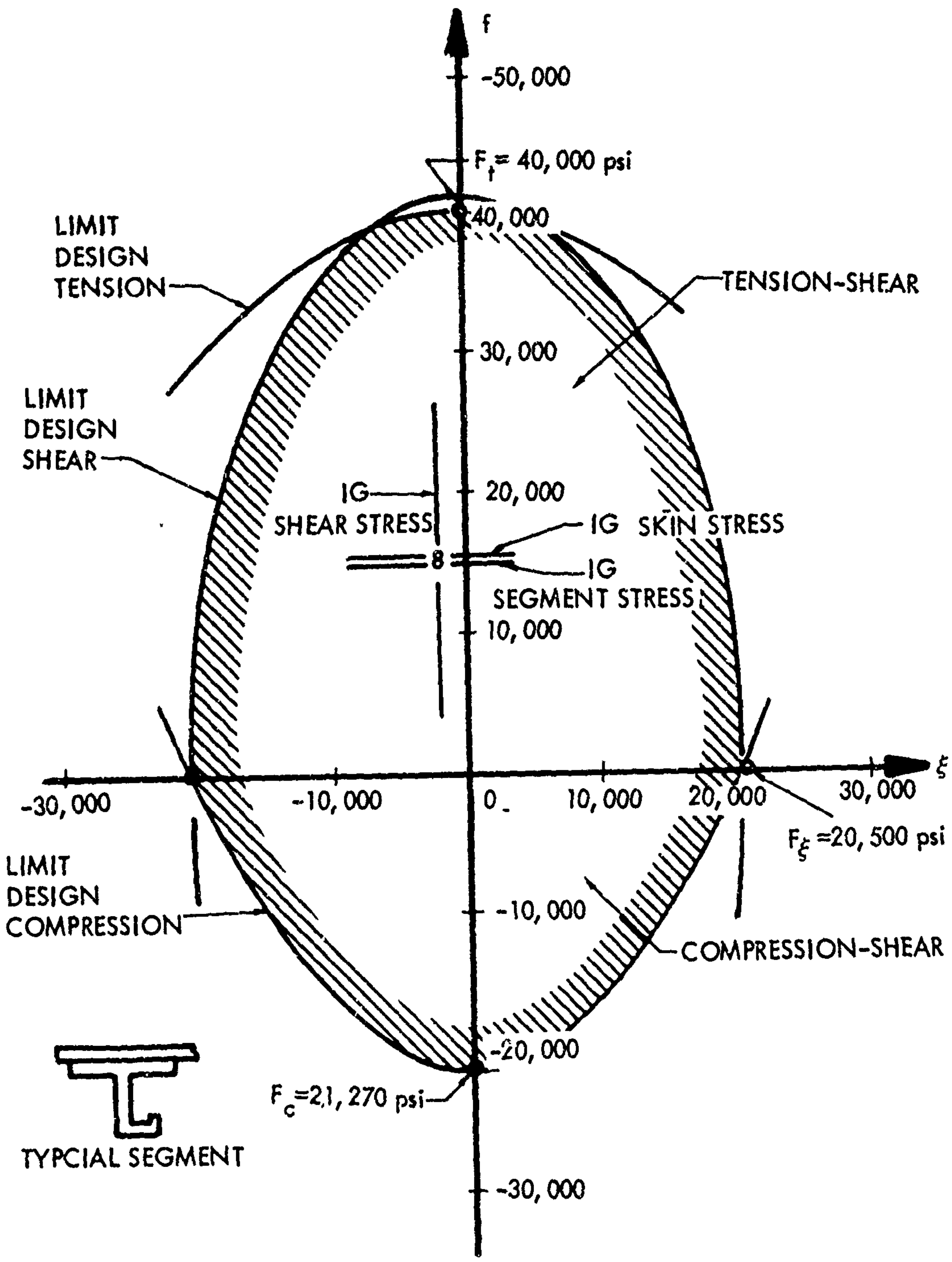

FIGURE 15. TYPICAL SKIN-STRINGER SEGMENT AND STRENGTH INTERACTION DIAGRAM

TABLE 9

NUMERICAL EXAMPLE
STRESS DATA FOR STATISTICAL ANALYSIS*

Level Flight Stresses (Based on Appropriate Effective Areas)	
Skin Stress, Tension f_{o_t}, psi	15,600
Segment Stress, Compression, f_{o_c}, psi	15,200
Shear, ξo, psi	-2,190
Dynamic Analysis Stress Data (Power Spectral Analysis-RMS Gust Velocity, σ_w = 1.0 ft. per sec.)	
RMS Tension Stress, $\overline{A}_{f_t}$, psi	184.19
RMS Compressive Stress, $\overline{A}_{f_c}$, psi	179.51
RMS Shear Stress, $\overline{A}_{\xi}$, psi	38.53
Correlation Coefficient (Axial and Shear Stresses)	-0.2141
Zero Crossings per sec	
Axial Stress, N_{O_f}	1.2205
Shear Stress, N_{O_ξ}	2.7235
RMS Stress Rates, psi per ft per sec	
Tension, σ_{β_t}	1,413
Compression, σ_{β_c}	1,377
Shear, σ_{α}	659
Allowable Limit Design Stresses, psi	
Tension, F_t	40,000
Compression, F_c	21,270
Shear, F_ξ	20,500

*See Appendix B for development of methods for Statistical Analysis of Combined Random Stresses

Table 9 and in Fig. 15. These are reference points for two joint probability stress distributions. The compression-shear or segment stress probability distribution was applied to the compression portion of the interaction diagram in Fig. 15, and the tension-shear or skin stress distribution was applied to the tension portion of the diagram. The volume of the compression-shear joint probability density function within the compression region of the interaction diagram was added to the volume of the tension-shear density function in the tension region to determine the probability that the limit design strength will not be exceeded. A typical plot of $P(MS < 0,\sigma_w)$ versus σ_w is shown in Fig. 16.

Certain structural elements in the fuselage near either the vertical or lateral bending axis are only subjected to fluctuating compression stresses and shear. They cannot be stressed in tension as a result of the gust loading. This occurs, because the location of the neutral plane through the fuselage section shifts across the element as the direction of the bending moment on the fuselage changes sign. The element is always on the compression side of the neutral plane. This compression-compression situation was handled in the statistical analysis of limit strength exceedances by removing the tension part of the interaction diagram and by subst'tuting another compression part. Now, these special cases could be treated in the same manner as normal elements.

The objective of the design envelope approach was to determine a level of gust i tensity, $\sigma_w\eta_d$, which when multiplied by a stress $\bar{A}$ value for a critical element would just equal the limit design strength for the element. Thus, the design envelope approach implies a one-dimensional probability distribution for design stress. The statistical distribution of stress values is assumed to be Gaussian and can be completely described by the rms stress value for a one-dimensional distribution.

When the probability of exceeding limit strength is governed by a joint probability function in two dimensions, three parameters, i.e. two rms stress values and a correlation coefficient, are required. As a result, no single statistical parameter can be scaled-up to a design strength level. However, the probability of exceeding the design strength of the element can be matched to : probability for exceeding an incremental cg acceleration* for the same flight condition. The distribution of

*The development that follows is essentially unchanged if the c.g. acceleration is replaced by a generalized load quantity, $y/\bar{A}$. Thus it can be seen that the numerical results are not dependent upon the choice of the particular output quantity for which the single-parameter probability distribution is obtained.

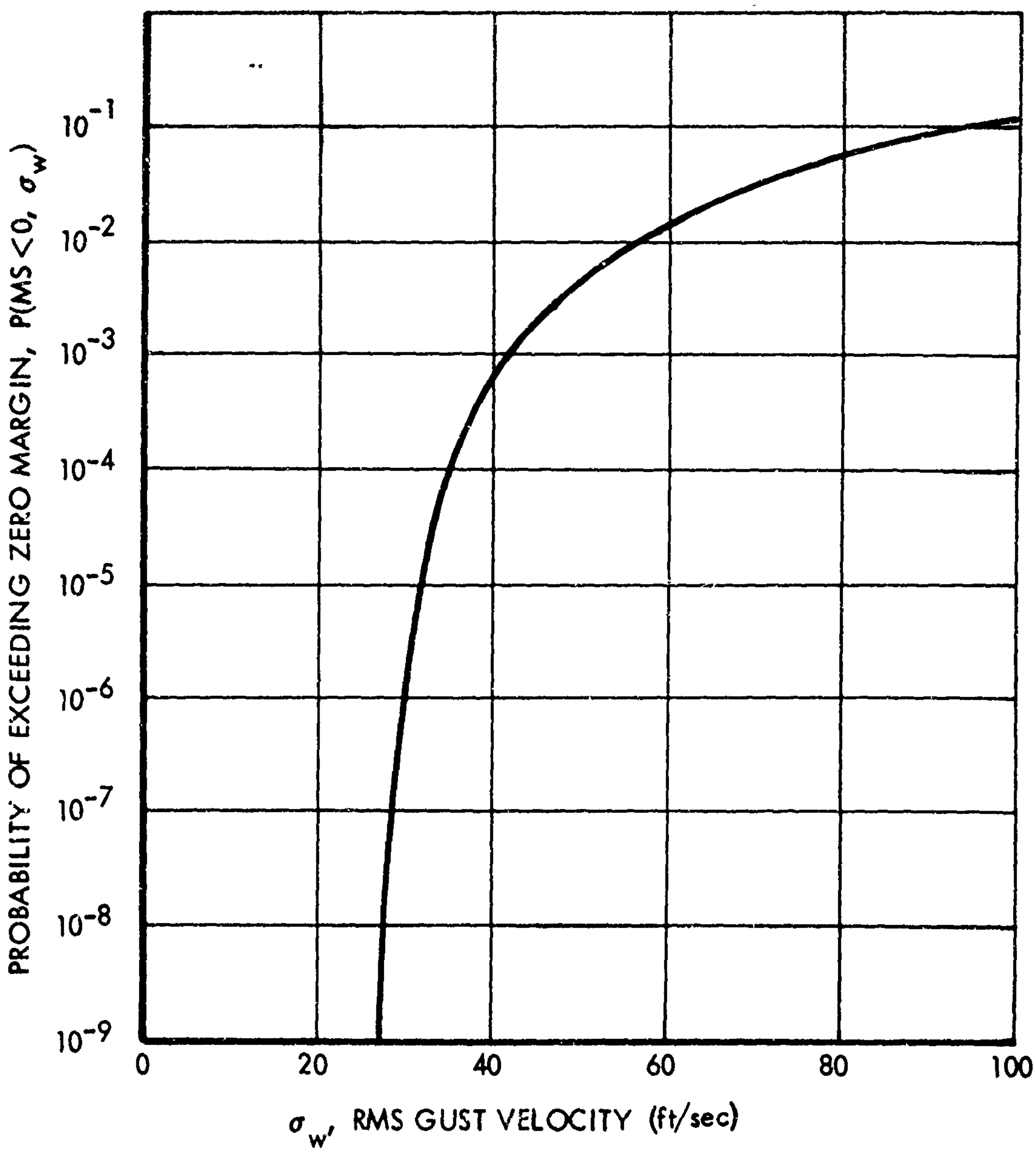

FIGURE 16. PROBABILITY OF EXCEEDING LIMIT DESIGN STRENGTH FOR VARIOUS RMS GUST VELOCITIES

incremental cg acceleration is a single parameter distribution, and a unique $\sigma_w \eta_d$ can be determined for that level of incremental cg acceleration.

The probability of exceeding specified values of incremental cg acceleration is determined as follows:

$$P(\Delta n > \Delta n_i,\ \sigma_w) = \frac{2}{\sqrt{2\pi}\,\bar{A}\sigma_w} \int_{\Delta n_i}^{\infty} e^{-\Delta n^2/2\bar{A}^2\sigma_w^2}\, d\Delta n \qquad (12)$$

This equation is evaluated for various specified $\bar{A}\sigma_w$ values to obtain the distribution functions shown in Fig. 17. It will be noted that the diagrams in Fig. 17 are universal, and can be applied to any airplane at any altitude.

Of course, the cumulative distribution functions shown in Figs. 16 and 17 will diff‸r, because the first is based on joint probability considerations, an‸ the second is a single parameter distribution. The two distributi‸‸ ‸unctions cannot be made to coincide everywhere. The question was, where ‸ ‸uld they be matched?

When each probability function is multiplied by $\hat{f}(\sigma_w)$, the probability density of rms gust velocity, and integrated over all σ_w, we obtain a new probability number indicating the chance of exceeding the design strength at any instant in time for all weather and seasonal conditions. Typical overall probability ‸ensity functions for incremental cg acceleration are shown in Fig. 18. Similar typical information for a structural element is shown in Fig. 19.

It is ovbious that one curve of the family of curves shown in Fig. 18 will best match the curve in Fig. 19. The cg acceleration curve that best matches the curve for the structural element is the one having very nearly the same area when integrated. It is noted that the maxima of the overall probability density curves for cg acceleration lie on a straight line as shown in Fig, 18, and it is possible to cross plot the maximum overall probability density versus acceleration level as shown in Fig. 20. This diagram is unique for the flight condition. The straight line will intersect the vertical axis at $\hat{f}(\sigma_w) = \hat{f}(0)$ since $P(\Delta n > 0) = 1.0$. Now it is possible to determine $\sigma_w \eta_d$ for the structural element by determining the maximum probability density in Fig. 19, $(9.0(10)^{-13})$. This maximum probability de‸sity wa‸ u‸e‸ in Fig. 20 to determine Δn_i, (1.39), and $\sigma_w \eta_d$ for the element.

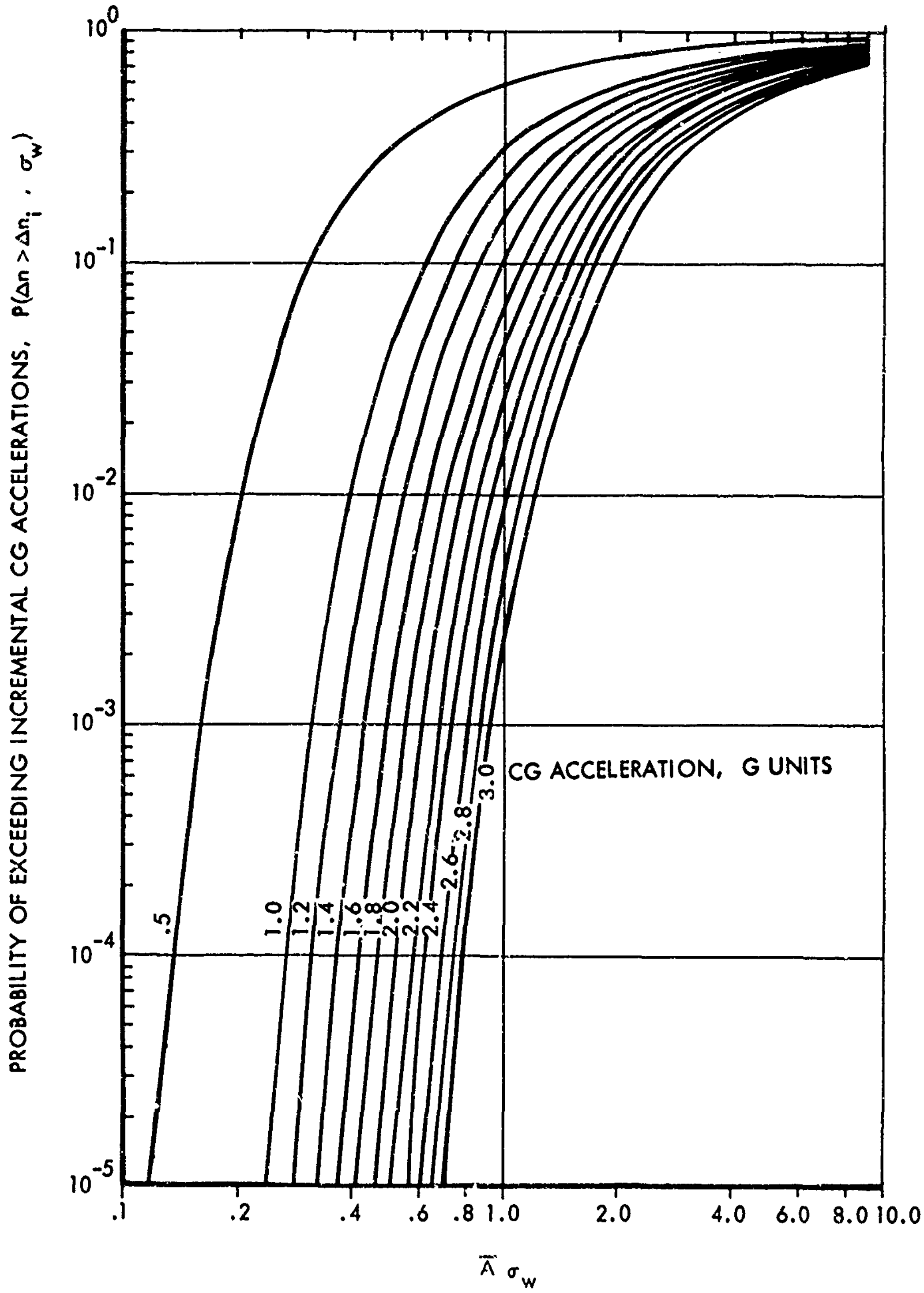

FIGURE 17. PROBABILITY OF EXCEEDING SPECIFIED INCREMENTAL CG ACCELERATIONS FOR VARIOUS RMS GUST VELOCITIES

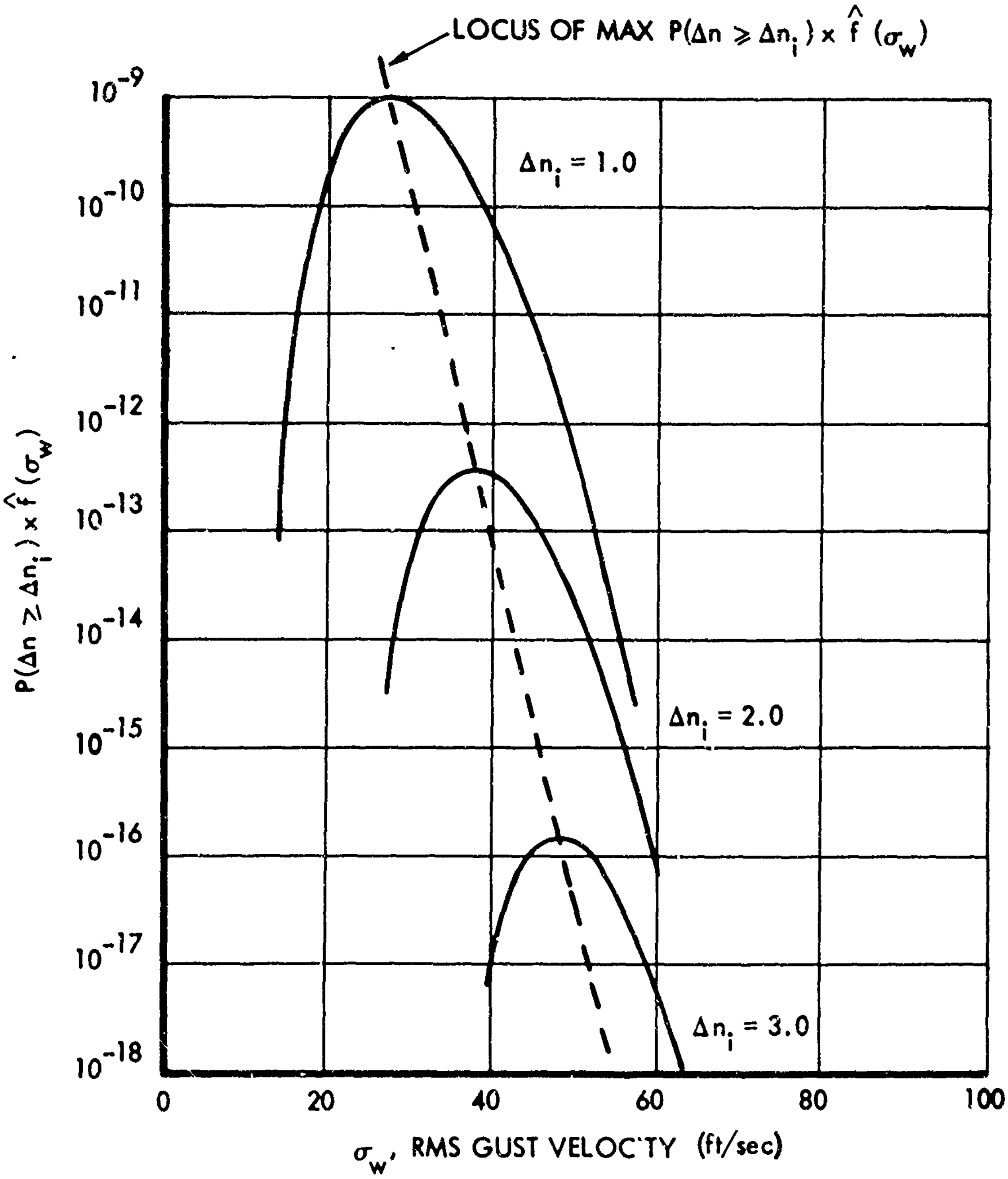

FIGURE 18. OVERALL PROBABILITY DENSITIES FOR EXCEEDING SPECIFIC INCREMENTAL CG ACCELERATIONS

$$\sigma_w \eta_d = \frac{\Delta n_i}{\sigma_{\Delta n}} = \frac{1.39}{.0138} = 137 \tag{13}$$

It is obvious that the limit design gust intensity, $\sigma_w \eta_d$, would vary with altitude, since the statistical characteristics of atmospheric turbulence changes with altitude. This variation is accounted for by use of Eq. (14).

$$N(y) = P_1 N_o \, e^{-y/b_1 \bar{A}} + P_2 N_o \, e^{-y/b_2 \bar{A}} \tag{14}$$

When we consider $y/\bar{A}$ to be a limit design gust velocity, $\sigma_w \eta_d$; then, Eq. (14) is rewritten as follows:

$$\frac{N(\sigma_w \eta_d)}{N_o} = P_1 \, e^{-(\sigma_w \eta_d)/b_1} + P_2 \, e^{-(\sigma_w \eta_d)/b_2} \tag{15}$$

$$(\bar{A} = 1.0)$$

The value, $N(\sigma_w \eta_d)/N_o$, is thought of as an <u>exceedance ratio</u>. It is the ratio of the number of gusts exceeding the <u>limit design gust</u> per unit time or distance at a given altitude to the total number of gusts per unit time or distance at that altitude.

The analysis procedure for the Design Envelope Approach was as follows: (1) Determine the lowest allowable values of $\sigma_w \eta_d$ or $\sigma_v \eta_d$ for the major components of the reference airplane, the 720B, (2) Determine the exceedance ratio for the critical elements or components of the airplane for a particular critical altitude, (3) Establish an acceptable exceedance ratio for each altitude from all design envelope analysis conditions. Determine the limit design $\sigma_w \eta_d$ for each altitude.

<u>Statistical Analysis - Flight Profile Approach</u>

The Flight Profile Approach involves the determination of the average number of times per hour that the limit strengths of the more critical structural components or elements are exceeded. The average number of limit strength exceedances is a weighted average number derived from the estimated airline usage of the 720B airplane.

The average number of limit strength exceedances per hour for a given flight condition is established by determining the number of times per foot travelled that the limit strength envelope is perforated or crossed, N_c. It is assumed that the number of limit strength exceedances is equal to one-half the number of perforations of the strength envelope. That is, there is one peak value exceeding limit strength for each two crossings. One-half of the number of strength envelope crossings per foot travelled times the airplane velocity in ft. per sec. times 3,600 sec. per hour gives the number of limit strength exceedances per flight hour for a given rms gust intensity σ_W or σ_V. A typical diagram showing the limit strength exceedances per ft. travelled for various rms gust intensities is shown in Fig. 21.

In order to account for the variation in rms gust intensity, the limit strength exceedances per hour is multiplied by the probability density function for rms gust velocity as shown in Fig. 22. The integral of this new probability function over all σ_W is, $\bar{G}$, the expected number of limit strength exceedances per hour. That is,

$$\bar{G} = 1800V \int_0^\infty N_c \, \hat{f}(\sigma_W) d\sigma_W. \qquad (16)$$

The limit strength exceedances per hour for the representative flight profiles is obtained by multiplying the exceedances per hour for each flight condition in the profile by the fraction of the total profile time spent at that condition, and then summing the exceedances per hour for all conditions in the particular profile.

The exceedances per average flight hour for total airplane usage is then determined by weighting the exceedances per hour of each profile by the fraction of total airplane usage represented by the particular profile and then summing over all the profiles. This process is represented by the following equation:

$$N_P = \sum_k \left[\sum_j \bar{G}_j \frac{t_j}{t_T} \right] t_k \qquad (17)$$

where

N_P total airplane exceedances per average flight hour

$\bar{G}_j$ exceedances per hour for a particular flight condition

$N_c/2$, EXCEEDANCES OF LIMIT DESIGN STRENGTH PER FT

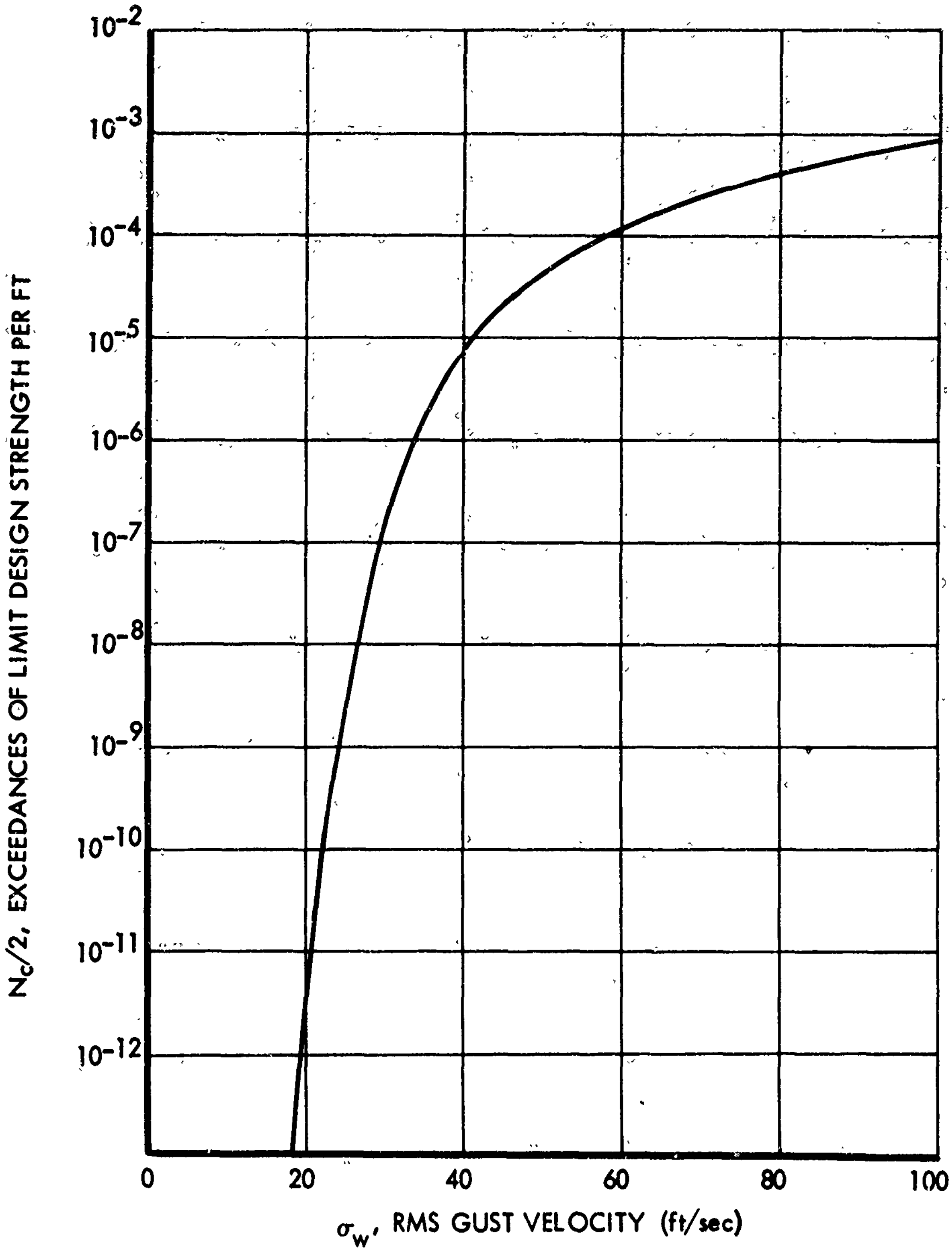

FIGURE 21. EXCEEDANCES OF LIMIT DESIGN STRENGTH PER FT. TRAVELED

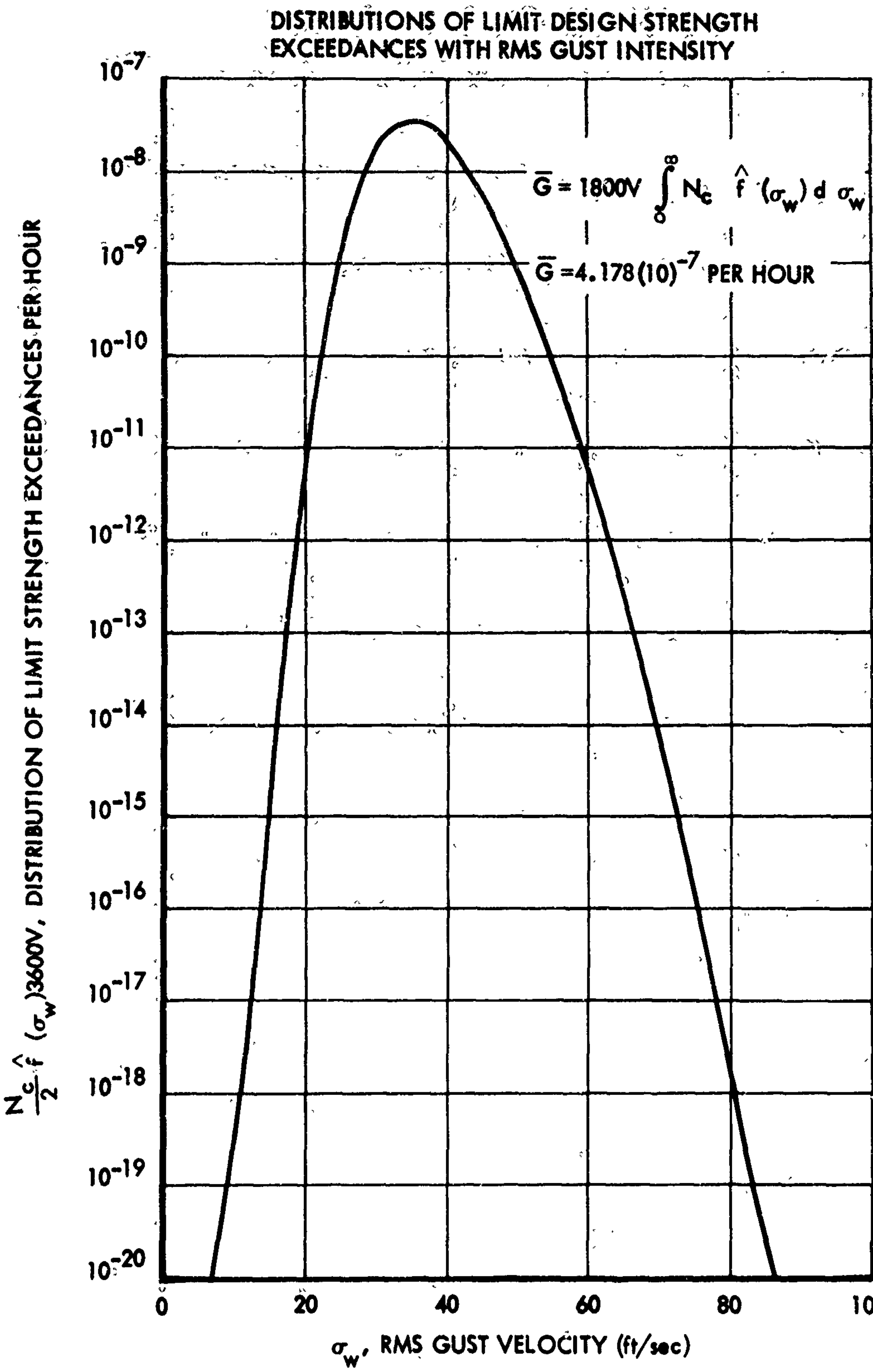

FIGURE 22. DISTRIBUTIONS OF LIMIT DESIGN STRENGTH EXCEEDANCES WITH RMS GUST INTENSITY

t_j	the time spent at a particular flight condition
t_T	the total profile flight time
t_k	fraction of total airplane usage represented by a particular profile
j	the number of conditions in a particular profile
k	the number of profiles used to represent the airplane usage

RESULTS

General Remarks

In the past, airplane power spectral gust analyses results have been used to determine the effects of airplane dynamic responses on the bending moments, shears, and torsions for the major components of an airplane. These incremental loads, usually the wing bending moments, were compared with comparable loads from a static aeroelastic analysis, using the gust load formula, to arrive at a dynamic factor. Then, the dynamic factor was applied to other aeroelastic solutions to obtain design incremental loads for all gust design conditions.

The basic results of a power spectral analysis, the rms loads, $\bar{A}$, and the number of times these loads cross their mean values with positive (or negative) slope per sec. or per ft., N_0, are not in themselves adequate to assess airplane strength. However, the bending moments, shears, and torsions, and the incremental cg accelerations do provide insight into an airplane dynamic responses in rough air, and can be used as guides to ascertain critical locations in the airplane structure. Then, the properly phased combined effects of the bending moments, shears, and torsions should be used to assess the strength at these critical locations.

The rms bending moments, shears, and torsions for the 720B airplane were determined at the locations indicated in Figs. 23 and 24 for the vertical and lateral analyses, respectively. The combined effects of vertical and lateral gust loads were studied for two locations on the aft fuselage, Body Balance Stations 1000 and 1280. Stress analyses were conducted for the most critical locations on the wing, fuselage, and the vertical tail. These locations consisted of one wing location, Wing Station 360 at Body Buttock Line 260 or 33 percent of the wing semi-span ($\eta = .33$). The stresses were studied for three body locations, Body Balance Stations 480, 1000, and 1280. One location on the vertical tail, Fin Station 165.5, Elastic Axis (EA) Station 158 was investigated.

Correlation of Dynamic and Aeroelastic Analyses

The total loads and stresses that were used to assess the airplane strength resulted from the incremental dynamic loads and the one-factor level flight loads. The level flight loads were obtained from aeroelastic solutions,[6,7] and the incremental dynamic loads were obtained from power spectral analysis. In order to determine if these two independent solutions represented the airplane in a consistent manner, the one-factor level flight loads were obtained for one analysis condition, Condition 1, using the dynamic analysis equations of motion. This was

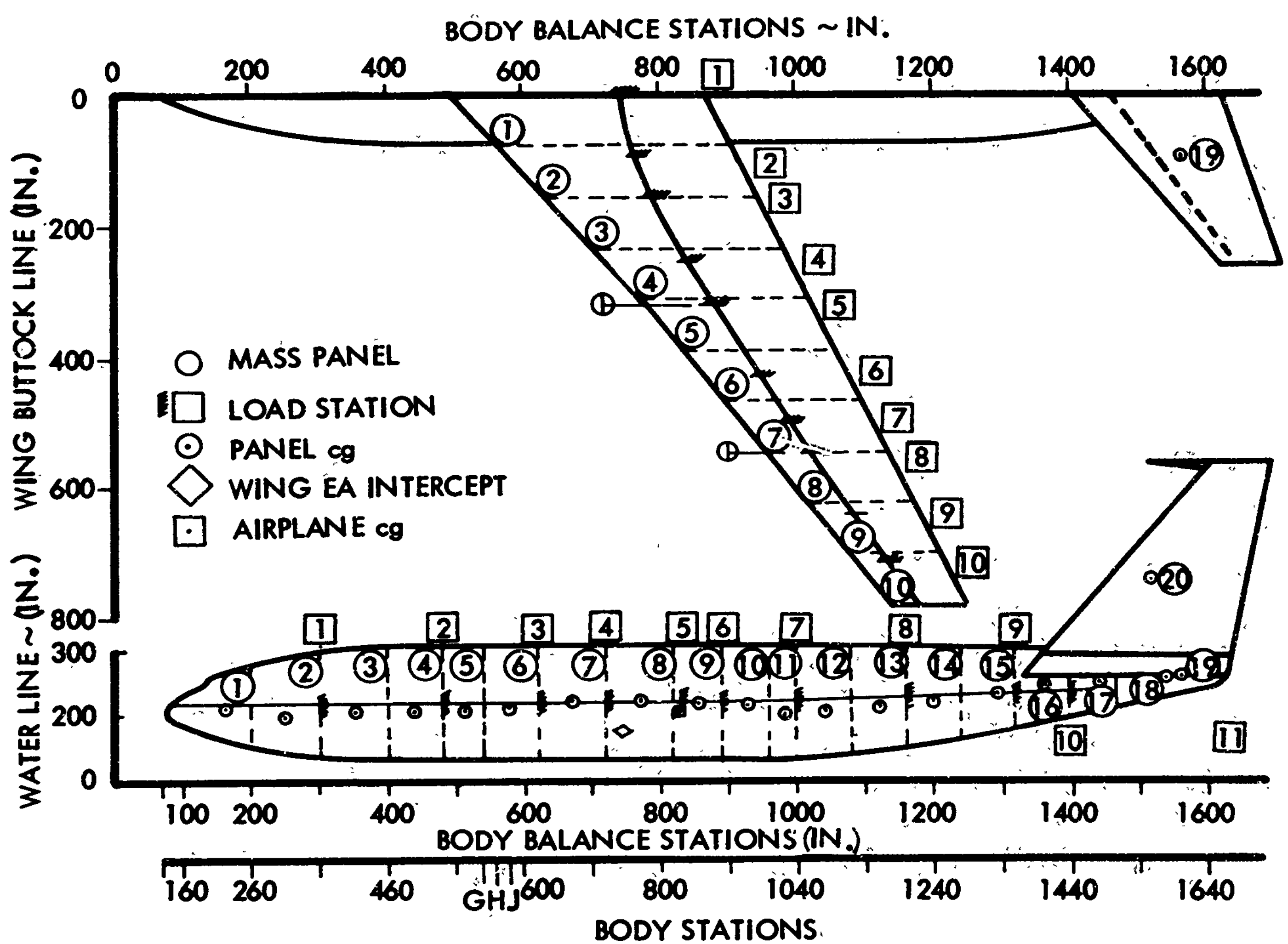

FIGURE 23. MODEL IDEALIZATION - VERTICAL ANALYSES

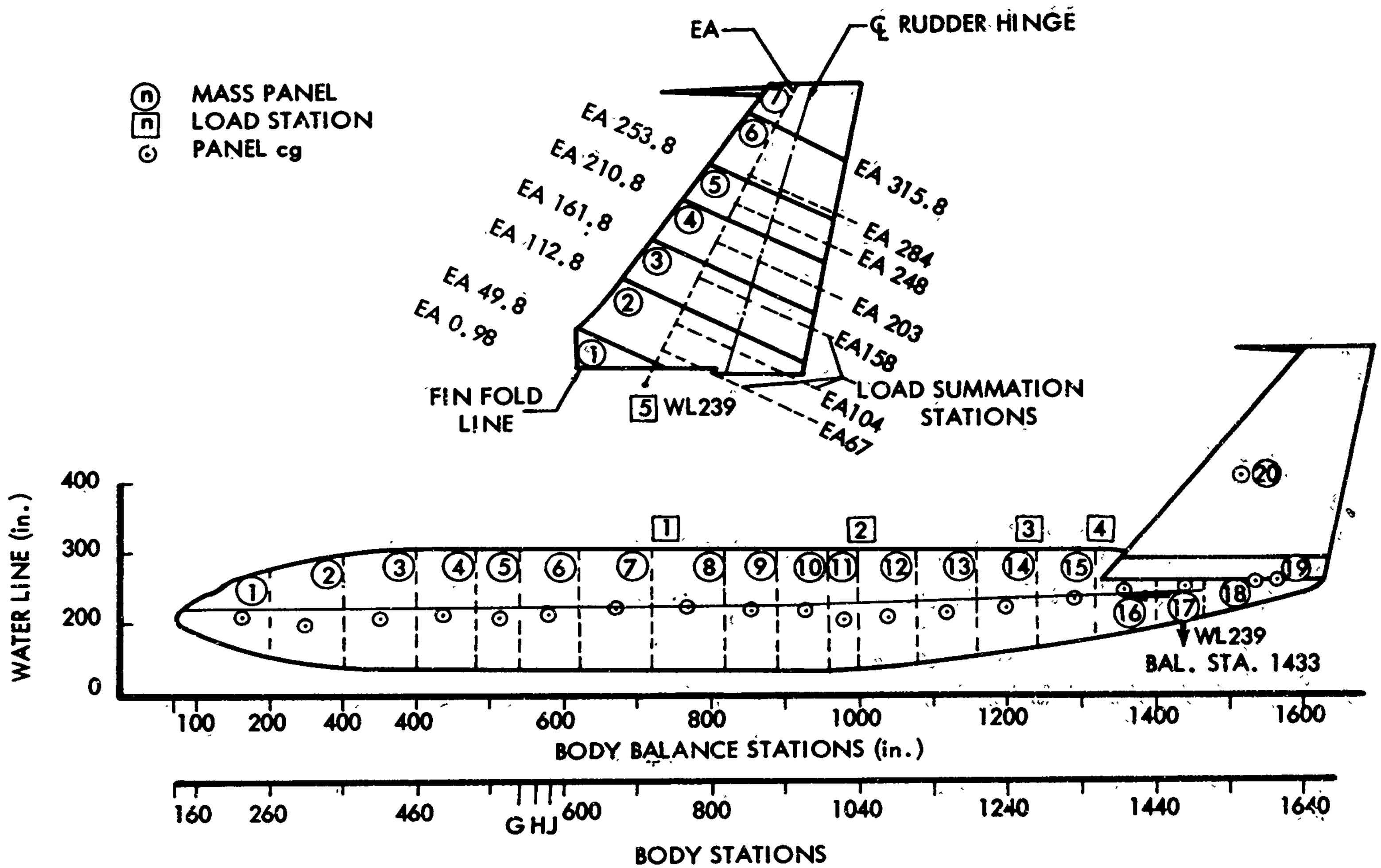

FIGURE 24. MODEL IDEALIZATION - LATERAL ANALYSIS

accomplished by setting the pitch and flexible generalized coordinate accelerations, the pitch and translation displacements, and all of the generalized coordinate velocities equal to zero. The vertical translation acceleration was set at 1.0g. In order to allow for a force balance in the vertical translation equation and a moment balance in the pitch equation, two unknowns were introduced to replace the airplane pitch and translation displacement freedoms. One of the unknowns was the angle of attack which gives rise to the lift necessary to offset the airplane weight plus the balancing tail load. The other unknown was the horizontal tail load which must balance the airplane pitching moments.

The wing bending moments, shears, and torsions, and the wing static deflections resulting from the reduced dynamic solution were obtained to compare with corresponding values from the aeroelastic solution. The aeroelastic wing loads shown in this comparison were obtained by subtracting a zero load factor solution from a one-factor solution. The comparison is made on the basis of a static incremental one-factor load. The results in Fig. 25 show the wing bending deflections obtained from the two solutions. The wing bending moment, shear, and torsion loads are compared in Fig. 26. The angle of attack required for level flight was 4.27 degrees for the reduced dynamic solution and 4.32 for the aeroelastic solution.

Frequency Response Functions

The equations of motion were solved to obtain steady state complex frequency response functions for the generalized coordinates due to 1.0 ft. per sec. sinusoidal gust excitation. Examples of the modulus of these frequency response functions for the Vertical Analyses, Condition 24, are presented in Figs. 27(a) through 27(j). The response quantities are identified as q_1 through q_7 for the seven free-free airplane symmetrical modes and q_T, q_P and q_X for the rigid airplane freedoms of vertical translation, pitch, and fore and aft translation, respectively. These frequency response functions illustrate the predominate responses for each individual generalized coordinate, and indicate the coupling that exists between the coordinates. The frequency response curve for airplane pitch, Fig. 27(i), shows the well damped airplane short period or pitch mode at 0.36 cps; 0.028 rad. per ft. The airplane pitch response has a large effect on the airplane loads, because of the high energy in atmospheric turbulence within this frequency range.

Typical generalized coordinate response curves for the lateral analyses, Conditions 10 and 10YD, are shown in Fig. 28(a) through 28(i) both with and without the yaw damper operating. The Dutch roll response at 0.20 cps or 0.0015 rad. per ft. is the major contributor to the lateral loads. Thus, the changes which effect the Dutch roll response have a large effect

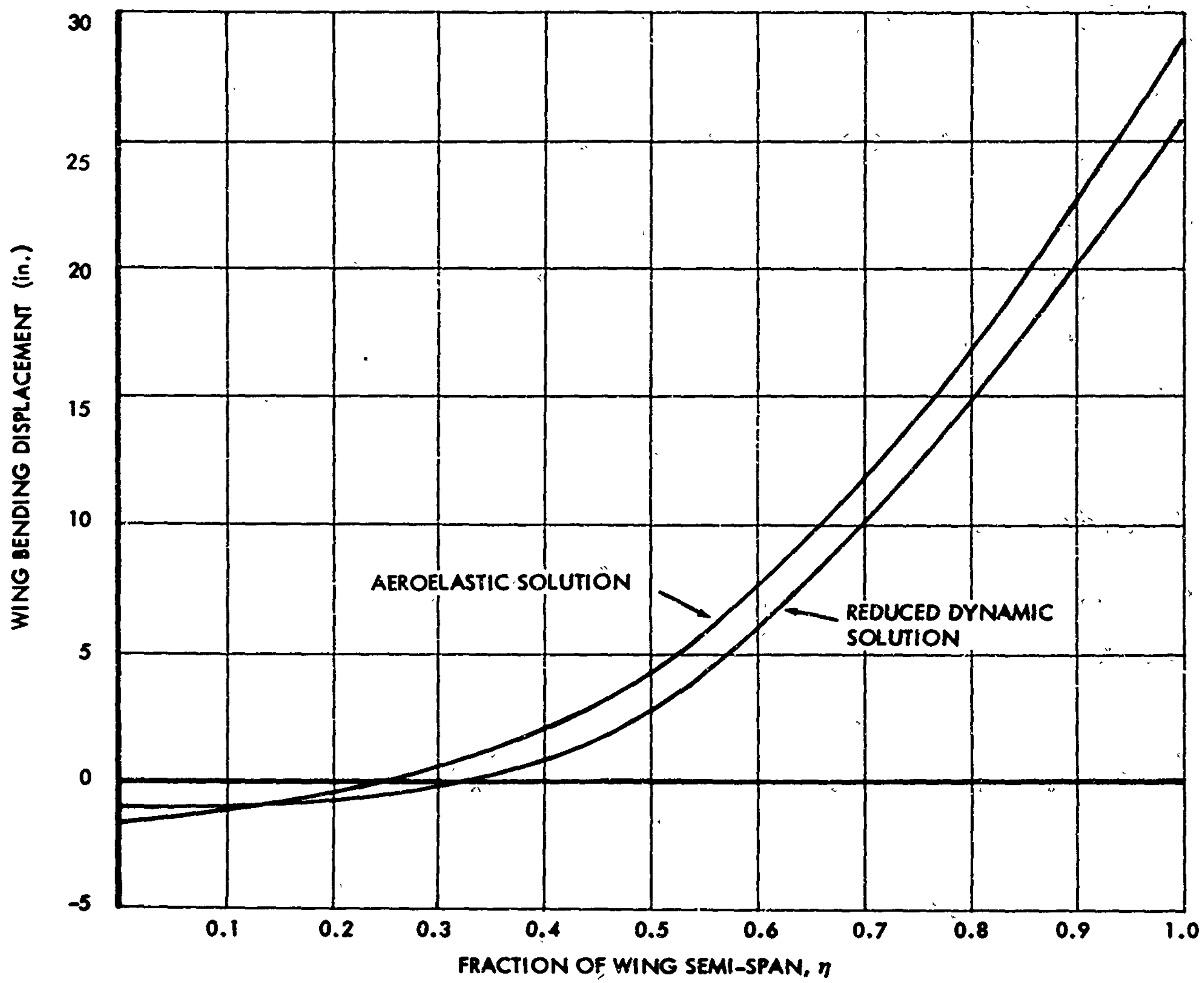

FIGURE 25. COMPARISON OF WING DEFLECTIONS FOR AEROELASTIC AND REDUCED DYNAMIC SOLUTIONS

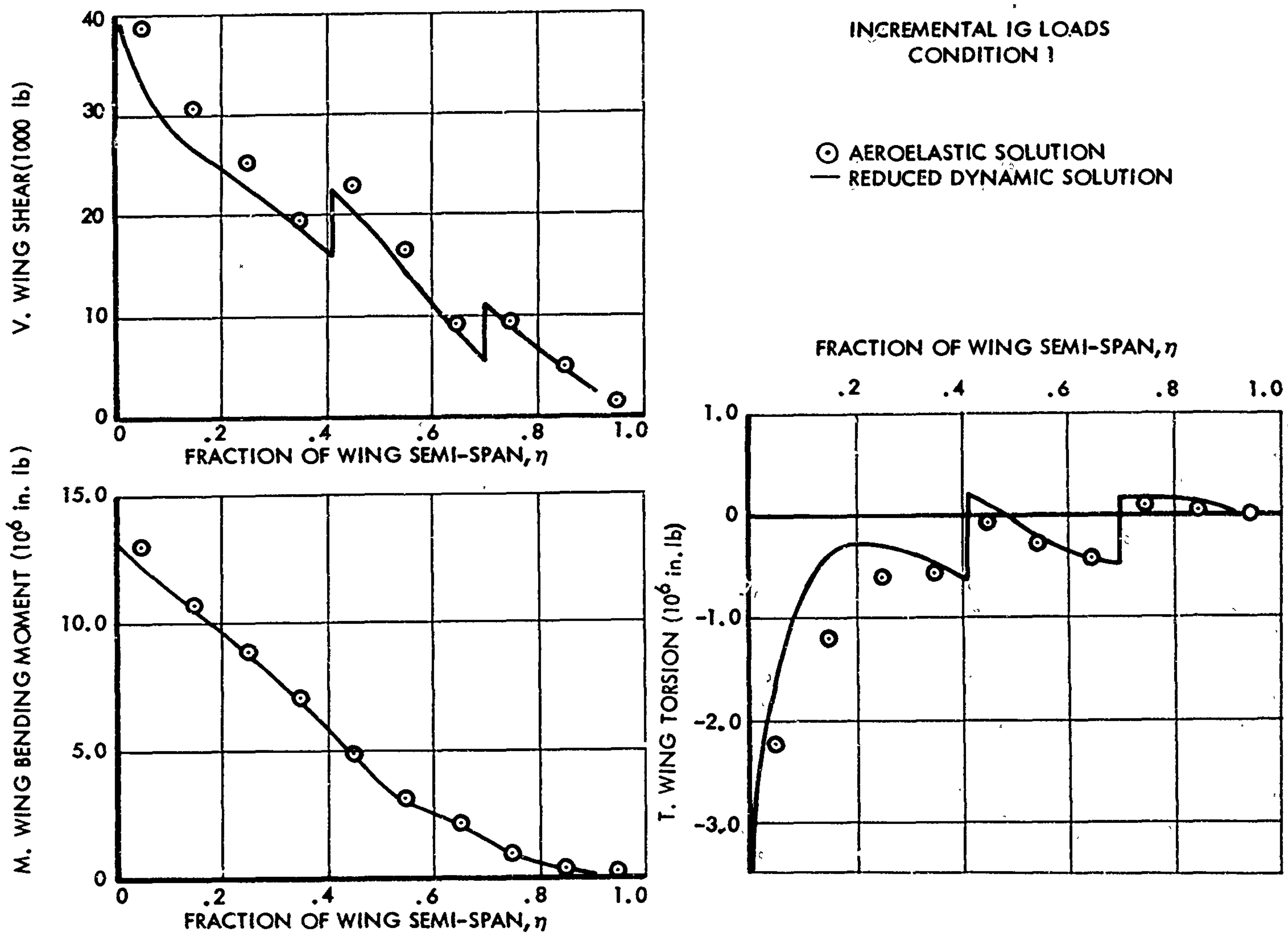

FIGURE 26. COMPARISON OF WING LOADS FOR AEROELASTIC AND REDUCED DYNAMIC SOLUTIONS

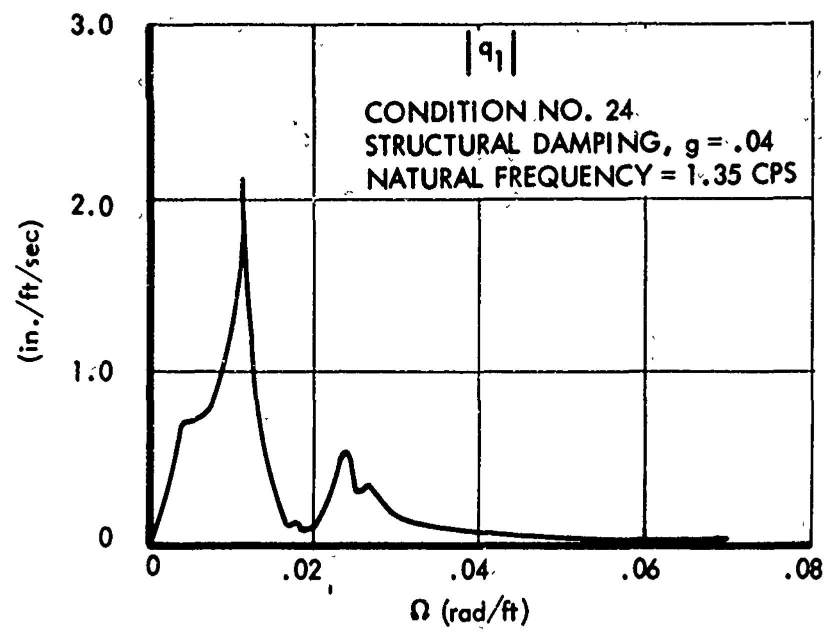

FIGURE 27a. FREQUENCY RESPONSE, FIRST SYMMETRICAL AIRPLANE MODE

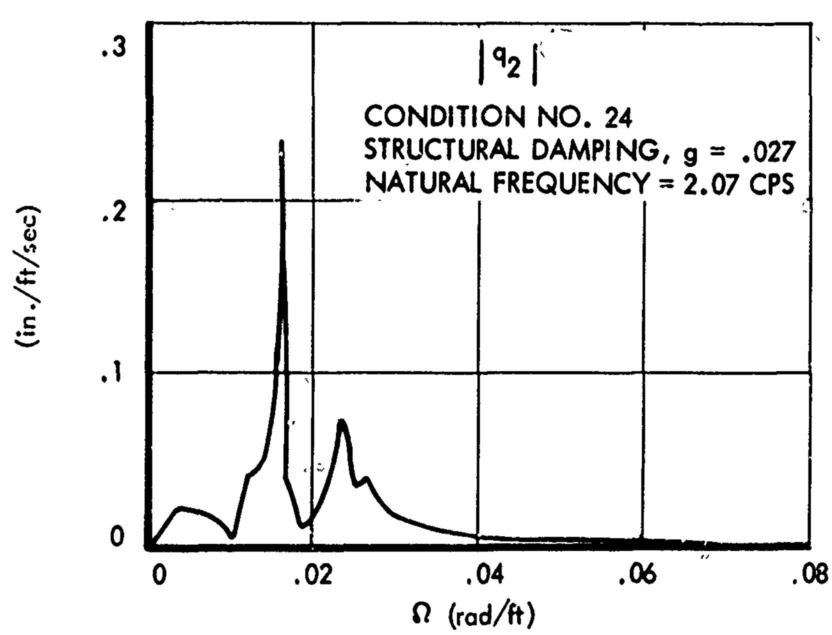

FIGURE 27b. FREQUENCY RESPONSE, SECOND SYMMETRICAL AIRPLANE MODE

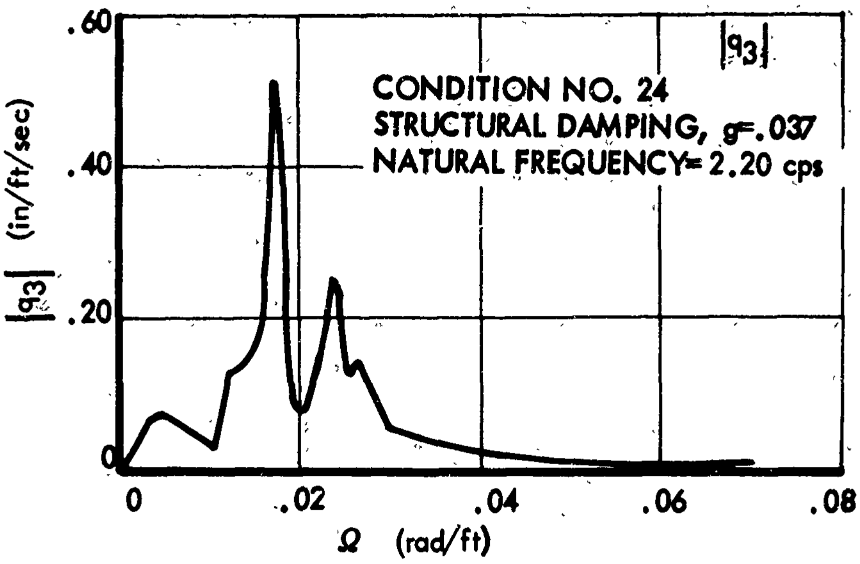

FIGURE 27c. FREQUENCY RESPONSE, THIRD SYMMETRICAL AIRPLANE MODE

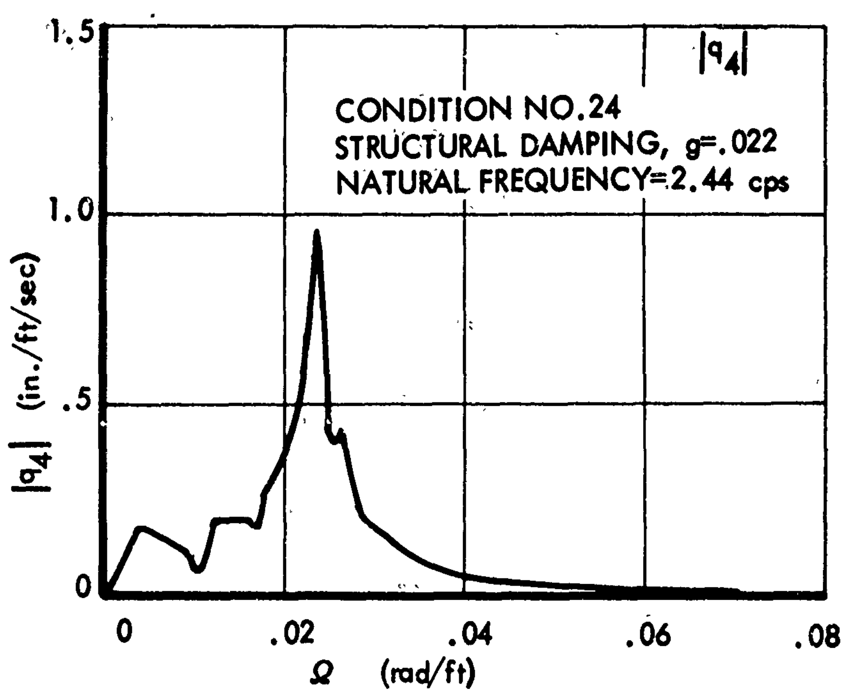

FIGURE 27d. FREQUENCY RESPONSE, FOURTH SYMMETRICAL AIRPLANE MODE

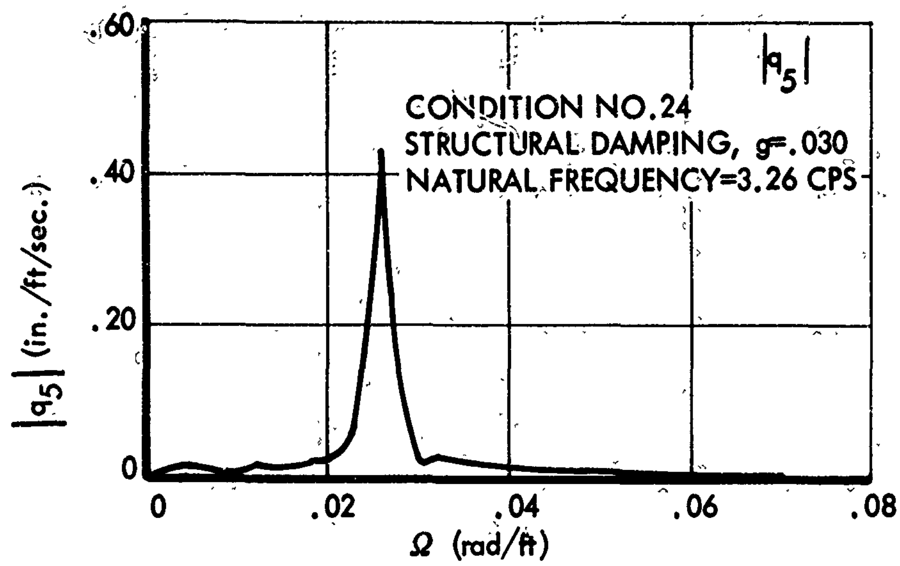

FIGURE 27e. FREQUENCY RESPONSE, FIFTH SYMMETRICAL AIRPLANE MODE

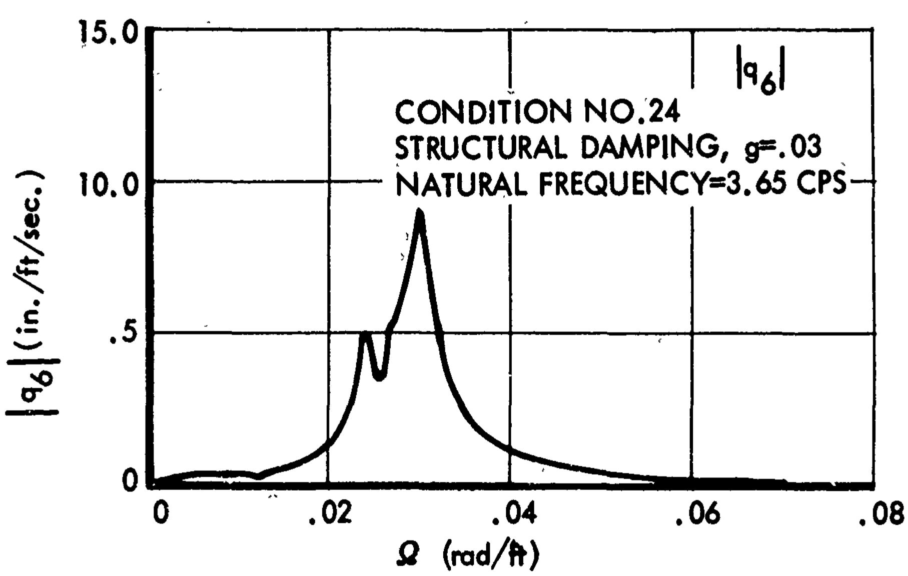

FIGURE 27f. FREQUENCY RESPONSE, SIXTH SYMMETRICAL AIRPLANE MODE

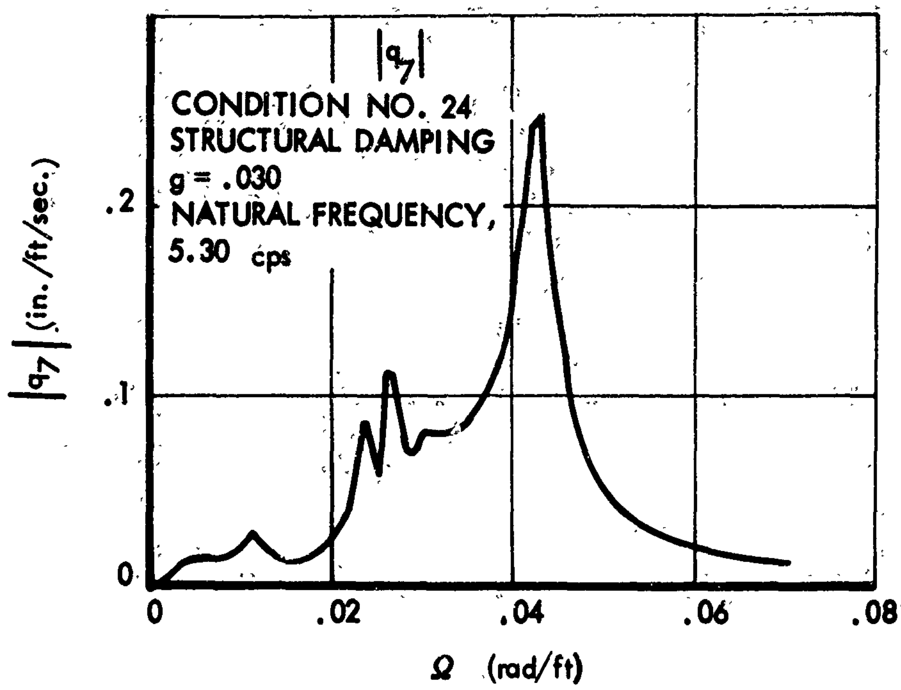

FIGURE 27g. FREQUENCY RESPONSE, SEVENTH SYMMETRICAL AIRPLANE MODE

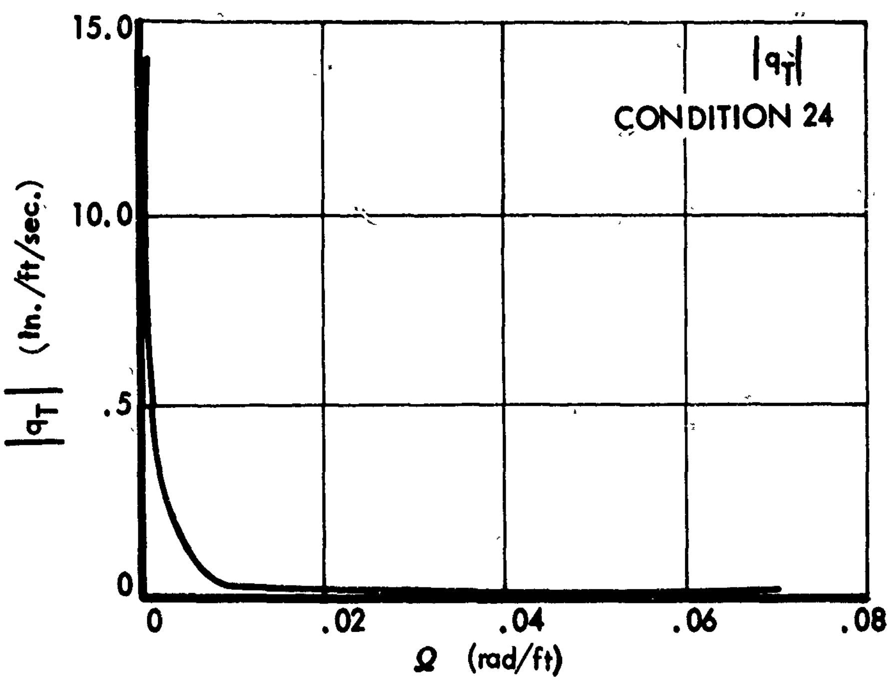

FIGURE 27h. FREQUENCY RESPONSE, AIRPLANE VERTICAL TRANSLATION

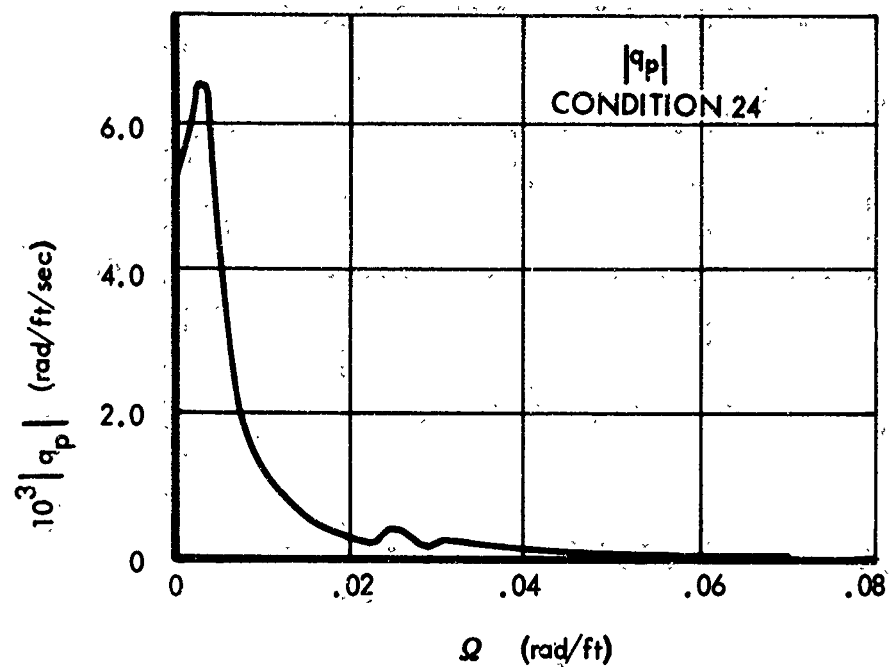

FIGURE 27i. FREQUENCY RESPONSE, AIRPLANE PITCH

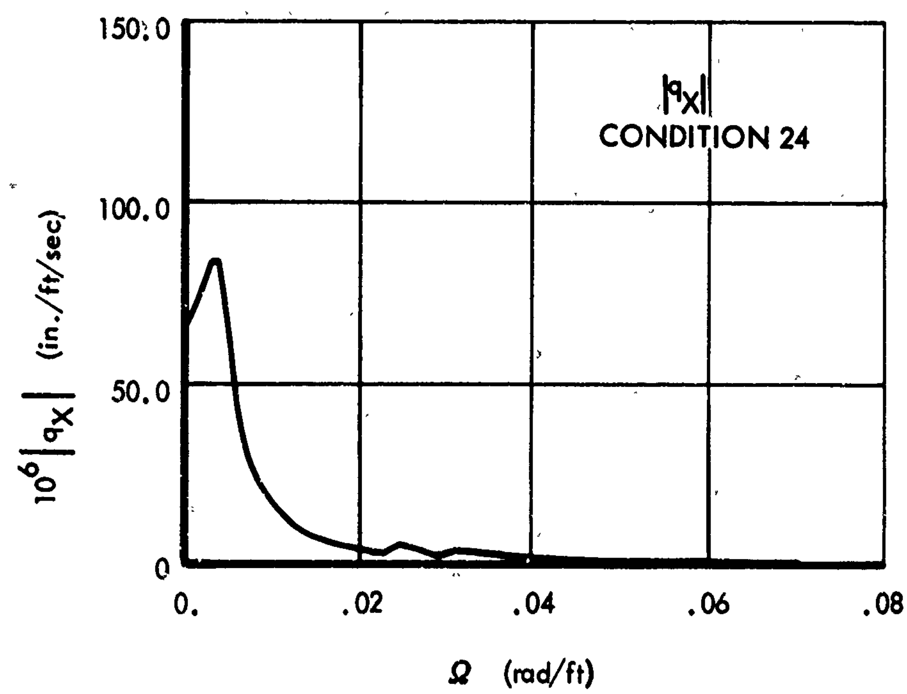

FIGURE 27j. FREQUENCY RESPONSE, AIRPLANE FORE AND AFT TRANSLATION

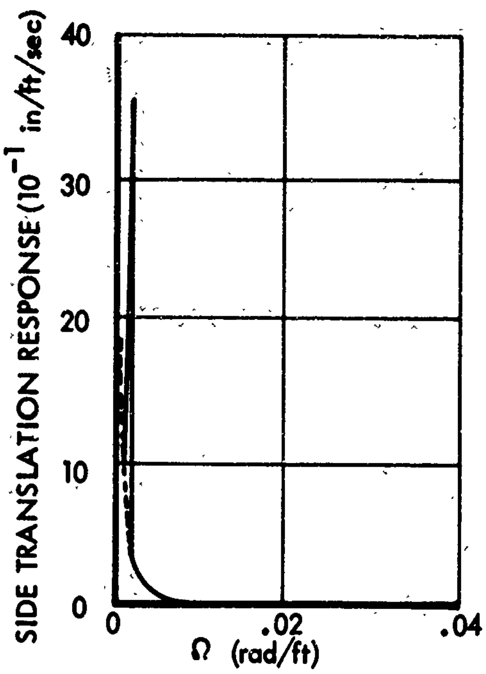

FIGURE 28a. FREQUENCY RESPONSE, AIRPLANE SIDE TRANSLATION

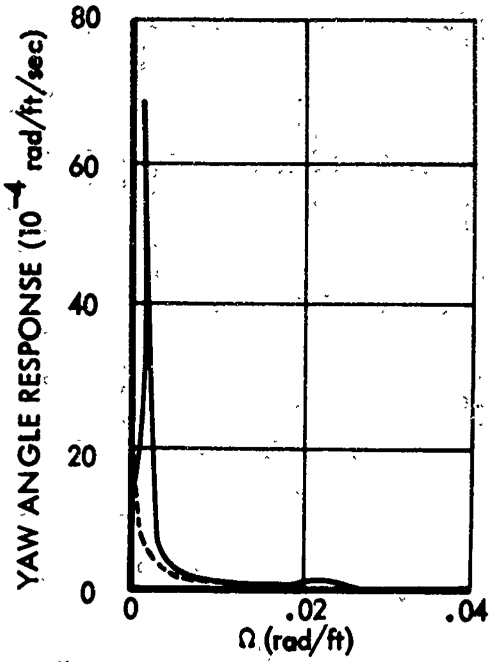

FIGURE 28b. FREQUENCY RESPONSE, AIRPLANE YAW

NOTE:

------------ YAW DAMPER ON

———— YAW DAMPER OFF

CONDITION 10, 10 YD

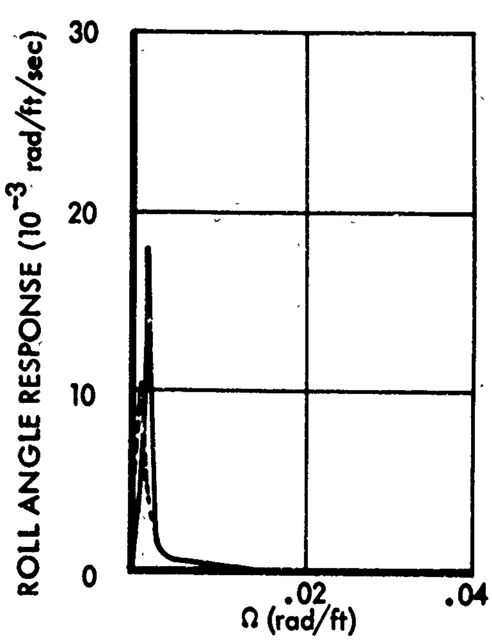

FIGURE 28c. FREQUENCY RESPONSE, AIRPLANE ROLL

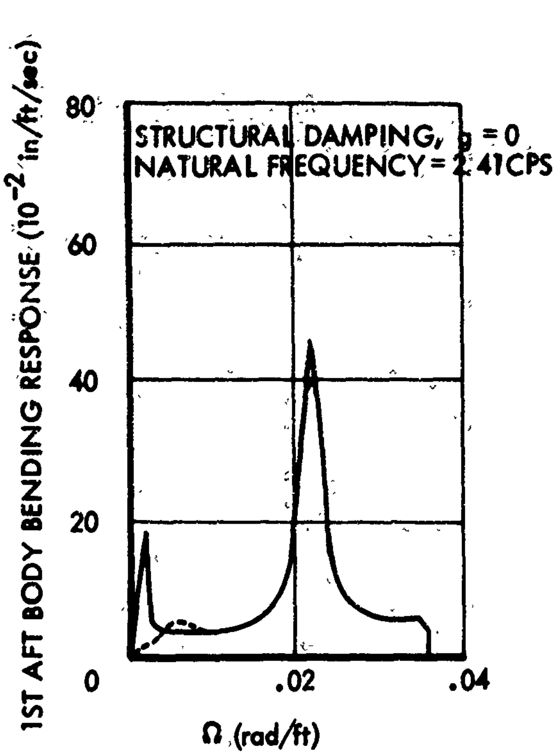

FIGURE 28d. FREQUENCY RESPONSE, FIRST CANTILEVERED AFT BODY SIDE BENDING MODE

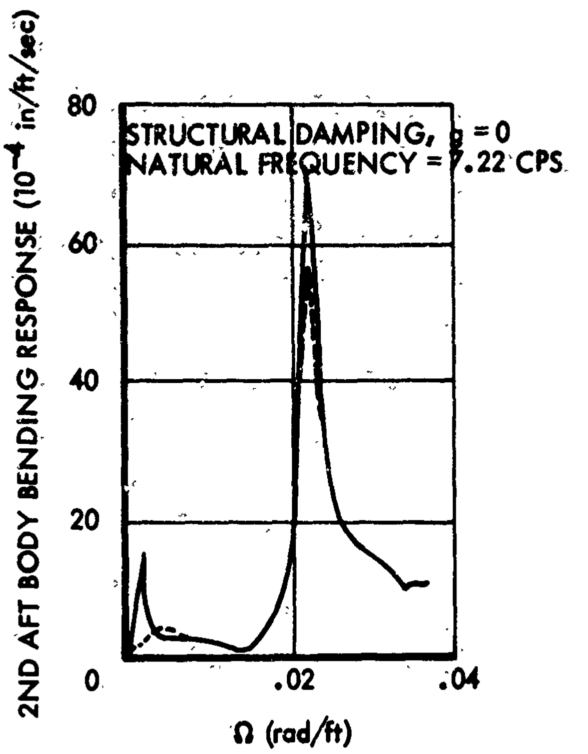

FIGURE 28e. FREQUENCY RESPONSE, SECOND CANTILEVERED AFT BODY SIDE BENDING MODE

NOTE:

------------ YAW DAMPER ON

———————— YAW DAMPER OFF

CONDITION 10, 10 YD

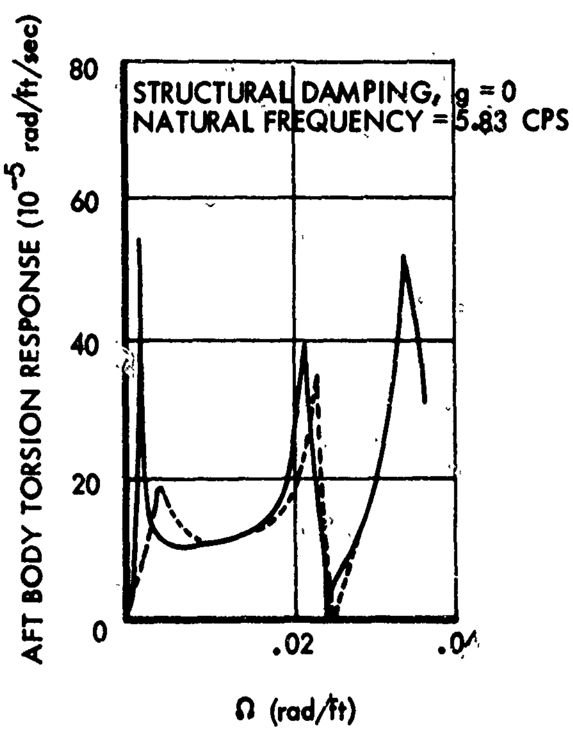

FIGURE 28f. FREQUENCY RESPONSE, FIRST CANTILEVERED AFT BODY TORSION MODE

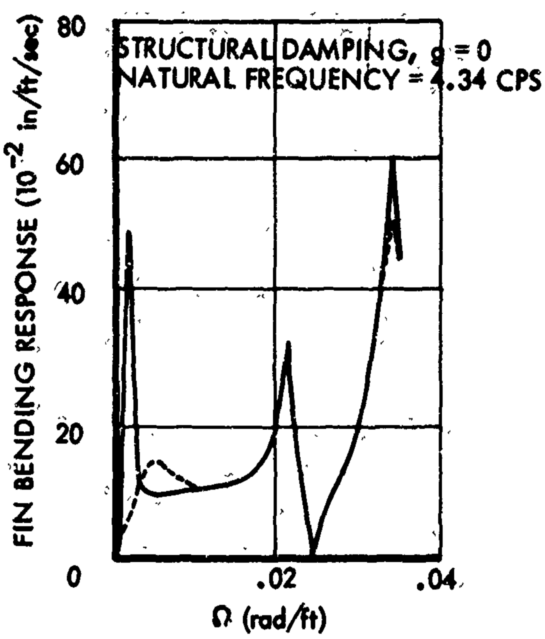

FIGURE 28g. FREQUENCY RESPONSE, FIRST CANTILEVERED FIN BENDING MODE

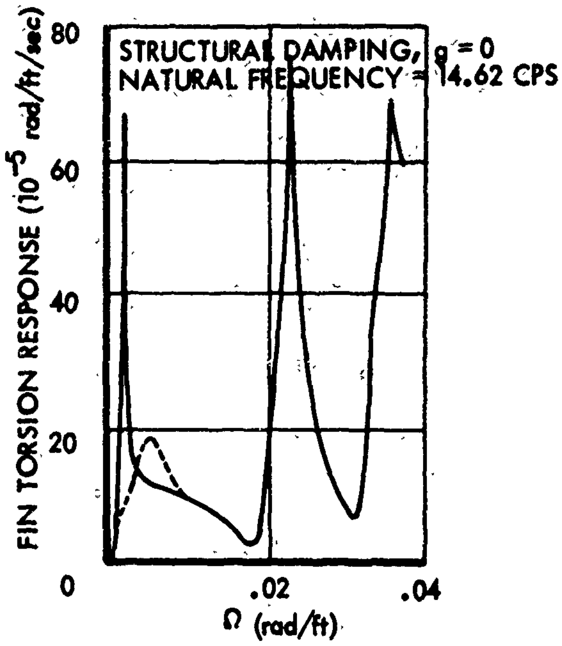

FIGURE 28h. FREQUENCY RESPONSE, FIRST CANTILEVERED FIN TORSION MODE

NOTE:

--------- YAW DAMPER ON

———— YAW DAMPER OFF

CONDITION 10, 10 YD

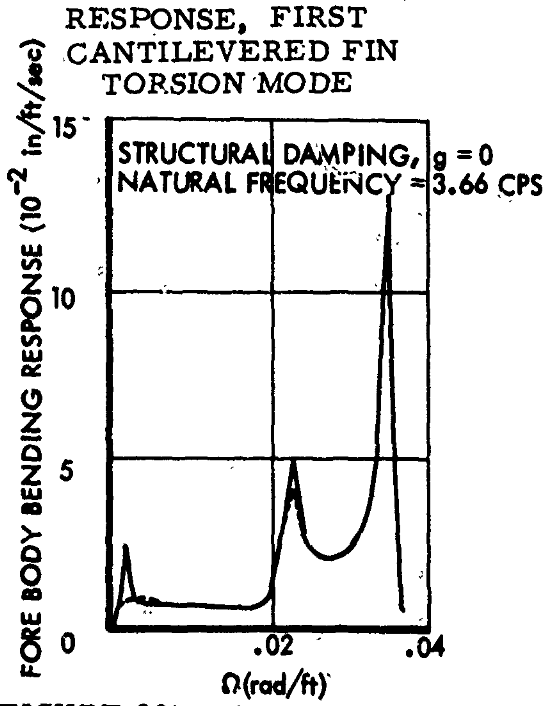

FIGURE 28i. FREQUENCY RESPONSE, FIRST FORE BODY CANTILEVERED SIDE BENDING

on magnitudes of the lateral loads. When the yaw damper is engaged, the rudder is commanded by the yaw damper servo system and will deflect in a manner to provide positive damping in the Dutch roll mode. The results of the yaw damper operation is readily apparent. By observing the decrease in the rigid airplane yaw response not only are the frequency response functions for the rigid airplane motions attenuated, but the frequency at which the maximum response occurs is reduced. This is reasonable, because at the Dutch roll frequency, 0.07 cps, the phase shift through the yaw damper system causes the rudder displacement to lead the yaw rate signal. This results in a rudder deflection that reduces the fin aerodynamic force due to yawing displacement which, in turn, causes a reduced Dutch roll resonant frequency.

The coupling between the flexible modes and the Dutch roll mode occurs at a higher frequency with the autopilot engaged. This may seem to contradict the effect evidenced by the rigid airplane response; however, this difference does exist, and there is a logical explanation. The explanation again lies with the phasing of the rudder deflection caused by the yaw damper output. In this case, the frequency, .63 cps, 0.0046 rad. per ft., is such that the rudder displacement lags the yaw rate signal; therefore, the rudder deflection adds to the fin aerodynamic force. This increase in force results in a larger flexible mode excitation at this frequency. As the response frequency increases toward a structural resonance frequency the cut-off filter in the yaw damper amplifier system attenuates the yaw damper output so that self-excitation will not occur.

Complex frequency responses for the loads were obtained by substituting the complex generalized coordinate responses into the airplane load equations. These load equations sum the incremental inertia loads, the airloads resulting from the coordinate responses, and the applied gust loading. Fig. 29 shows the load responses for Vertical Analyses, Condition 24, for wing bending moment, shear, and torsion at the most critical wing station, Wing Eta Station 0.33. Similar load frequency response functions are shown for Wing Eta Station 0.12. Fuselage vertical shear and bending moment frequency responses at the critical forward body station, Body Station 540 and at Aft Body Station 1360, are shown in Fig. 30.

Fig. 31 gives the vertical tail load frequency responses for lateral analysis Conditions 10 and 10YD. These frequency responses are for vertical tail bending moment, shear, and torsion at the vertical tail Elastic Axis Stations 67 and 158 with and without the yaw damper operating. Fig. 32 shows the lateral bending moment, shear, and torsion frequency response functions for Body Station 1375 with and without the yaw damper operating.

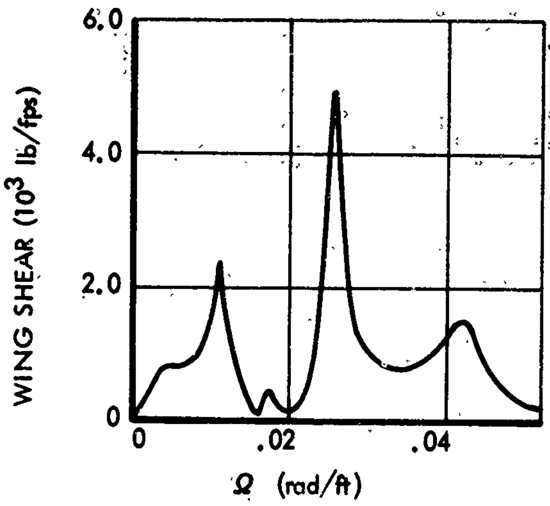

FIGURE 29a. FREQUENCY RESPONSE, WING VERTICAL SHEAR

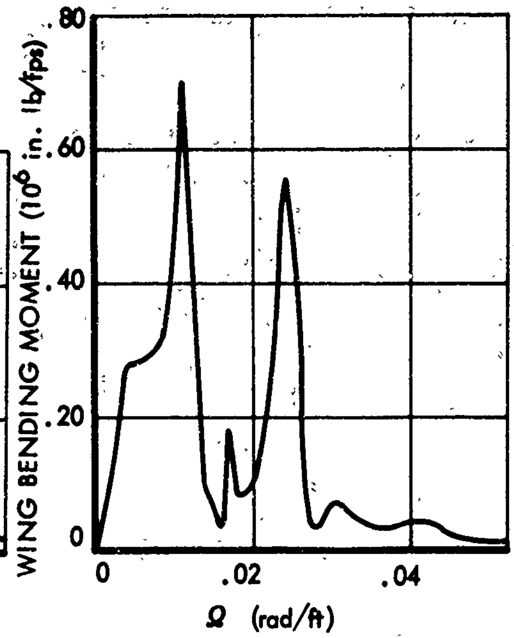

FIGURE 29b. FREQUENCY RESPONSE. WING BENDING MOMENT

NOTE: CONDITION 24 WING STATION, η = 0.33

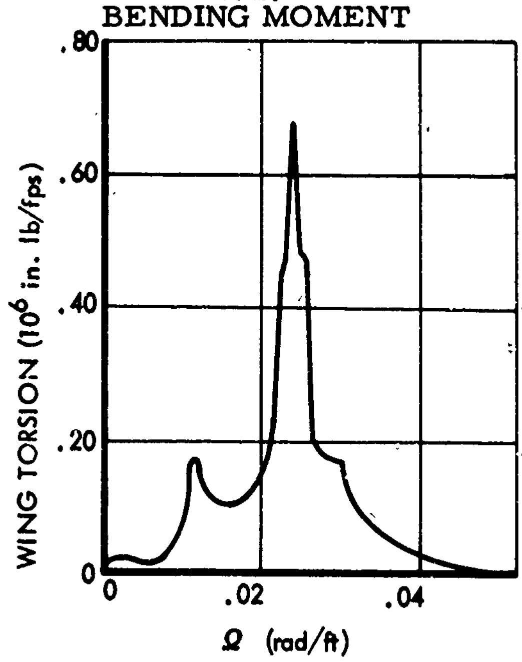

FIGURE 29c. FREQUENCY RESPONSE, WING TORSION

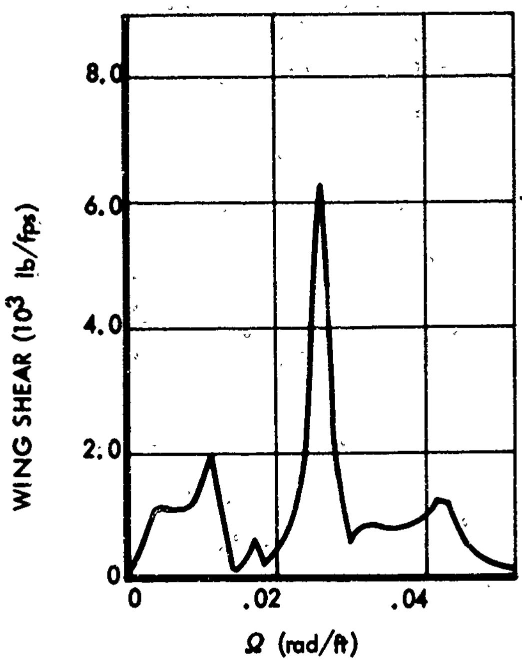

FIGURE 29d. FREQUENCY RESPONSE, WING VERTICAL SHEAR

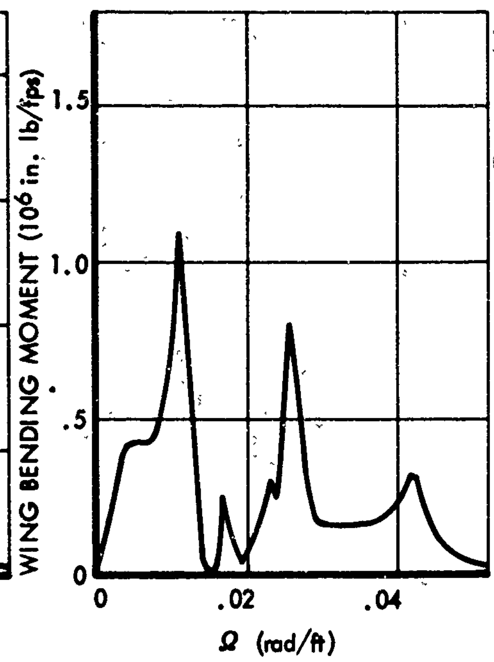

FIGURE 29e. FREQUENCY RESPONSE, WING BENDING MOMENT

NOTE: CONDITION 24 WING STATION $\eta = 0.12$

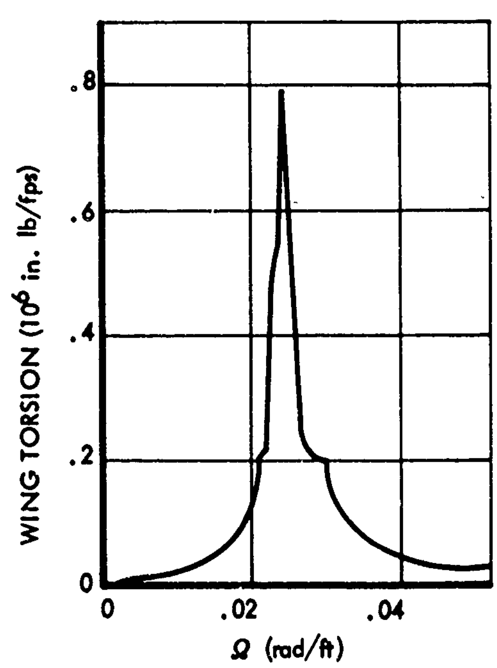

FIGURE 29f. FREQUENCY RESPONSE, WING TORSION

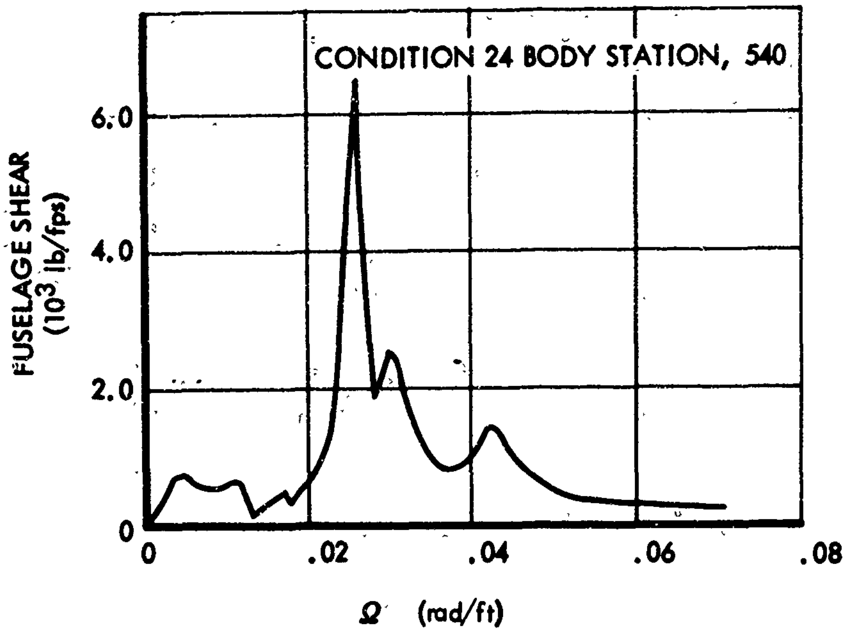

FIGURE 30a. FREQUENCY RESPONSE, FUSELAGE VERTICAL SHEAR

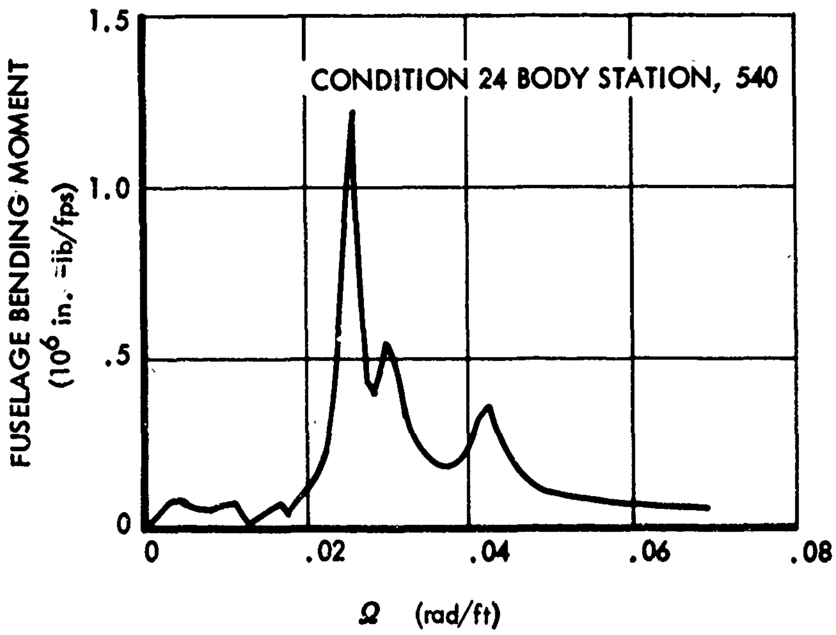

FIGURE 30b. FREQUENCY RESPONSE, FUSELAGE VERTICAL BENDING MOMENT

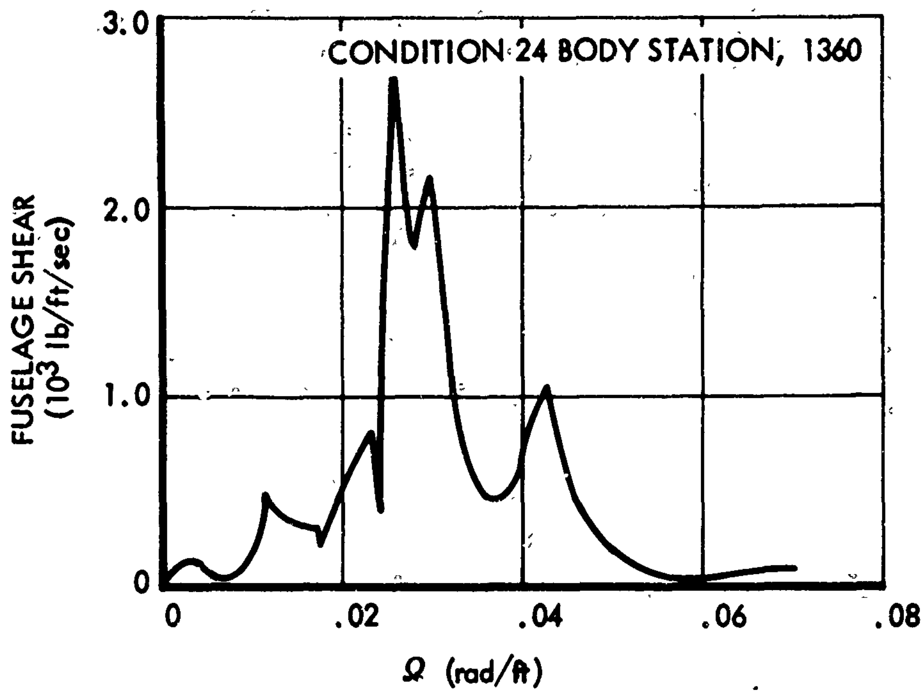

FIGURE 30c. FREQUENCY RESPONSE, FUSELAGE VERTICAL SHEAR

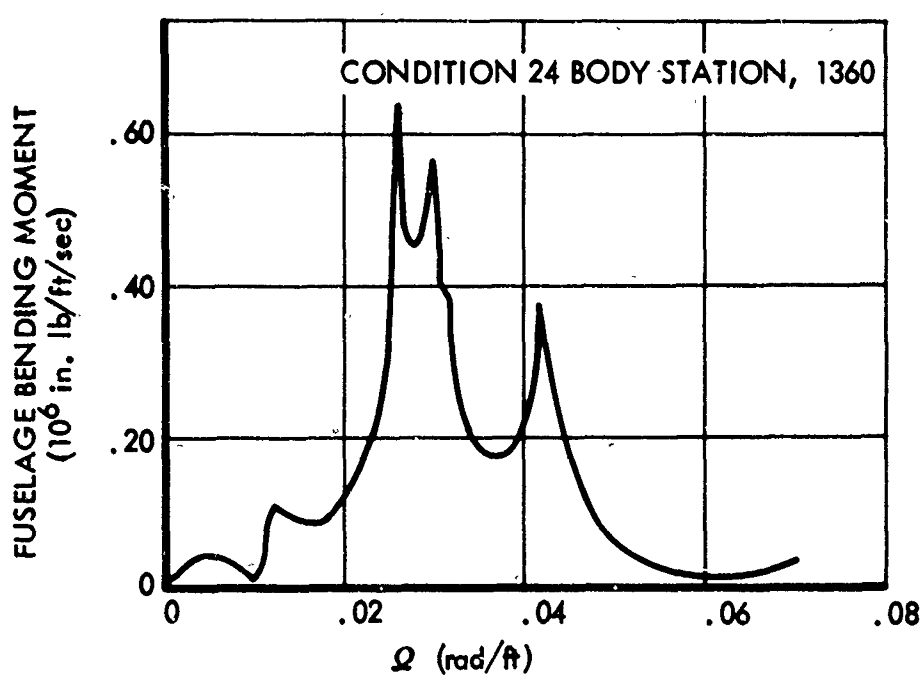

FIGURE 30d. FREQUENCY RESPONSE, FUSELAGE VERTICAL BENDING MOMENT

IEAR

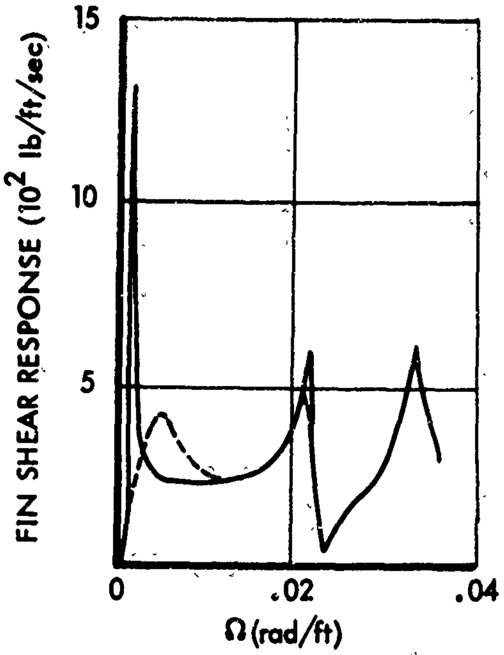

FIGURE 31a. FREQUENCY RESPONSE, FIN SHEAR

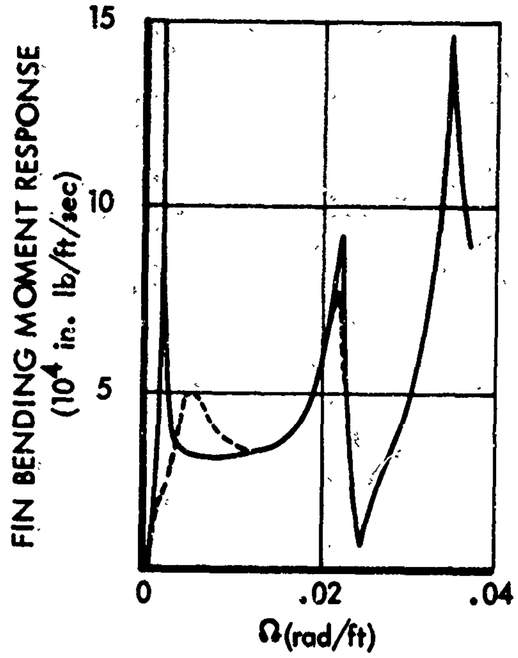

FIGURE 31b. FREQUENCY RESPONSE, FIN BENDING MOMENT

NOTE:

---------- YAW DAMPER ON

———— YAW DAMPER OFF

CONDITION 10, 10 YD
FIN ELASTIC AXIS
STA. 67

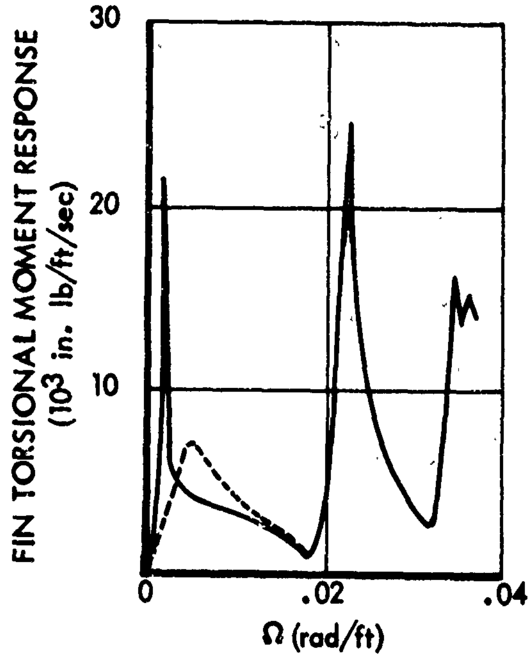

FIGURE 31c. FREQUENCY RESPONSE, FIN TORSION

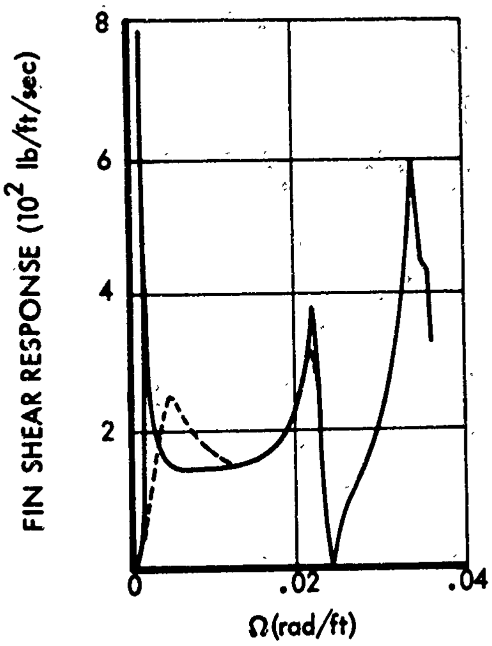

FIGURE 31d. FREQUENCY RESPONSE, FIN SHEAR

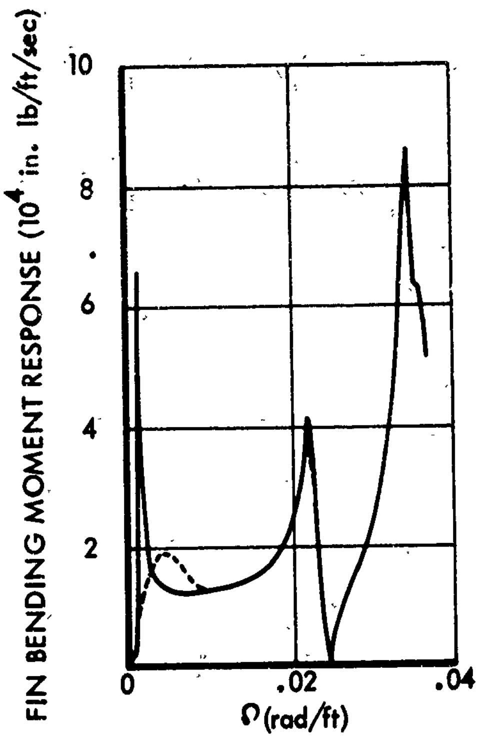

FIGURE 31e. FREQUENCY RESPONSE, FIN TORSION

NOTE

- - - - - - - - YAW DAMPER ON

———————— YAW DAMPER OFF

CONDITION 10, 10 YD
FIN E.A. STA. 158

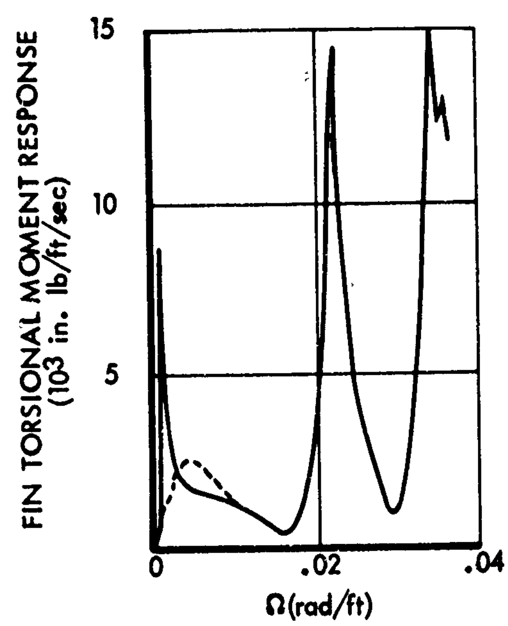

FIGURE 31f. FREQUENCY RESPONSE, FIN BENDING MOMENT

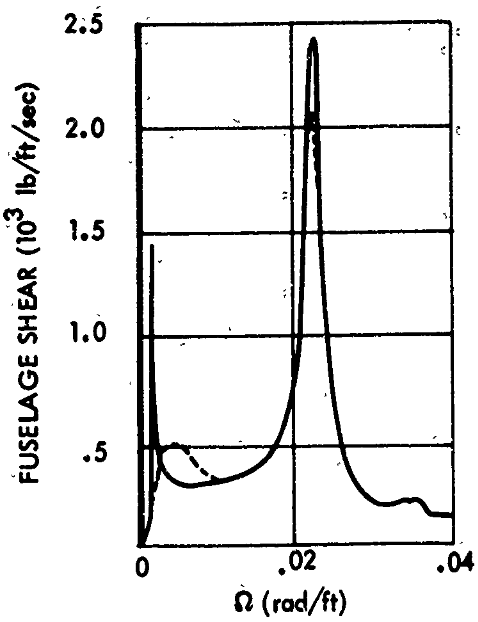

FIGURE 32a. FREQUENCY RESPONSE, FUSELAGE LATERAL SHEAR

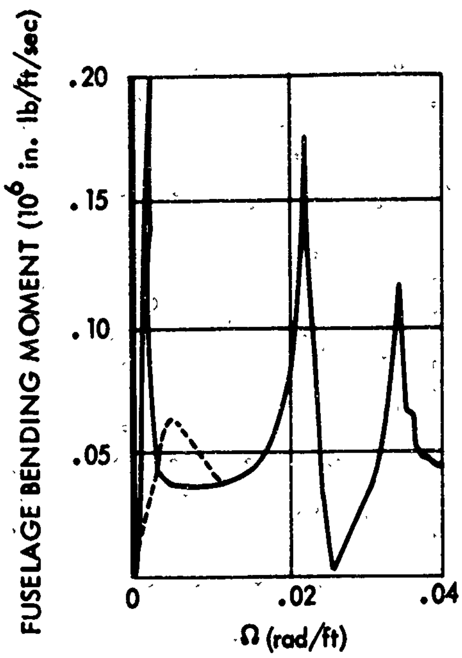

FIGURE 32b. FREQUENCY RESPONSE, FUSELAGE LATERAL BENDING MOMENT

NOTE

---------- YAW DAMPER ON

———— YAW DAMPER OFF

CONDITION 10, 10 YD
BODY STATION 1375

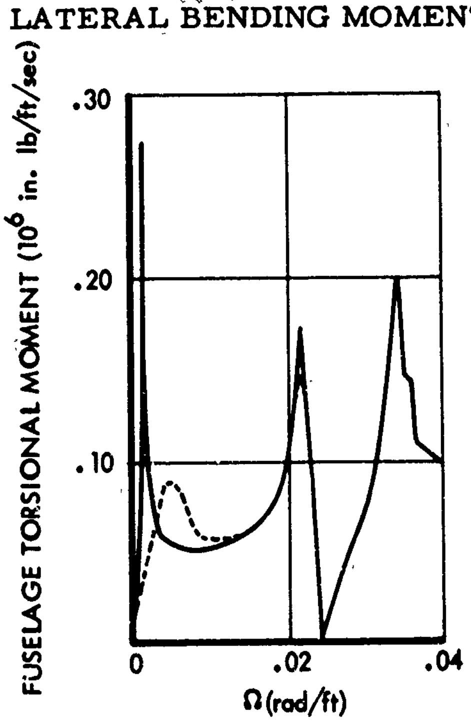

FIGURE 32c. FREQUENCY RESPONSE, FUSELAGE TORSIONAL MOMENT

The major response peaks for the wing loads result from airplane pitch and from the first and fifth flexible modes. This is reasonable, because the first and fifth flexible modes constitute the largest part of the coupled wing bending deflection. The wing torsion loads receive their major responses from the airplane pitch and first and fourth flexible modes, the fourth mode is primarily wing torsion. The second and third flexible modes are predominantly nacelle side bending modes; therefore, they contribute relatively little to the overall wing loads. The fuselage vertical bending moment and shear loads are derived mainly from the fifth flexible airplane mode, which is predominantly fuselage vertical bending.

The primary response for the vertical tail results from the Dutch roll mode; however, when the yaw damper is on the fin and aft body flexible modes become more important. The principal side bending moment, shear, and torsion at Body Balance Station 1360 again results from the Dutch roll response when the yaw damper is off. All of the frequency response functions shown in Figs. 27 through 32 are the modulus of the complex frequency responses. The load frequency response functions were multiplied by the gust power spectra which resulted in output load power spectra. The rms loads were obtained by taking the square root of the area under the load power spectra. Typical variations of the rms load for the wing, fuselage, and vertical tail are shown in Figs. 33, 34, 35 and 36, respectively.

Determination of Critical Flight Conditions and Critical Structure, Vertical Analyses

Initial efforts to arrive at design frequencies of exceedance using the mission profile concept and to arrive at values of $\sigma_w \eta_d$ using the design envelope approach were based on limit allowable bending moments. The use of bending moments alone to estimate allowable limit strength is not exactly correct, because the limit design stresses result from combined loading; therefore, properly combined shear, moment, and torsion loads should be considered. Since the stresses in critical areas are more sensitive to bending moment, and reasonable assumptions are made as to the magnitude and phasing of the associated shear and torsion, it was assumed that the critical structural areas and the critical conditions could be established by a bending moment criteria.

Four weight conditions were analyzed in the vertical analyses for an altitude of 22,000 ft. at the design cruise speed of 375 kt. EAS. The resulting rms wing and body bending moments for a unit rms gust velocity were obtained and divided into the incremental limit allowable bending moments to give allowable values of $\sigma_w \eta_d$. These allowable $\sigma_w \eta_d$ values are plotted in Fig. 37 versus fraction of wing semi-span and in Fig. 38 versus Body Balance Station. It will be noted from Fig. 37 that two

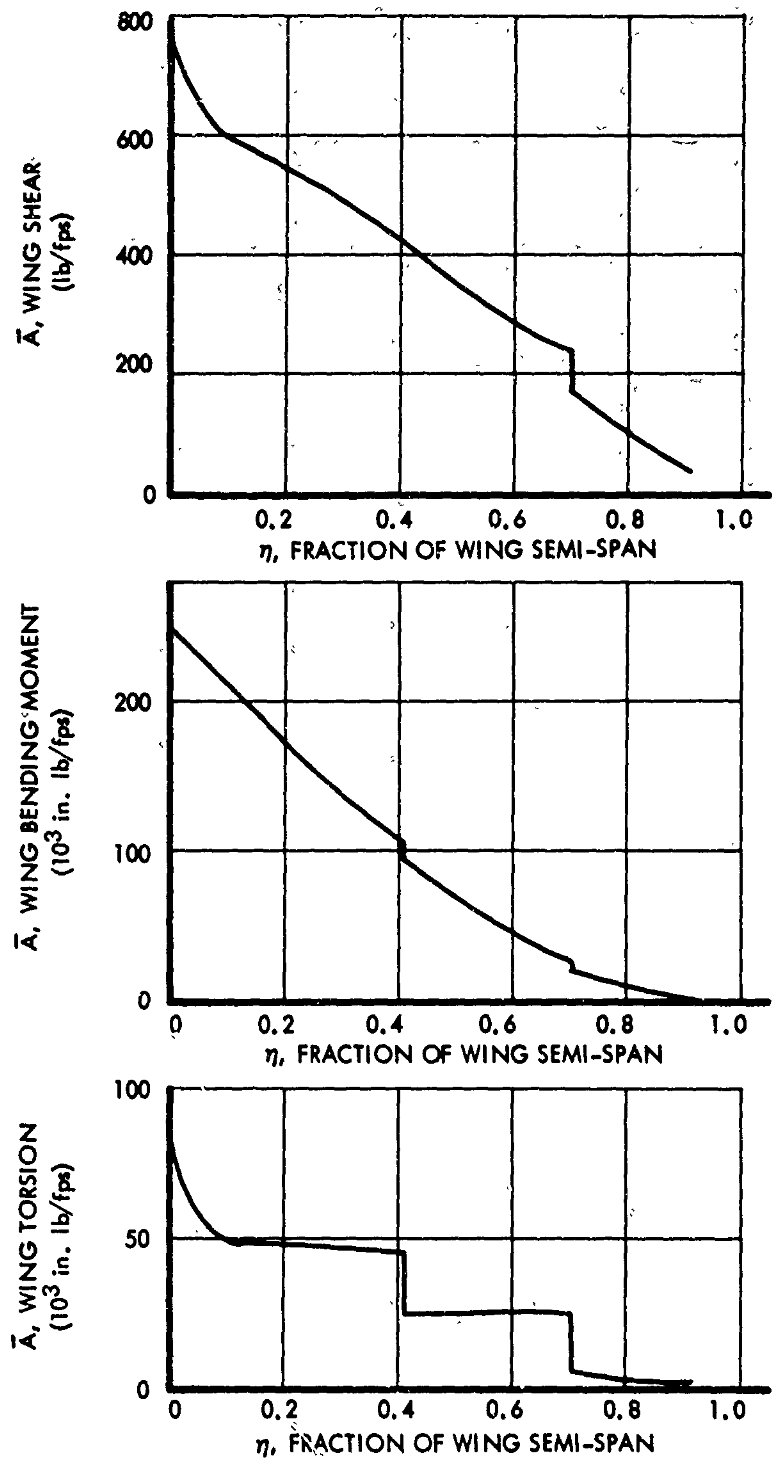

FIGURE 33. DISTRIBUTION OF RMS WING LOADS - CONDITION 24

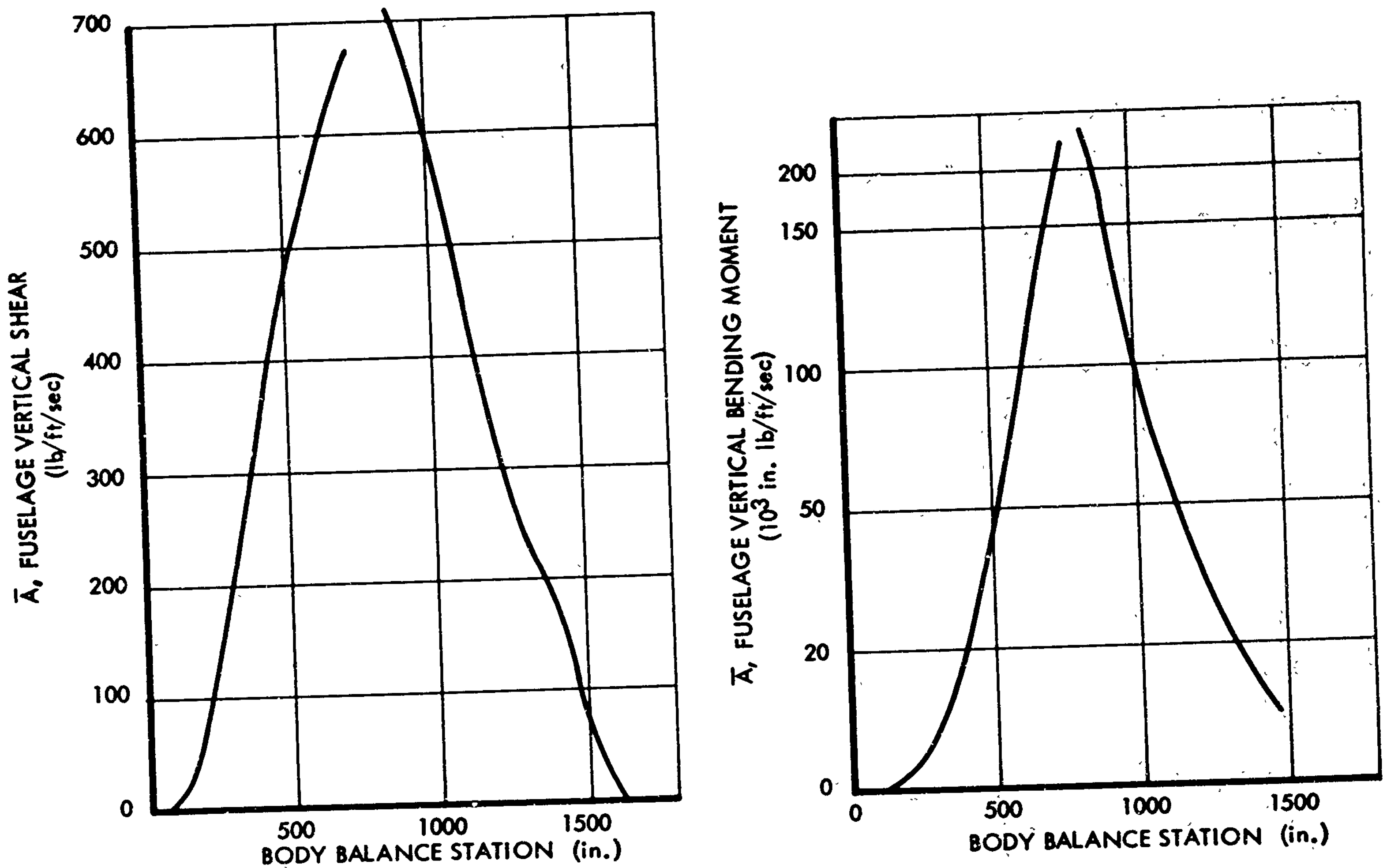

FIGURE 34. DISTRIBUTION OF RMS FUSELAGE LOADS, VERTICAL ANALYSIS - CONDITION 24

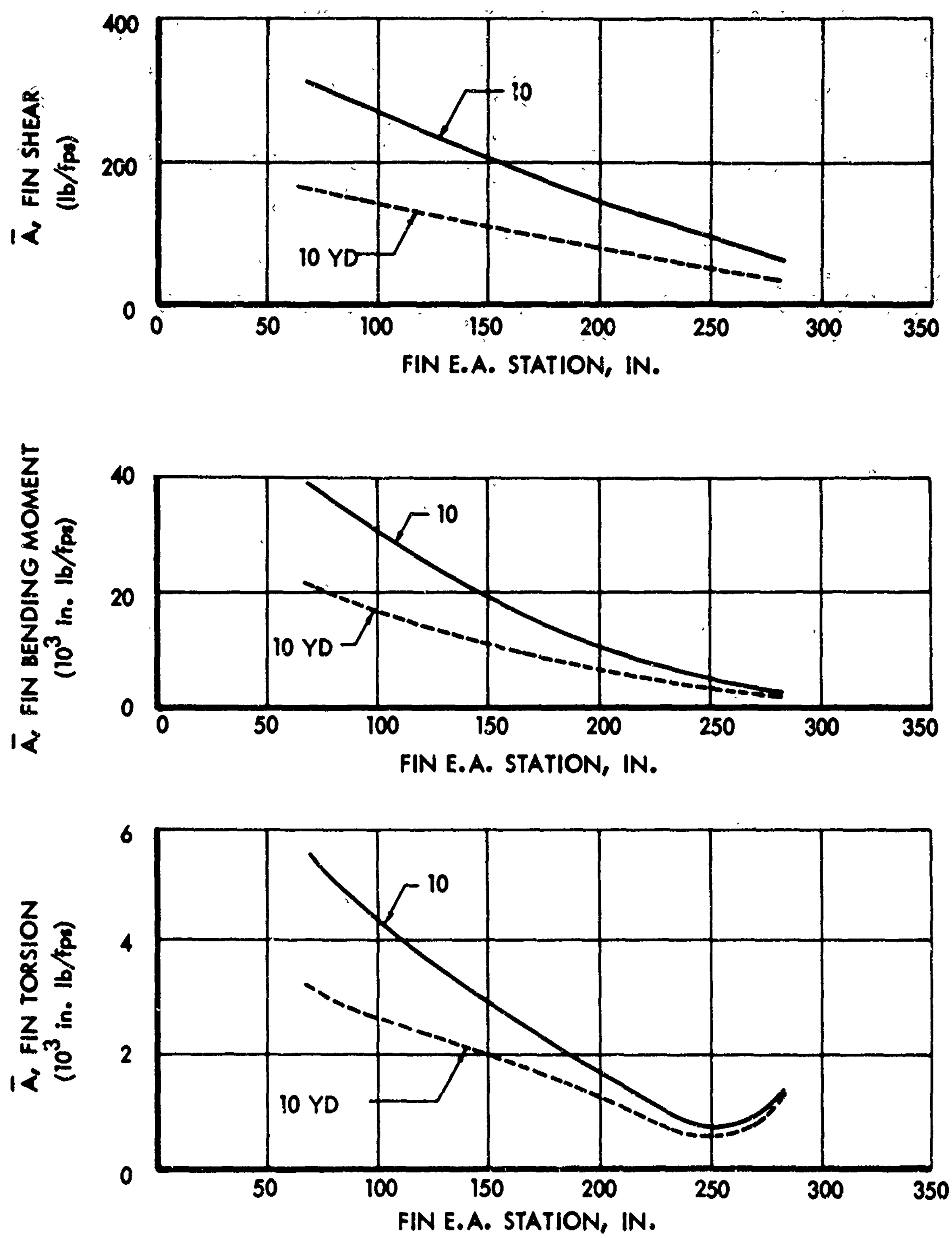

FIGURE 35. DISTRIBUTION OF RMS FIN LOADS - CONDITION 10, 10YD

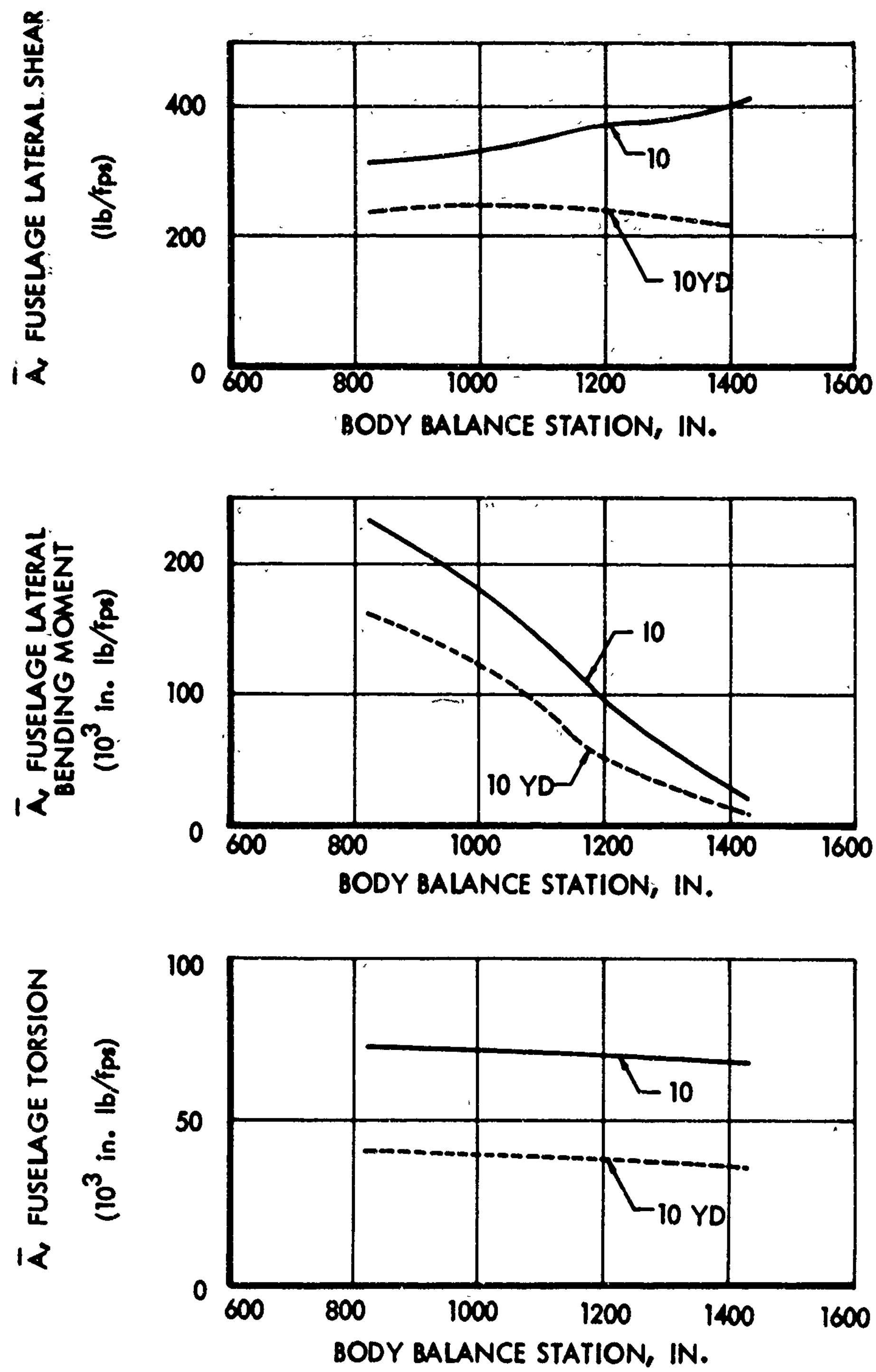

FIGURE 36. DISTRIBUTION OF RMS BODY LOADS, LATERAL ANALYSIS - CONDITION 10, 10YD

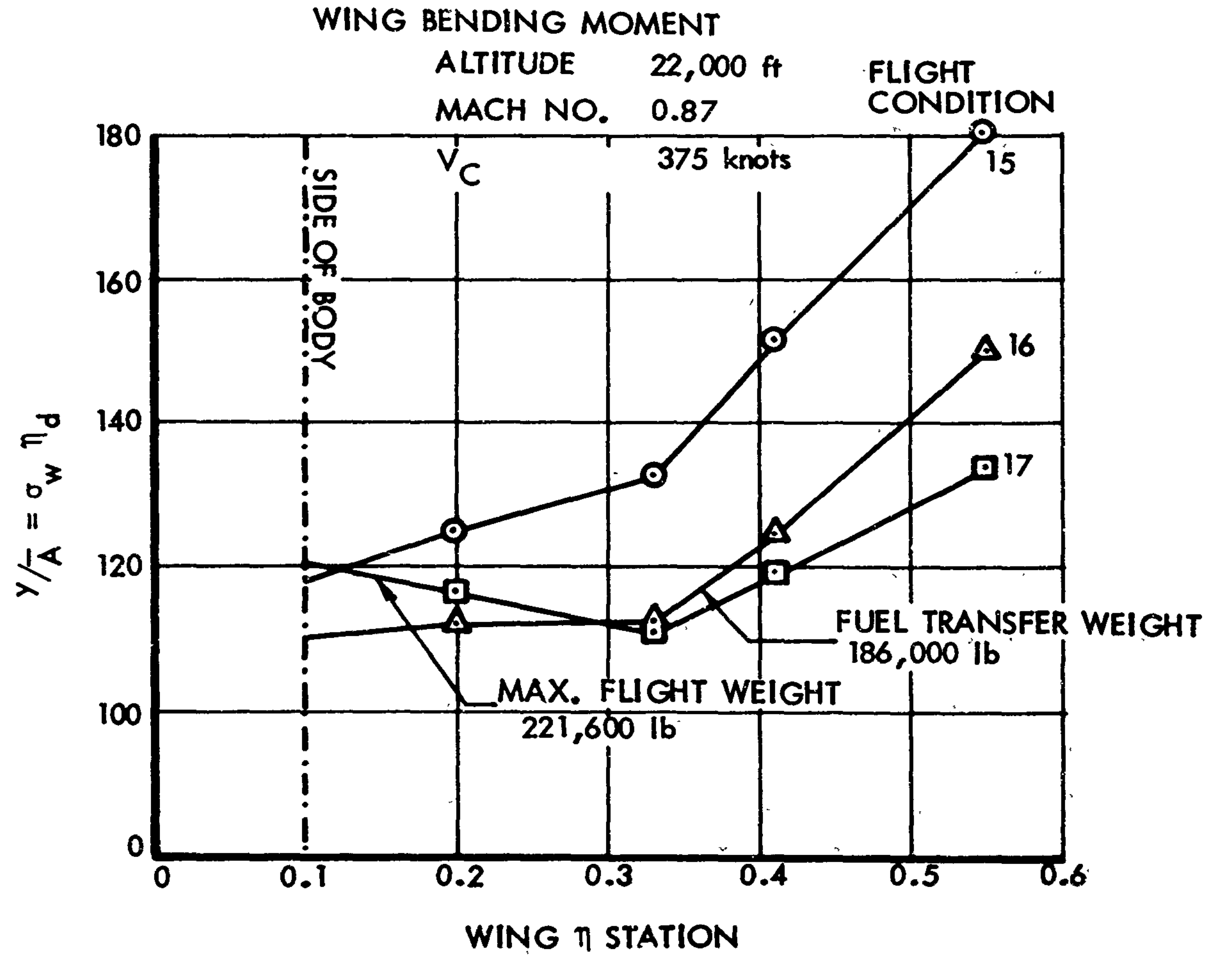

FIGURE 37. WING $\sigma_w \eta_d$ BASED ON BENDING MOMENTS

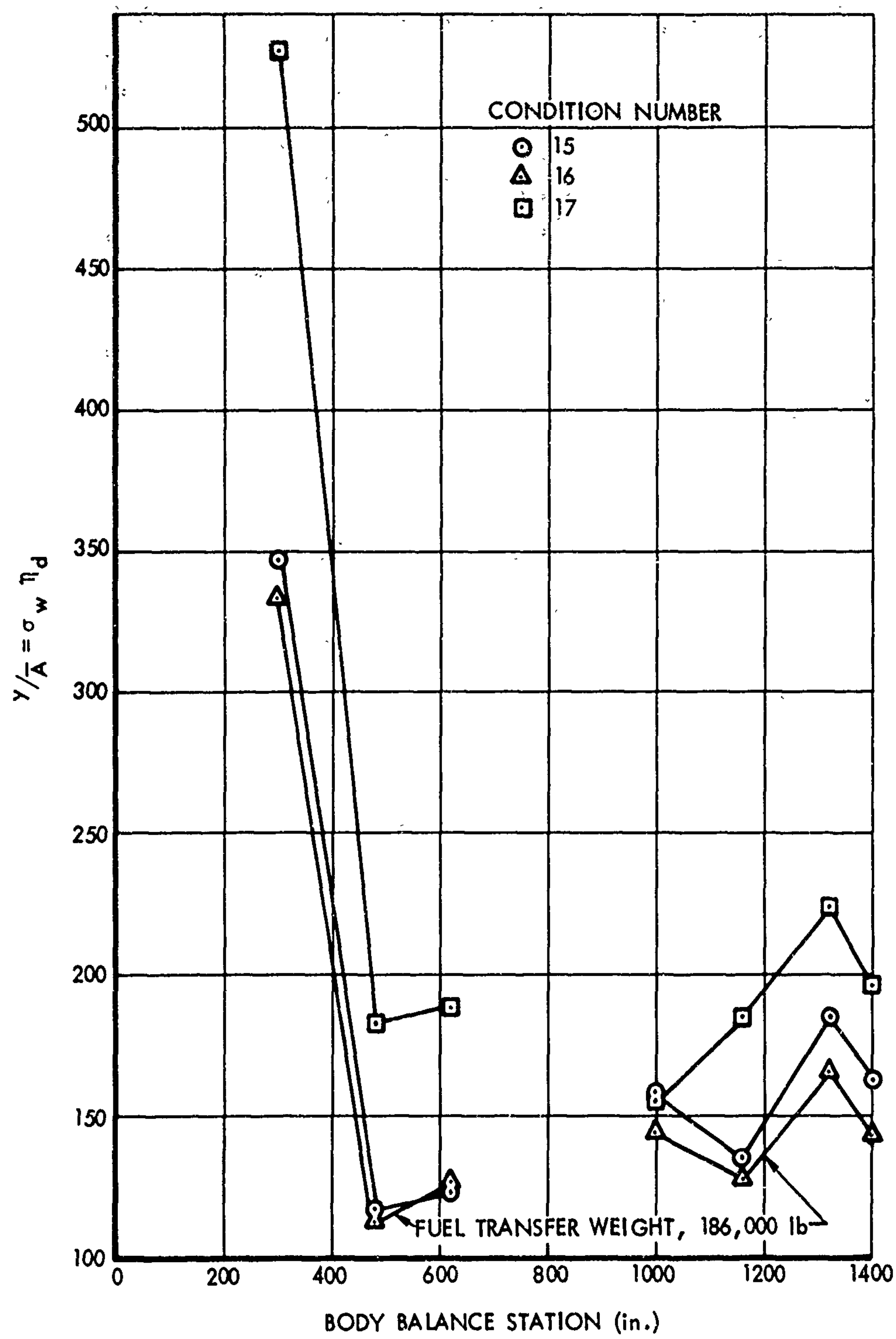

FIGURE 38. FUSELAGE $\sigma_w \eta_d$ BASED ON VERTICAL BENDING MOMENT

weight conditions, the fuel transfer weight condition, 186,000 lb., and the maximum flight weight condition, 221,600 lb., appear to be equally critical inboard of 33 percent wing semi-span. Since neither condition was clearly critical, both weight conditions were further examined for flight altitudes of 5,000, 15,000, 30,000, and 40,000 ft. The results of these altitude variations are given in Fig. 39, wherein values of $\bar{A}$ are plotted for wing bending moment at Wing Eta Stations .12 and .33. The corresponding altitude variations of the one factor aeroelastic loads are given in Fig. 40. The altitude conditions were analyzed at design cruise velocity, V_C; thus, the true airspeed and Mach number increased with altitude until the design cruise Mach number was reached. Above this altitude the true airspeed decreases for a constant design Mach number up to 35,000 ft. Above 35,000 ft. the true airspeed remains constant with increasing altitude. The effect of this variation of true airspeed is apparent in the altitude trends for the rms and one factor flight bending moments.

Values for $\sigma_W \eta_d$ were calculated for each of the two weight configurations mentioned previously for various altitudes. This information is shown in Fig. 41. The discontinuities in the curves reflect the abrupt change in cruise velocity at 24,000 ft. The preliminary boundary of minimum $\sigma_W \eta_d$ is defined by Conditions 26, 27, 17, 28 and 21 at 5,000, 15,000, 22,000, 30,000 and 40,000 ft., respectively.

Speed variations to further define the boundary of minimum $\sigma_W \eta_d$ were examined for altitudes of 15,000 and 22,000 ft. The velocities chosen were the gust penetration speed, V_B, 253 kt. EAS; an average cruise speed, 300 kt. EAS, and the design dive speed, V_D, 445 kt. EAS or M_D, .95. The fuel transfer weight condition was chosen for the 22,000 ft. speed variation, and the maximum flight weight was chosen for the 15,000 ft. variation. These conditions were deemed to be the most critical for the respective altitudes. The results of the speed variations are given in Figs. 42 and 43. The most critical speed for the 15,000 ft. altitude, maximum flight weight condition, appeared to be very near the design cruise speed, V_C, 375 kt. EAS or 472 kt. TAS; however, at 22,000 ft. the critical speed was found to be less than V_C. One additional condition was analyzed for 22,000 ft. to pinpoint the critical speed at 340 kt. EAS or 480 kt. TAS. Finally, center of gravity variations were studied for this condition, and the minimum $\sigma_W \eta_d$ values were obtained for a cg location at .25 MAC, Condition 24C. The resulting boundary of minimum $\sigma_W \eta_d$ is presented on Fig. 44. As can be determined from this figure, the most critical or least value of $\sigma_W \eta_d$ for Flight Condition 24C, Wing Eta Station .33 is 108.3.

Minimum values of $\sigma_W \eta_d$ for the fuselage were obtained by observing the variation of rms fuselage bending moments with altitude and speed. The forward fuselage appeared to be more critical than the aft fuselage. The one factor loads for the forward body remained nearly the same for

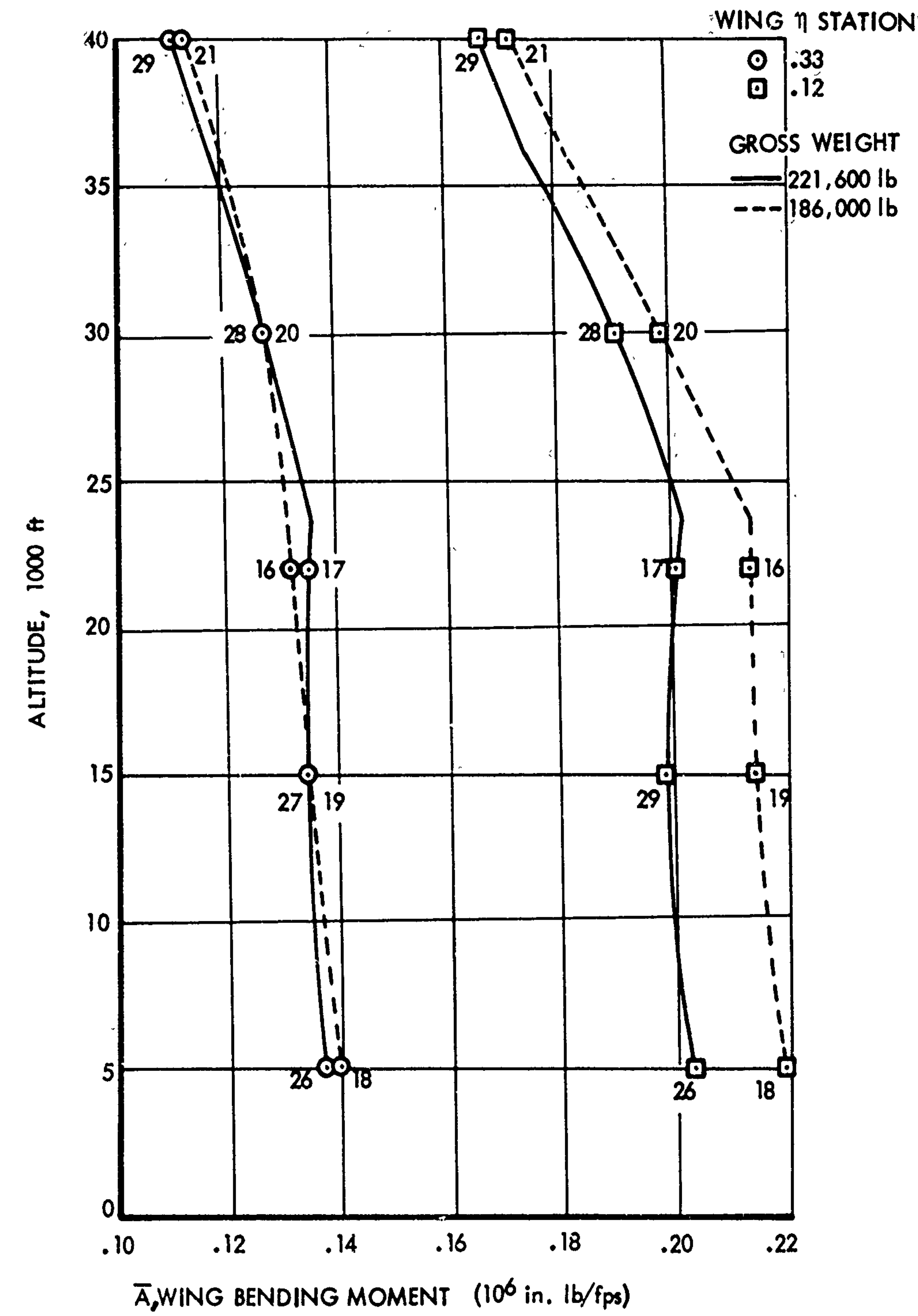

FIGURE 39. VARIATION OF RMS WING BENDING MOMENTS WITH ALTITUDE

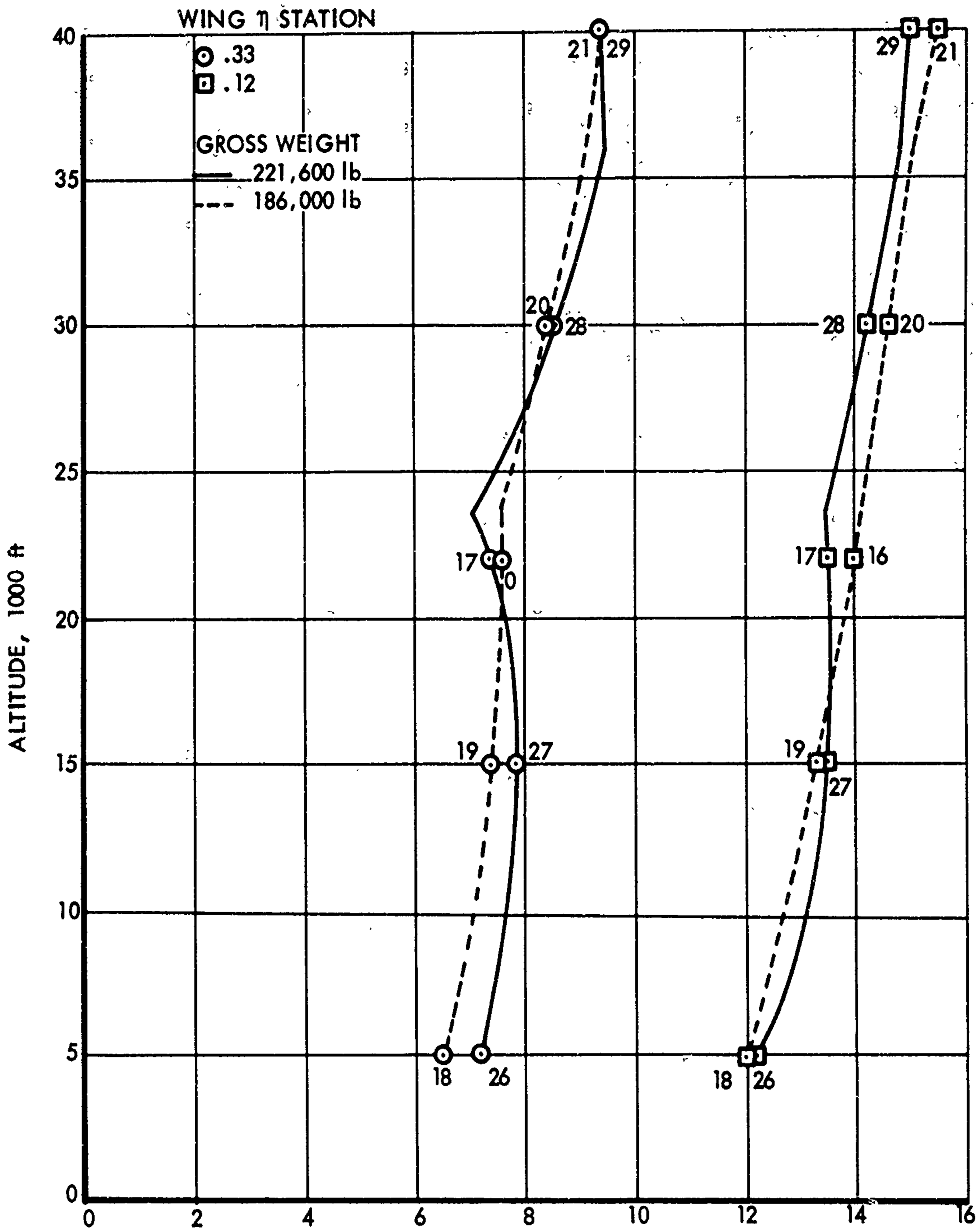

FIGURE 40. VARIATION OF LEVEL FLIGHT WING BENDING MOMENTS WITH ALTITUDE

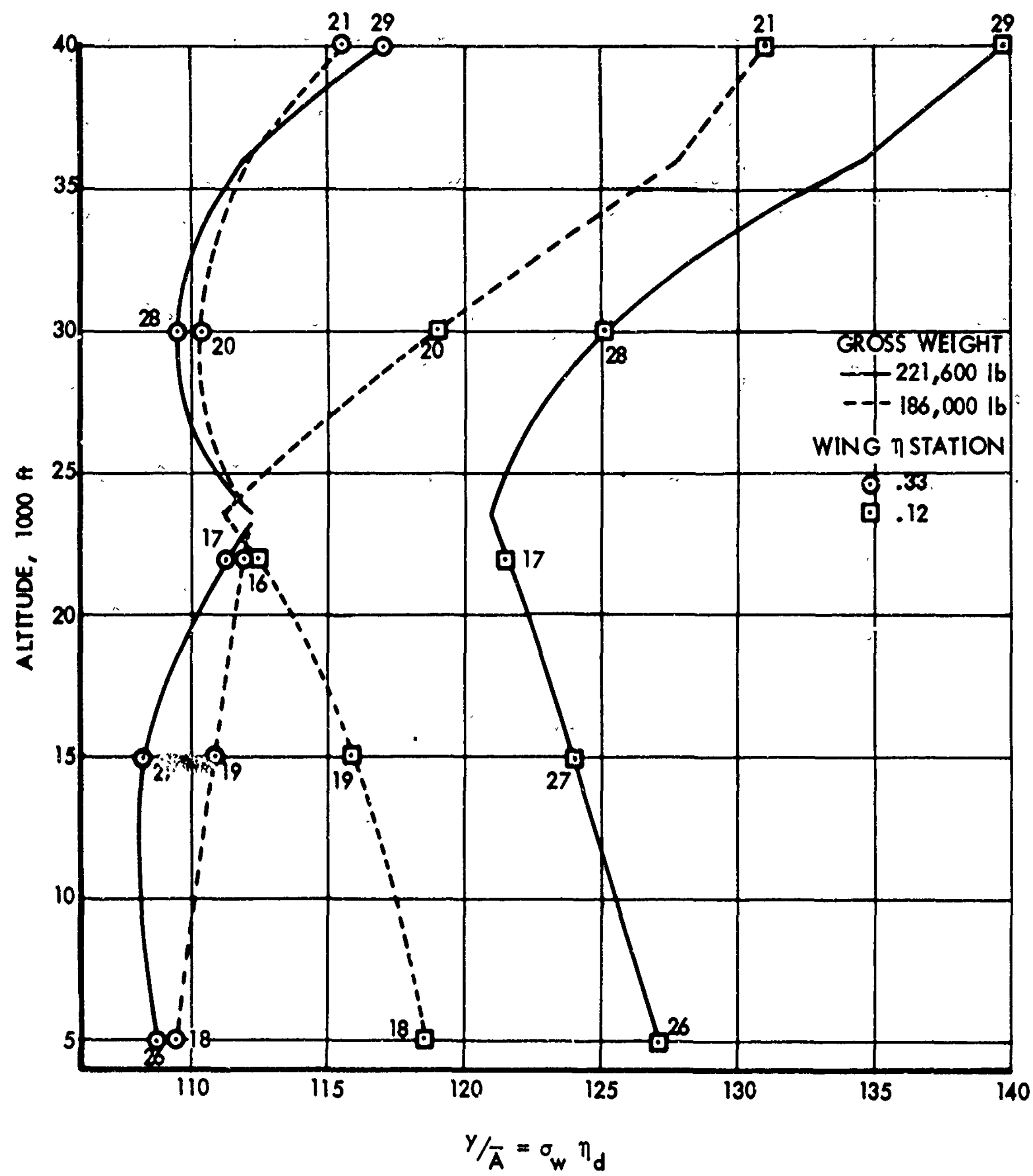

FIGURE 41. VARIATION OF WING BENDING MOMENT $\sigma_w \eta_d$ WITH ALTITUDE

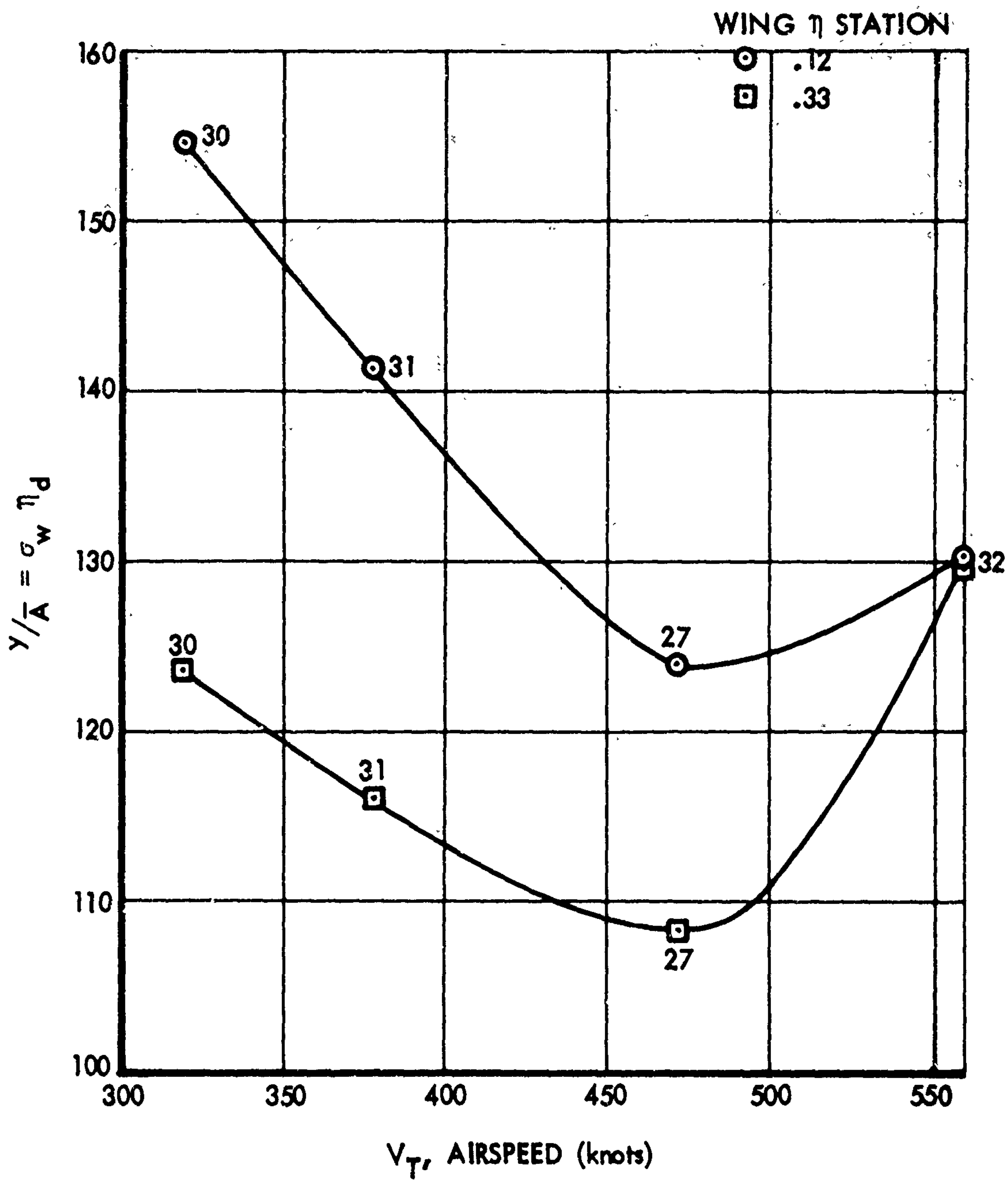

FIGURE 42. EFFECT OF SPEED ON WING BENDING MOMENT $\sigma_w \eta_d$ 15,000 FT. ALTITUDE

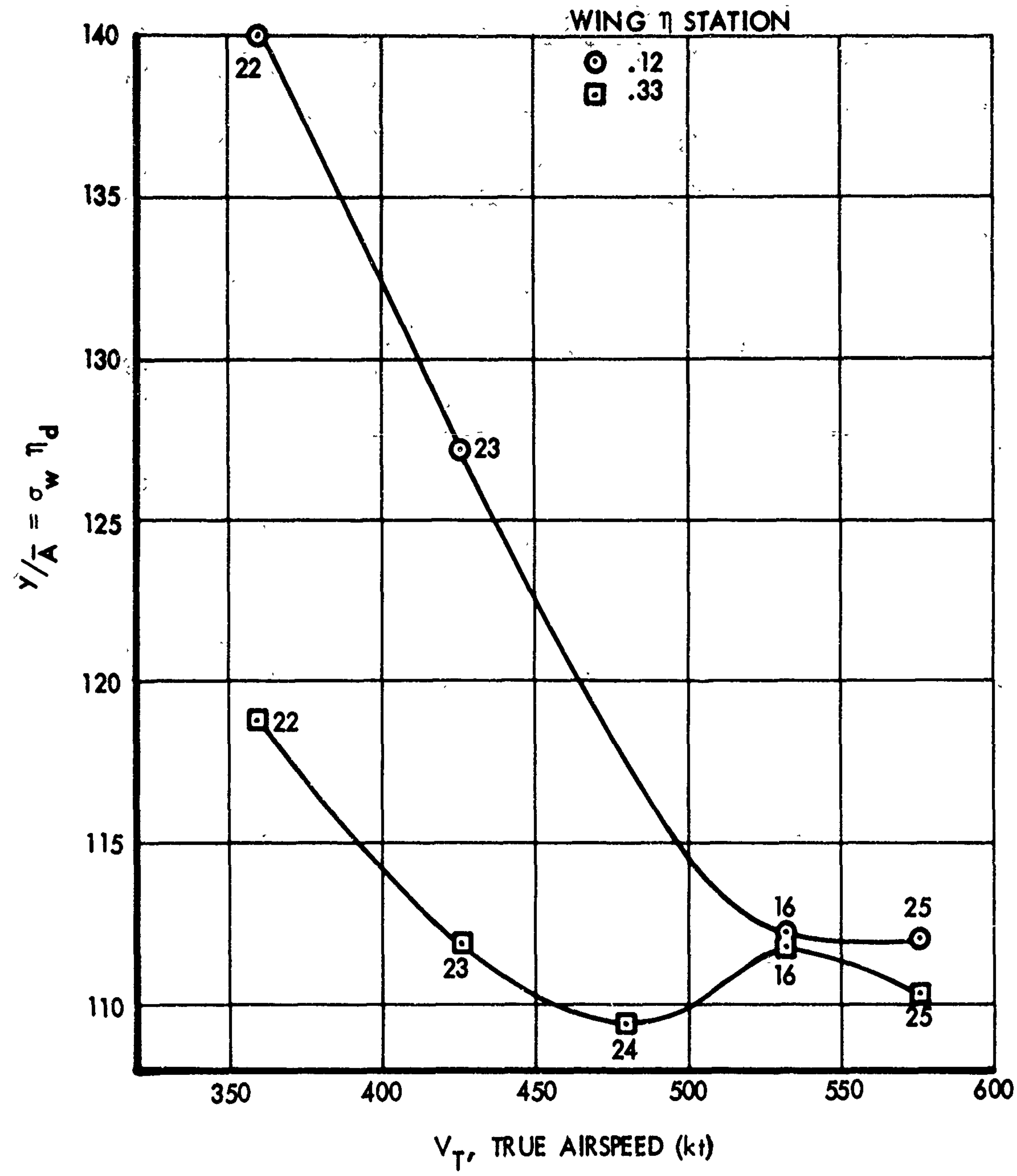

FIGURE 43. EFFECT OF SPEED ON WING BENDING MOMENT $\sigma_w \eta_d$, 22,000 FT. ALTITUDE

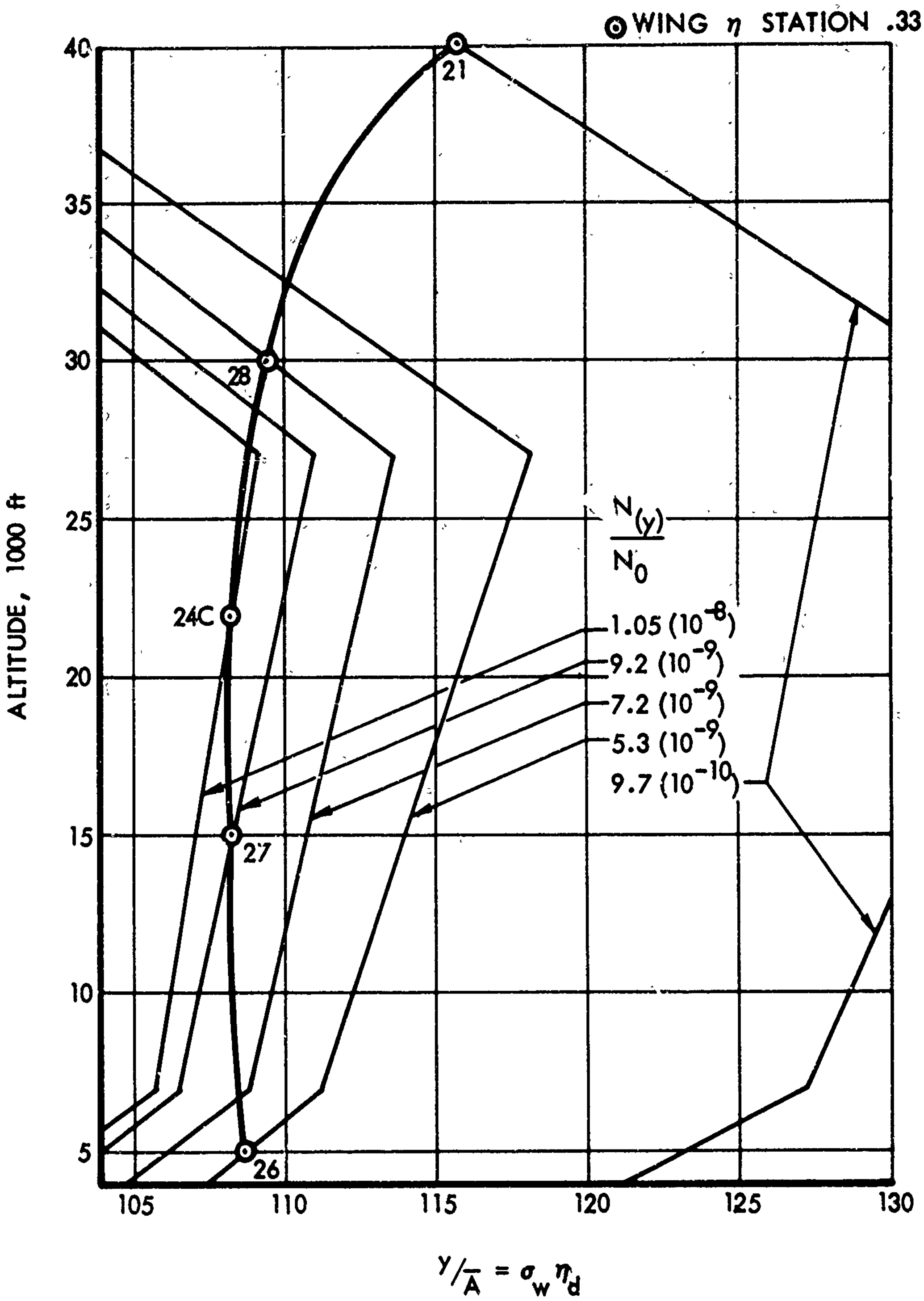

FIGURE 44. VARIATION OF MINIMUM WING BENDING MOMENT $\sigma_w \eta_d$ WITH ALTITUDE

all gross weight conditions; therefore, the variation in $\sigma_w \eta_d$ was largely a function of the incremental bending moments. The variation of fuselage $\bar{A}$ values with altitude at design cruise velocity is given in Fig. 45(a). The effect of speed variations on the rms bending moments at 22,000 ft. is given in Fig. 45(b). Representing these variation as $\sigma_w \eta_d$ in Fig. 46, it was concluded that the vertical gust loading on the fuselage was most critical at Body Balance Station 480,* for Flight Condition 16. The minimum value of $\sigma_w \eta_d$ for this body station was 112.2.

The average number of exceedances per hour of limit vertical bending moment were calculated for the wing for Wing Eta Stations .12 and .33 and for the fuselage for Body Balance Stations 480* and 1160. These results, shown in Figs. 47 and 48 respectively, were based on the flight profiles describing the average airplane usage described in Analyses Conditions. The design frequency of exceedance for the wing was determined as $3.7(10)^{-6}$ exceedances per hour. The corresponding design exceedance level for the fuselage is $3.3(10)^{-7}$ exceedances per hour. It will be observed that the highest or most critical frequency of exceedance occurs at Wing Eta Station .33, the same station that showed the minimum $\sigma_w \eta_d$. The highest frequency of exceedance for the body also occurs at the same body balance station that gave the minimum $\sigma_w \eta_d$ for the fuselage, Body Balance Station 480. Therefore, it appears that these two rather different approaches are consistent in arriving at the most critical stations based on the bending moment criteria. A comparison of the mission profile and design envelope frequencies of exceedance of wing limit strength may be of interest. By examining Fig. 44 herein, it is seen that the critical $\sigma_w \eta_d$ occurs in the altitude range 22,000 to 27,000 ft., and corresponds to an $N(y)/N_0$ value of 1.1×10^{-8}. For the critical condition the bending moment zero crossings are 1.20 per sec., which gives the following $N(y)$ value:

$$(1.1 \times 10^{-8})\ (1.20)\ (3600) \ = \ 4.8 \times 10^{-5} \text{ exceedances per hour}$$

As shown in Fig. 47, the frequency of exceedance value as calculated by the flight profile analysis is 3.7×10^{-6}. The ratio of design envelope to flight profile frequency of exceedance at the limit strength level, is therefore

$$\frac{4.8 \times 10^{-5}}{3.7 \times 10^{-6}} = 13.0$$

To extend the comparison to a load basis let us suppose that the flight profile frequency of exceedance were to be applied on a design envelope

*This corresponds to Body Station 540 (See Fig. 23)

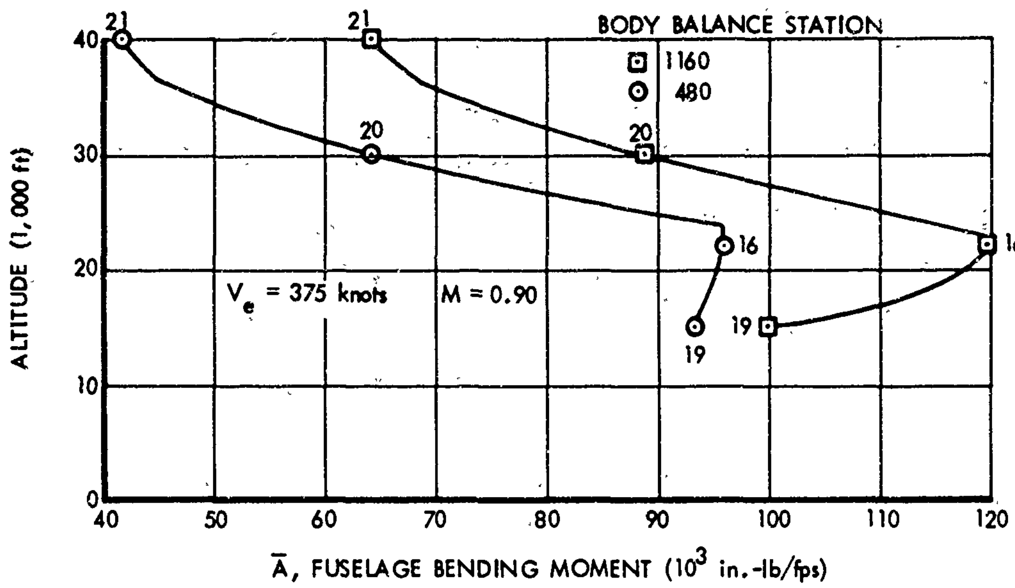

FIGURE 45. (a) VARIATION OF FUSELAGE RMS VERTICAL BENDING MOMENTS WITH ALTITUDE

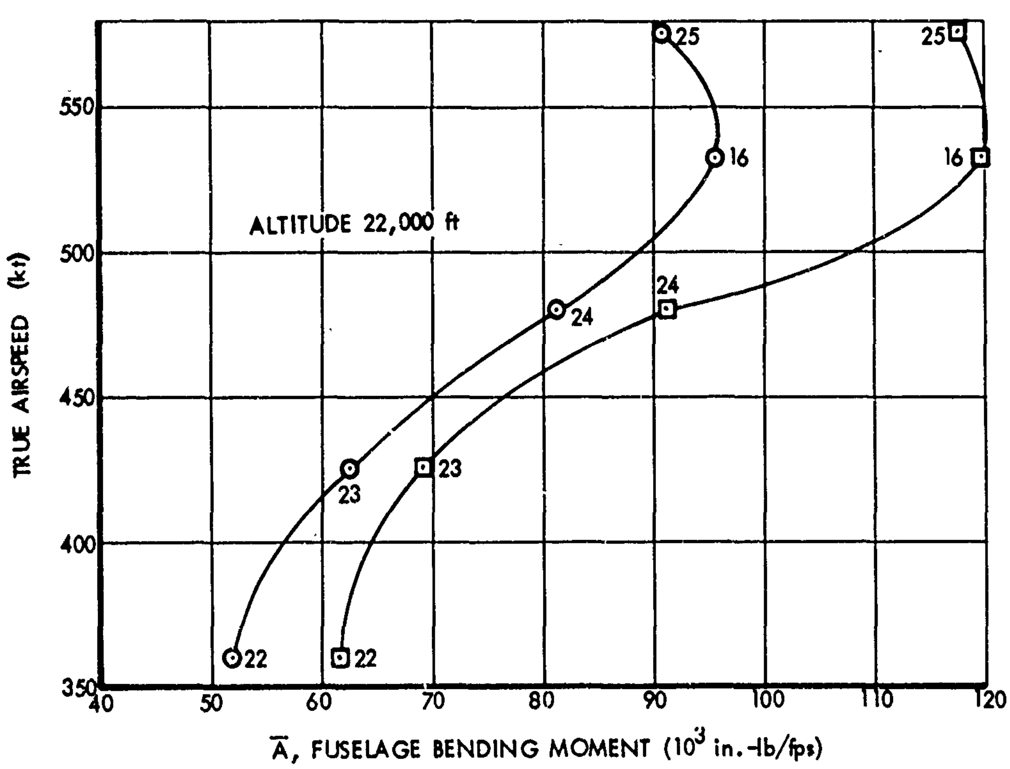

FIGURE 45. (b) VARIATION OF FUSELAGE RMS VERTICAL BENDING MOMENTS WITH SPEED

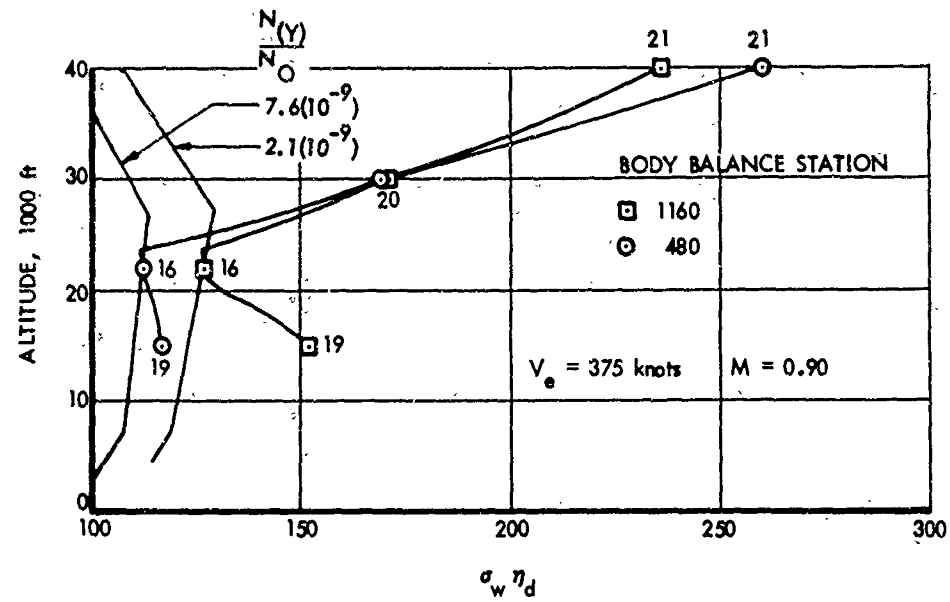

FIGURE 46. (a) VARIATION OF ALLOWABLE FUSELAGE $\sigma_w \eta_d$ WITH ALTITUDE BASED ON VERTICAL BENDING MOMENTS

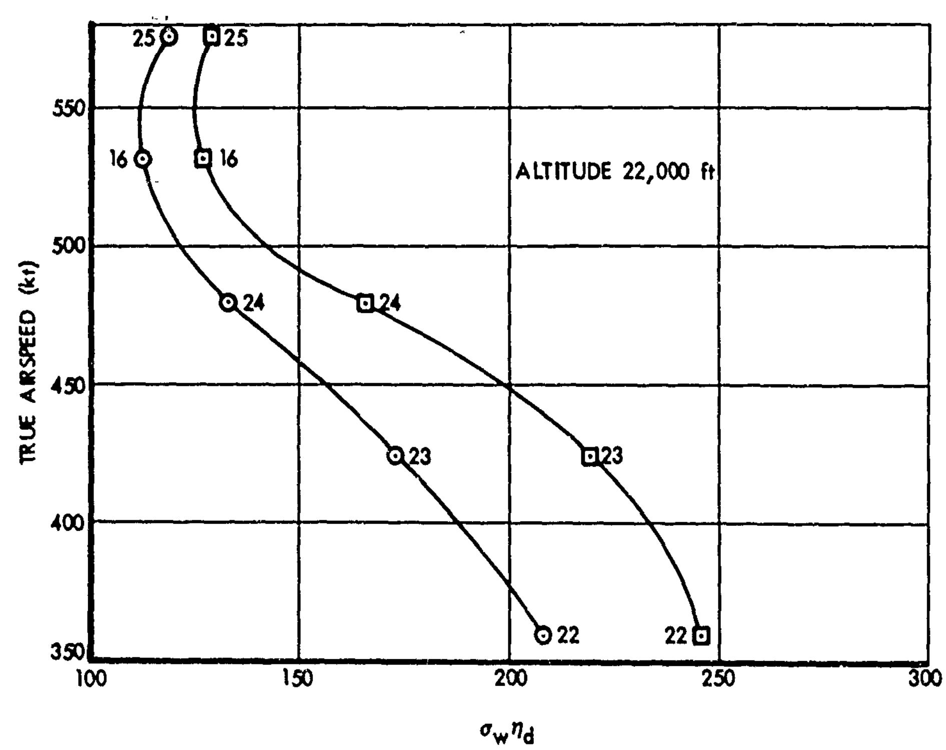

FIGURE 46. (b) VARIATION OF ALLOWABLE FUSELAGE $\sigma_w \eta_d$ WITH SPEED BASED ON VERTICAL BENDING MOMENTS

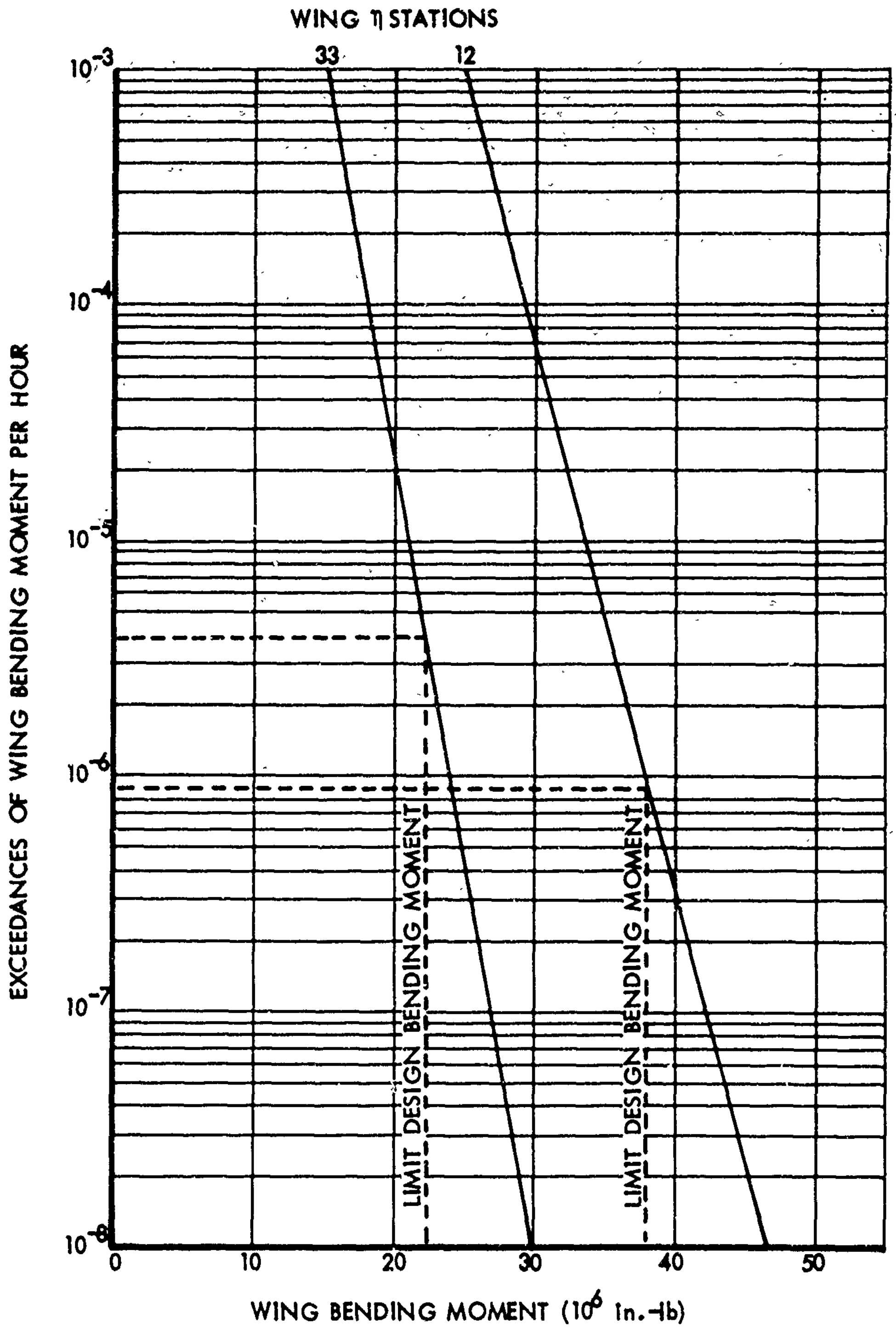

FIGURE 47. EXCEEDANCES OF WING BENDING MOMENT, WING ETA STATION .33

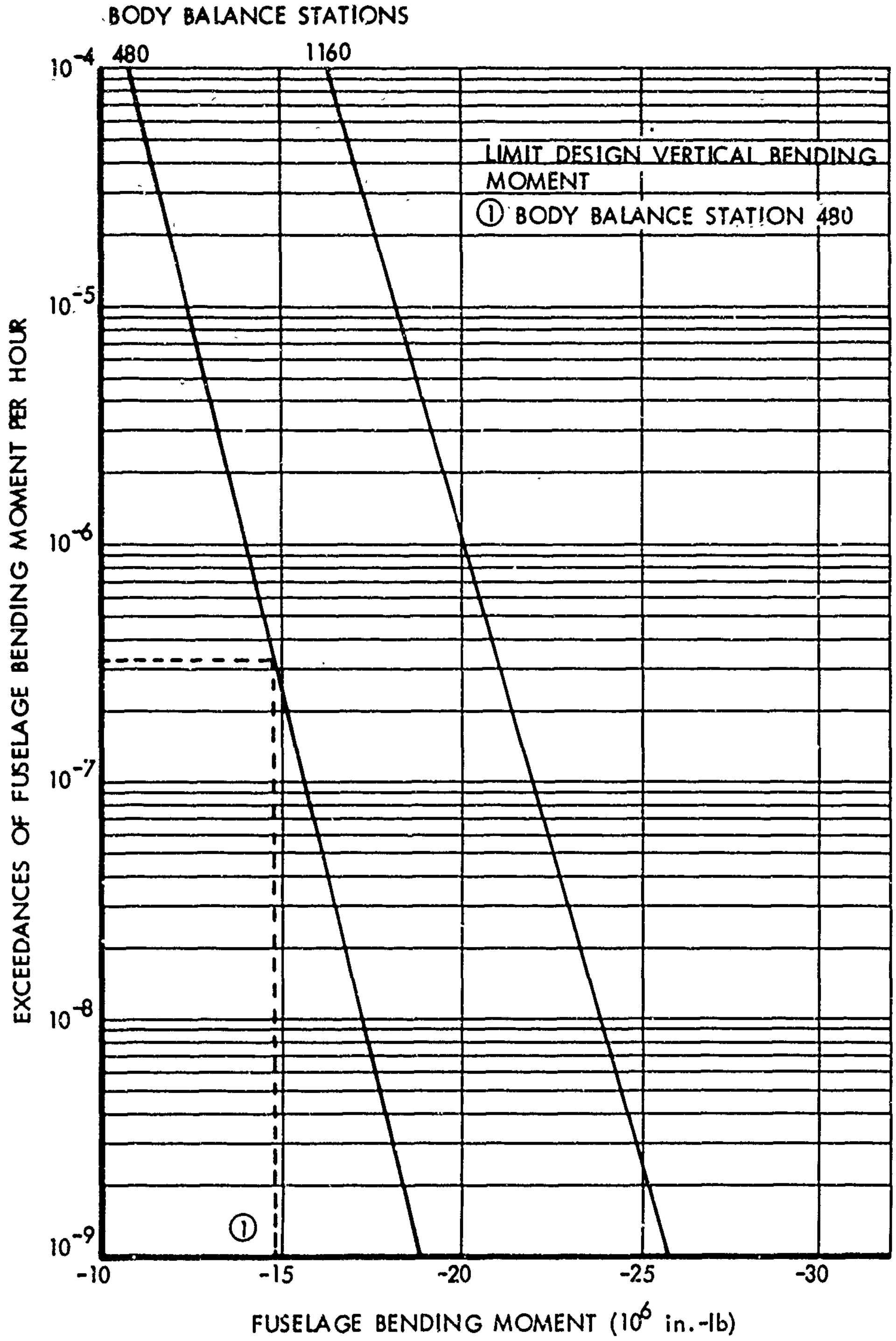

FIGURE 48. EXCEEDANCES OF FUSELAGE VERTICAL BENDING MOMENT, BODY BALANCE STATIONS 480, 1160

basis - for example, in order to provide for operation of the airplane 100% of the time at its most critical flight condition. The $N(y)/N_o$ value for the critical design envelope condition using the flight profile $N(y)$ with the design envelope N_o is:

$$\frac{N(y)}{N_o} = (3.7\times10^{-6}) \left(\frac{1}{1.20}\right) \left(\frac{1}{3600}\right) = 8.6\times10^{-10}$$

At an altitude of 22,000 ft., the corresponding $\sigma_w \eta_d$, from Fig. 47 is 138 ft. per sec. But strength has been provided only for $\sigma_w \eta_d$ = 108.3 ft. per sec. As a result, the incremental loads would have to be increased in the ratio 138/108.3 = 1.27. The corresponding ratio of increase of net loads, assuming a one-factor bending moment of 8.00×10^6 in.lb. and a limit allowable bending moment of 22.25×10^6 in.lb., is

$$\frac{(22.25 - 8.00)\ (1.27) + 8.00}{22.25} = 1.17$$

Determination of Critical Flight Conditions and Critical Structure, Lateral Analyses

Previous lateral analyses of 707/720 type airplanes have indicated that the magnitudes of the gust loads for flight in continuous turbulence is largely dependent on the Dutch roll stability of the airplane. Naturally, the loads are influenced by the damping in the Dutch roll mode, and can reach large amplitudes as the damping decreases. There are regions within the flight regime where the Dutch roll damping decreases to the extent that the Dutch roll response would reach significant amplitudes if the controls were locked. However, the pilot would apply corrective control inputs either manually or automatically through the yaw damper system before such a situation would develop. Since this corrective action is at the discretion of the pilot, it is beyond the scope of this study to establish a threshold for corrective control.

Therefore, the lateral analyses for the design envelope approach were conducted for flight conditions defined by the design cruise velocity, V_C, at a variety of altitudes. An airplane configuration was chosen to give the greatest Dutch roll response. This configuration exhibits the maximum airplane yaw inertia, a high gross weight and a large yaw-roll product of inertia, all of which are associated with reduced Dutch roll stability. The rms fin and aft fuselage bending moments were divided into the limit allowable bending moments for the fin and aft fuselage, respectively, to give values of $\sigma_v \eta_d$. These $\sigma_v \eta_d$ values were plotted against Fin Elastic Axis Station and Body Balance Station, and are shown in Figs. 49 and 50. The minimum value of $\sigma_v \eta_d$, 61.9, for the fin occurs at Fin Elastic Axis Station 158. The most critical aft body balance

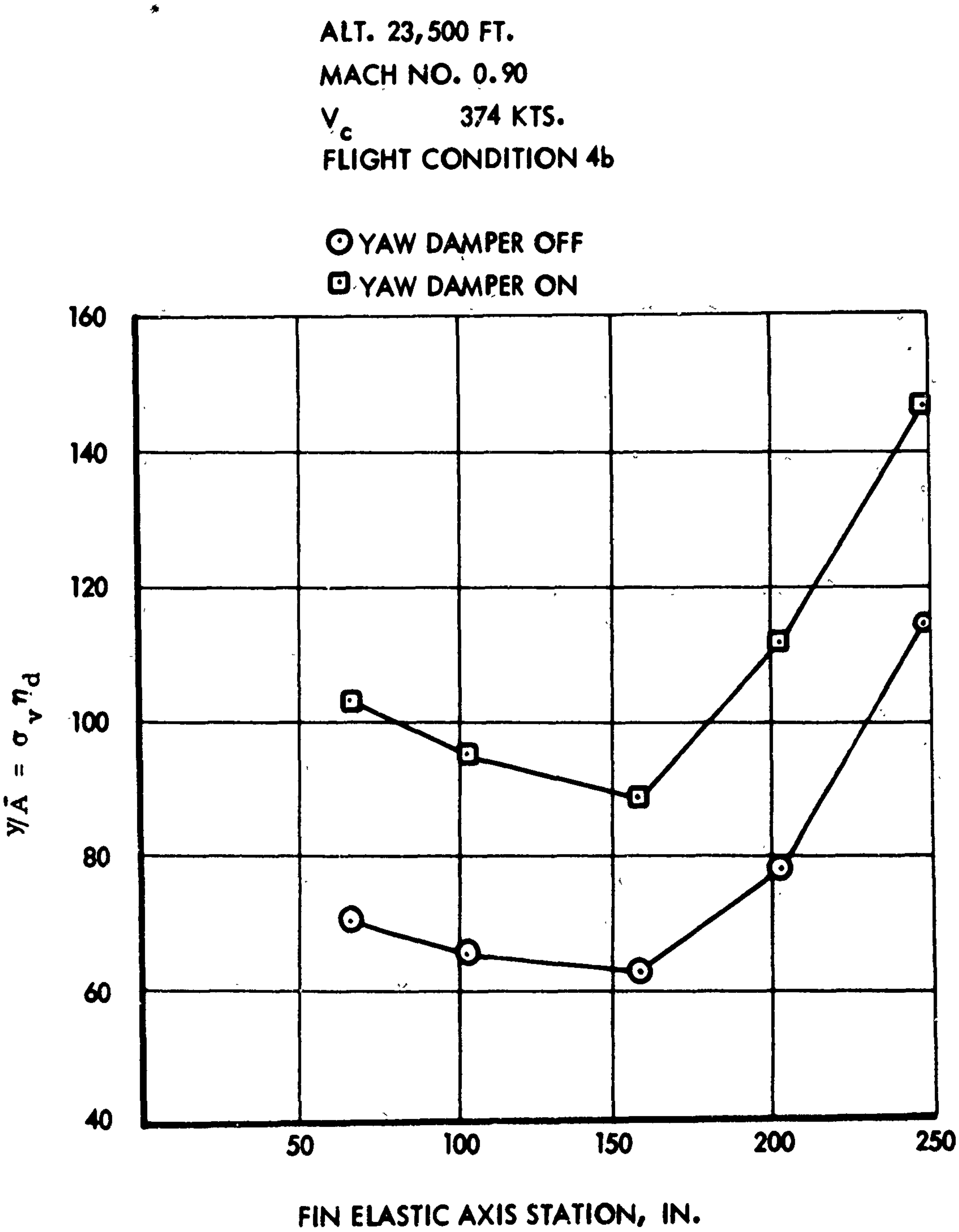

FIGURE 49. FIN $\sigma_v \eta_d$ BASED ON BENDING MOMENTS

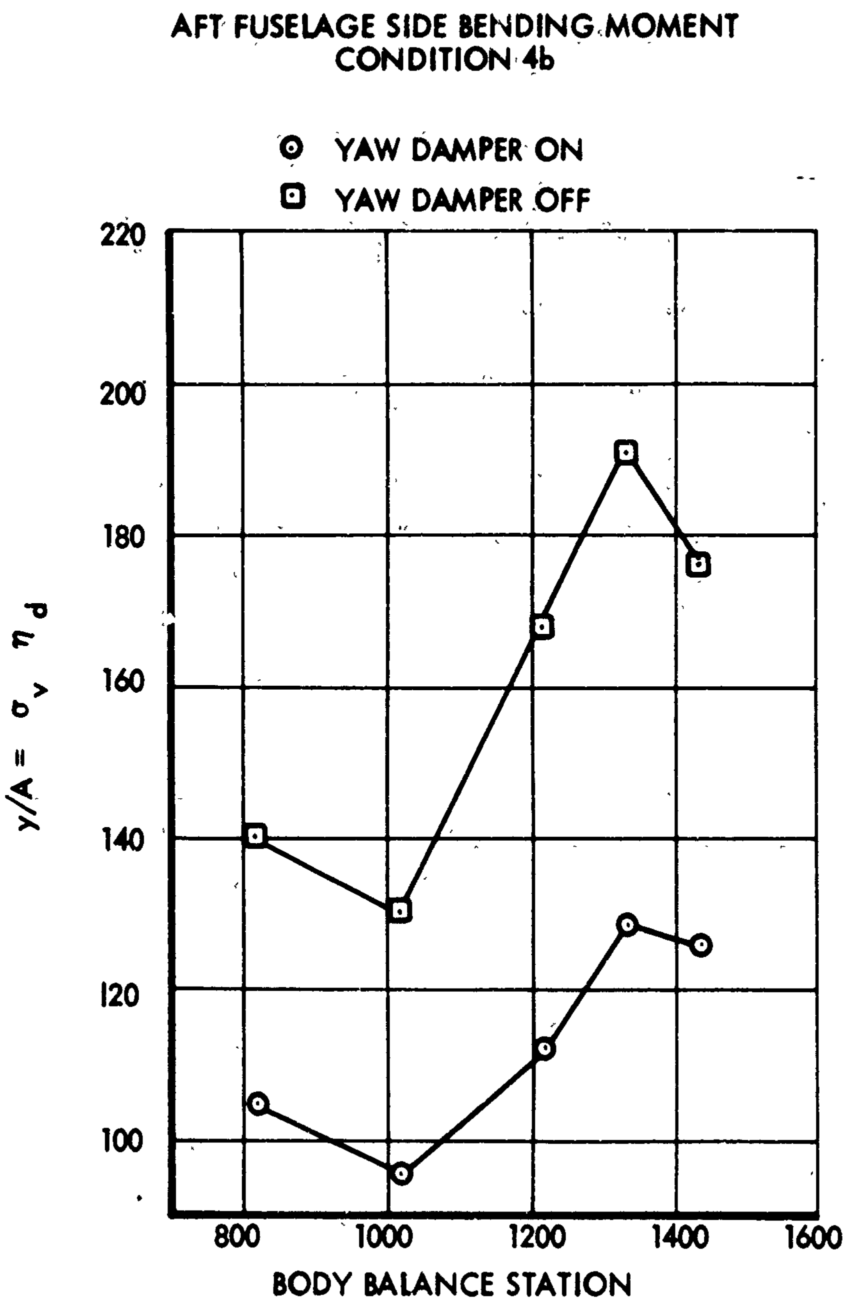

FIGURE 50. BODY $\sigma_v \eta_d$ BASED ON AFT FUSELAGE SIDE BENDING MOMENTS - CONDITION 4b

station is 1080 where the $\sigma_V \eta_d$ value was 94.3. The critical aft fuselage station from the lateral analysis standpoint is very nearly the same as critical aft fuselage station determined from the vertical analyses. Resultant values of $\sigma_V \eta_d$ obtained for other altitude points on the design cruise speed envelope are shown in Figs. 51 and 52. The critical altitude for both the aft fuselage and fin is 23,500 ft. All of the above analyses conditions were repeated with the electronic yaw damper engaged. It will be noted from the results shown in Figs. 51 and 52 that the yaw damper is very effective in reducing the peak amplitude of the Dutch roll response, and therefore provides a large reduction, approximately 40 to 60 percent, in the fin and fuselage loads. The degree to which the yaw damper is effective in reducing the loads is largely dependent upon the effective Dutch roll damping it can provide.

The number of exceedances of limit design bending moment per average flight hour were calculated for the vertical tail Elastic Axis Stations 67 and 158 and Aft Fuselage Balance Stations 1020 and 1335. These values, obtained both with the yaw damper engaged and disengaged, are shown in Figs. 53, 54, 55, and 56. The most critical design value for the vertical tail, $1.05(10)^{-4}$ exceedances per hour, occurs at Elastic Axis Station 158 with the yaw damper disengaged. When the yaw damper is operating full time the value is increased to $4.0(10)^{-6}$ exceedances per hour, thus showing the capability of yaw damper system to reduce the level of the lateral dynamic loads. The design frequency of exceedance for the aft fuselage occurs at Body Balance Station 1020 and with the yaw damper disengaged is $2.0(10)^{-7}$ exceedances per hour. The corresponding values with the yaw damper engaged is $1.50(10)^{-9}$ exceedances per hour.

The critical or design values of $\sigma_V \eta_d$ based on bending moment from the lateral analyses occur at the same vertical tail station and aft body station as the critical design frequency of exceedance obtained by the flight profile approach.

A summary of the exceedances of limit design load, as obtained from the Flight Profile Analyses using the bending moment criteria, are given in Fig. 57. Also shown in this figure, expressed as exceedance ratios, are the design values of $\frac{N(\sigma_W \eta_d)}{N_o}$ and $\frac{N(\sigma_V \eta_d)}{N_o}$ as determined from the Design Envelope Analyses.

Results - Incremental CG Acceleration

The rms values, $\bar{A}$, of incremental center of gravity acceleration due to unit rms gust velocity are shown in Fig. 58 for gross weights of 221,600 lb. and 186,000 lb. These values were obtained from the dynamic loads solution for points on the design cruise speed boundary of 375 kt. EAS

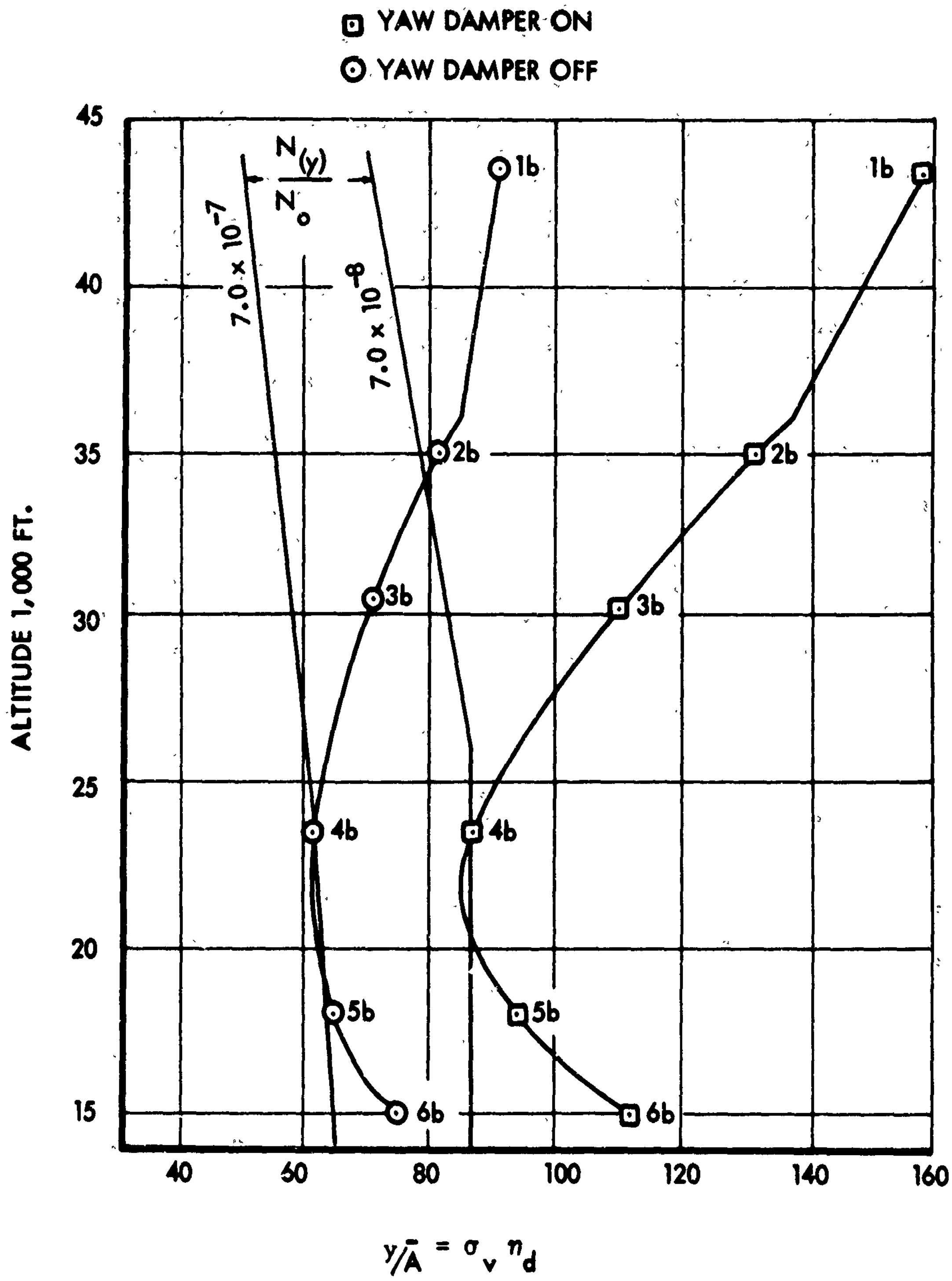

FIGURE 51. VARIATION OF FIN BENDING MOMENT $\sigma_v \eta_d$ WITH ALTITUDE

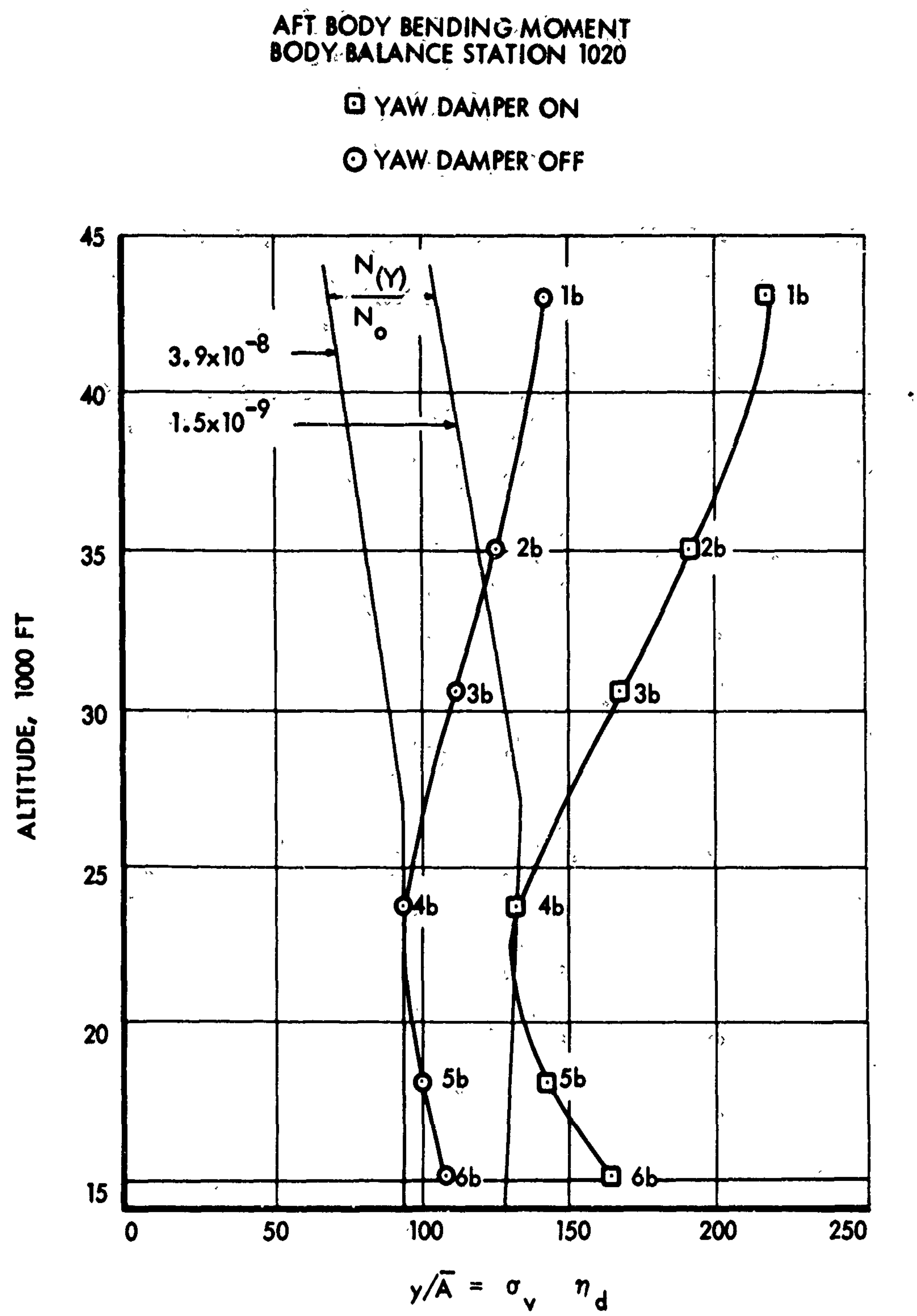

FIGURE 52. VARIATION OF BODY BENDING MOMENT $\sigma_v \cdot \eta_d$ WITH ALTITUDE

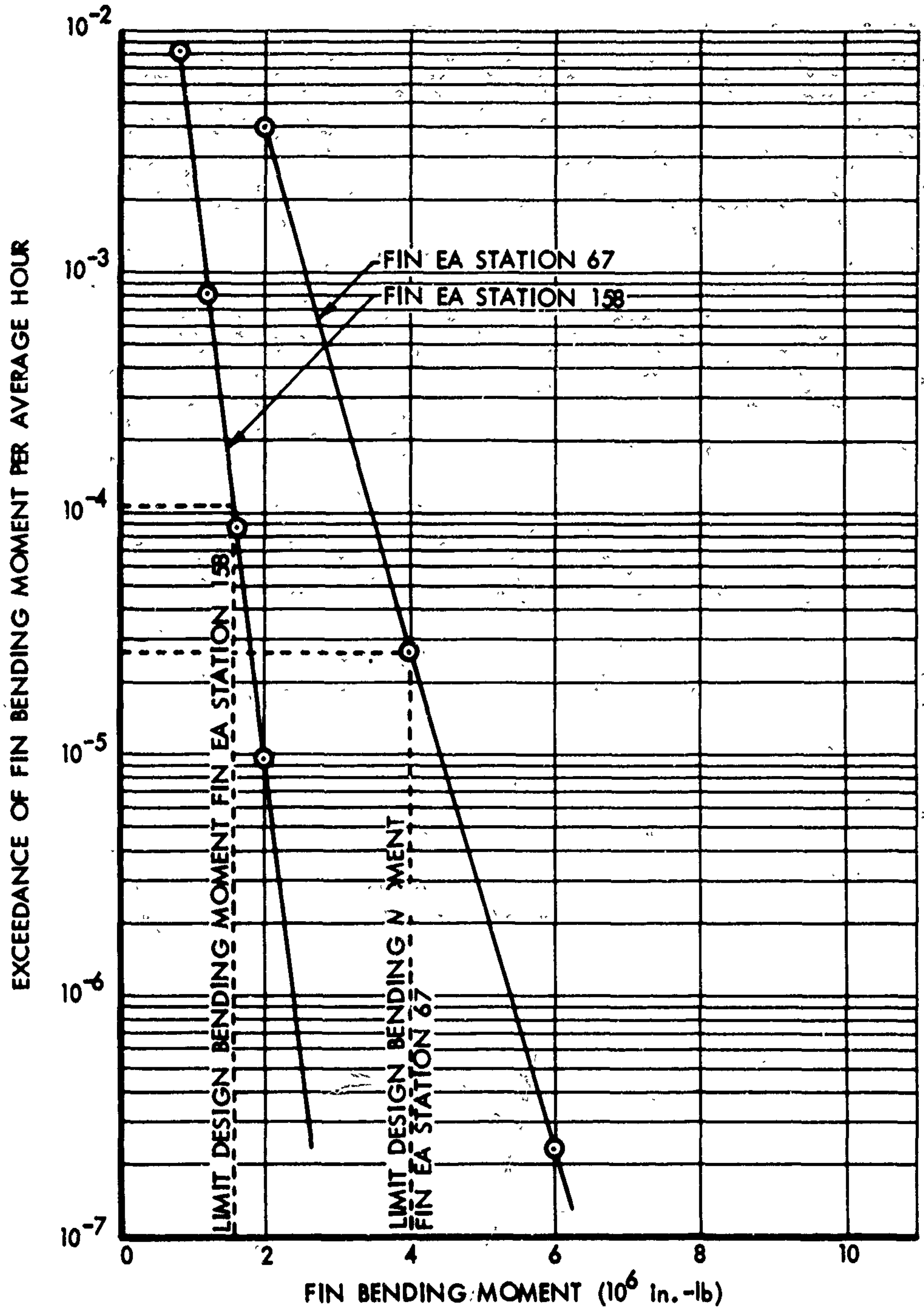

FIGURE 53. EXCEEDANCES OF FIN BENDING MOMENT, YAW DAMPER OFF

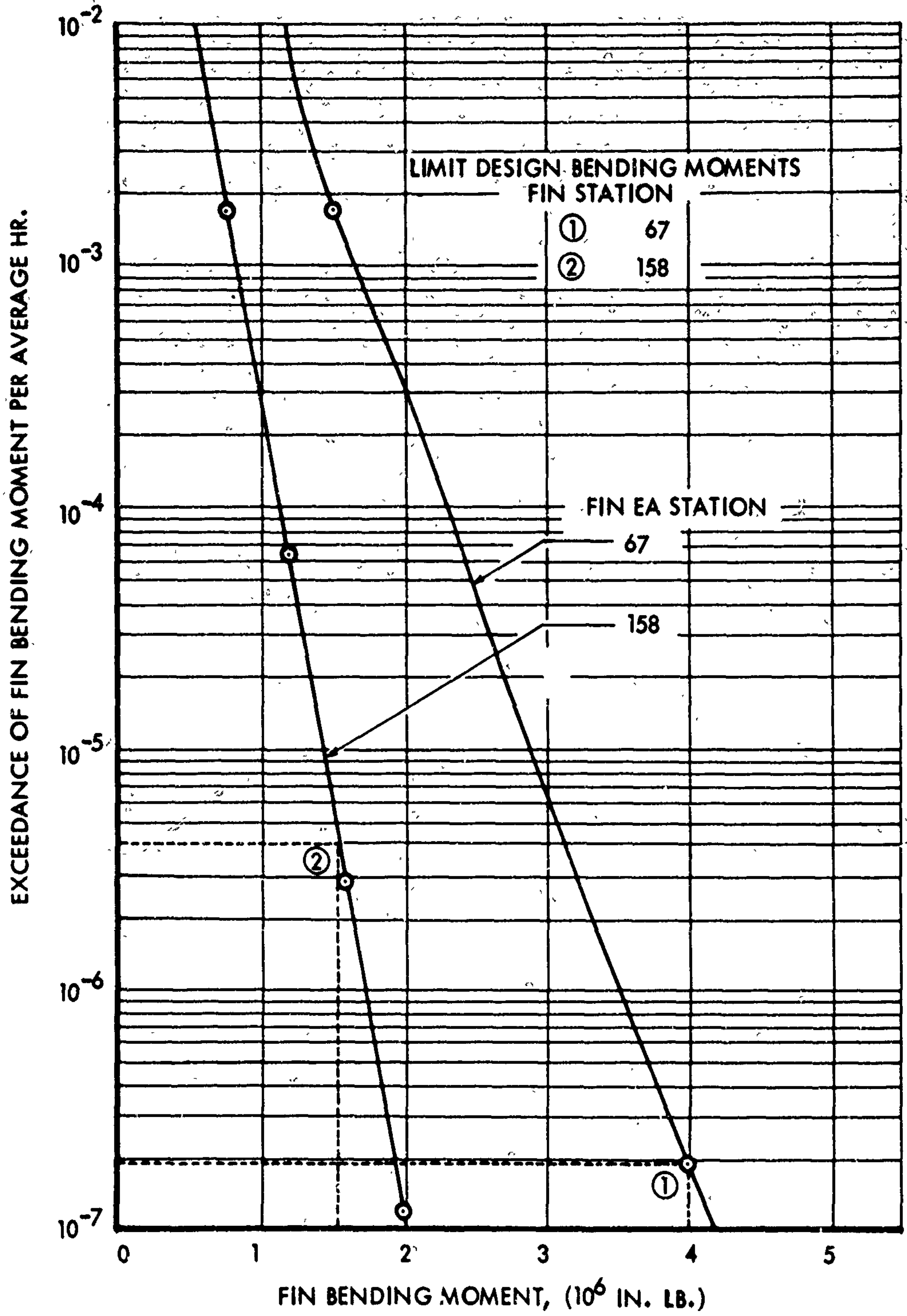

FIGURE 54. EXCEEDANCES OF FIN BENDING MOMENT, YAW DAMPER ON

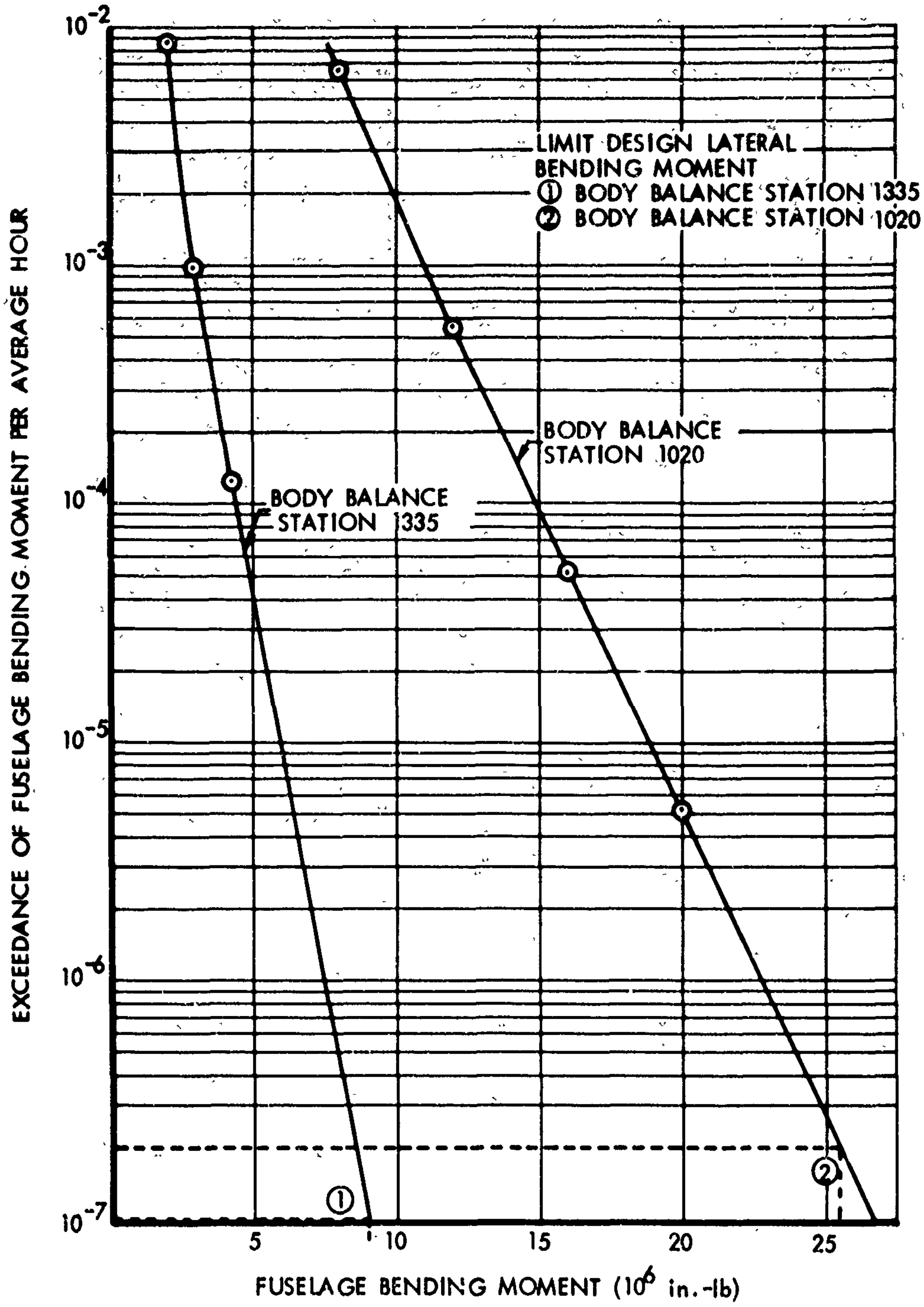

FIGURE 55. EXCEEDANCES OF FUSELAGE LATERAL BENDING MOMENT, YAW DAMPER OFF

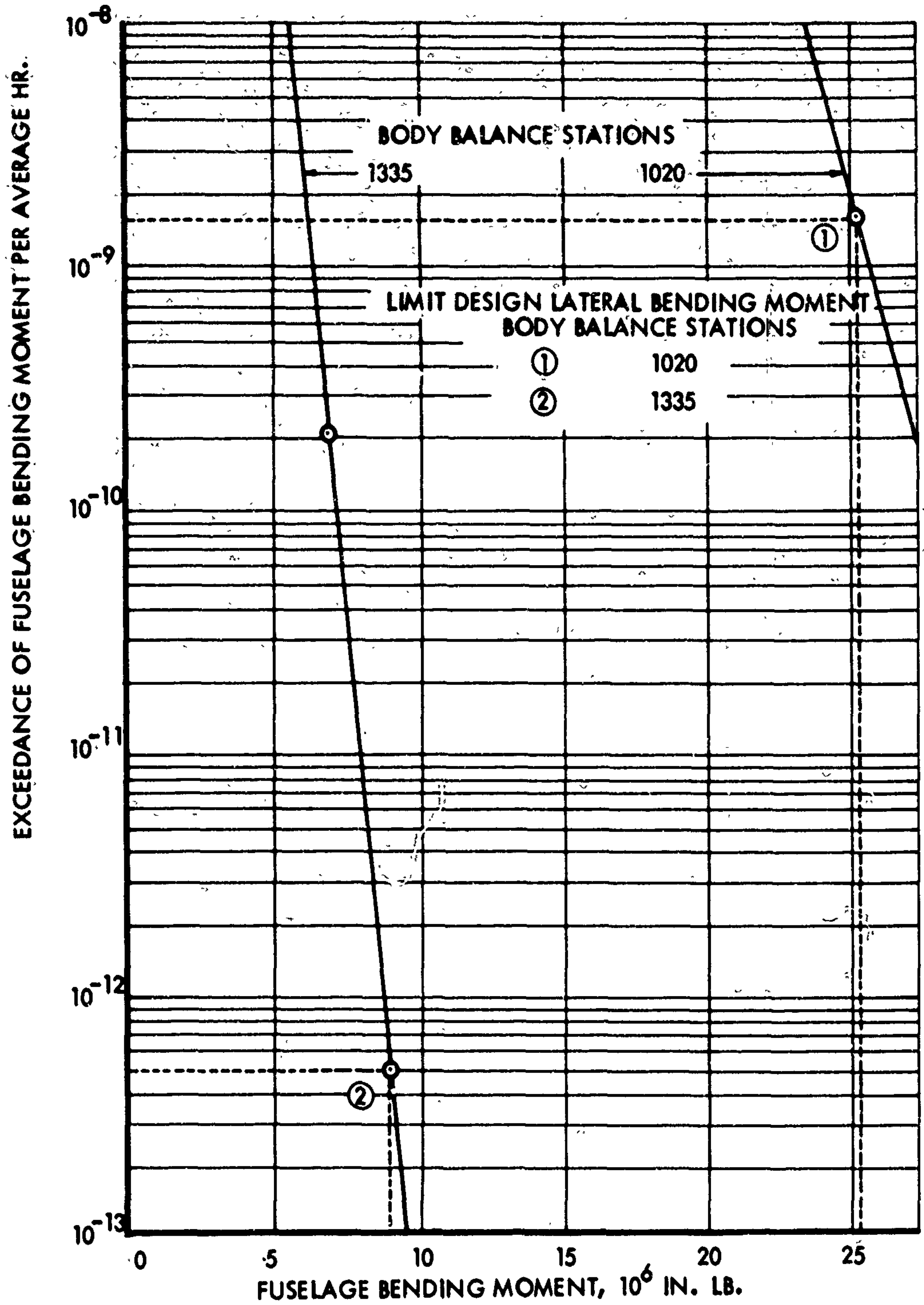

FIGURE 56. EXCEEDANCES OF FUSELAGE LATERAL BENDING MOMENT, YAW DAMPER ON

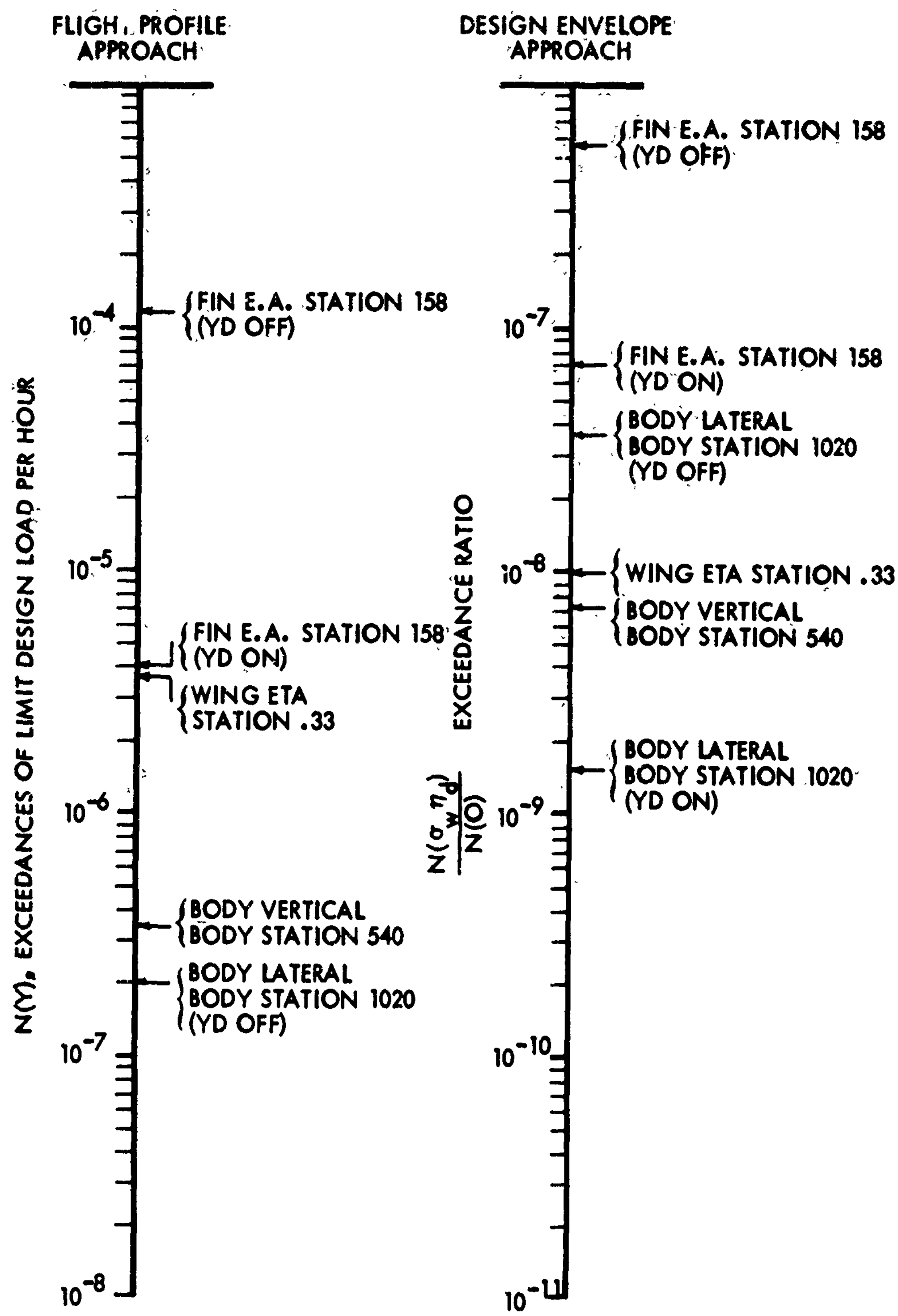

FIGURE 57. SUMMARY OF DESIGN VALUES OF EXCEEDANCE RATIOS AND FREQUENCY OF EXCEEDANCES BASED ON BENDING MOMENTS

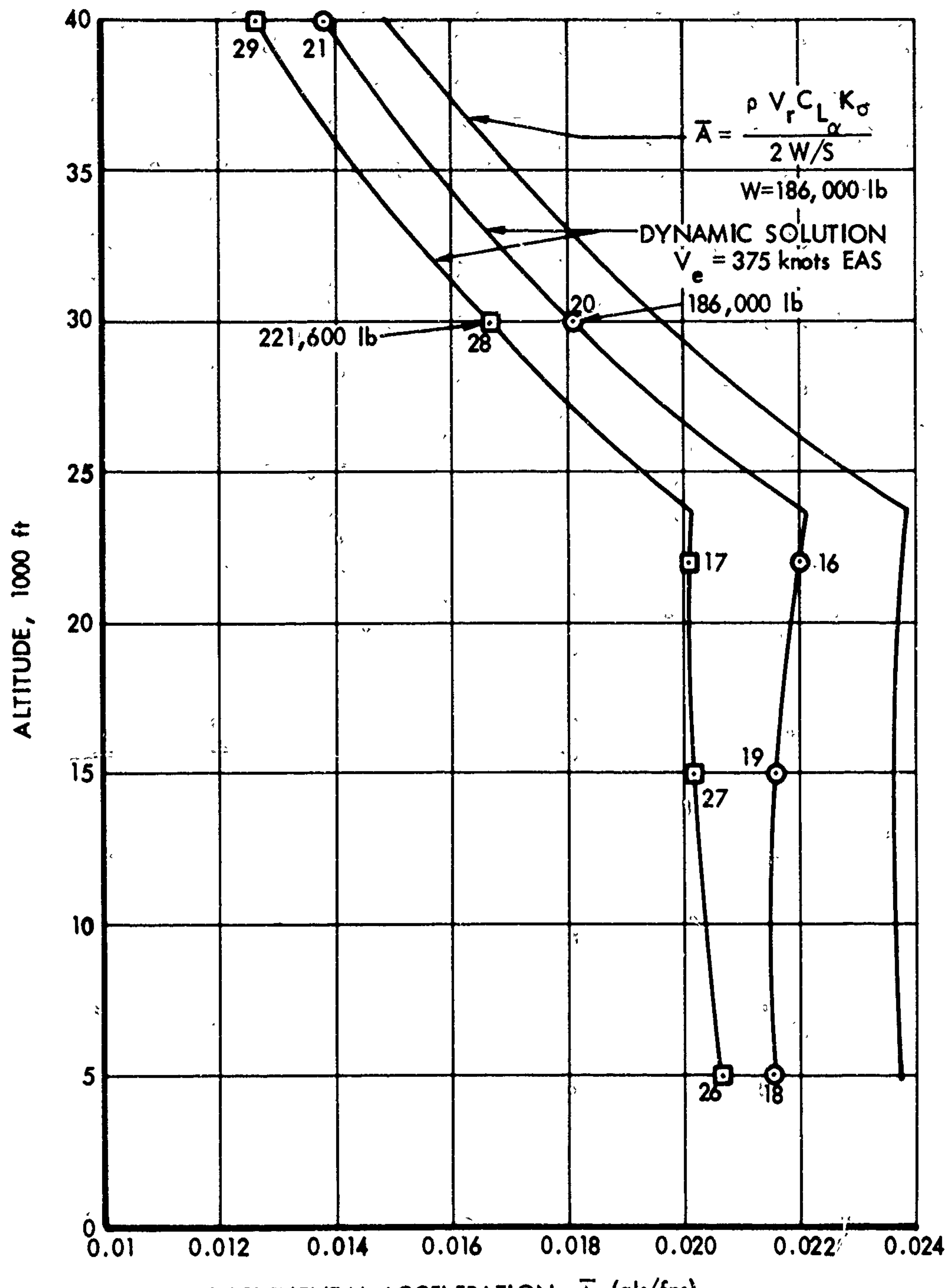

FIGURE 58. ALTITUDE VARIATION OF INCREMENTAL CG ACCELERATION

to Mach .90. As a matter of interest, the $\bar{A}$ values for 186,000 lb. gross weight were also calculated using the one dimensional expression developed by Y. C. Fung[16] and given below:

$$\bar{A}_{\Delta n} = \frac{\rho V_T C_{L\alpha}}{2(W/S)} K_\sigma \qquad (19)$$

where,

ρ — atmospheric density at altitude, slugs per cu. ft.

V_T — true airspeed, ft. per sec.

$C_{L\alpha}$ — flexible airplane life curve slope, per rad.

W — airplane gross weight, lb.

S — airplane wing area, ft.

K_σ — gust response factor based upon the isotropic turbulence spectrum and a scale of turbulence factor of 2500 ft.

The $\bar{A}_{\Delta n}$ values determined by the one-dimensional equation are about ten percent higher than those obtained from the full dynamic solution. This difference can be attributed to flexibility and aerodynamic effects which are more precisely accounted for in the dynamic solution.

Values for the frequency of exceedance per hour for incremental center of gravity acceleration are shown in Fig. 59. These values were determined from flight profile analysis. The cg acceleration exceedances for the 707-300 series airplanes are also shown in Fig. 59. These data were collected by NASA from actual airline operations[3]. At the time of this report, sufficient acceleration data was not available for the 720B airplane, so an attempt was made to adjust the 707-300 data to represent 720B usage. This adjusted data can be compared to the 720B analytical data in Fig. 59. This comparison indicates that the predicted cg acceleration exceedances are somewhat higher than the adjusted usage values. The disagreement increases as the acceleration level increases. This would indicate that the turbulence intensity parameters, P_1, P_2, b_1, and b_2 should be readjusted.

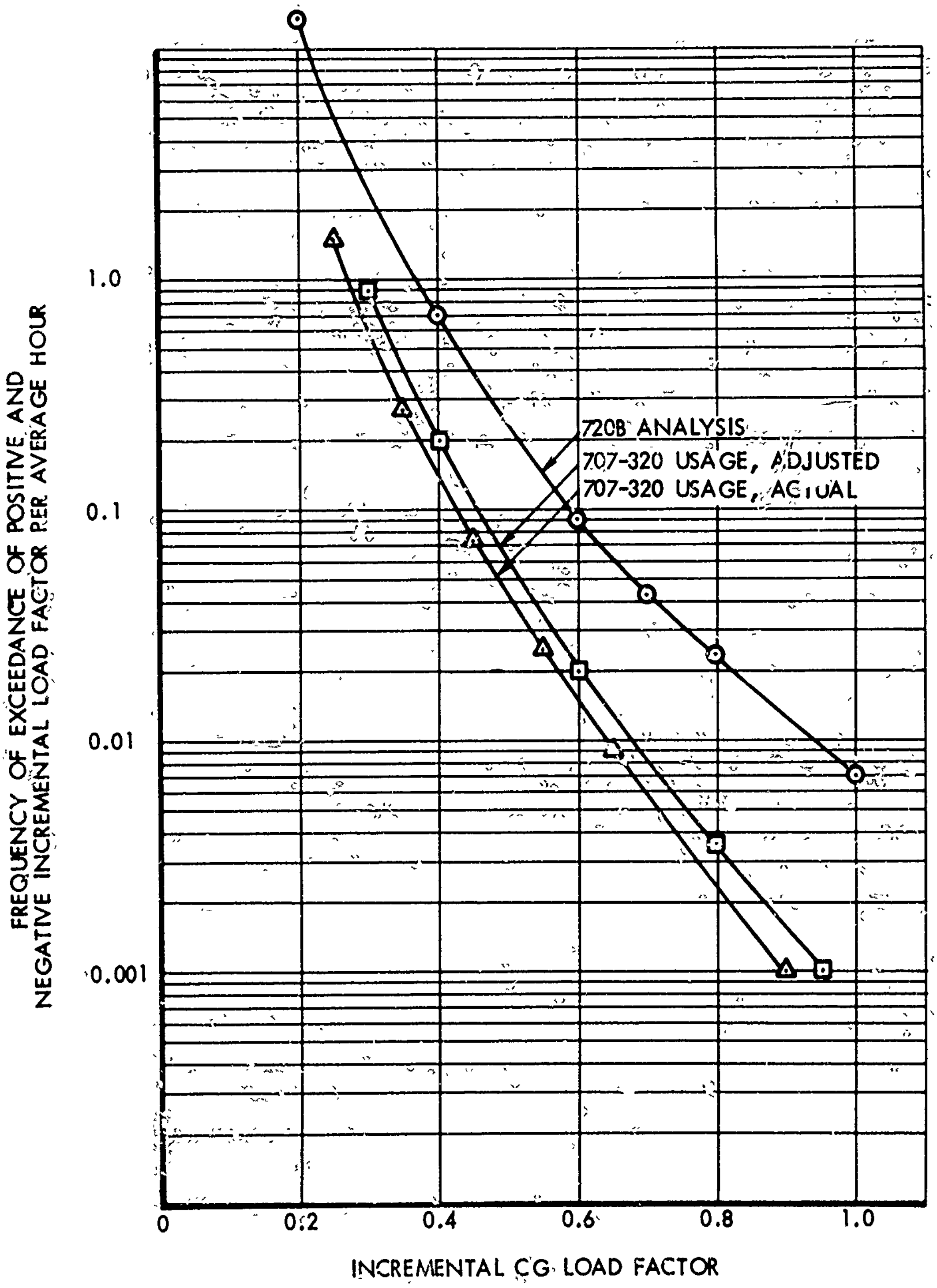

FIGURE 59. EXCEEDANCES OF INCREMENTAL CG ACCELERATION

Boeing Analysis Results for Lockheed Model 749

A comparative analysis was conducted by The Boeing Company on the Lockheed Model 749 airplane. The Lockheed-California Company furnished the basic airplane data in the form of lumped mass distribution, bending and torsional stiffness distributions, wing lift distribution, and basic airplane lift and moment data. From this description, the analysis was conducted by Boeing using the analysis procedures used for the 720B study. The results of this analysis are expressed as $\bar{A}$, the rms load due to a one ft. per sec. rms gust velocity, and N_0, the number of zero crossings per second for wing shear, bending moment, and torsion. A comparison of these values with those obtained by Lockheed are shown in Figs. 60 and 61. Values for $\bar{A}$ and N_0 for cg incremental acceleration are also listed. The agreement between the Boeing and Lockheed $\bar{A}$ values is generally not as good as might be desired. Possible reasons for this disagreement are explored in Reference 18. The agreement of the N_0 values is seen to be much more satisfactory.

Parametric Variations - Vertical Analyses

The results of the parametric variations conducted for the vertical analyses are shown in Fig. 62 as they affected the rms wing bending moment at the critical wing station. Fig. 63 shows how these parametric variations affect the airplane incremental cg acceleration. The trends exhibited by bending moment and cg acceleration are similar for all variations except for the variation of wing torsional stiffness. In this case, a reduction in wing torsional stiffness of 20 percent resulted in a slight, less than one percent, increase in cg acceleration while the rms wing bending moment actually decreased by one percent. The wing rms bending moment and incremental cg acceleration are quite insensitive to variations in wing torsional stiffness.

When gradual penetration effects were neglected, the resulting rms wing bending moment and the airplane incremental cg acceleration were reduced by 10-12 percent. This implies that results obtained from analyses in which gradual penetration was neglected may be unconservative. The rms wing bending moments and incremental cg acceleration were also affected by the inclusion of structural damping. Including structural damping in the amount of $g = .03$ reduced the rms wing bending moment and cg acceleration levels from 5 to 8 percent. Moving the airplane center of gravity aft by 9 percent of the MAC increased the wing bending moment and cg acceleration 2 to 3 percent.

The rms wing bending moment level was reduced about 8 percent when the wing bending stiffness was decreased to 80 percent of its nominal value.

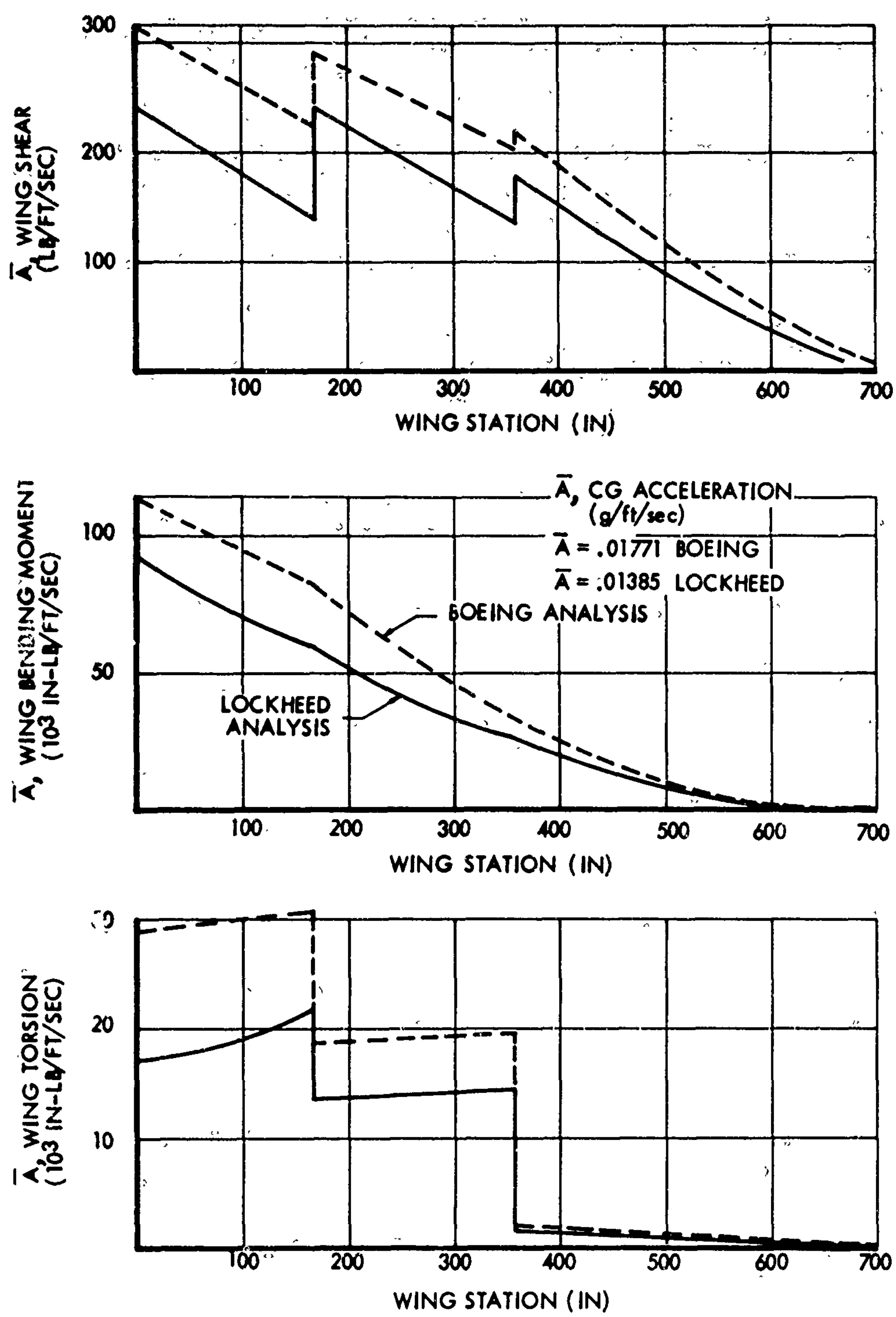

FIGURE 60. COMPARISON OF RMS LOADS FOR THE LOCKHEED MODEL 749

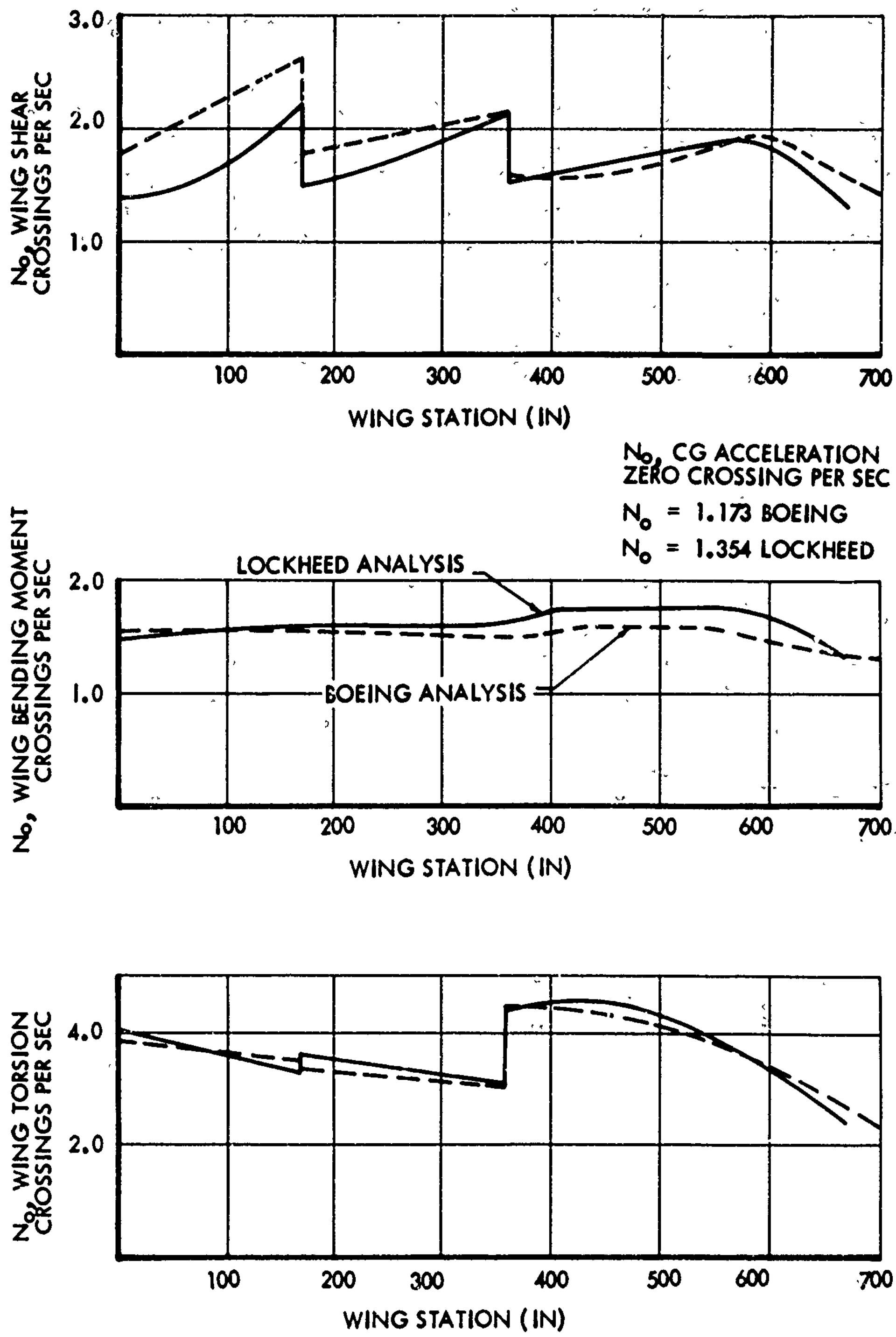

FIGURE 61. COMPARISON OF NUMBER OF ZERO CROSSINGS

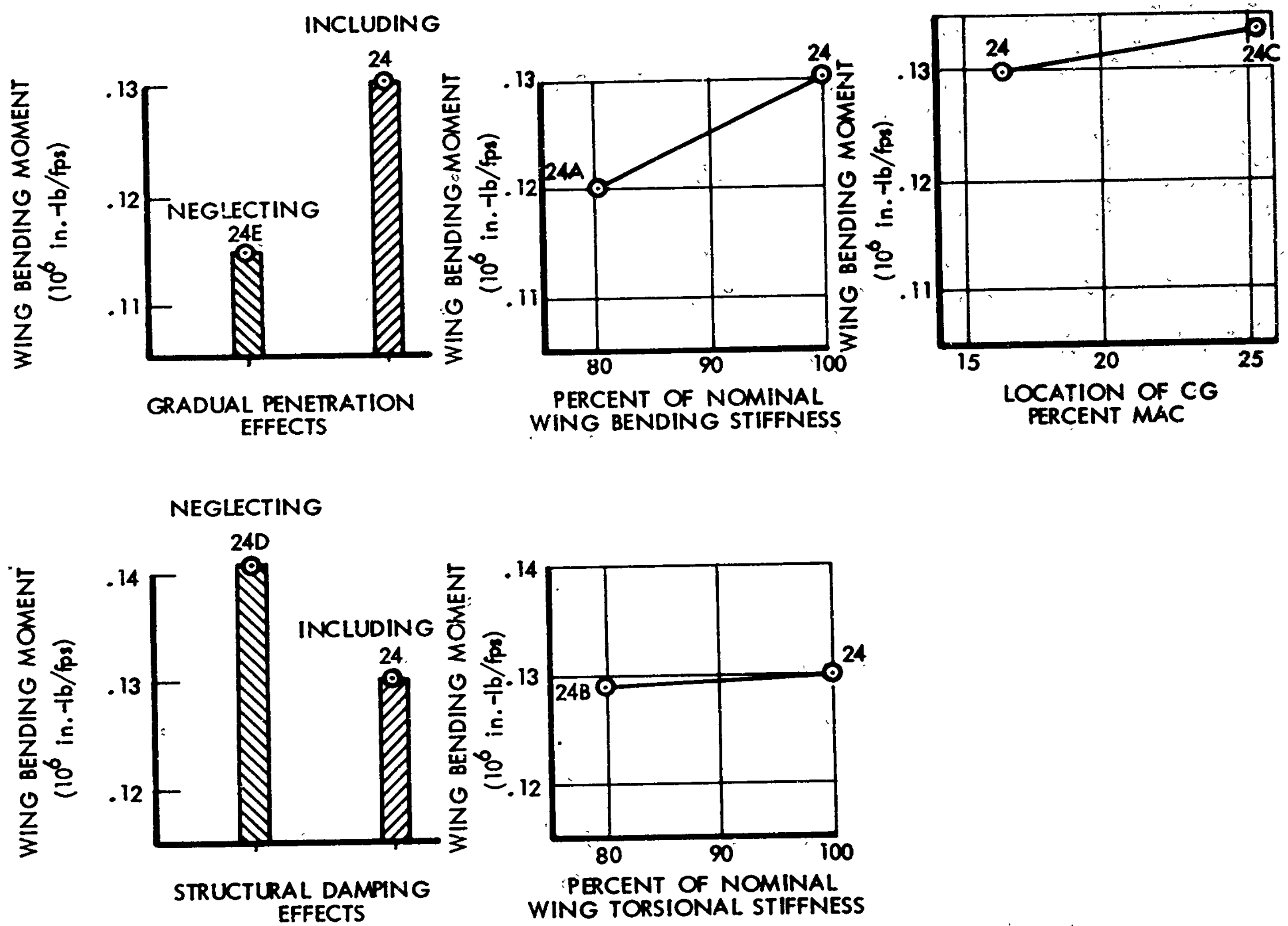

FIGURE 62. WING BENDING MOMENT RESULTS OF PARAMETRIC VARIATIONS, VERTICAL ANALYSES

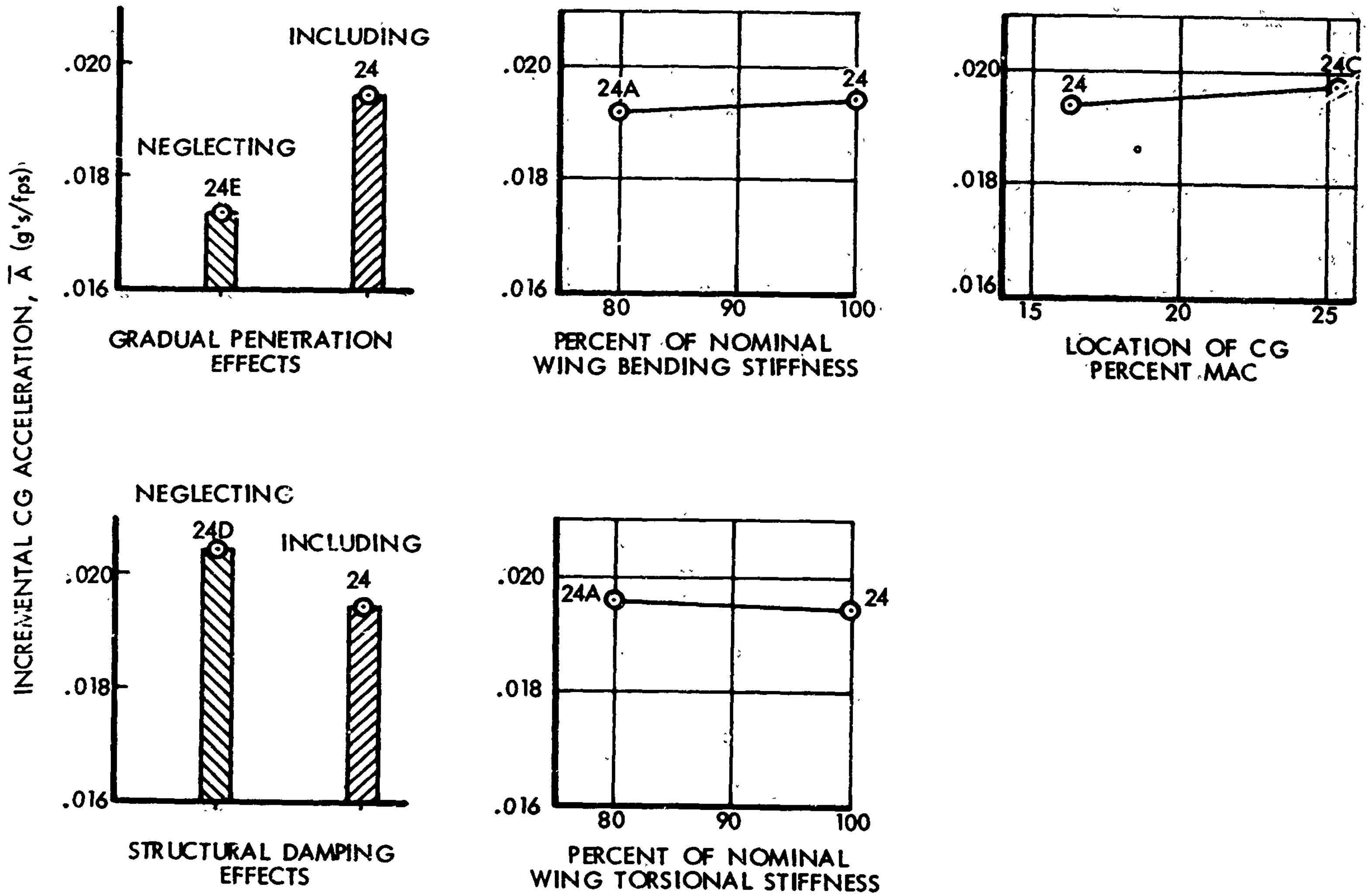

FIGURE 63. CG ACCELERATION RESULTS OF PARAMETRIC VARIATIONS, VERTICAL ANALYSES

The general conclusions that can be drawn from the vertical analyses parametric variations is that the dynamic analyses should include gradual penetration and structural damping effects.

Parametric Variations - Lateral Analyses

The results of the parametric variations conducted for the lateral analysis are given in terms of vertical tail bending moment at Fin Elastic Axis Station 158. These results are shown in Figs. 64 through 66(c). Variations in $\bar{A}$ for fin shear, bending moment, and torsion are shown in Fig. 64 for changes in airplane gross weight. The gross weight changes were made by adding wing fuel. The addition of wing fuel causes a corresponding increase in airplane yaw and roll inertia. The trends in the rms loads, therefore, reflect the influence of these inertia changes as well as the weight changes. These results indicate a 11 percent increase in the rms fin loads for a 25 percent increase in gross weight.

The variation in $\bar{A}$ for fin loads, resulting from changes in altitude, with gross weight, Mach number and true airspeed constant at 475 kt., are shown in Fig. 65. The effects of increasing altitude under these circumstances is to decrease the dynamic pressure and decrease Dutch roll damping. The reduction of Dutch roll damping would tend to increase the resulting loads; however, for this airspeed, the reduction of dynamic pressure more than offsets the effect of the damping loss, and the end result was an overall decrease in the loads. Previous studies on similar airplanes indicate that increasing the altitude at reduced airspeeds can increase the loads significantly due to a loss of Dutch roll stability.

The curves in Figs. 66(a) through 66(c) show the effects on rms fin loads of variations in the yaw damping derivative, $C_{n_{b\dot{\psi}/2V}}$, the yaw-roll coupling derivative, $C_{n_{b\dot{\phi}/2V}}$, and the airplane product of inertia, I_{xy}. As was mentioned previously in Analysis, the lateral gust loads are closely associated with the Dutch roll damping. When the Dutch roll damping is large, variation in the damping derivatives and airplane product of inertia have only a small effect on the lateral dynamic loads; however, when the amount of inherent Dutch roll damping is low, these same parameters can have a tremendous effect on the dynamic stability and the resultant dynamic loads.

Statistical Correlation Between Wing Loads

Prior to conducting the detailed combined stress analysis it was decided to obtain the correlations between the wing shear, bending moment and torsion loads. These correlation coefficients were obtained for each

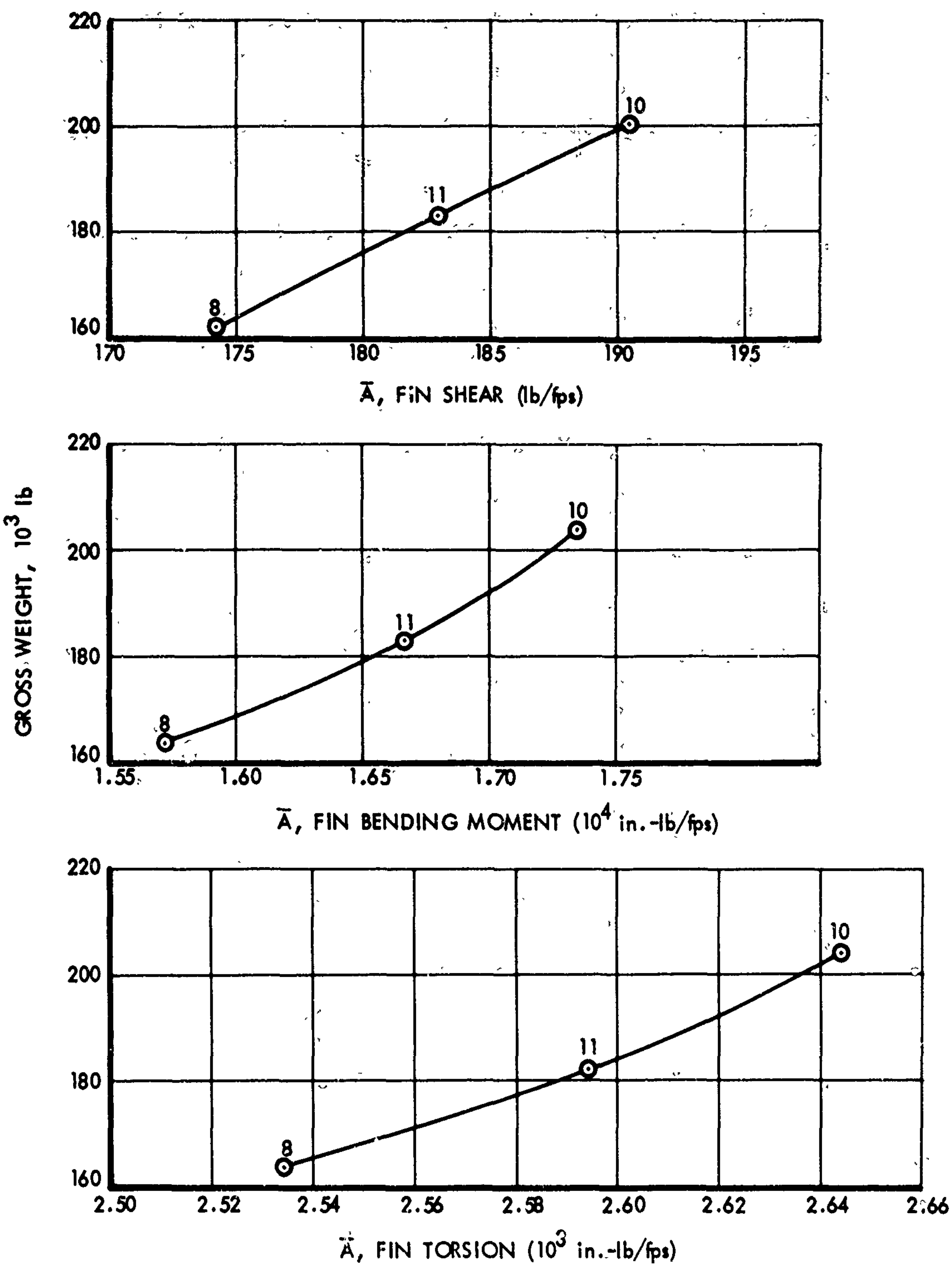

FIGURE 64. VARIATION OF RMS FIN LOADS WITH GROSS WEIGHT, FIN E.A. STATION 158

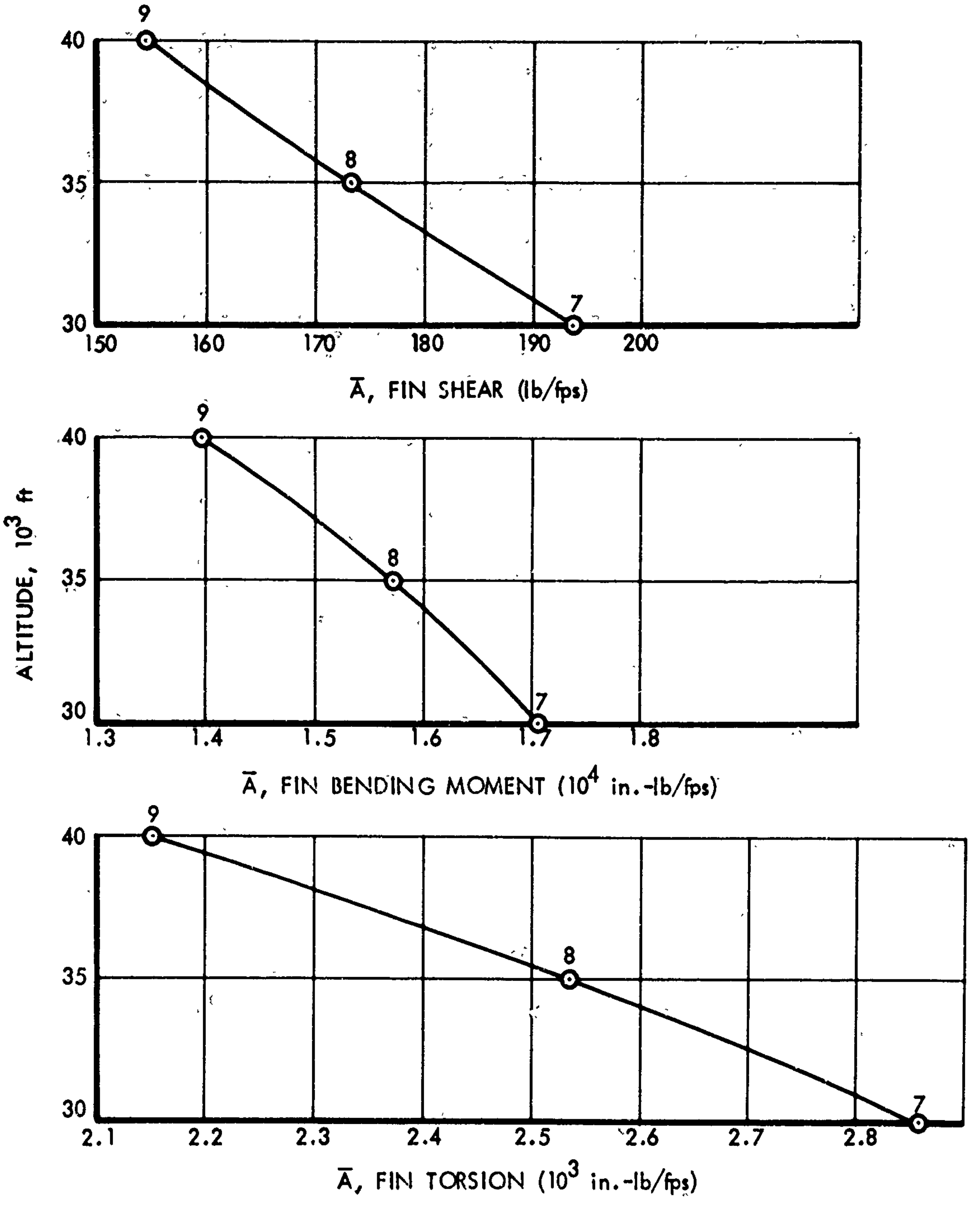

FIGURE 65. VARIATION OF RMS FIN LOADS WITH ALTITUDE, FIN E. A. STATION 158

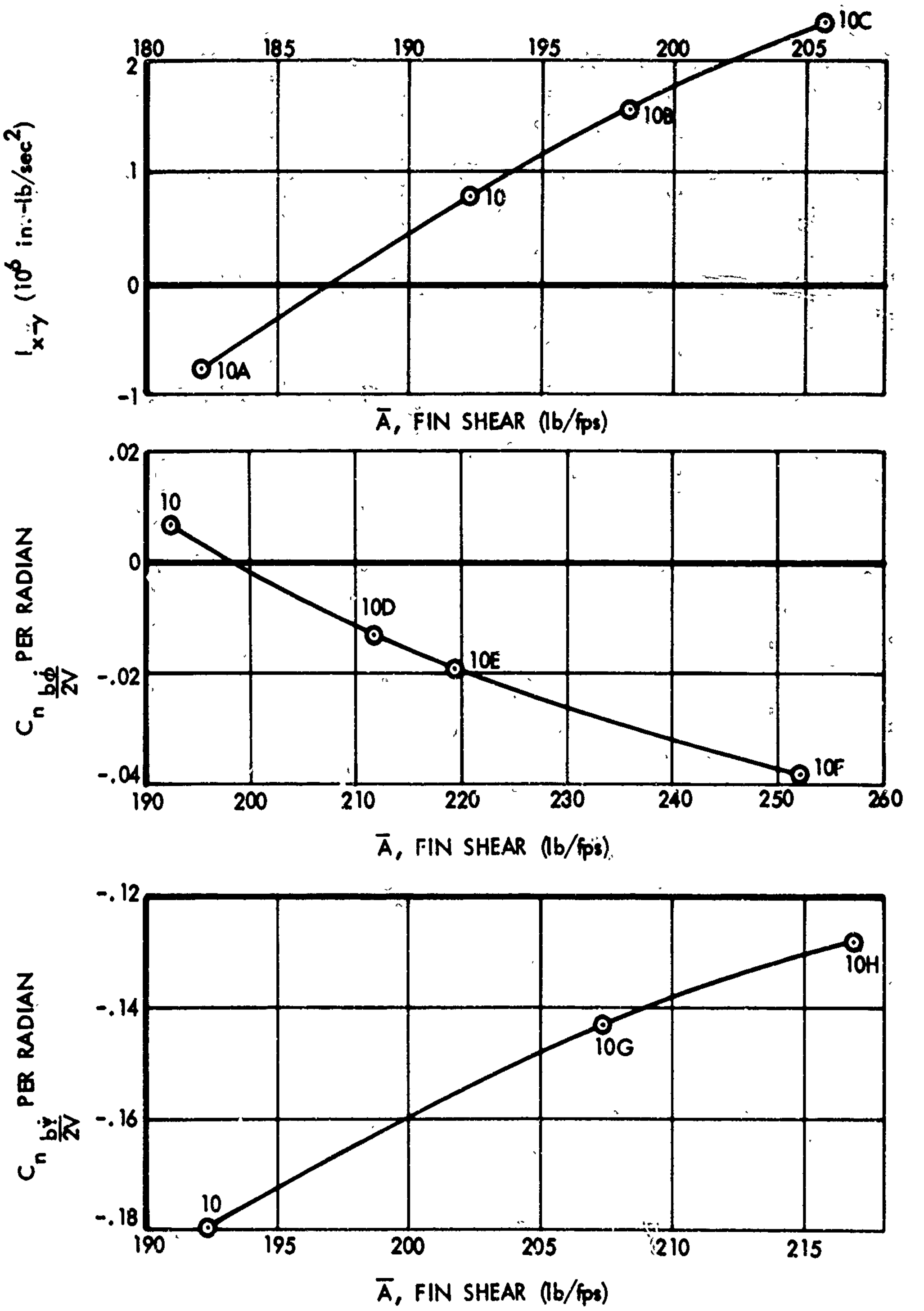

FIGURE 66. (a) FIN SHEAR RESULTS OF PARAMETRIC VARIATIONS, LATERAL ANALYSES, FIN E.A. STATION 158

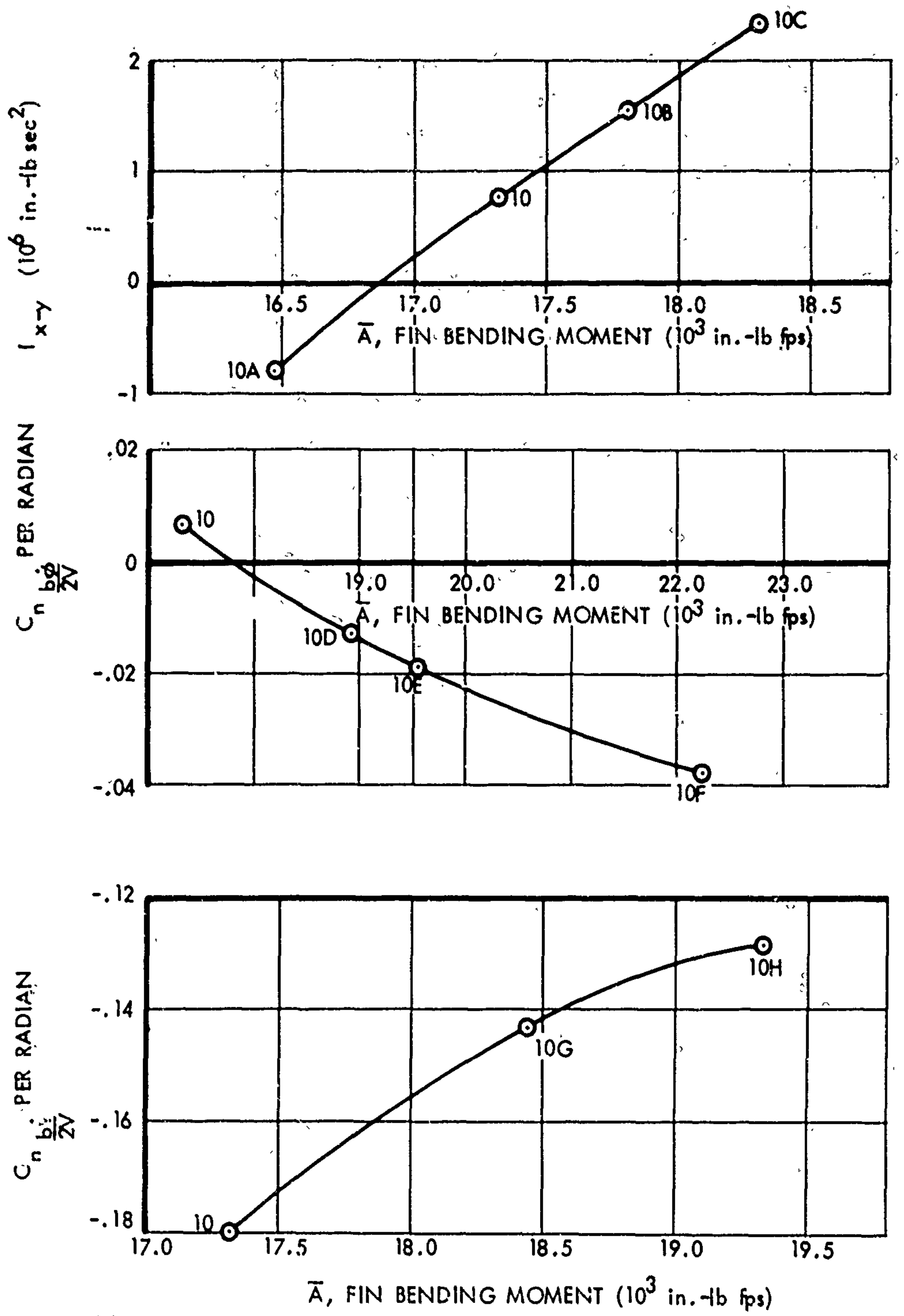

FIGURE 66. (b) FIN BENDING MOMENT RESULTS OF PARAMETRIC VARIATIONS, LATERAL ANALYSES

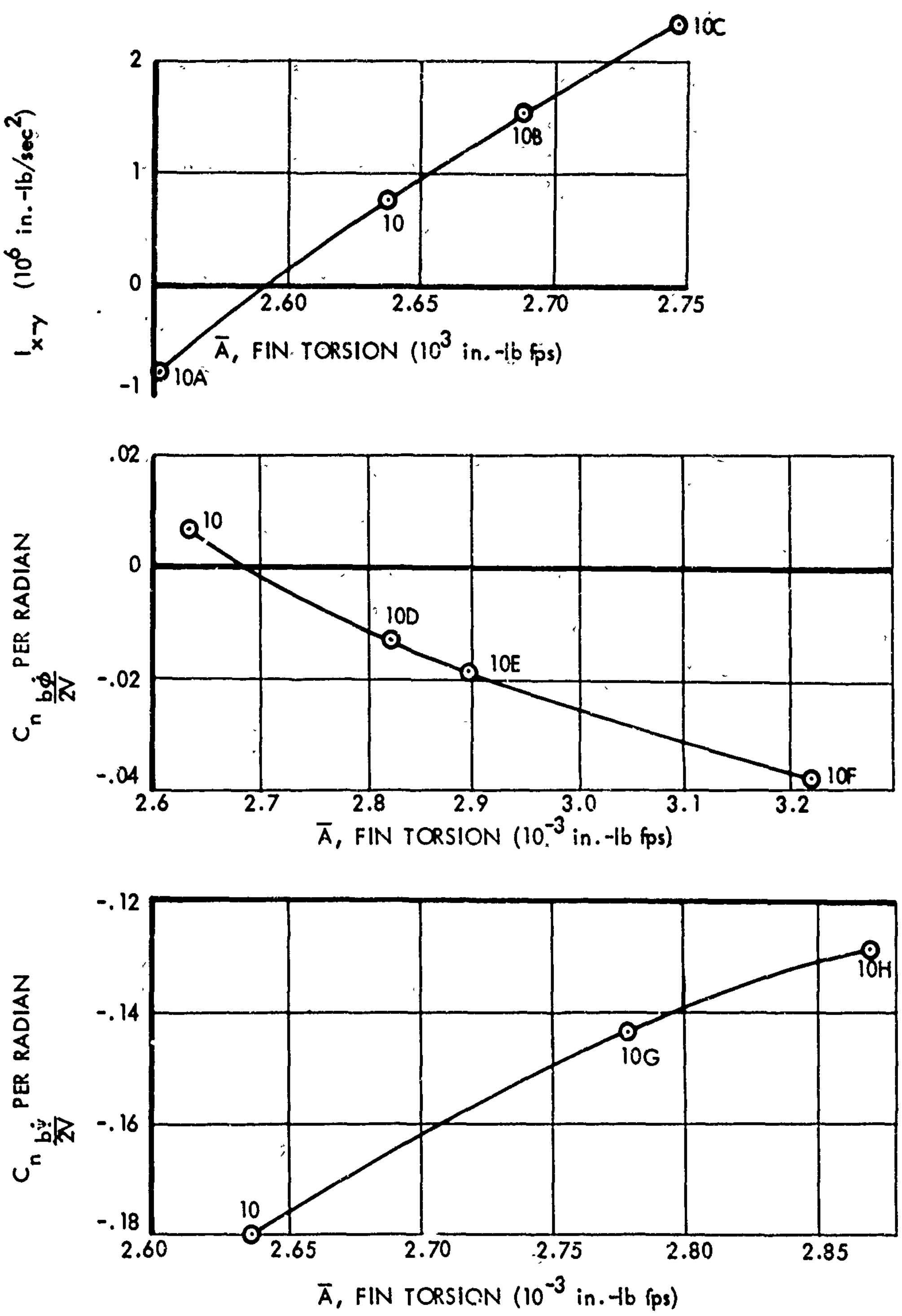

FIGURE 66 (c). FIN TORSION RESULTS OF PARAMETRIC VARIATIONS, LATERAL ANALYSES set of load quantities using cross power spectral density equations derived in Appendix B. The results are plotted versus Wing Eta Station in Fig. 67.

Outboard of the outboard nacelle the wing shear and bending moment are almost exactly correlated while the torsion and bending moment are correlated very poorly. This indicates that shear and bending are very nearly in phase but that torsion is very nearly independent of either bending moment or shear. Inboard of the outboard nacelle, the effects of the nacelle are readily apparent. The correlation between shear and bending moment is poorer due to shear loads arising from the outboard nacelle. However, the correlation between shear and torsion is improved, due to the nacelle inertia loads. A somewhat similar tendency is shown at the inboard nacelle. The correlation between the three load quantities improves inboard of the inboard nacelle. This is a result of transferring shear and bending moment into torsion as the elastic axis sweep angle changes near the wing root.

Results - RMS Stress Analysis

The individual structural elements for the detailed stress analysis were selected at locations around the critical wing, body and fin stations to give the best strength evaluation possible. Included among these elements are those which demonstrated the least margin of safety as determined by the static stress analysis.[11,12,13] The numbering system used for all the elements is the same as that used in the stress analysis referenced above. In Fig. 68 is a sketch identifying the structural elements of the wing box at Wing Eta Station .33. The elements for which design values of $\sigma_W \eta_d$ and number of exceedances were calculated are indicated by the solid circles. The structural element array and the elements analyzed for Body Stations* 540, 1040, and 1360 are shown in Figs. 69(a), 69(b), and 69(c), respectively. The same elements were analyzed in both the lateral and vertical analyses with the exception of Forward Body Station 540 which was analyzed for the vertical analyses only. The detailed stresses for the critical Vertical Tail Elastic Axis Station 158 were calculated for the elements shown in Fig. 70. The stress analysis for the fin was conducted assuming the elements on the left and right side were symmetrical about the fin chord line.

The rms loads were transformed into axial and shear stresses using the stress coefficients obtained from the conventional stress analysis. The rms stress quantities for the structural elements at Wing Eta Station .33, Condition 24C, are shown in Tables 10(a) and 10(b). The rms shear,

*Corresponds to Body Balance Stations 480, 1000, and 1320 (see Fig. 21)

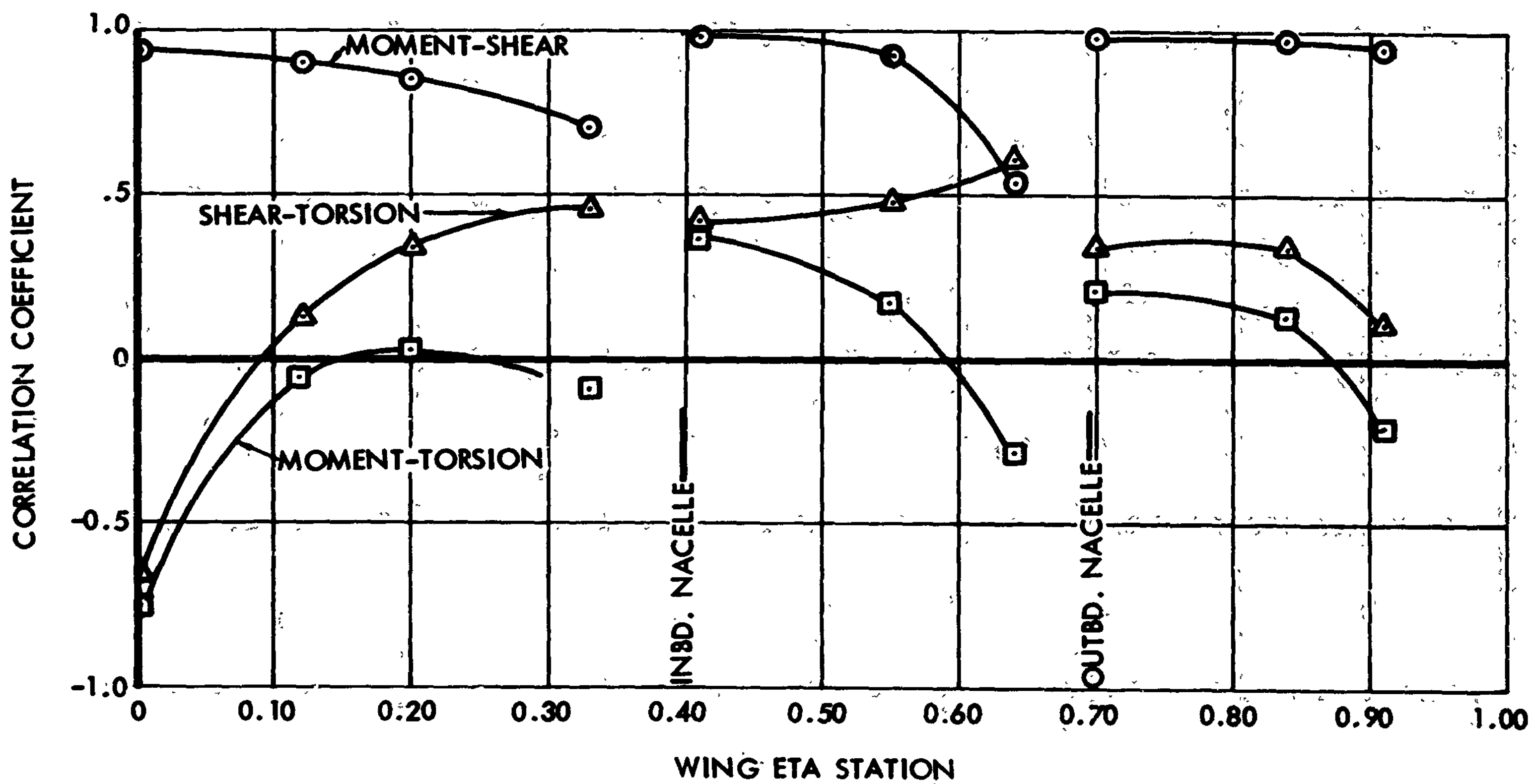

FIGURE 67. SPANWISE CORRELATION BETWEEN THE WING LOADS OF SHEAR-BENDING MOMENT-TORSION - CONDITION 24

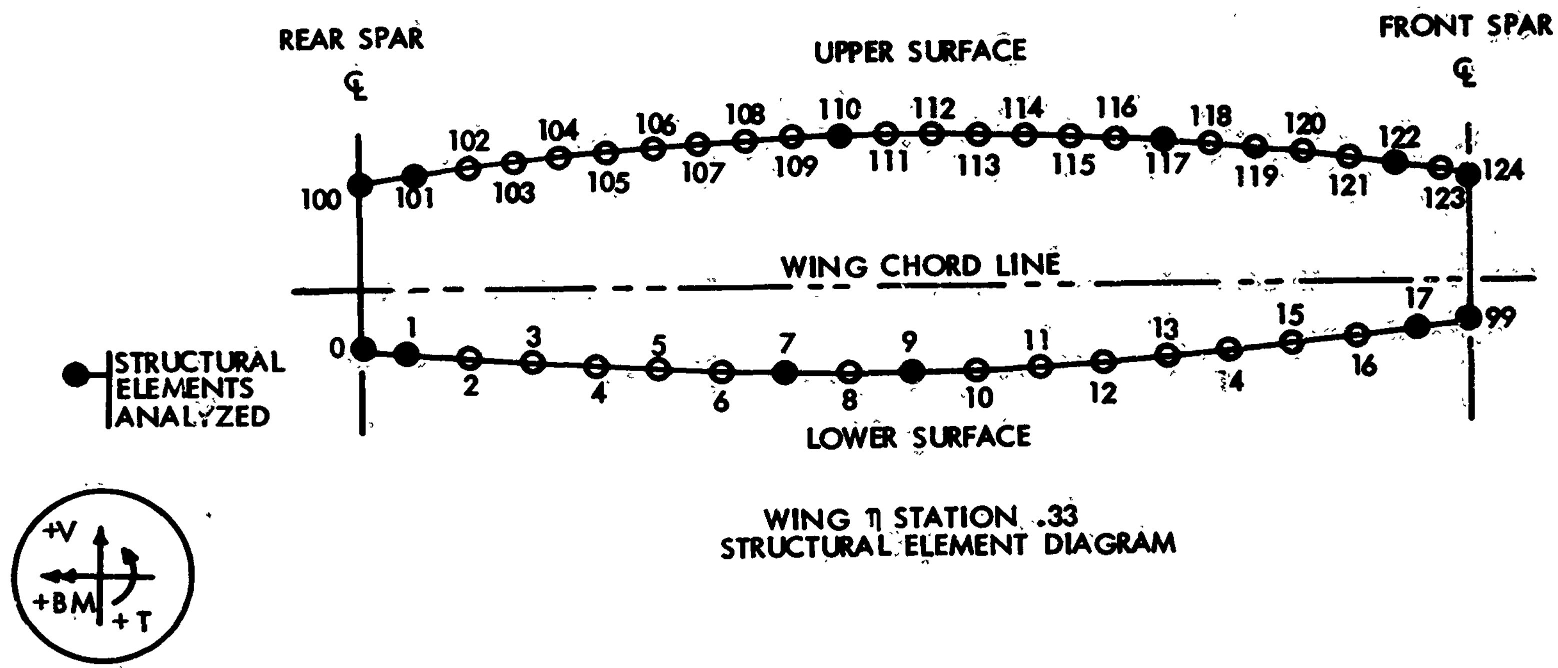

FIGURE 68. ARRAY OF STRUCTURAL ELEMENTS, WING ETA STATION .33

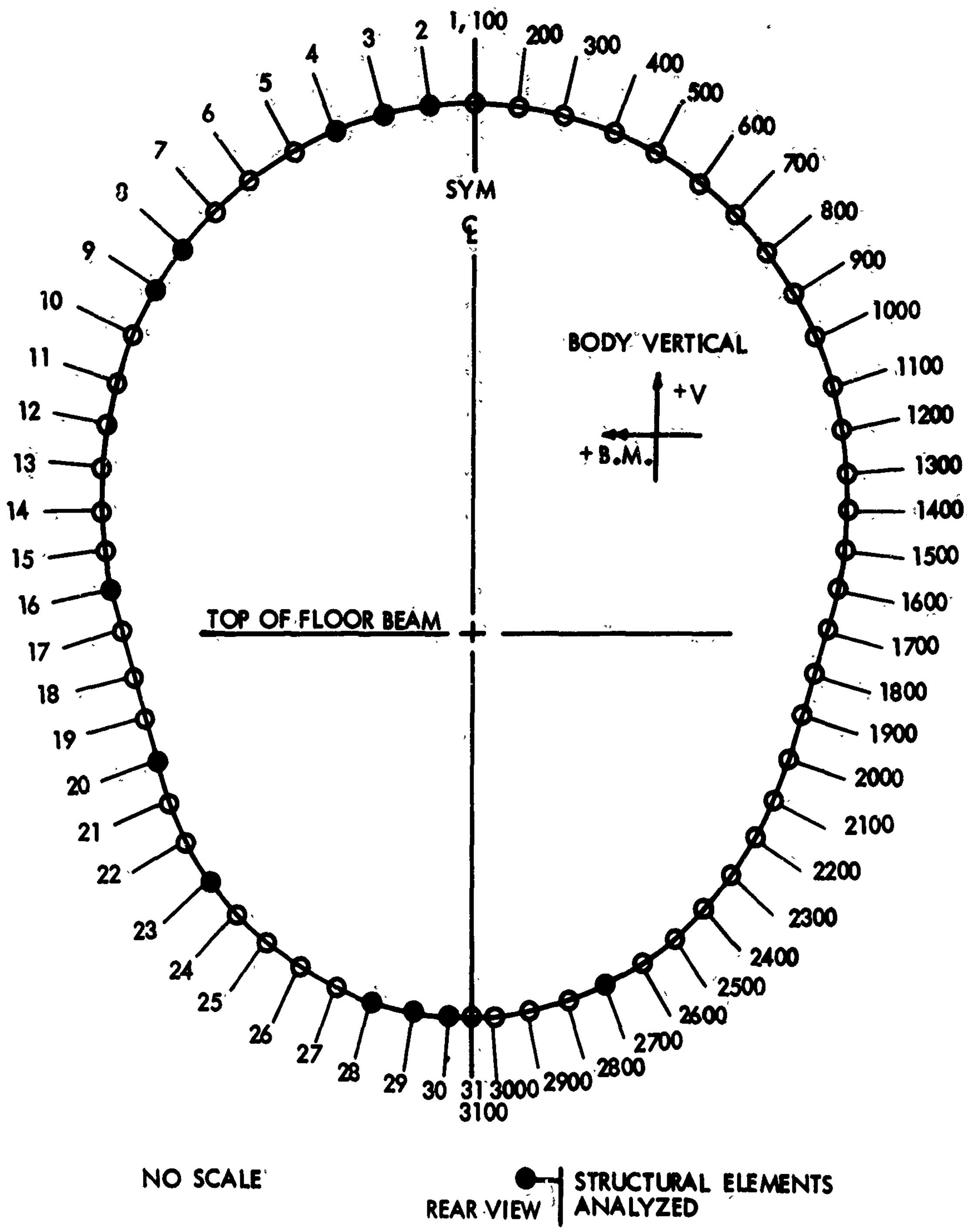

FIGURE 69 (a). ARRAY OF STRUCTURAL ELEMENTS, BODY STATION 540

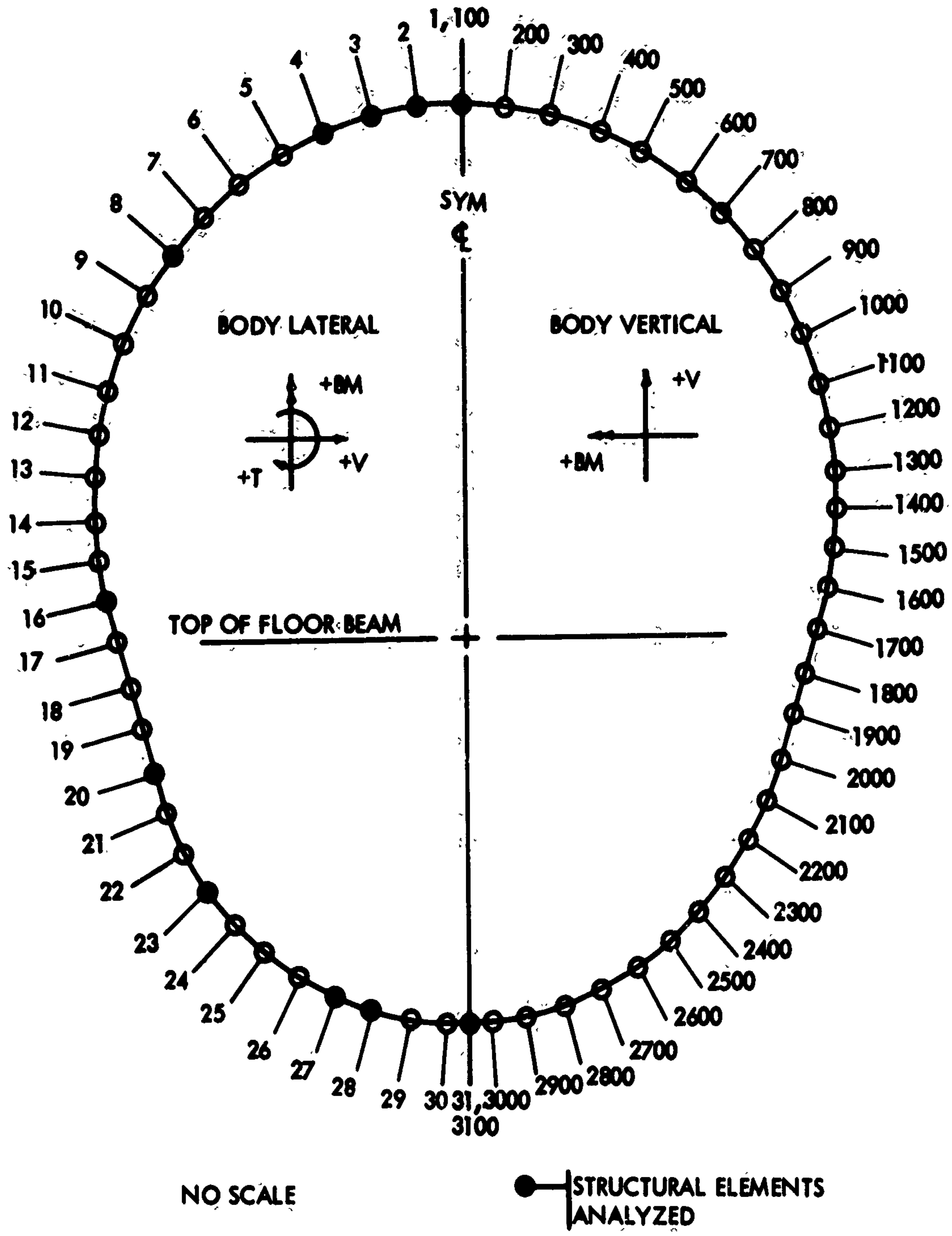

REAR VIEW

FIGURE 69 (b). ARRAY OF STRUCTURAL ELEMENTS, BODY STATION 1040

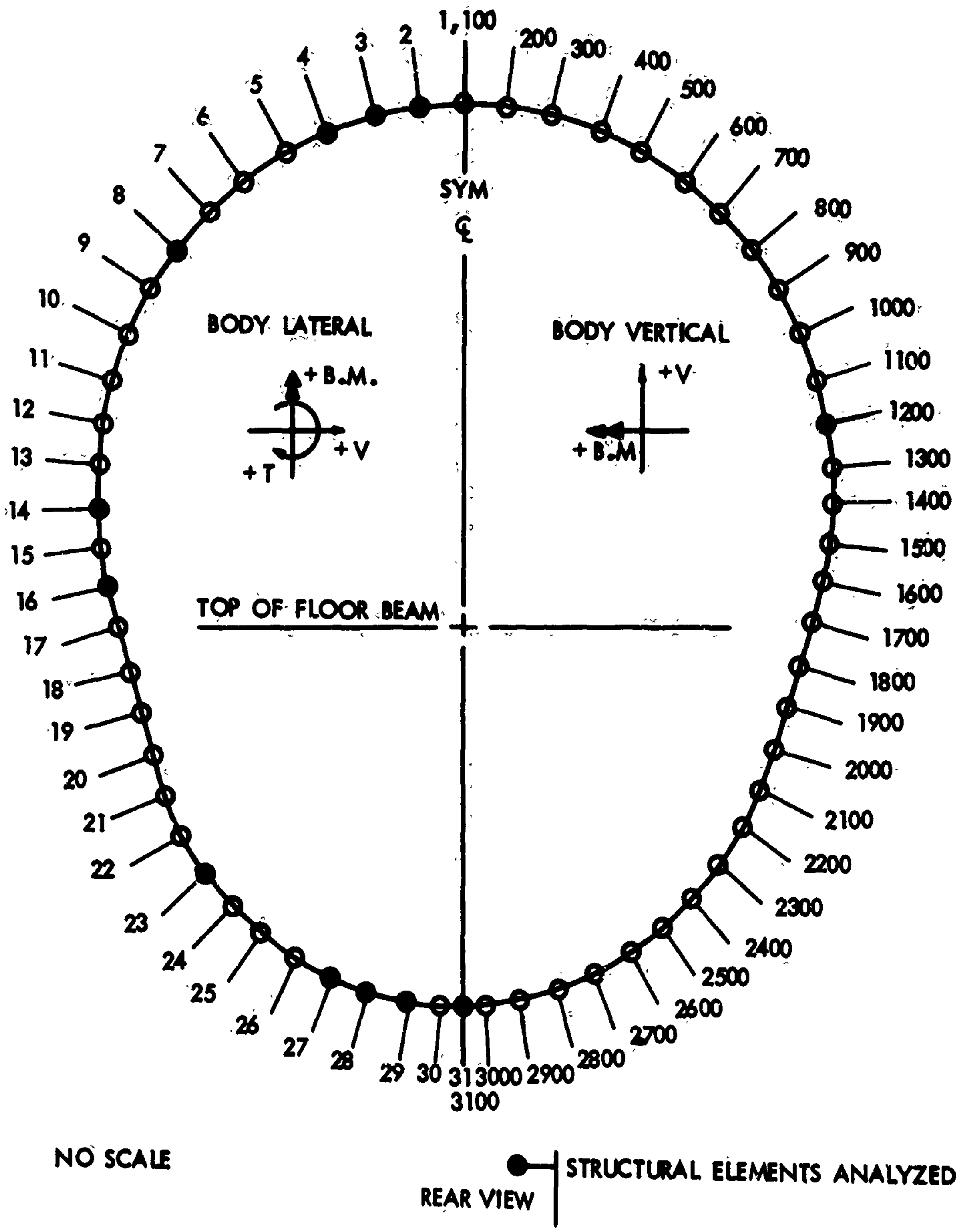

FIGURE 69 (c). ARRAY OF STRUCTURAL ELEMENTS, BODY STATION 1360

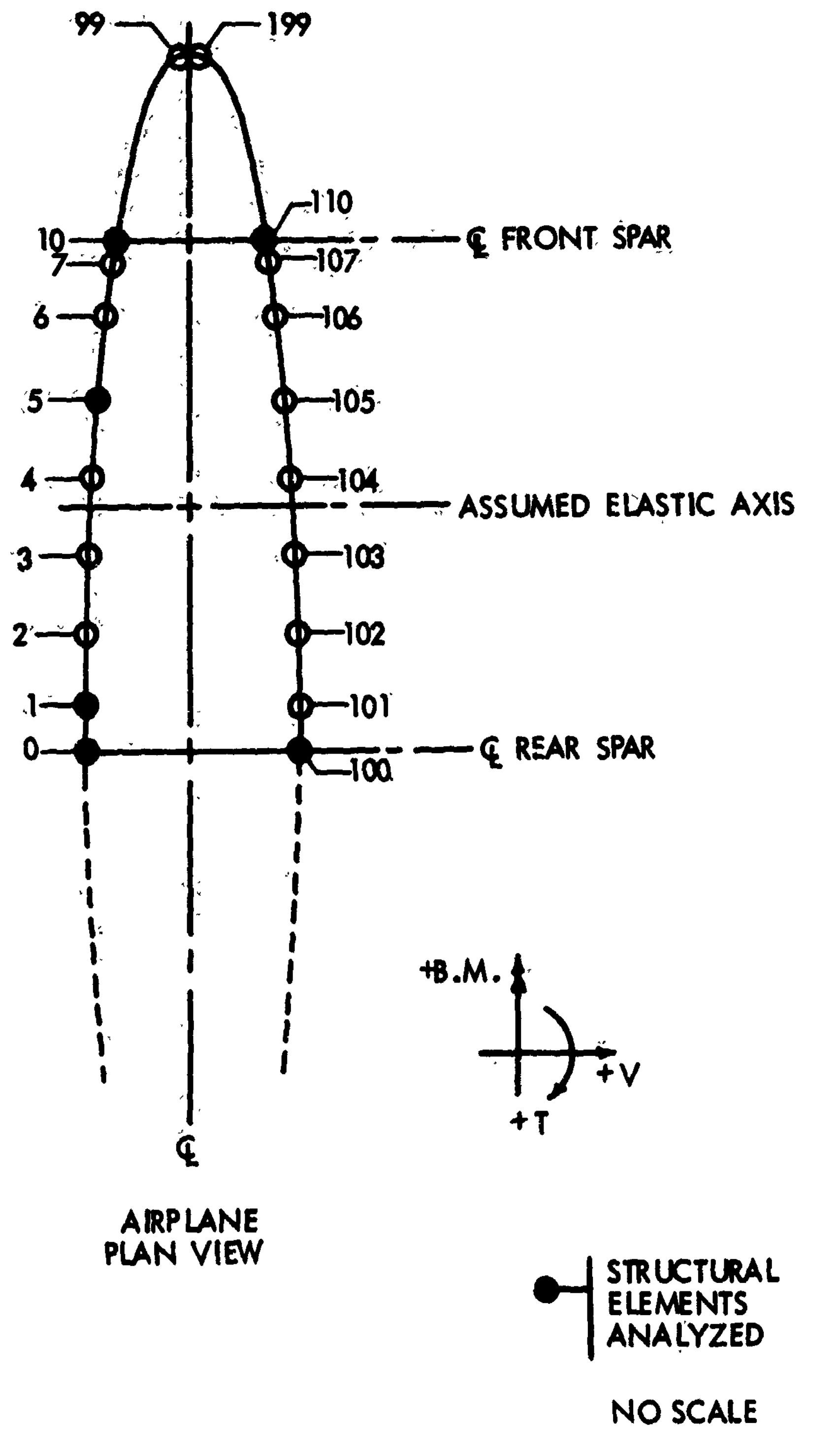

FIGURE 70. ARRAY OF STRUCTURAL ELEMENTS, FIN ELASTIC AXIS STATION 158

TABLE 10a. RMS STRESS AND ZERO CROSSINGS

7200 CONDITION 24C VERTICAL GUST ANALYSIS

WING ETA STATION=.33

ELEMENT NO.	ABAR (PSI)			ZERO CROSSINGS PER ST		
	SHEAR STRESS	SKIN STRESS	SEGMENT STRESS	SHEAR STRESS	SKIN STRESS	SEGMENT STRESS
0	30.3210	166.7673	157.9920	0.0030208	0.0014958	0.0014958
1	40.4127	176.3221	169.4365	0.0037390	0.0014958	0.0014958
2	40.7619	186.3639	169.7639	0.0036741	0.0014958	0.0014958
3	41.2727	197.3093	190.6673	0.0036122	0.0014958	0.0014958
4	37.9697	205.7631	199.5441	0.0035650	0.0014958	0.0014958
5	40.1347	213.4755	207.6770	0.0035316	0.0014958	0.0014958
6	43.4356	219.2919	213.4962	0.0035332	0.0014958	0.0014958
7	45.4972	222.2269	216.5099	0.0035647	0.0014958	0.0014958
8	56.9277	223.1722	217.4147	0.0034606	0.0014958	0.0014958
9	62.2240	222.3742	215.0876	0.0034626	0.0014958	0.0014958
10	67.0859	220.1669	212.8756	0.0036670	0.0014958	0.0014958
11	71.5464	216.3543	210.0245	0.0037255	0.0014958	0.0014958
12	75.9709	209.9701	203.6529	0.0037511	0.0014958	0.0014958
13	80.1559	202.9647	196.6364	0.0037741	0.0014958	0.0014958
14	100.5336	194.0499	188.1799	0.0037966	0.0014958	0.0014958
15	104.7739	186.0110	177.4001	0.0039117	0.0014958	0.0014958
16	112.9217	173.6922	167.4216	0.0039219	0.0014958	0.0014958
17	116.0267	161.5132	154.9601	0.0039149	0.0014958	0.0014958
99	101.5308	150.4909	141.5567	0.0039464	0.0014958	0.0014958
199	105.1913	115.5307	106.5597	0.0039464	0.0014958	0.0014958
122	127.0940	163.2238	136.2711	0.0030392	0.0014958	0.0014958
121	123.4072	155.2603	146.8677	0.0038296	0.0014958	0.0014958
120	129.9629	165.9566	155.7021	0.0039215	0.0014958	0.0014958
119	117.3099	175.1706	165.0159	0.0039107	0.0014958	0.0014958
118	153.5290	183.2063	173.0497	0.0037905	0.0014958	0.0014958
117	104.0226	190.2205	181.7216	0.0037467	0.0014958	0.0014958
116	73.1264	195.0923	186.9695	0.0037650	0.0014958	0.0014958
115	69.7328	200.7296	189.5091	0.0037612	0.0014958	0.0014958
114	65.3899	204.2649	193.0591	0.0037149	0.0014958	0.0014958
113	61.5725	207.1770	195.7646	0.0036496	0.0014958	0.0014958
112	57.0239	208.4092	200.3135	0.0036537	0.0014958	0.0014958
111	52.6040	209.1640	200.6590	0.0035661	0.0014958	0.0014958
110	47.3949	208.2136	198.9210	0.0035701	0.0014958	0.0014958
109	45.2213	205.0341	197.0277	0.0035290	0.0014958	0.0014958
108	42.4699	202.4960	193.6457	0.0035099	0.0014958	0.0014958
107	40.5099	197.0759	188.2693	0.0035022	0.0014958	0.0014958
106	39.0556	191.3310	183.0009	0.0035107	0.0014958	0.0014958
105	37.5977	183.6703	175.3420	0.0035367	0.0014958	0.0014958
104	36.7272	175.3636	166.9744	0.0035760	0.0014958	0.0014958
103	36.2156	165.7705	157.2075	0.0036270	0.0014958	0.0014958
102	36.0175	155.5405	147.0695	0.0036491	0.0014958	0.0014958
101	36.0745	144.6829	136.0329	0.0037530	0.0014958	0.0014958
100	28.9651	132.5006	124.1004	0.0038267	0.0014958	0.0014958

TABLE 10b. CORRELATION COEFFICIENTS AND STRESS RATES

7200 CONDITION 24C VERTICAL GUST ANALYSIS:

WING ETA STATION=.33

ELEMENT NO.	CORRELATION COEFFICIENT	RMS STRESS RATES (PSI/FPS) SHEAR	SKIN	SEGMENT
0	-0.4196008	0.7290667	1.9673769	1.6766422
1	-0.4071061	0.9596933	1.6971782	1.9026445
2	-0.3961229	0.9610626	1.7327596	1.5999602
3	-0.3799018	0.9159321	1.8551790	1.7919962
4	-0.3595776	0.8506765	1.9330823	1.8763719
5	-0.3271068	0.8964102	2.0063670	1.9519778
6	-0.2893156	0.9666659	2.0610339	2.0065639
7	-0.2716043	1.0132090	2.0886180	2.0356390
8	-0.1119215	1.2929790	2.0979036	2.0631987
9	-0.1465342	1.4320739	2.0900031	2.0215192
10	-0.1808676	1.5583656	2.0692389	2.0007301
11	-0.1557687	1.6767689	2.0336240	1.9739907
12	-0.1439021	1.7907827	1.9734977	1.9160693
13	-0.1363917	1.9094961	1.9079810	1.8601075
14	-0.1259910	2.3982306	1.8237966	1.7690290
15	-0.1204087	2.6067001	1.7296387	1.6710713
16	-0.1163996	2.7036629	1.6370851	1.5739620
17	-0.1137966	2.7956613	1.5179956	1.4964079
18	-0.1109698	2.6517631	1.4144017	1.5394139
123	0.1109711	2.9619042	1.0899906	1.0019102
122	0.1149222	3.0667776	1.3469940	1.2007962
121	0.1294670	2.9799063	1.4992769	1.3003409
120	0.1315858	2.9039276	1.5508191	1.4633797
119	0.1393319	2.8087062	1.6463557	1.5509162
118	0.1477039	2.7099610	1.7216616	1.6204221
117	0.1567680	2.6734053	1.7079790	1.7079634
116	0.1692769	1.7299665	1.8411106	1.7372396
115	0.1960135	1.6276444	1.9864497	1.7011096
114	0.2000368	1.5262647	1.9199301	1.8144022
113	0.2176512	1.4258740	1.9671713	1.8617902
112	0.2376594	1.3276647	1.9674738	1.8026641
111	0.3501943	1.1707282	1.9656994	1.9059100
110	0.2292349	1.0576694	1.9569115	1.9695704
109	0.3230850	1.0030137	1.9349870	1.8517021
108	0.3474925	0.9409776	1.9011769	1.6293717
107	0.3698141	0.8914173	1.8522352	1.7694999
106	0.3945373	0.8569762	1.7982406	1.7199640
105	0.4030996	0.8350140	1.7242410	1.8679665
104	0.4149312	0.8249578	1.6491670	1.9601932
103	0.4214679	0.8295215	1.5599641	1.6702795
102	0.4235112	0.8344090	1.4619450	1.3021606
101	0.4216023	0.8507290	1.3598109	1.2749162
100	0.4156718	0.6964119	1.2453180	1.1671190

skin, and segment stress levels, $\bar{A}$, are given in Table 10(a) with their associated number of zero crossings. Table 10(b) contains the correlation coefficients between the shear and axial stresses and the respective stress rates. Similar values were calculated for all the structural elements indicated in Figs. 68 through 70.

Results - Statistical Analysis

Following the procedure outlined in the Analysis section, the rms stresses, correlation coefficients, and stress rates were used to determine the probability of exceeding limit strength, $P(MS < 0, \sigma_W)$, and the number of times per hour that the limit strength envelope is penetrated. The resultant probabilities, $P(MS < 0, \sigma_W)$, are given in Table 11 for Structural Element 9, Condition 24C. The probability, $P(MS < 0, \sigma_W)$, for all the structural elements analyzed by the design envelope approach were plotted and are shown in Figs. 71(a) through 74(d). The most critical element for each profile condition, i.e., the element which demonstrates the highest probability of exceeding limit strength, was selected using the techniques described on Page 58. The values resulting from the multiplication of these critical $P(MS < 0, \sigma_W)$ with $\hat{f}(\sigma_W)$ are shown in Figs. 75 through 78. The maximum values of these overall probability curves were used with the curves of $P(\Delta n > \Delta n_1)\hat{f}(\sigma_W)$ in Figs. 79 and 80 to determine the design incremental cg acceleration. The design levels of $\sigma_W \eta_d$ and $\sigma_V \eta_d$ were then calculated and appear in Table 12. Corresponding exceedance ratios as determined by Eq. (15) are also given in Table 12.

The altitude variation of $\sigma_W \eta_d$ determined by the joint probability method is shown in Fig. 81 for Wing Eta Station .33 and for the vertical tail E. A. Station 158. Similar information is given in Fig. 82.

The altitude trends obtained by the joint probability approach indicate that the critical altitude of 23,500 ft. for the lateral analyses and 22,000 ft. for the vertical analyses as chosen by the bending moment criteria were correct.

The variation of $\sigma_W \eta_d$ around the wing structural box at Wing Eta Station .33, Condition 24C, as determined by the joint probability method, is shown in Fig. 83. The static margin of safety for each element as obtained by the static stress analysis [12] for a high bending moment condition is also shown in Fig. 83. The comparison indicates that the strength capability as determined by the statistical approach exhibits the same trend as the static margin of safety. There is, however, a difference in which element is most critical. Element 9 and the lower surface has the lowest margin of safety while Elements 117 and 122 on the upper surface display the lowest $\sigma_W \eta_d$. The significance of this

TABLE 11. VALUES OF P(MS<0) f (σ_w)

720B CONDITION 24C VERTICAL GUST ANALYSIS

WING ETA STATION = 0.33 STRUCTURAL ELEMENT 9

TURBULENCE PARAMETERS

P1 = 0.032000
P2 = 0.000125
B1 = 3.200000
B2 = 11.700000

1G STRESSES (PSI)

SHEAR	SKIN	SEGMENT
-2240.0	12221.0	12498.0

V TRUE (FT/SEC) =810.7

RMS GUST VELOCITY (FT/SEC)	PROBABILITY OF EXCEEDING LIMIT DESIGN STRENGTH	F (SIGW)	P X F(SIGW)
28.	0.	0.4864215E-06	0.
29.	0.	0.3949974E-06	0.
30.	0.	0.3184221E-06	0.
31.	0.00005	0.2548235E-06	0.1392634E-10
32.	0.00014	0.2024432E-06	0.2825186E-10
33.	0.00025	0.1596593E-06	0.3994703E-10
34.	0.00039	0.1250008E-06	0.4921112E-10
35.	0.00058	0.9715360E-07	0.5611083E-10
40.	0.00238	0.2469449E-07	0.5878047E-10
50.	0.01313	0.9224421E-09	0.1211255E-10
60.	0.03635	0.1659663E-10	0.6032457E-12
70.	0.07136	0.1438279E-12	0.1026337E-13
80.	0.11492	0.6003548E-15	0.6899351E-16
90.	0.16345	0.1207021E-17	0.1972825E-18
100.	0.21403	0.1168864E-20	0.2501691E-21
110.	0.26462	0.5451987E-24	0.1442718E-24
120.	0.31390	0.1224863E-27	0.3844790E-28
130.	0.36102	0.1325449E-31	0.4785148E-32
140.	0.40553	0.6908435E-36	0.2801543E-36
150.	0.44717	0.	0.
160.	0.48588	0.	0.

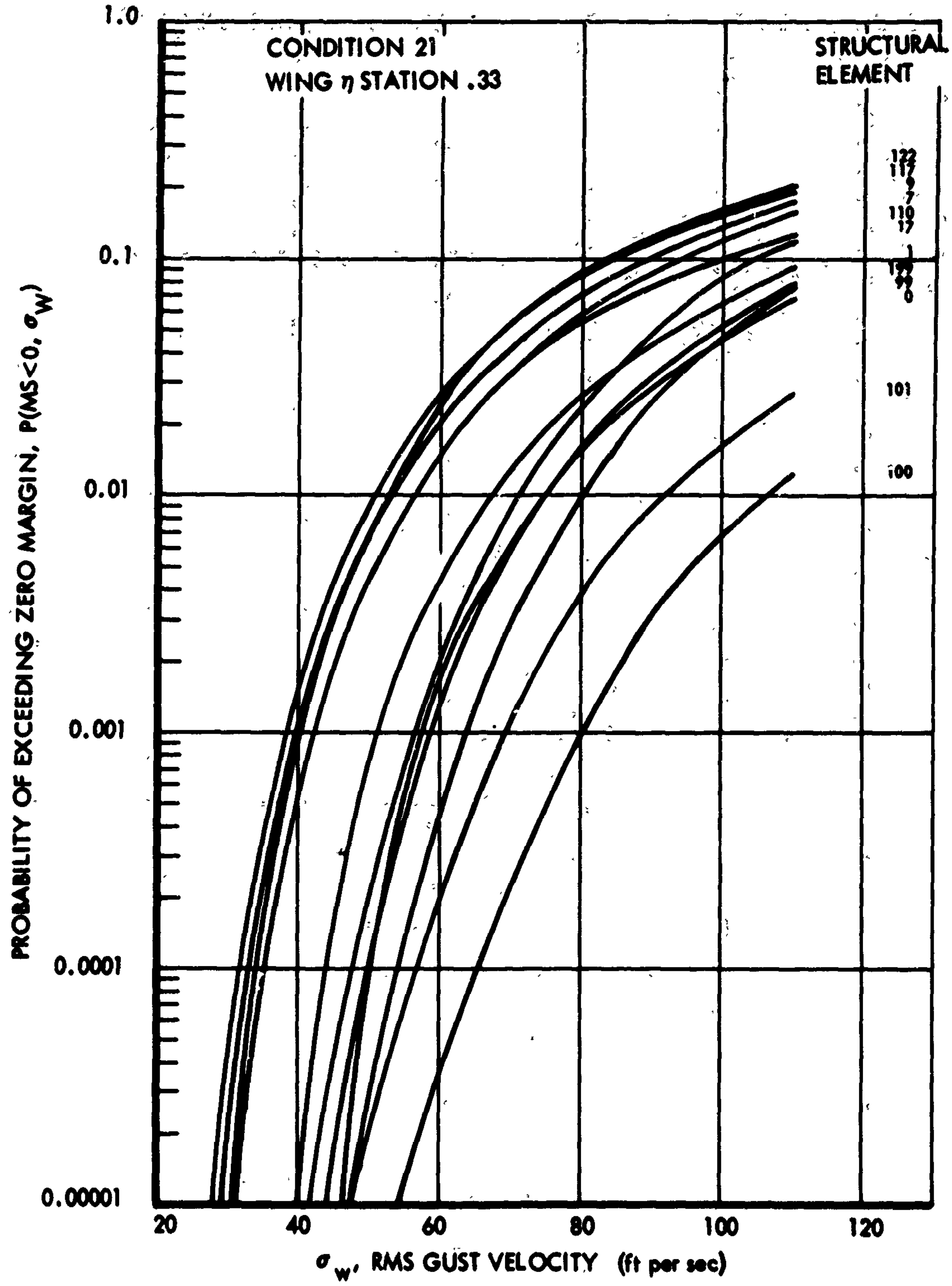

FIGURE 71 (a). PROBABILITY OF EXCEEDING ZERO MARGIN - CONDITION 21

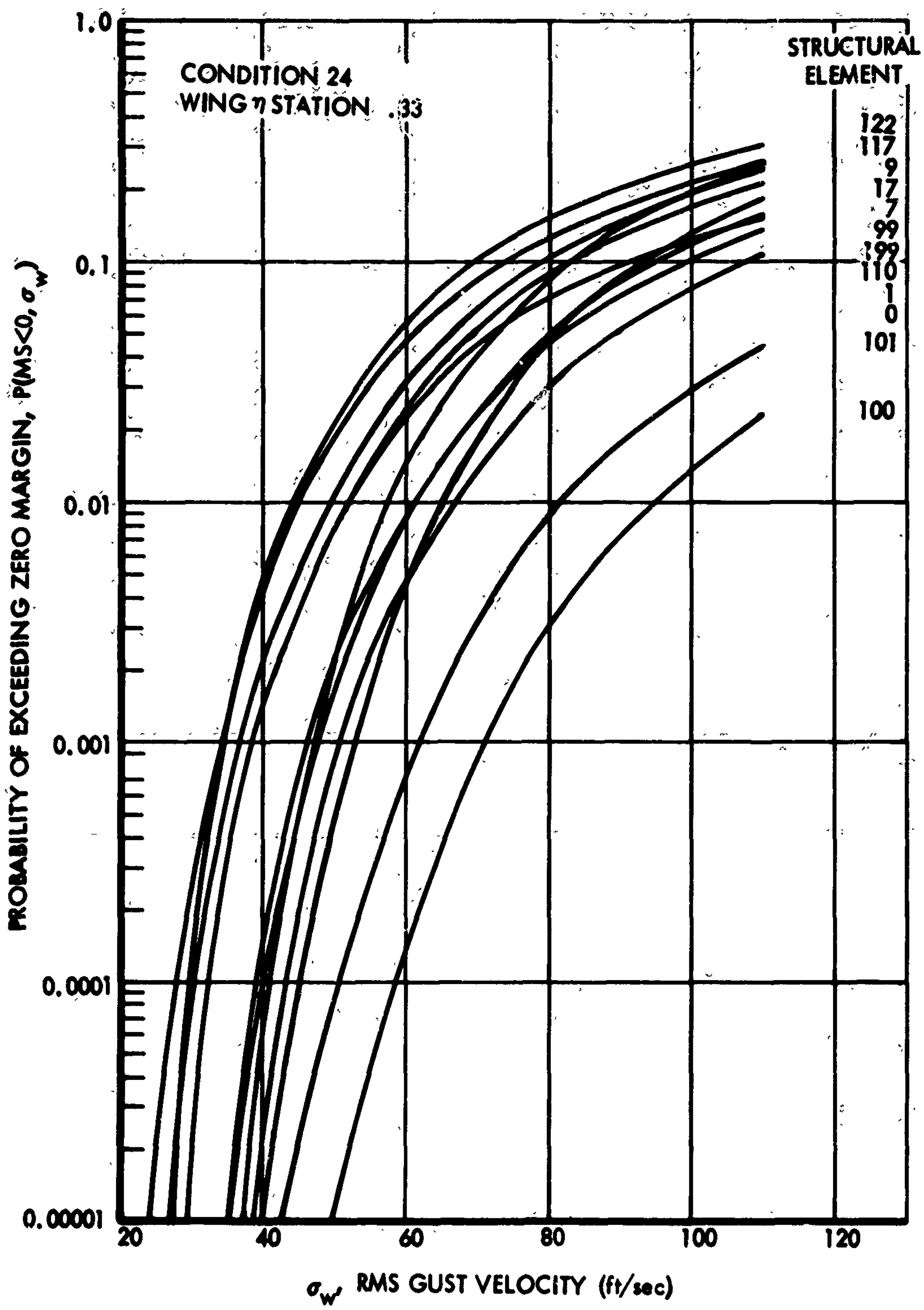

FIGURE 71 (b). PROBABILITY OF EXCEEDING ZERO MARGIN - CONDITION 24

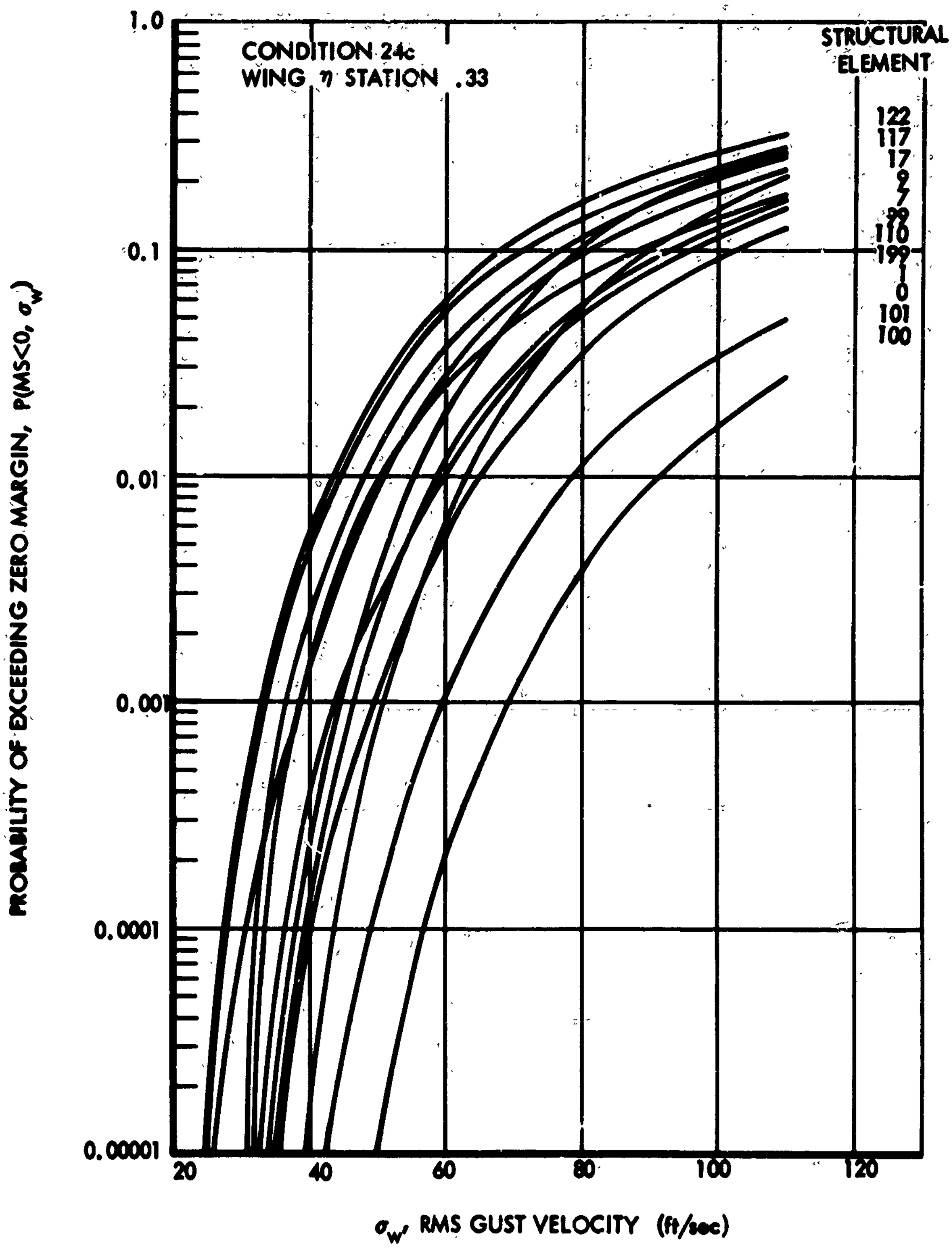

FIGURE 71 (c). PROBABILITY OF EXCEEDING ZERO MARGIN - CONDITION 24C

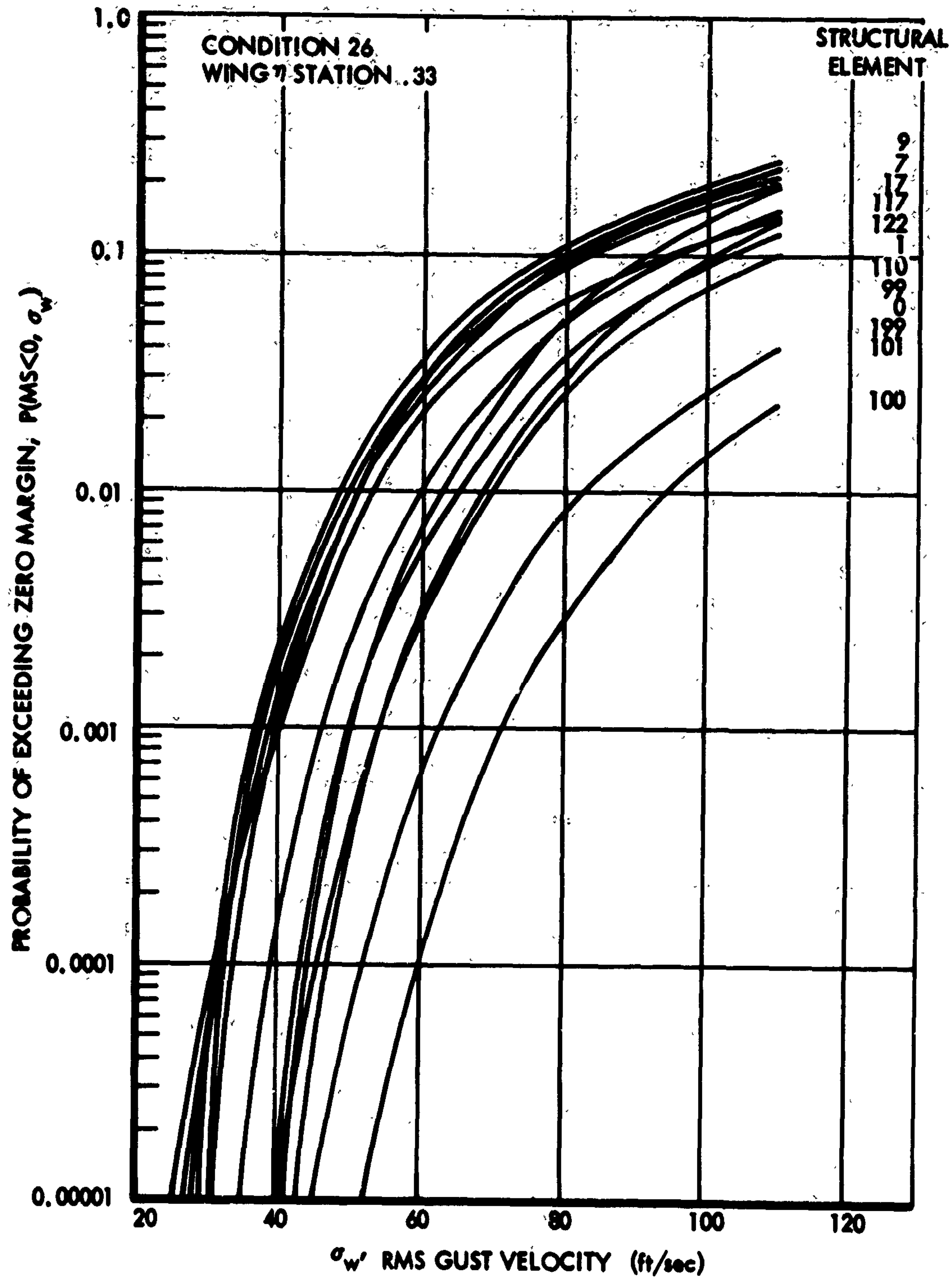

FIGURE 71 (d). PROBABILITY OF EXCEEDING ZERO MARGIN - CONDITION 26

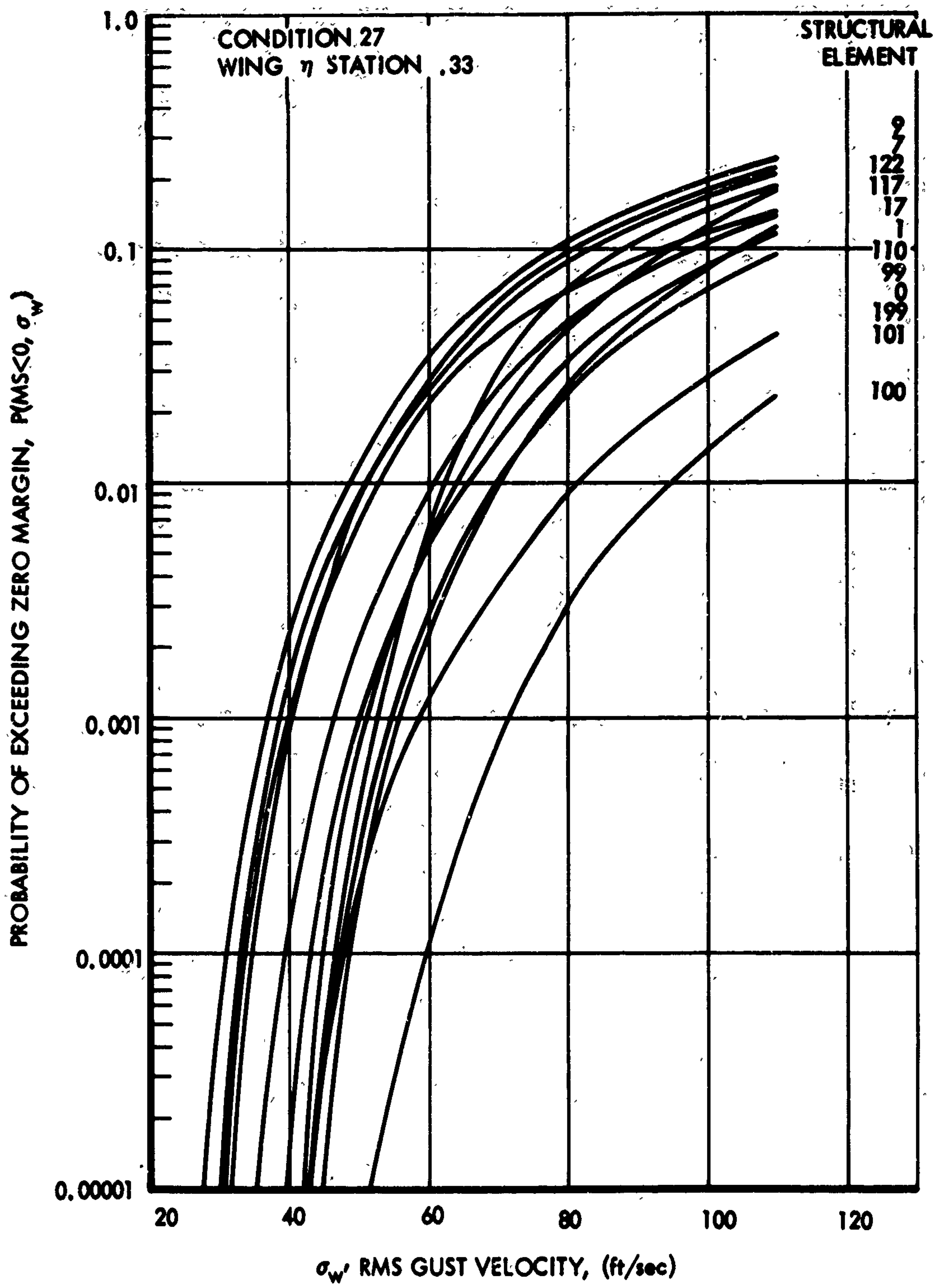

FIGURE 71 (e). PROBABILITY OF EXCEEDING ZERO MARGIN - CONDITION 27

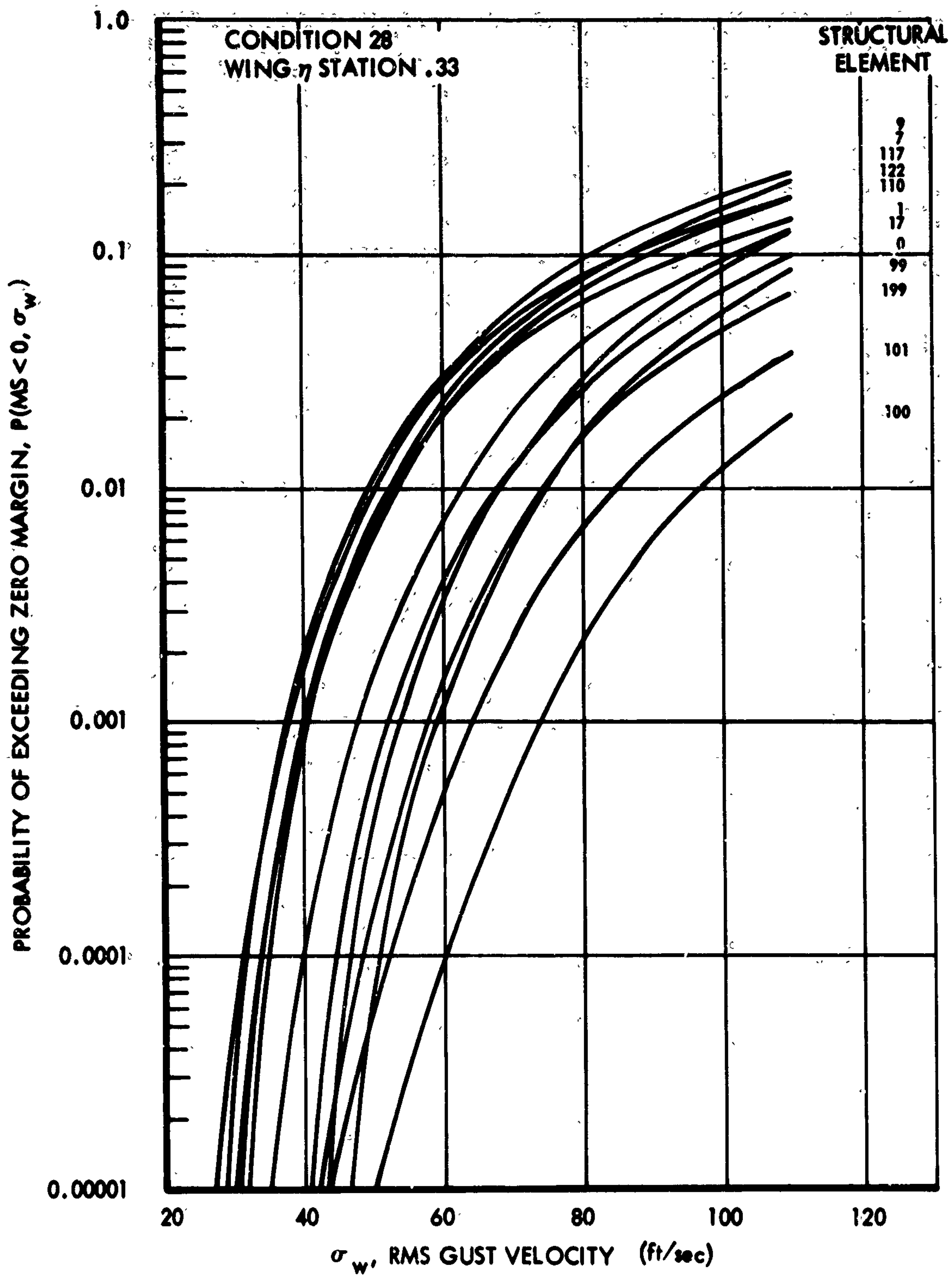

FIGURE 71 (f). PROBABILITY OF EXCEEDING ZERO MARGIN - CONDITION 28

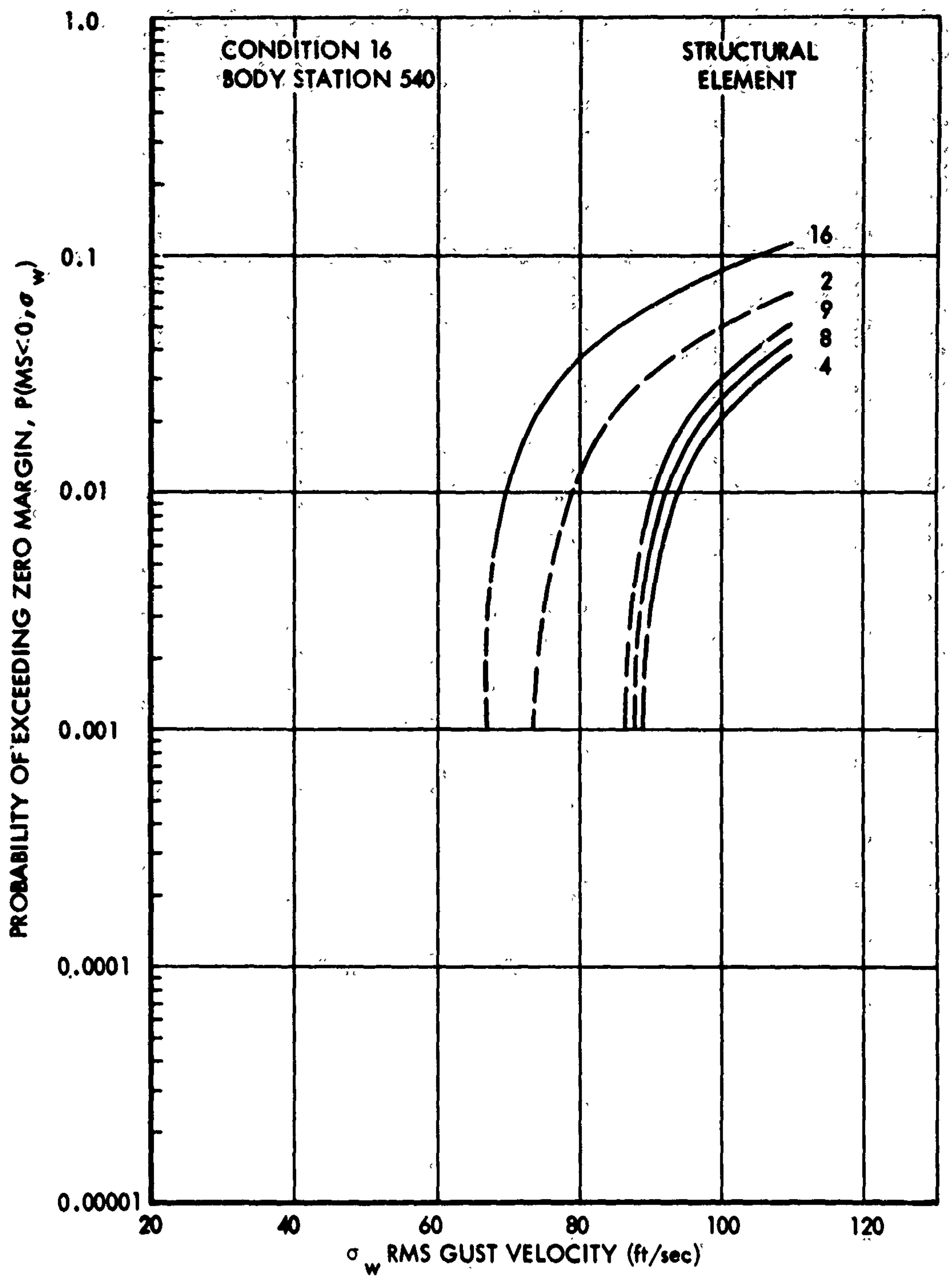

FIGURE 72 (a). PROBABILITY OF EXCEEDING ZERO MARGIN - CONDITION 16

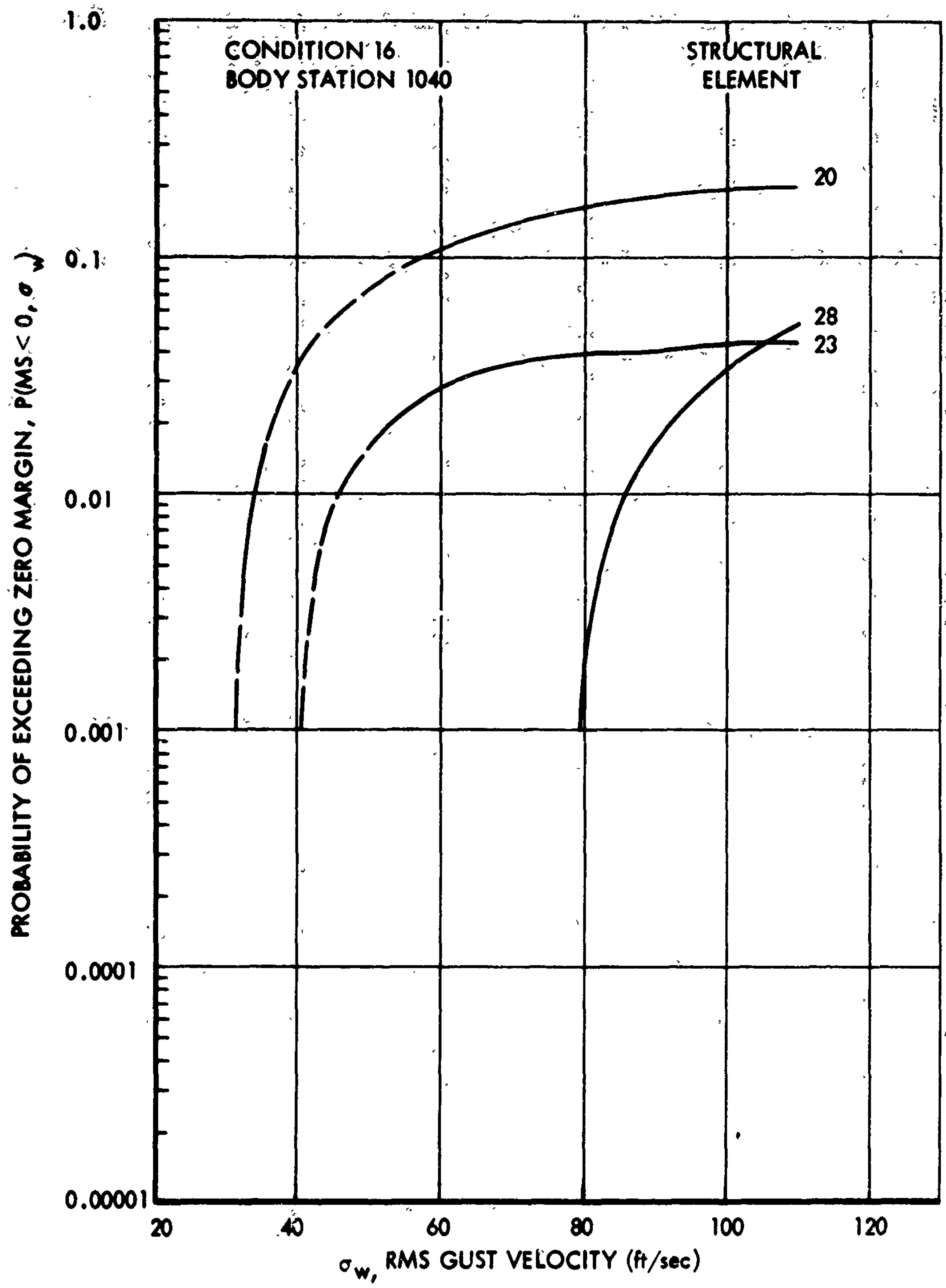

FIGURE 72 (b). PROBABILITY OF EXCEEDING ZERO MARGIN - CONDITION 16

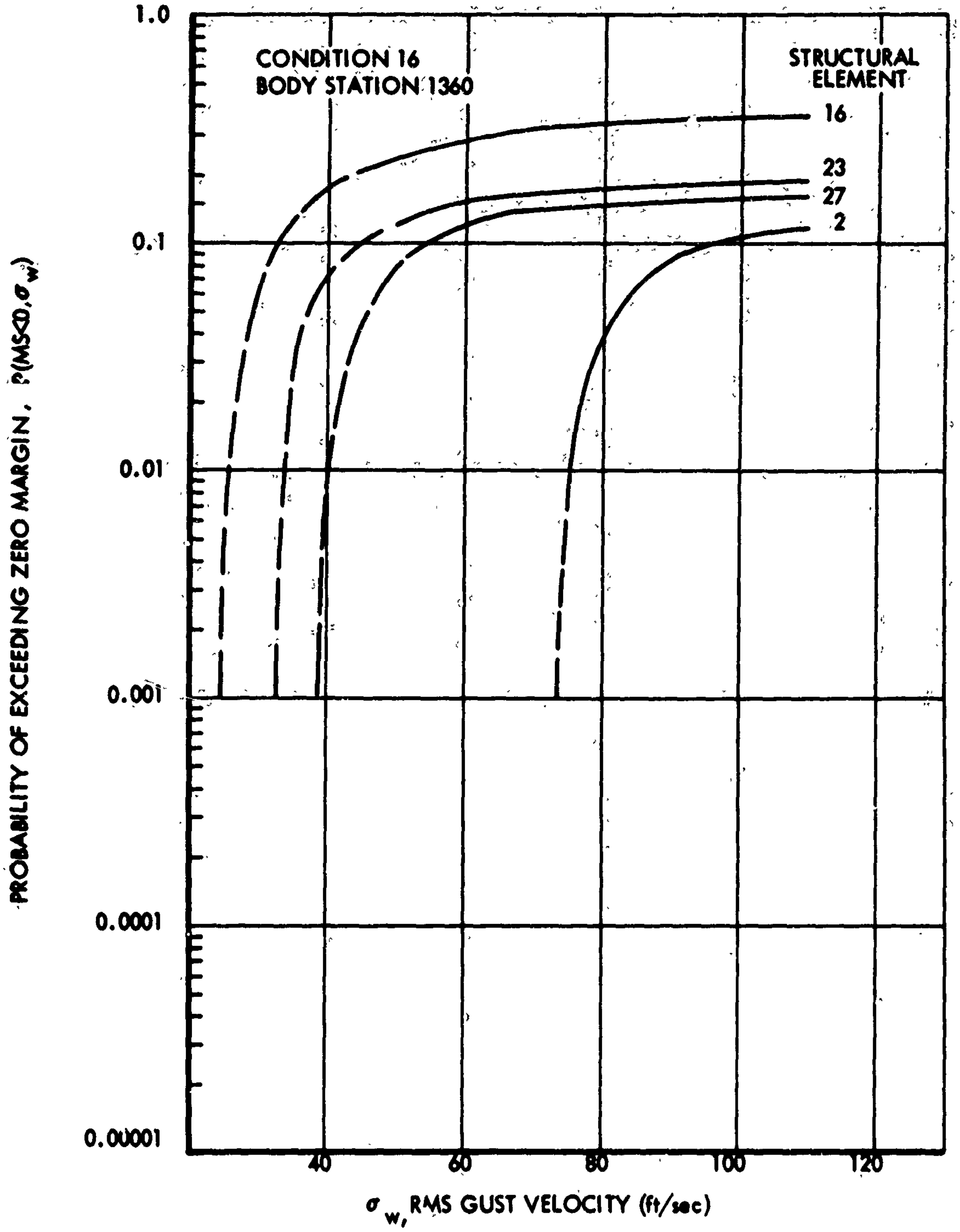

FIGURE 72 (c). PROBABILITY OF EXCEEDING ZERO MARGIN - CONDITION 16

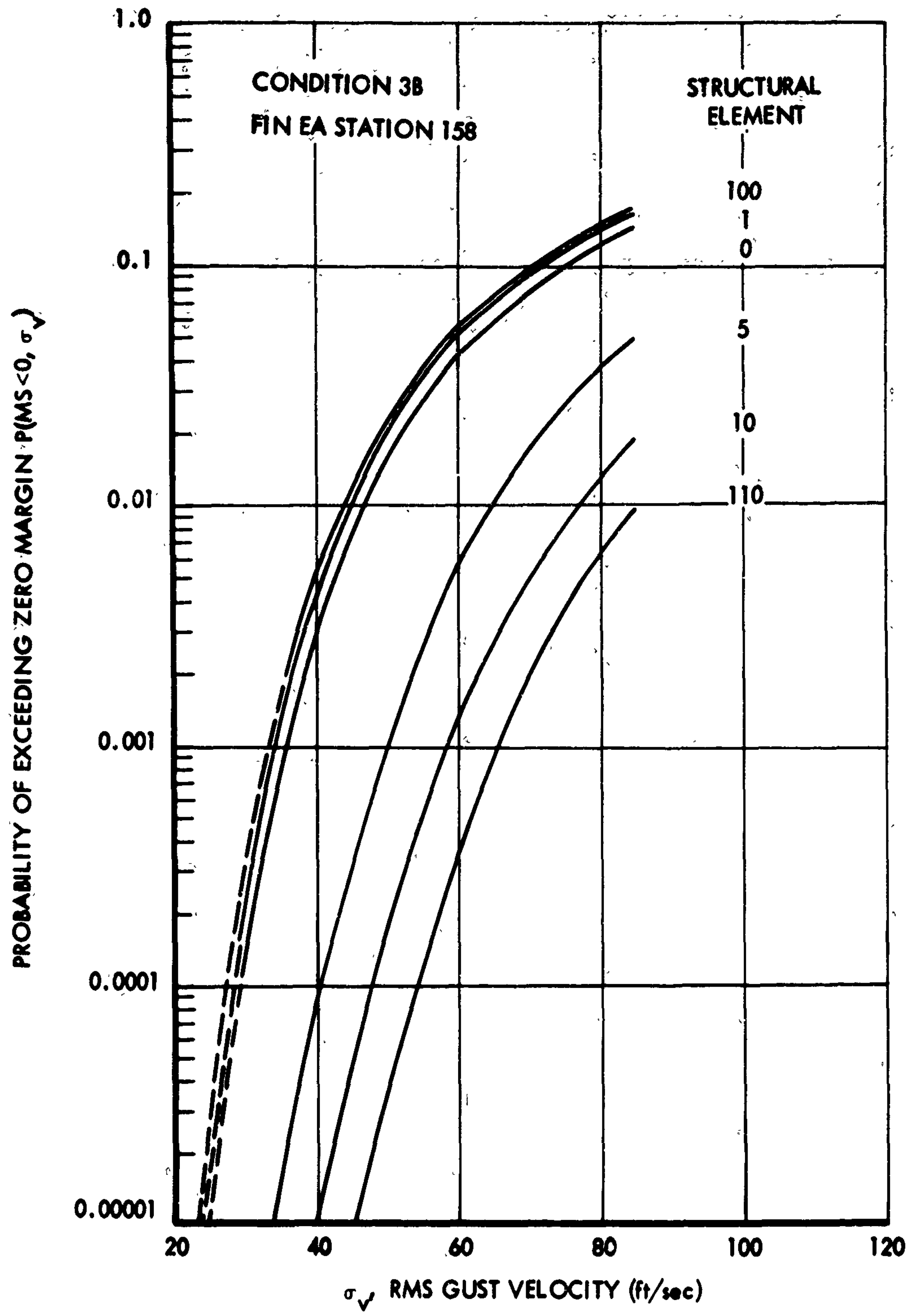

FIGURE 73 (a). PROBABILITY OF EXCEEDING ZERO MARGIN - CONDITION 3B

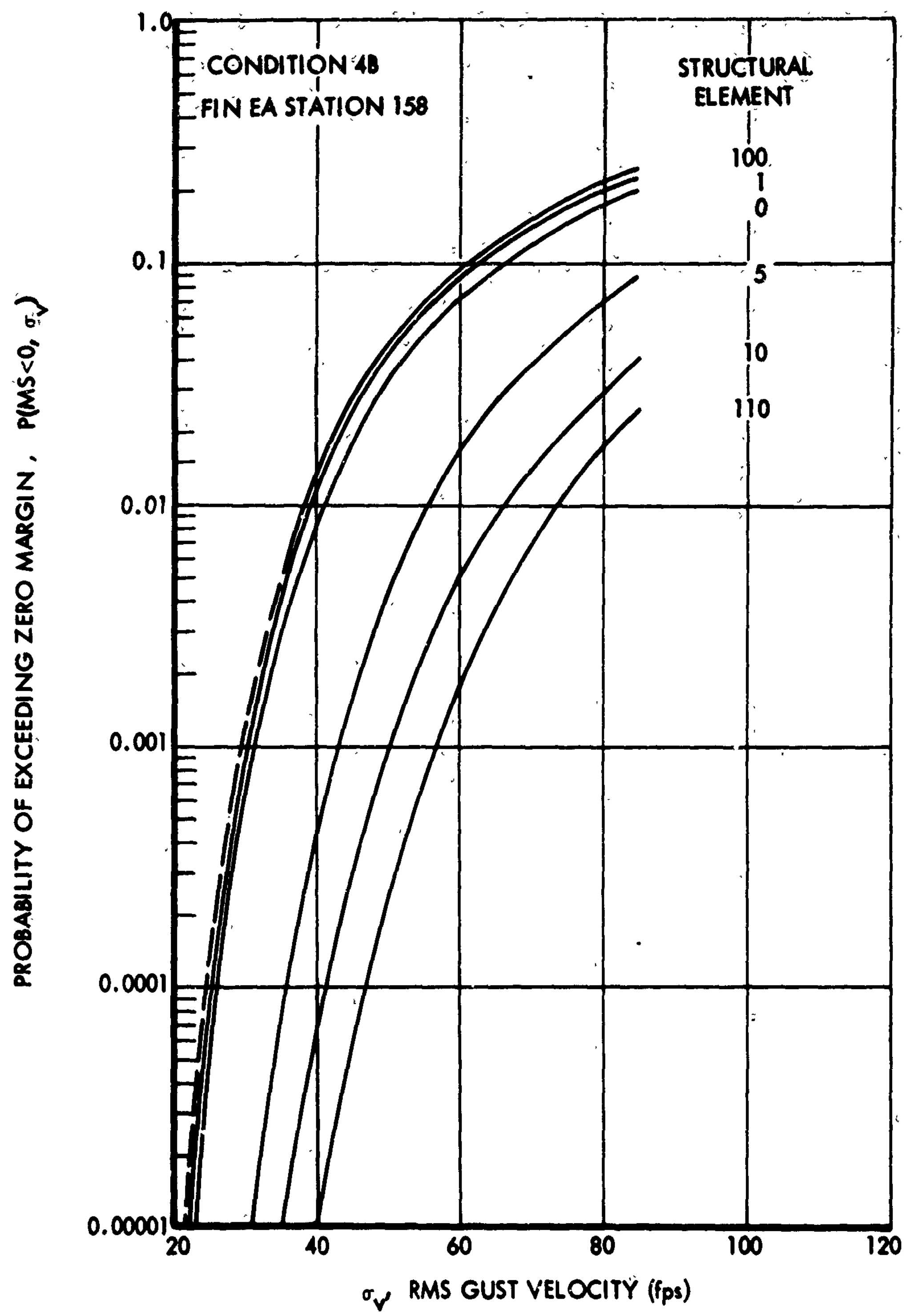

FIGURE 73 (b). PROBABILITY OF EXCEEDING ZERO MARGIN - CONDITION 4B

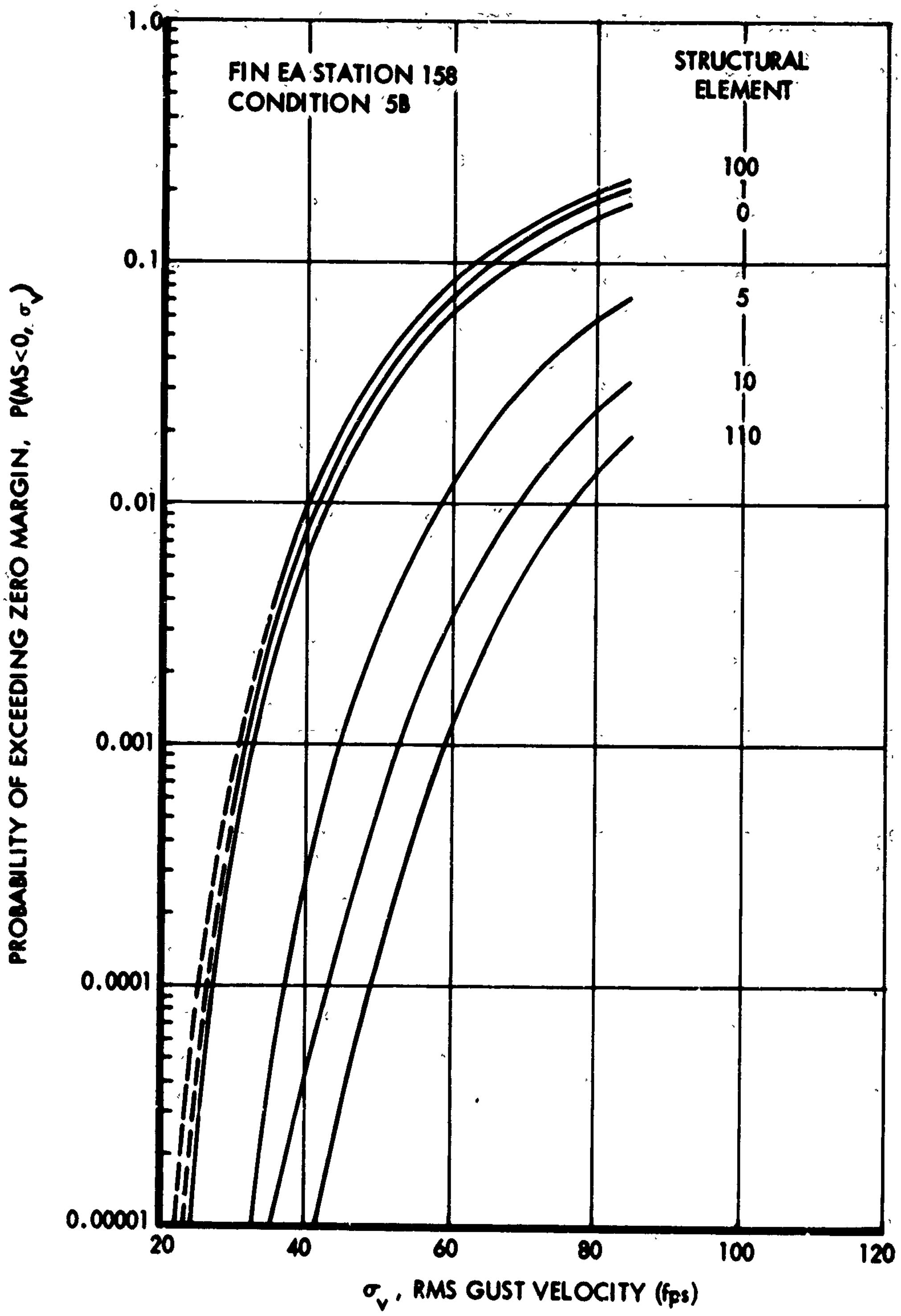

FIGURE 73 (c). PROBABILITY OF EXCEEDING ZERO MARGIN - CONDITION 5B

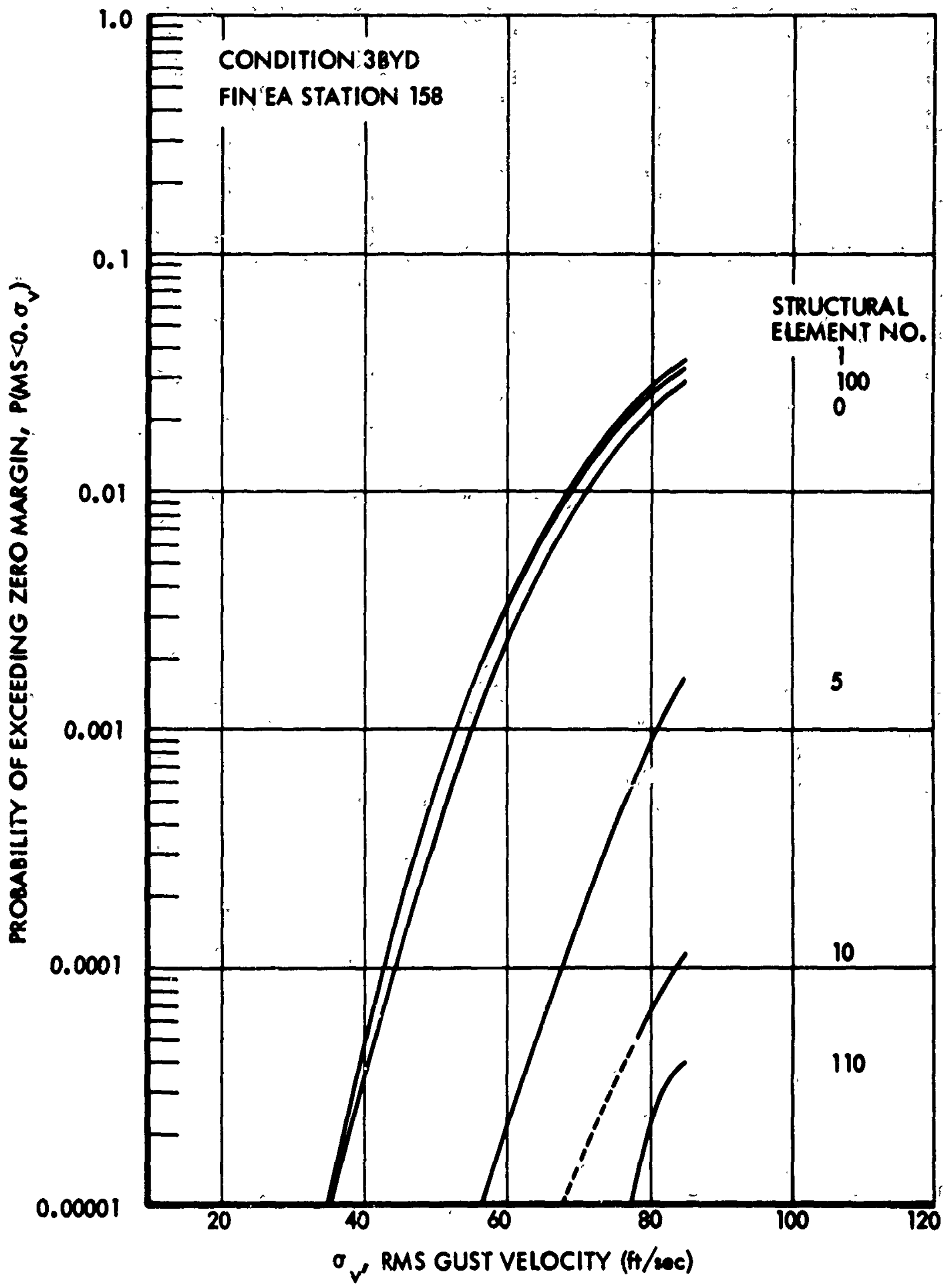

FIGURE 73 (d). PROBABILITY OF EXCEEDING ZERO MARGIN - CONDITION 3BYD

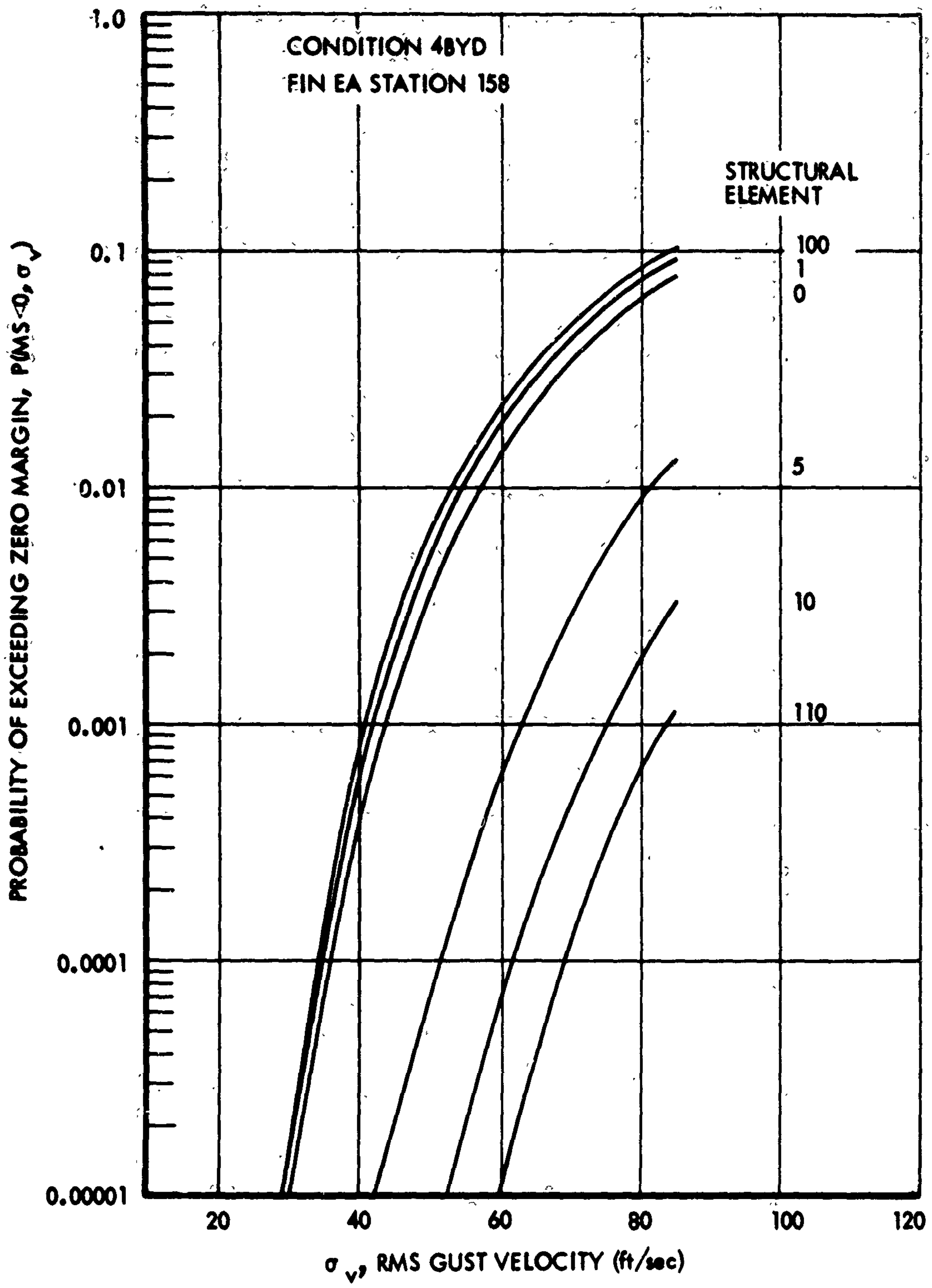

FIGURE 73 (e). PROBABILITY OF EXCEEDING ZERO MARGIN - CONDITION 4BYD

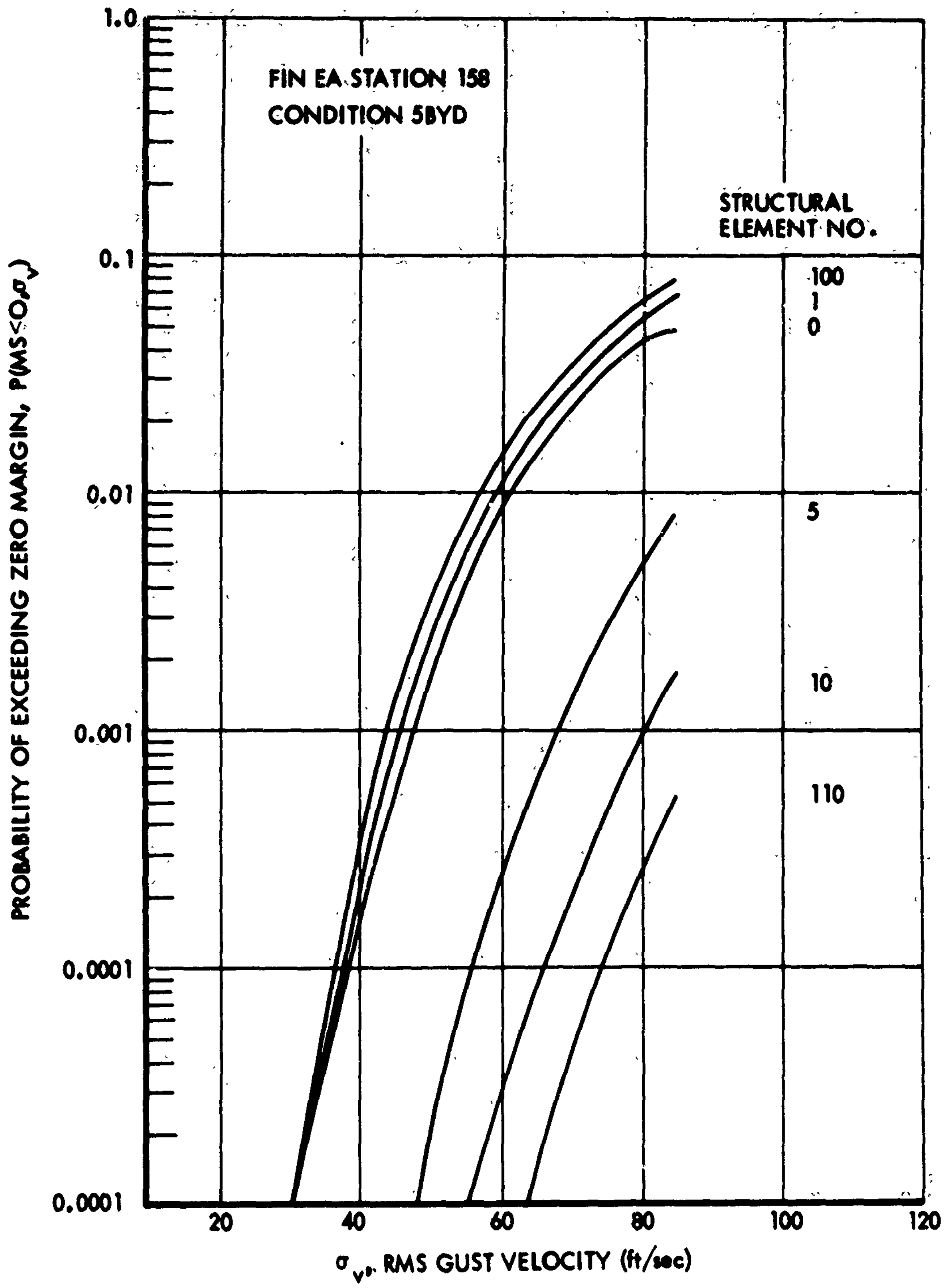

FIGURE 73 (f). PROBABILITY OF EXCEEDING ZERO MARGIN - CONDITION 5BYD

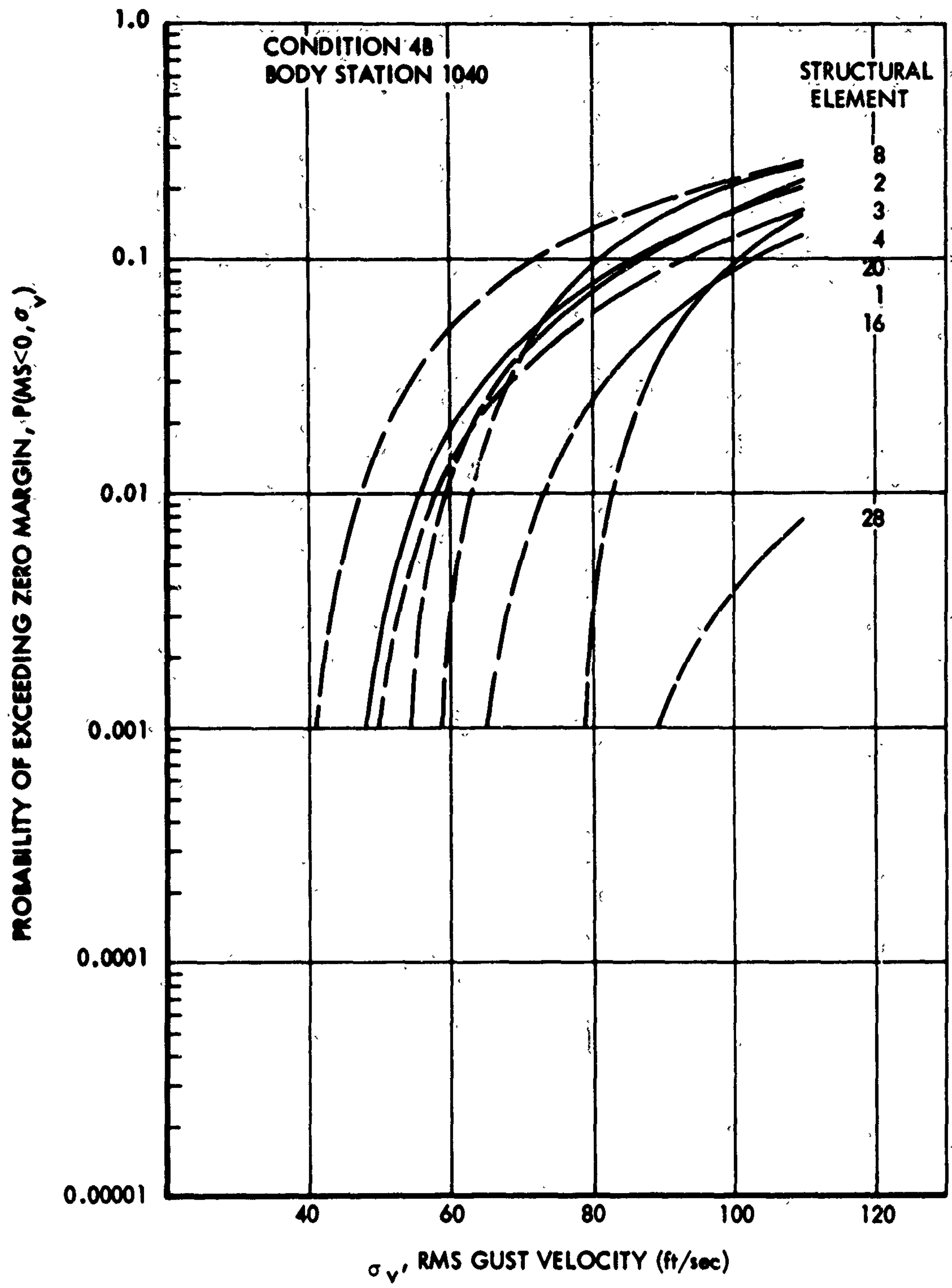

FIGURE 74 (a). PROBABILITY OF EXCEEDING ZERO MARGIN - CONDITION 4B

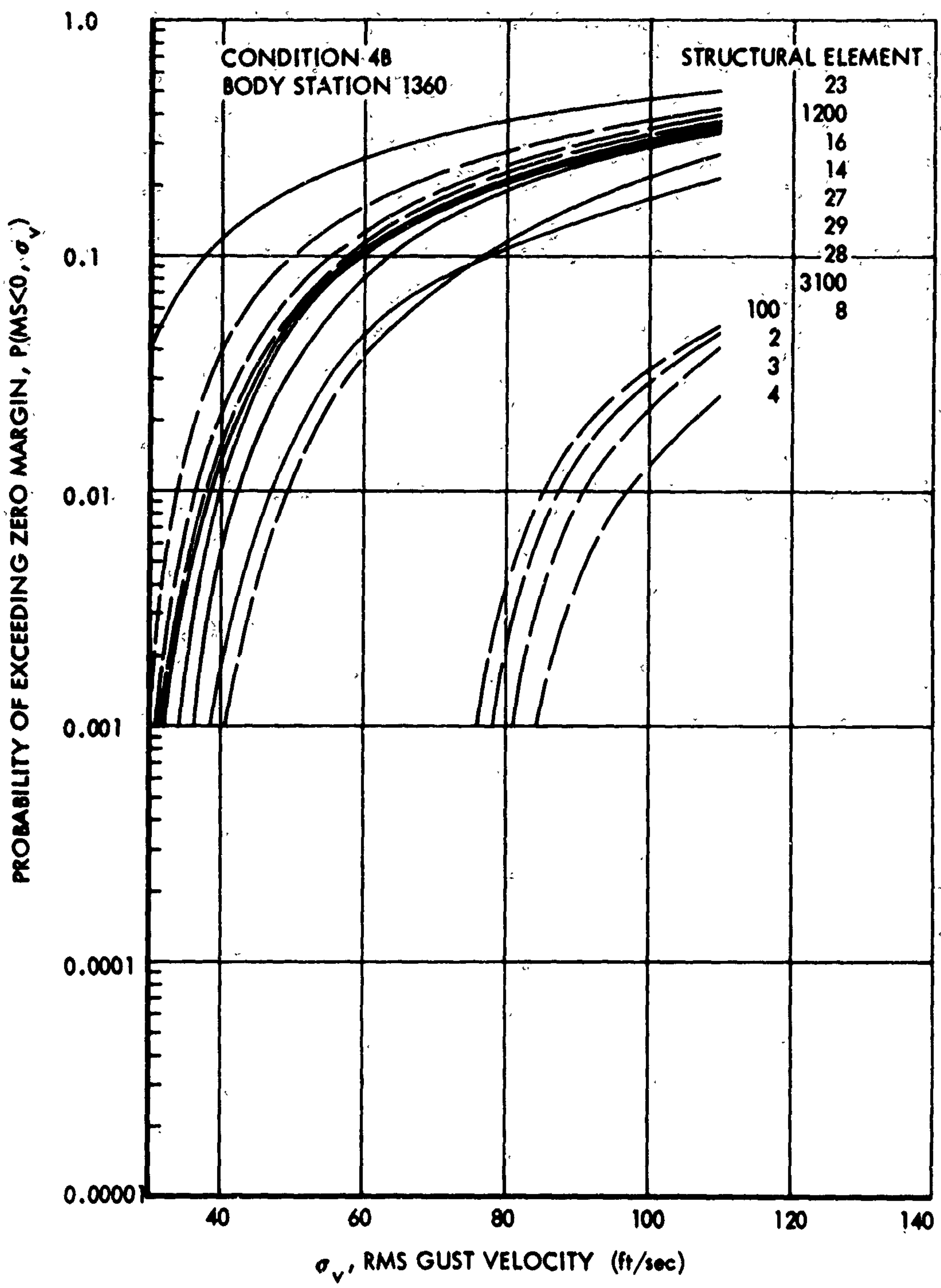

FIGURE 74 (b). PROBABILITY OF EXCEEDING ZERO MARGIN - CONDITION 4B

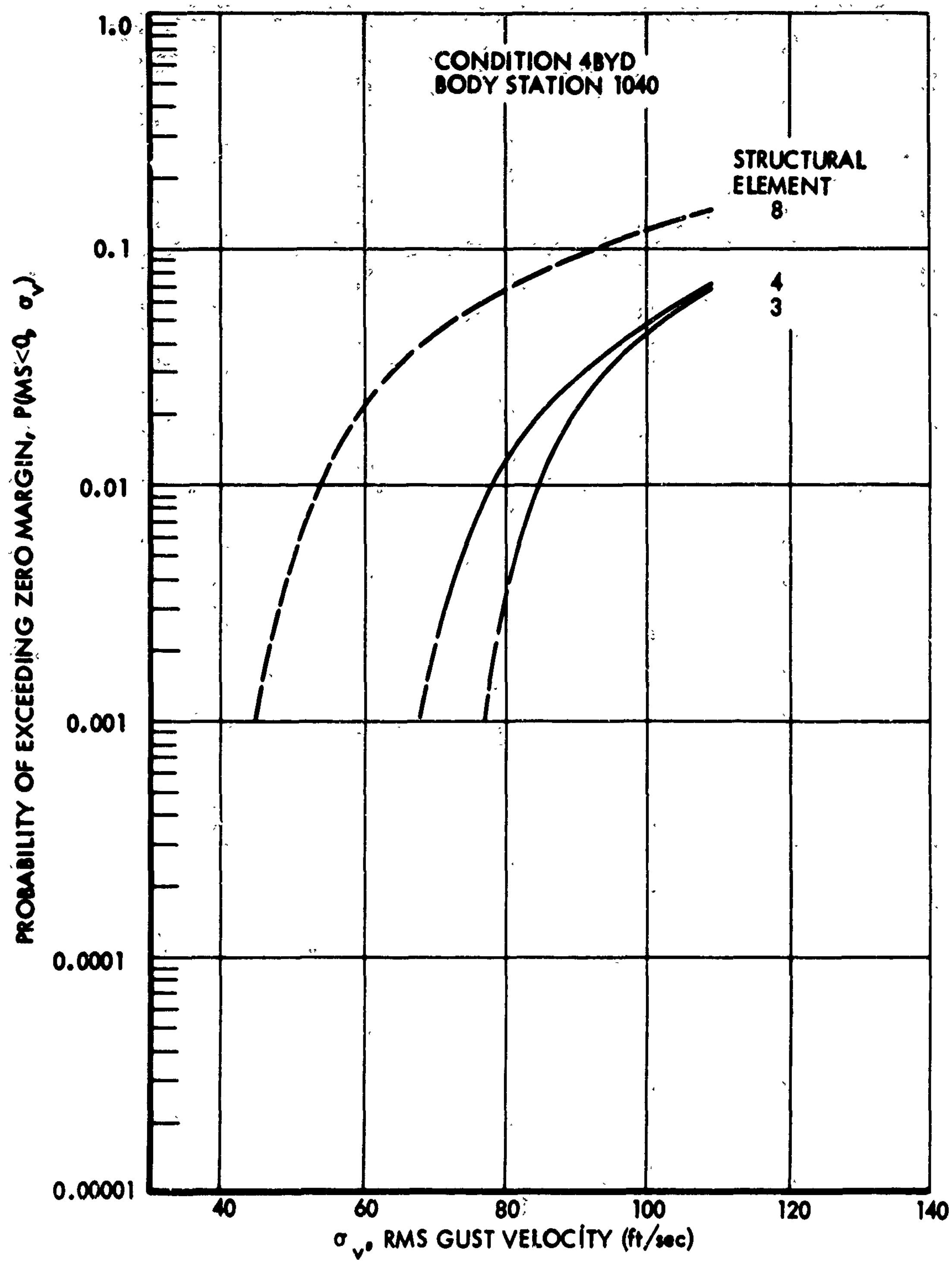

FIGURE 74 (c). PROBABILITY OF EXCEEDING ZERO MARGIN - CONDITION 4BYD

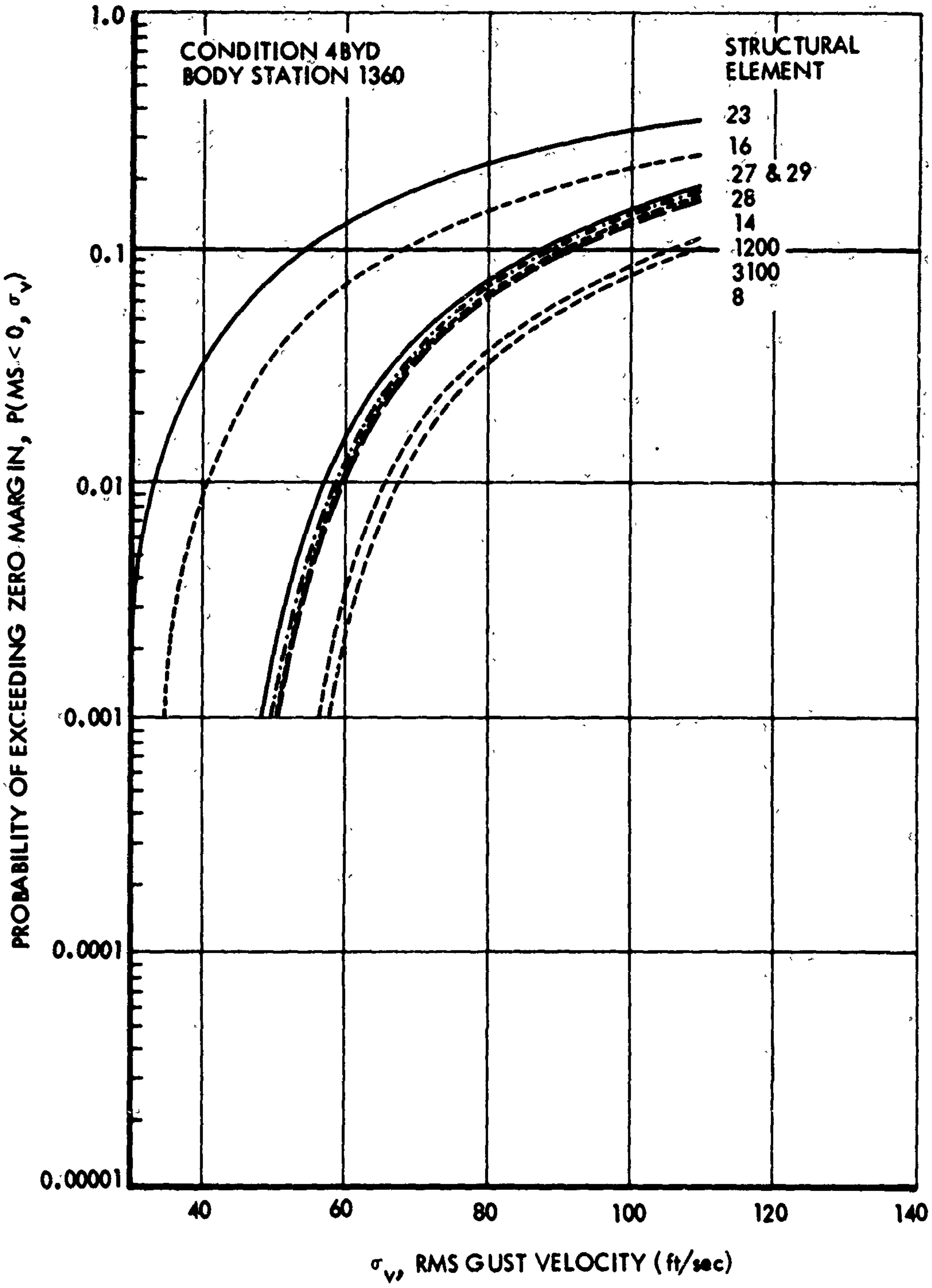

FIGURE 74 (d). PROBABILITY OF EXCEEDING ZERO MARGIN - CONDITION 4BYD

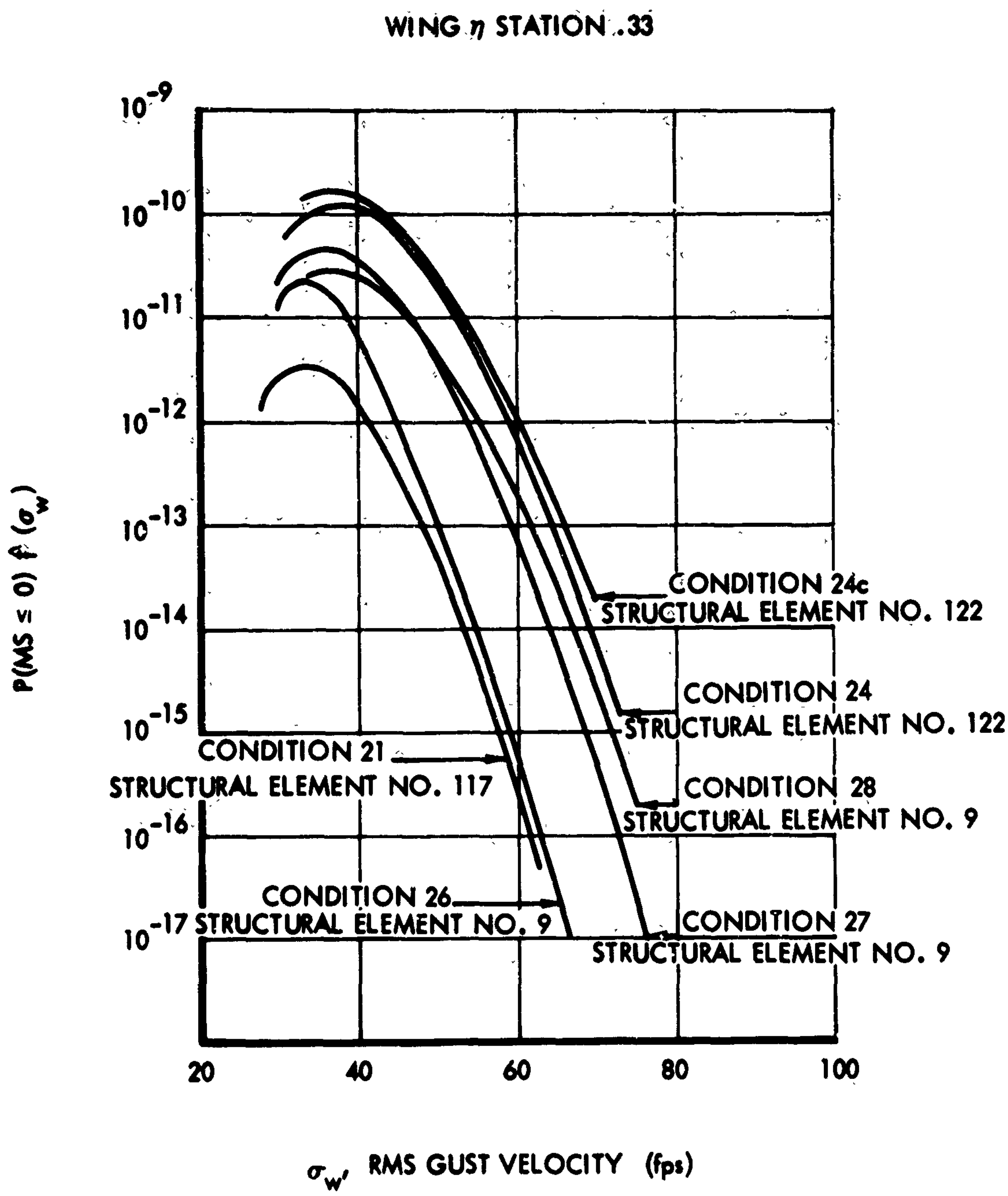

FIGURE 75. OVERALL PROBABILITY OF FAILURE FOR CRITICAL ELEMENTS-WING, VERTICAL ANALYSIS

Values of $P \times \hat{f}(\sigma_w)$ plotted in this figure are based on one dimensional value of $P(MS \leq 0)$ vs σ_w. The reason is that the correlation coefficients are very near unity and the predominance of one stress over the other has led to inconsistent numerical integration of the joint probability function. It is believed that the one dimensional value is sufficiently accurate to represent airplane strength.

BODY VERTICAL ANALYSIS
CONDITION 16

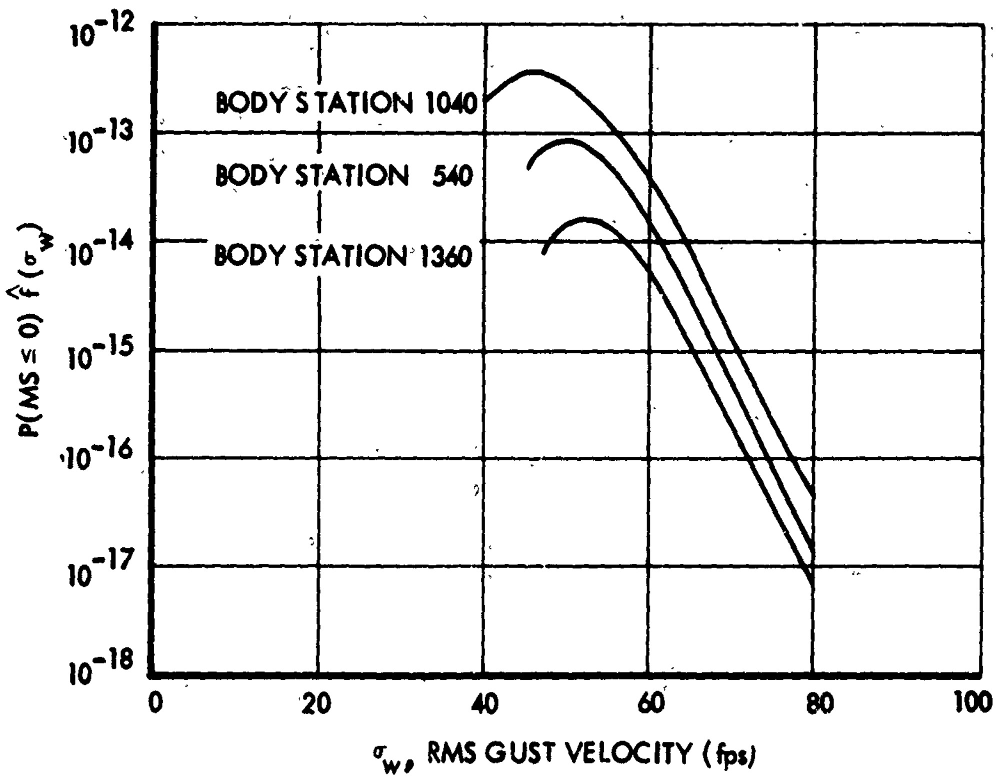

FIGURE 76. OVERALL PROBABILITY OF FAILURE FOR CRITICAL ELEMENTS-BODY, VERTICAL ANALYSIS

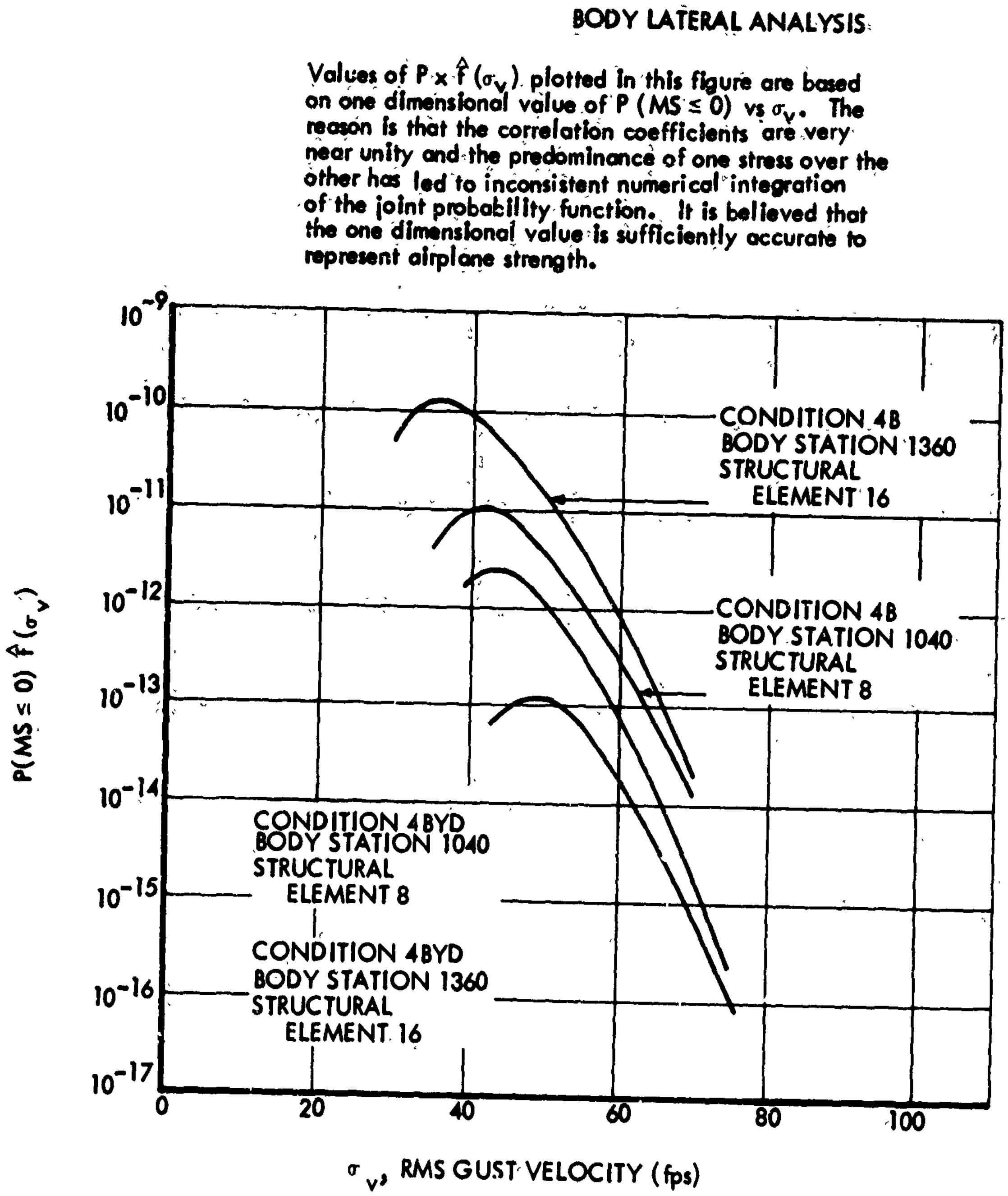

FIGURE 77. OVERALL PROBABILITY OF FAILURE FOR CRITICAL ELEMENTS-BODY, LATERAL ANALYSIS

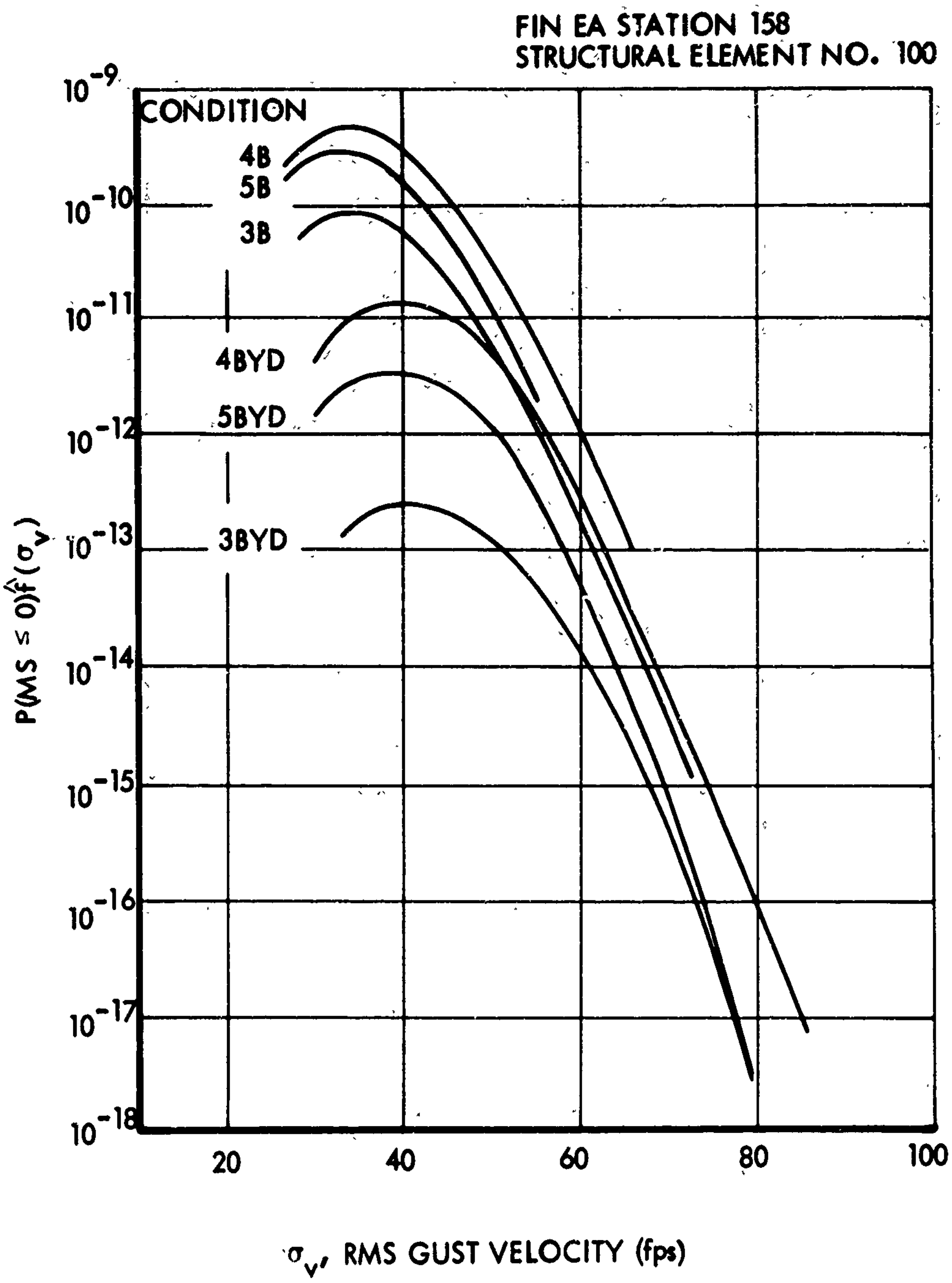

FIGURE 78. OVERALL PROBABILITY OF FAILURE FOR CRITICAL ELEMENTS-VERTICAL TAIL, LATERAL ANALYSIS

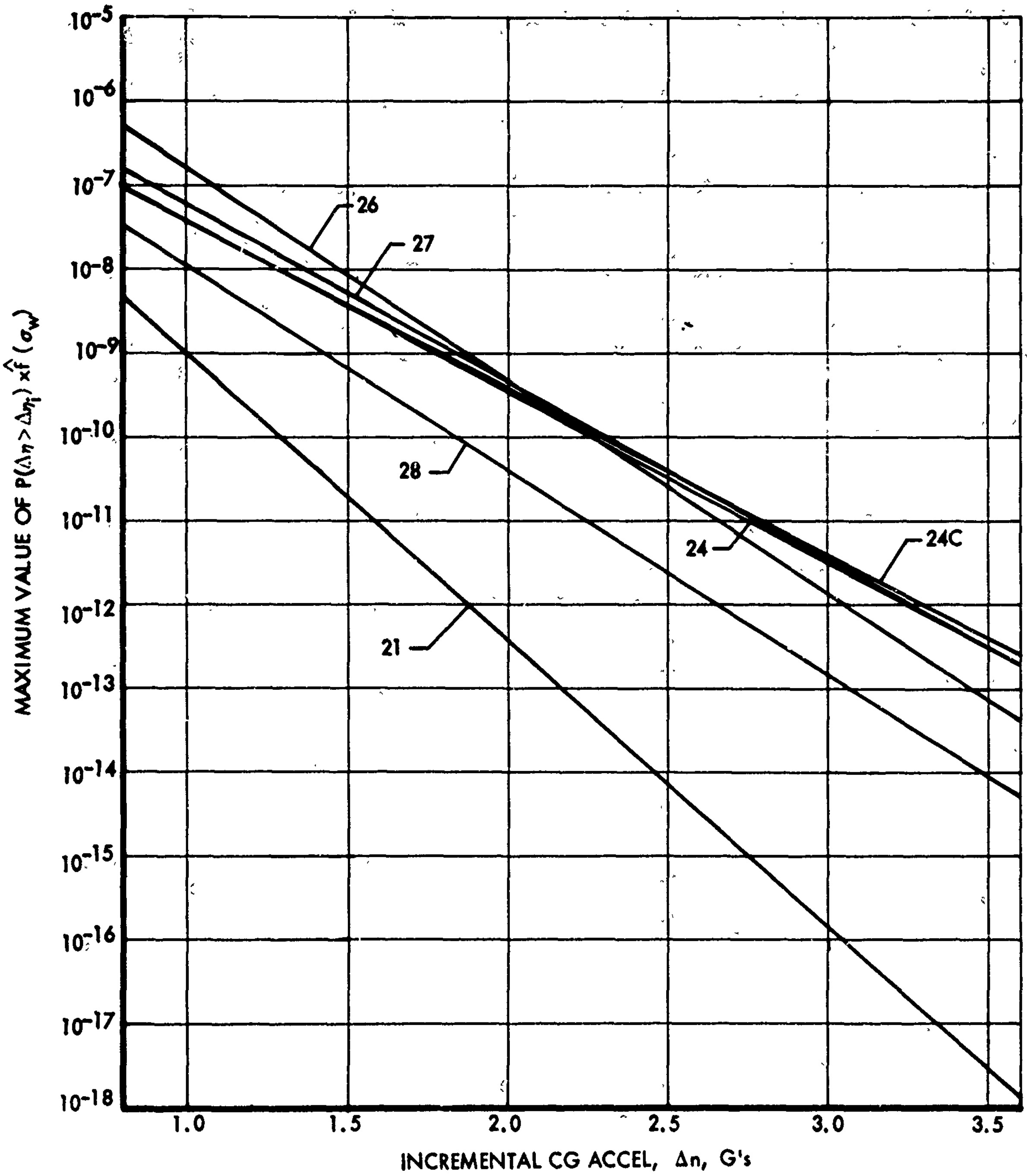

FIGURE 79. VARIATION OF MAXIMUM VALUE OF $P(\Delta n > \Delta n_i) x \hat{f}(\sigma_W)$ WITH INCREMENTAL CG ACCEL, Δn

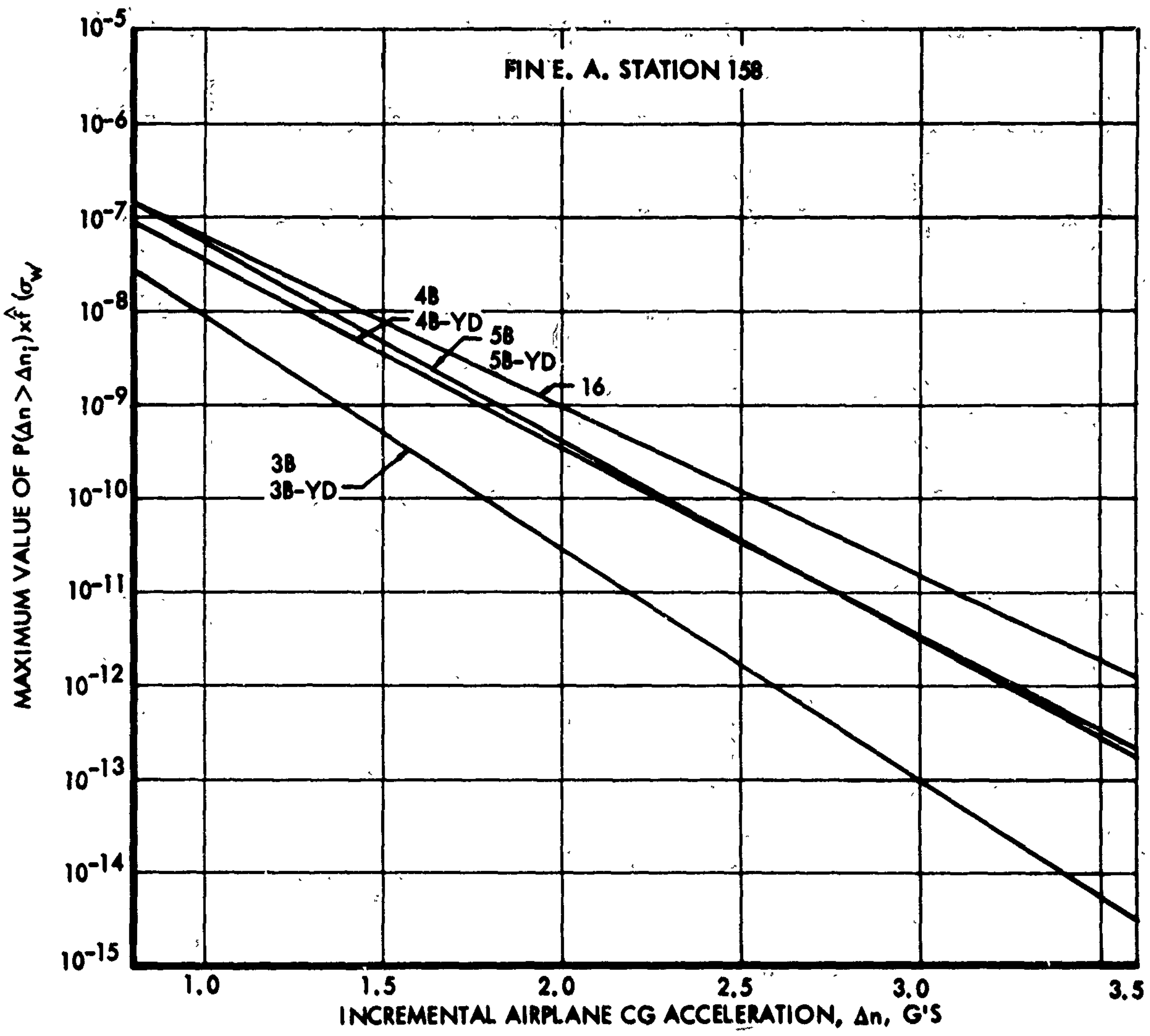

FIGURE 80. VARIATION OF MAXIMUM VALUE OF $P(\Delta n > \Delta n_i) x \hat{f}(\sigma_W)$ WITH INCREMENTAL AIRPLANE CG ACCELERATION, Δn

TABLE 12

SUMMARY OF EXCEEDANCE RATIO VALUES FOR DESIGN ENVELOPE CONDITIONS

Analysis Condition	Station		$\bar{A}\,\Delta n$	Δni Design	$\sigma_w \eta_d$	$\sigma_v \eta_d$	$\frac{N(\sigma_w \eta_d)}{N(o)}$	$\frac{N(\sigma_v \eta_d)}{N(o)}$
21	Wing	.33	.01380	1.71	124.7		$4.8(10^{-10})$	
24	Wing	.33	.01942	2.18	112.7		$7.2(10^{-9})$	
24C	Wing	.33	.01977	2.19	110.8		$8.1(10^{-9})$	
26	Wing	.33	.02066	2.51	121.5		$1.2(10^{-9})$	
27	Wing	.33	.02027	2.40	118.4		$3.2(10^{-9})$	
28	Wing	.33	.01670	2.06	123.3		$2.2(10^{-9})$	
16	Body	540	.02206	4.21	190.8		$1.0(10^{-11})$	
	Body	1040	.02206	3.87	175.4		$3.5(10^{-11})$	
	Body	1360	.02206	4.61	209.0		$1.8(10^{-12})$	
3B	Fin E.A.	158	.0164	1.81		110.4		$6.0(10^{-9})$
4B	Body	1040	.0196	2.76		140.8		$7.2(10^{-10})$
	Body	1360	.0196	2.20		112.2		$8.0(10^{-9})$
	Fin E.A.	158	.0196	1.93		98.5		$2.3(10^{-8})$
5B	Fin E.A.	158	.0202	2.04		101.0		$2.3(10^{-8})$
3B(YD)	Fin E.A.	158	.0164	3.35		168.9		$5.0(10^{-11})$
4B(YD)	Body	1040	.0196	3.71		189.3		$1.3(10^{-11})$
	Body	1360	.0196	3.05		155.6		$2.1(10^{-10})$
	Fin E.A.	158	.0196	3.15		136.7		$1.0(10^{-9})$
5B(YD)	Fin E.A.	158	.0202	3.44		147.5		$2.8(10^{-10})$

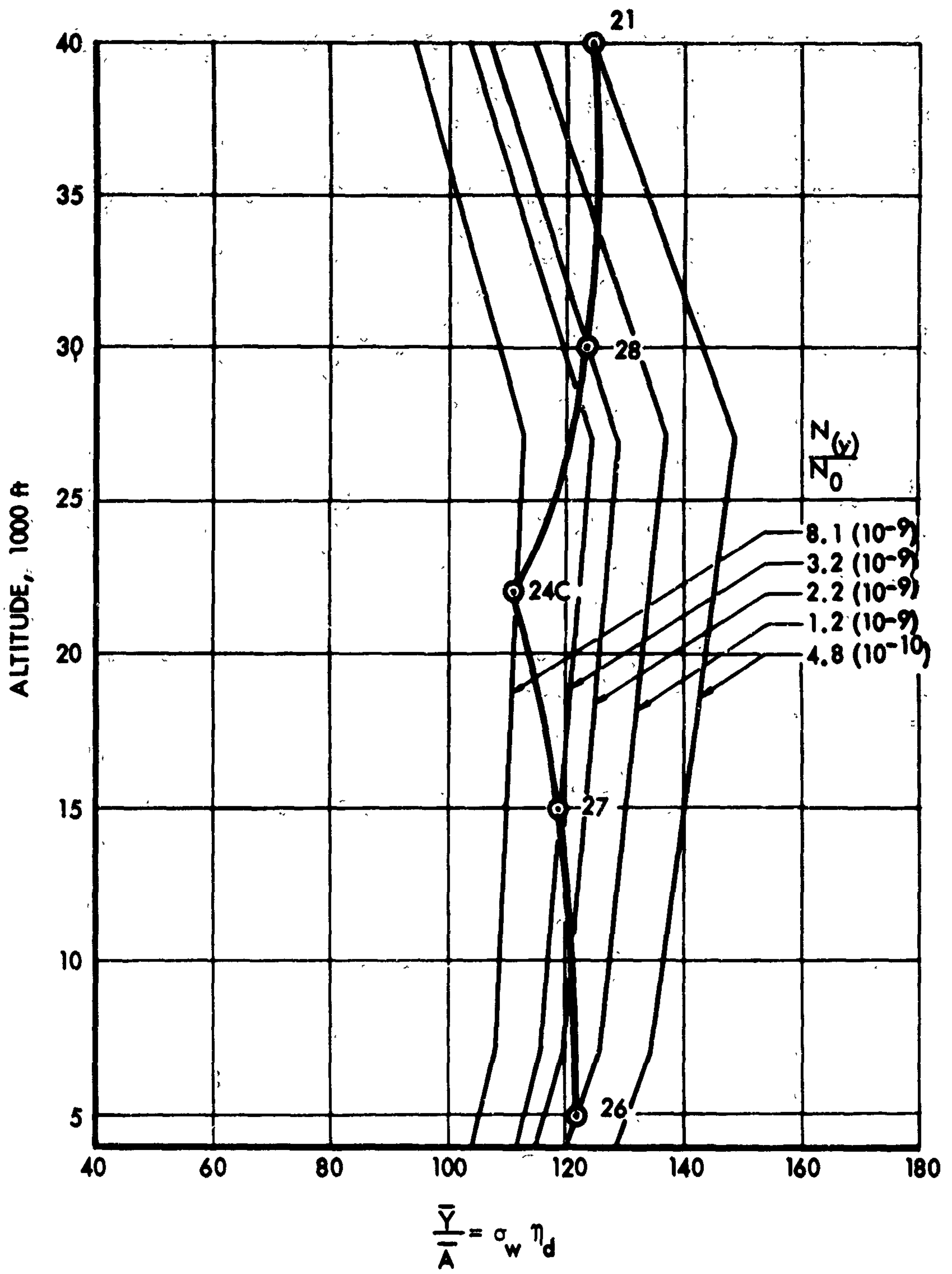

FIGURE 81. VARIATION OF COMBINED STRESS PROBABILITY $\sigma_w \eta_d$ WITH ALTITUDE

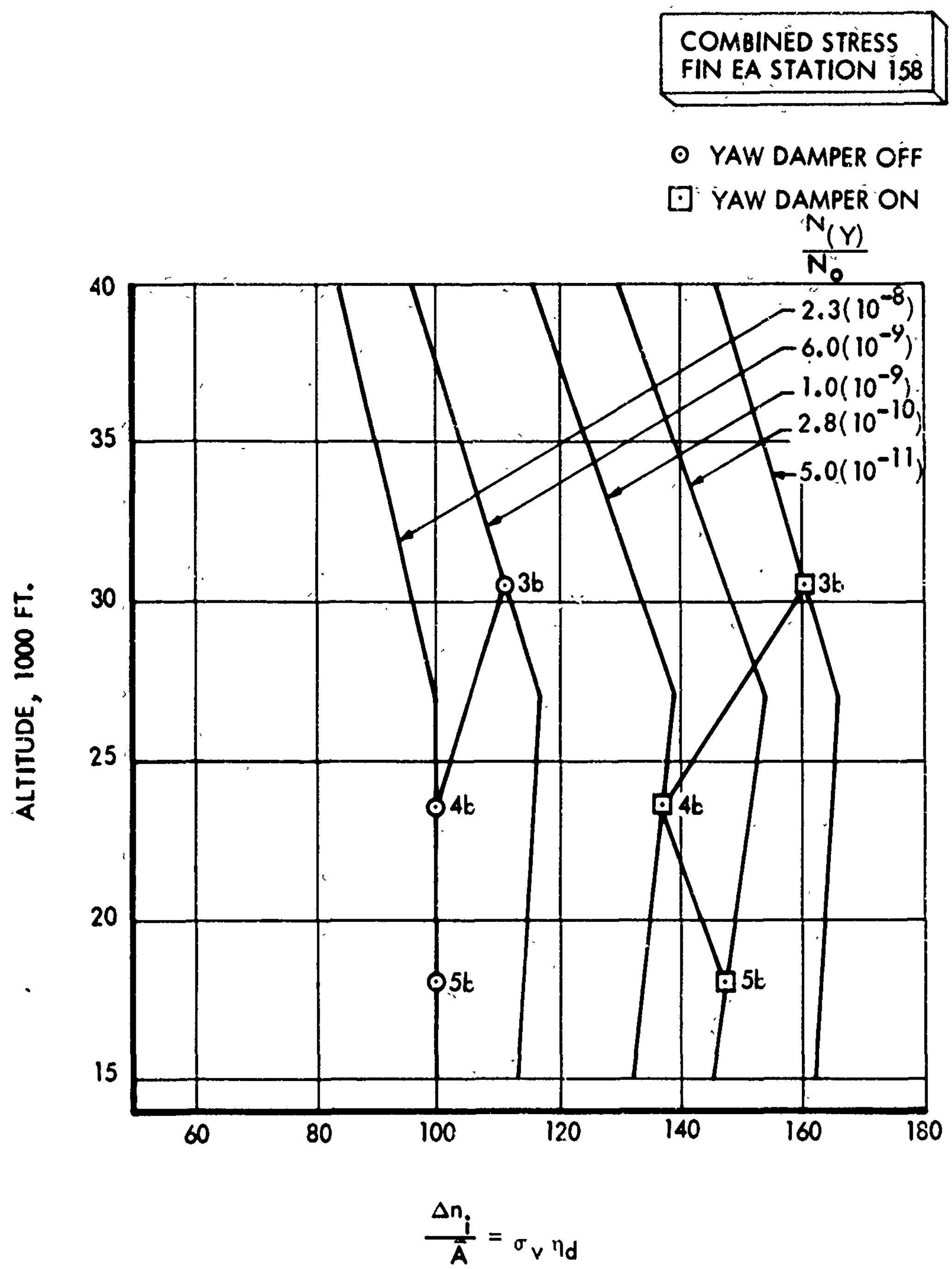

FIGURE 82. VARIATION OF COMBINED STRESS PROBABILITY $\sigma_v \eta_d$ WITH ALTITUDE

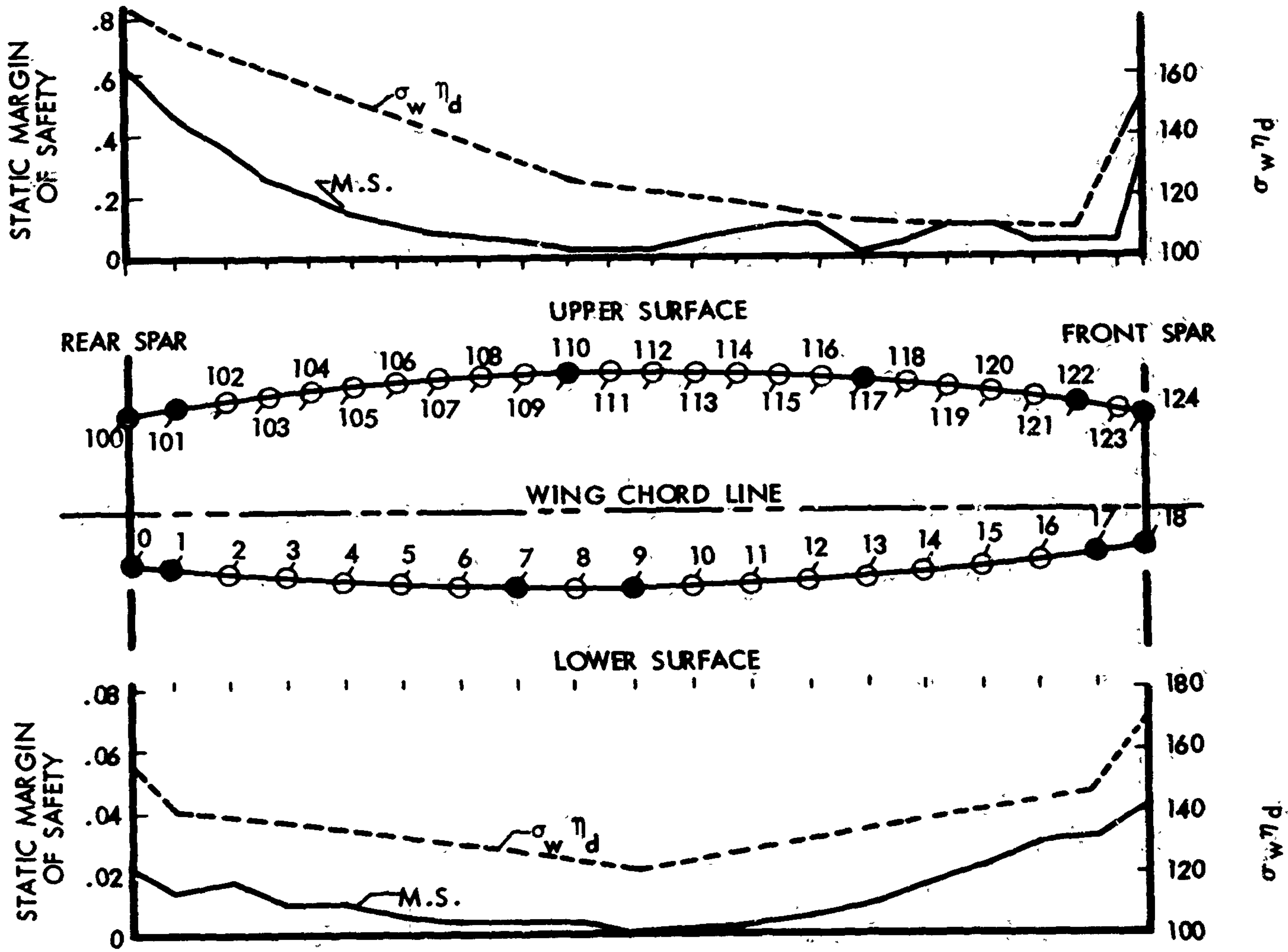

FIGURE 83. COMPARISON OF STATIC MARGIN OF SAFETY WITH $\sigma_w \eta_d$ - WING ETA STATION .33

difference is that an allowable bending moment for the section would probably be determined by Element 9 while actually under a random type of loading Elements 117 and 122 may be the most critical.

The evaluation of strength capability following the Flight Profile Approach results in number of exceedances per hour of the limit strength envelope. Representative values of the number of exceedances per hour, $\bar{G}$, for structural Element 110 are given in Tables 13 through 25 for all the flight profile conditions. The $\bar{G}$ values for the remaining elements and conditions appears in Volume II, Data Report. The total number of exceedances of the limit design envelope per average flight hour, N_p, were obtained by multiplying the $\bar{G}$ values by the appropriate time factors. These values are summarized in Tables 26(a), 26(b) and 26(c).

A summary of the exceedances per hour obtained for the Flight Profile Analysis using the joint probability approach are given in Fig. 84. Also shown in this figure are the design values of $\sigma_w \eta_d$ and $\sigma_v \eta_d$ expressed as exceedance ratios $\frac{N(\sigma_w \eta_d)}{N(o)}$ and $\frac{N(\sigma_v \eta_d)}{N(o)}$.

TABLE 13. EXCEEDANCES PER HOUR - CONDITION 2

7208 CONDITION 2 VERTICAL GUST ANALYSIS

WING ETA STATION = 0.33 STRUCTURAL ELEMENT 110

TURBULENCE PARAMETERS

P1 = 0.055000
P2 = 0.000260
B1 = 3.370000
B2 =10.600000

1G STRESSES (PSI)

SHEAR	SKIN	SEGMENT
-1699.0	-11970.0	-11440.0

V TRUE (FT/SEC) =624.9

G BAR = 0.3404693E-05 PER HOUR

RMS GUST VELOCITY (FT/SEC)	NC (PER FT)	F (SIGW)	NC F(SIGW) X 1800V
10.	0.	0.1719984E-03	0.
15.	0.1153180E-19	0.7840254E-05	0.1016999E-18
20.	0.5396531E-12	0.3300692E-05	0.2003609E-11
22.	0.2773744E-10	0.2271063E-05	0.7085801E-10
24.	0.5548958E-09	0.1508094E-05	0.9413113E-09
26.	0.5710621E-08	0.9664748E-06	0.6207902E-08
28.	0.3630455E-07	0.5976501E-06	0.2440628E-07
30.	0.1614155E-06	0.3566687E-06	0.6475955E-07
32.	0.5473124E-06	0.2054103E-06	0.1264594E-06
34.	0.1505583E-05	0.1141613E-06	0.1933379E-06
36.	0.3515394E-05	0.6122861E-07	0.2421150E-06
38.	0.7205064E-05	0.3169051E-07	0.2568387E-06
40.	0.1329642E-04	0.1582862E-07	0.2367398E-06
45.	0.4372390E-04	0.2388290E-08	0.1174625E-06
50.	0.1024688E-03	0.2884700E-09	0.3324957E-07
55.	0.1924672E-03	0.2789229E-10	0.6038573E-08
60.	0.3109628E-03	0.2158926E-11	0.7551610E-09
65.	0.4519064E-03	0.1337707E-12	0.6797906E-10
70.	0.6083729E-03	0.6635201E-14	0.4540643E-11
75.	0.7741492E-03	0.2634615E-15	0.2294271E-12
80.	0.9444643E-03	0.8374330E-17	0.8896702E-14

TABLE 14. EXCEEDANCES PER HOUR - CONDITION 4

7208 CONDITION 4 VERTICAL GUST ANALYSIS

WING ETA STATION = 0.33 STRUCTURAL ELEMENT 110

TURBULENCE PARAMETERS

P1 = 0.055000
P2 = 0.000260
B1 = 3.370000
B2 =10.600000

1G STRESSES (PSI)

SHEAR	SKIN	SEGMENT
-1747.0	-10650.0	-10180.0

V TRUE (FT/SEC) =624.9

G BAR = 0.1394977E-05 PER HOUR

RMS GUST VELOCITY (FT/SEC)	NC (PER FT)	F (SIGW)	NC F(SIGW) X 1800V
10.	0.	0.1719984E-03	0.
15.	0.2927206E-22	0.7840254E-05	0.2581528E-21
20.	0.1879234E-13	0.3300692E-05	0.6977170E-13
22.	0.1734891E-11	0.2271063E-05	0.4431951E-11
24.	0.5419869E-10	0.1508094E-05	0.9194129E-10
26.	0.7891885E-09	0.9664248E-06	0.8579111E-09
28.	0.6608456E-08	0.5976501E-06	0.4442633E-08
30.	0.3669767E-07	0.3566687E-06	0.1472302E-07
32.	0.1492705E-06	0.2054103E-06	0.3448972E-07
34.	0.4774964E-06	0.1141613E-06	0.6131720E-07
36.	0.1265207E-05	0.6122861E-07	0.8713839E-07
38.	0.2886112E-05	0.3169051E-07	0.1028811E-06
40.	0.5835854E-05	0.1582862E-07	0.1039061E-06
45.	0.2291970E-04	0.2388290E-08	0.6157288E-07
50.	0.6098791E-04	0.2884700E-09	0.1978964E-07
55.	0.1258393E-03	0.2789229E-10	0.3948154E-08
60.	0.2183767E-03	0.2158926E-11	0.5303193E-09
65.	0.3355208E-03	0.1337707E-12	0.5048635E-10
70.	0.4721346E-03	0.6635201E-14	0.3523817E-11
75.	0.6227358E-03	0.2634615E-15	0.1845502E-12
80.	0.7825570E-03	0.8374330E-17	0.7371561E-14

TABLE 15. EXCEEDANCES PER HOUR - CONDITION 5

7208 CONDITION 5 VERTICAL GUST ANALYSIS

WING ETA STATION = 0.33 STRUCTURAL ELEMENT 110

TURBULENCE PARAMETERS

P1 = 0.055000
P2 = 0.000260
B1 = 3.370000
B2 =10.600000

1G STRESSES (PSI)

SHEAR	SKIN	SEGMENT
-1701.0	-11820.0	-11290.0

V TRUE (FT/SEC) =624.9

G BAR = 0.3014469E-05 PER HOUR

RMS GUST VELOCITY (FT/SEC)	NC (PER FT)	F (SIGW)	NC F(SIGW) X 1800V
10.	0.	0.1719984E-03	0.
15.	0.1178477E-19	0.7840254E-05	0.1039309E-18
20.	0.5139476E-12	0.3300692E-05	0.1908171E-11
22.	0.2595945E-10	0.2271063E-05	0.6631596E-10
24.	0.5123709E-09	0.1508094E-05	0.8691731E-09
26.	0.5217883E-08	0.9664248E-06	0.5672256E-08
28.	0.3289814E-07	0.5976501E-06	0.2211626E-07
30.	0.1453013E-06	0.3566687E-06	0.5829454E-07
32.	0.4900137E-06	0.2054103E-06	0.1132202E-06
34.	0.1341939E-05	0.1141613E-06	0.1723237E-06
36.	0.3121549E-05	0.6122861E-07	0.2149898E-06
38.	0.6377445E-05	0.3169051E-07	0.2273366E-06
40.	0.1173683E-04	0.1582862E-07	0.2089717E-06
45.	0.3838632E-04	0.2388290E-08	0.1031233E-06
50.	0.8959862E-04	0.2884700E-09	0.2907338E-07
55.	0.1677697E-03	0.2789229E-10	0.52637[illegible]E-08
60.	0.2703872E-03	0.2158926E-11	0.6566247E-09
65.	0.3921508E-03	0.1337707E-12	0.5900755E-10
70.	0.5270784E-03	0.6635201E-14	0.3933895E-11
75.	0.6698677E-03	0.2634615E-15	0.1985179E-12
80.	0.8165000E-03	0.8374330E-17	0.7691299E-14

TABLE 16. EXCEEDANCES PER HOUR - CONDITION 6

720B CONDITION 6 VERTICAL GUST ANALYSIS

WING ETA STATION = 0.33 STRUCTURAL ELEMENT 110

TURBULENCE PARAMETERS

P1 = 0.055000
P2 = 0.000260
B1 = 3.370000
B2 =10.600000

1G STRESSES (PSI)

SHEAR	SKIN	SEGMENT
-1133.0	-11970.0	-11440.0

V TRUE (FT/SEC) =624.9

G BAR = 0.2208273E-05 PER HOUR

RMS GUST VELOCITY (FT/SEC)	NC (PER FT)	F (SIGW)	NC F(SIGW) X 1800V
10.	0.	0.1719984E-03	0.
15.	0.1209854E-20	0.7840254E-05	0.1066981E-19
20.	0.1436026E-12	0.3300692E-05	0.5331637E-12
22.	0.9116727E-11	0.2271063E-05	0.2328958E-10
24.	0.2143667E-09	0.1508094E-05	0.3636463E-09
26.	0.2503280E-08	0.9664248E-06	0.2721266E-08
28.	0.1760008E-07	0.5976501E-06	0.1183191E-07
30.	0.8489839E-07	0.3566687E-06	0.3406104E-07
32.	0.3077842E-06	0.2054103E-06	0.7111514E-07
34.	0.8950631E-06	0.1141613E-06	0.1149396E-06
36.	0.2189714E-05	0.6122861E-07	0.1508117E-06
38.	0.4669008E-05	0.3169051E-07	0.1664360E-06
40.	0.8912478E-05	0.1582862E-07	0.1586847E-06
45.	0.3129838E-04	0.2388290E-08	0.8408185E-07
50.	0.7680043E-04	0.2884700E-09	0.2494652E-07
55.	0.1495137E-03	0.2783229E-10	0.4690927E-08
60.	0.2480278E-03	0.2154926E-11	0.6023258E-09
65.	0.3679045E-03	0.1337707E-12	0.5535917E-10
70.	0.5033467E-03	0.6635[illegible]1E-14	0.3756771E-11
75.	0.6449000E-03	0.[illegible]E-15	0.1922744E-12
80.	0.[illegible]97630E-03	0.9374330E-17	0.7533639E-14

TABLE 17. EXCEEDANCES PER HOUR - CONDITION 7

7208 CONDITION 7 VERTICAL GUST ANALYSIS

WING ETA STATION = 0.33 STRUCTURAL ELEMENT 110

TURBULENCE PARAMETERS

P1 = 0.016500
P2 = 0.000090
B1 = 3,050000
B2 =11,400000

1G STRESSES (PSI)

SHEAR	SKIN	SEGMENT
-2274.0	-11740.0	-11220.0

V TRUE (FT/SEC) =810.7

G BAR = 0.2418557E-05 PER HOUR

RMS GUST VELOCITY (FT/SEC)	NC (PER FT)	F (SIGW)	NC F(SIGW) X 1800V
10.	0.	0.2427838E-04	0.
15.	0.1119441E-20	0.2674668E-05	0.4369217E-20
20.	0.1367588E-12	0.1351946E-05	0.2697834E-12
22.	0.8729709E-11	0.9785274E-06	0.1246538E-10
24.	0.2060932E-09	0.6868347E-06	0.2065612E-09
26.	0.2414129E-08	0.4674816E-06	0.1646864E-08
28.	0.1701507E-07	0.3085388E-06	0.7660814E-08
30.	0.8223965E-07	0.1974640E-06	0.2369746E-07
32.	0.2986331E-06	0.1225460E-06	0.5340351E-07
34.	0.8696330E-06	0.7374682E-07	0.9358624E-07
36.	0.2129936E-05	0.4303487E-07	0.1337580E-06
38.	0.4545960E-05	0.2435177E-07	0.1615433E-06
40.	0.8684816E-05	0.1336207E-07	0.1693429E-06
45.	0.3054843E-04	0.2604658E-08	0.1161107E-06
50.	0.7512609E-04	0.4188745E-09	0.4592059E-07
55.	0.1462309E-03	0.5557420E-10	0.1185892E-07
60.	0.2427509E-03	0.6083012E-11	0.2154826E-08
65.	0.3602802E-03	0.5493134E-12	0.2887974E-09
70.	0.4931336E-03	0.4092398E-13	0.2944931E-10
75.	0.6358298E-03	0.2515311E-14	0.2333809E-11
80.	0.7838896E-03	0.1275445E-15	0.1458980E-12

TABLE 18. EXCEEDANCES PER HOUR - CONDITION 7 (31,000 FT.)

720B CONDITION 7 VERTICAL GUST ANALYSIS

WING ETA STATION = 0.33 STRUCTURAL ELEMENT 110
ALTITUDE 31,000 FT.

TURBULENCE PARAMETERS

P1 = 0.015000
P2 = 0.000090
B1 = 3.000000
B2 =11.250000

1G STRESSES (PSI)

SHEAR	SKIN	SEGMENT
-2274.0	-11740.0	-11220.0

V TRUE (FT/SEC) =810.7

G BAR = 0.2056369E-05 PER HOUR

RMS GUST VELOCITY (FT/SEC)	NC (PER FT)	F (SIGW)	NC F(SIGW) X 1800V'
10.	0.	0.1977267E-04	0.
15.	0.1119441E-20	0.2639028E-05	0.4310997E-20
20.	0.1367588E-12	0.1314431E-05	0.2623165E-12
22.	0.8729709E-11	0.9437267E-06	0.1201568E-10
24.	0.2060937E-09	0.6557961E-06	0.1977265E-09
26.	0.2414129E-08	0.4417695E-06	0.1556284E-08
28.	0.1701502E-07	0.2883346E-06	0.7159157E-08
30.	0.8223965E-07	0.1823358E-06	0.2188194E-07
32.	0.2996331E-06	0.1117175E-06	0.4868463E-07
34.	0.8676330E-06	0.6632002E-07	0.8416147E-07
36.	0.2129936E-05	0.3814541E-07	0.1185609E-06
38.	0.4545960E-05	0.2125759E-07	0.1410173E-06
40.	0.8684816E-05	0.1147783E-07	0.1454637E-06
45.	0.3054843E-04	0.2141284E-08	0.9545435E-07
50.	0.7512609E-04	0.3278701E-09	0.3594391E-07
55.	0.1462309E-03	0.4120434E-10	0.8792547E-08
60.	0.2427509E-03	0.4250083E-11	0.1505535E-08
65.	0.3602802E-03	0.3598035E-12	0.1891640E-09
70.	0.4931336E-03	0.2500039E-13	0.1799053E-10
75.	0.6358298E-03	0.1425744E-14	0.1322864E-11
80.	0.7838896E-03	0.6673441E-16	0.7633740E-13

TABLE 19. EXCEEDANCES PER HOUR - CONDITION 8

720B CONDITION 8 VERTICAL GUST ANALYSIS

WING ETA STATION = 0.33 STRUCTURAL ELEMENT 110

TURBULENCE PARAMETERS

P1 = 0.010500
P2 = 0.000020
B1 = 2.950000
B2 = 0.950000

1G STRESSES (PSI)

SHEAR	SKIN	SEGMENT
-2242.0	-12360.0	-11810.0

V TRUE (FT/SEC) =802.3

G BAR = 0.2047245E-06 PER HOUR

RMS GUST VELOCITY (FT/SEC)	NC (PER FT)	F (SIGW)	NC F(SIGW) X 1800V
10.	0.	0.1343433E-04	0.
15.	0.4392395E-22	0.2293403E-05	0.1454677E-21
20.	0.2190014E-13	0.9279908E-06	0.2934495E-13
22.	0.1912570E-11	0.6014662E-06	0.1662273E-11
24.	0.5731040E-10	0.3746223E-06	0.3100359E-10
26.	0.8082305E-09	0.2237600E-06	0.2611661E-09
28.	0.6600714E-08	0.1282526E-06	0.1222481E-08
30.	0.3593097E-07	0.7054160E-07	0.3660153E-08
32.	0.1439104E-06	0.3723226E-07	0.7732052E-08
34.	0.4539670E-06	0.1885769E-07	0.1236223E-07
36.	0.1189647E-05	0.9165630E-08	0.1574548E-07
38.	0.2688633E-05	0.4274755E-08	0.1659696E-07
40.	0.5393723E-05	0.1913228E-08	0.1490185E-07
45.	0.2096166E-04	0.2140765E-09	0.6449156E-08
50.	0.5490091E-04	0.1851253E-10	0.1467887E-08
55.	0.1123810E-03	0.1237248E-11	0.2007901E-09
60.	0.1938156E-03	0.6390609E-13	0.1788611E-10
65.	0.2962093E-03	0.2551068E-14	0.1091494E-11
70.	0.4150863E-03	0.7870332E-16	0.4711758E-13
75.	0.5451336E-03	0.1876571E-17	0.1477246E-14
80.	0.6819978E-03	0.3454924E-19	0.3605118E-16

TABLE 20. EXCEEDANCES PER HOUR - CONDITION 8 (33,000 FT.)

7208 CONDITION 8 VERTICAL GUST ANALYSIS

WING ETA STATION = 0.33 STRUCTURAL ELEMENT 110
ALTITUDE 33,000 FT.

TURBULENCE PARAMETERS

P1 = 0.012500
P2 = 0.000070
B1 = 2.970000
B2 =10.400000

1G STRESSES (PSI)

SHEAR	SKIN	SEGMENT
-2247.0	-12360.0	-11810.0

V TRUE (FT/SEC) =802.3

G BAR = 0.4429345E-06 PER HOUR

RMS GUST VELOCITY (FT/SEC)	NC (PER FT)	F (SIGW)	NC F(SIGW) X 1800V
10.	0.	0.1594628E-04	0.
15.	0.4392395E-22	0.2449926E-05	0.1553958E-21
20.	0.2190014E-13	0.1086651E-05	0.3436544E-13
22.	0.1912570E-11	0.7369660E-06	0.2035400E-11
24.	0.5731040E-10	0.4816636E-06	0.3986228E-10
26.	0.8082385E-09	0.3033744E-06	0.3540816E-09
28.	0.6600714E-08	0.1841420E-06	0.1755209E-08
30.	0.3593097E-07	0.1077124E-06	0.5588814E-08
32.	0.1438104E-06	0.6071798E-07	0.1260935E-07
34.	0.4539660E-06	0.3298434E-07	0.2162300E-07
36.	0.1189647E-05	0.1726780E-07	0.2966472E-07
38.	0.2688633E-05	0.8711743E-08	0.3382373E-07
40.	0.5393723E-05	0.4235571E-08	0.3299024E-07
45.	0.2086166E-04	0.5938290E-09	0.1788938E-07
50.	0.5490881E-04	0.6607368E-10	0.5239084E-08
55.	0.1123830E-03	0.5834627E-11	0.9468880E-09
60.	0.1938156E-03	0.4088984E-12	0.1144430E-09
65.	0.2962882E-03	0.2274234E-13	0.9730483E-11
70.	0.4150862E-03	0.1003859E-14	0.6017219E-12
75.	0.5451336E-03	0.3516637E-16	0.2768314E-13
80.	0.6818978E-03	0.9776875E-18	0.9627295E-15

TABLE 21. EXCEEDANCES PER HOUR - CONDITION 9

720B CONDITION 9 VERTICAL GUST ANALYSIS

WING ETA STATION = 0.33 STRUCTURAL ELEMENT 110

TURBULENCE PARAMETERS

P1 = 0.007000
P2 = 0.000108
B1 = 3.050000
B2 = 9.370000

1G STRESSES (PSI)

SHEAR	SKIN	SEGMENT
-1667.0	-12830.0	-12260.0

V TRUE (FT/SEC) =802.3

G BAR = 0.3465593E-07 PER HOUR

RMS GUST VELOCITY (FT/SEC)	NC (PER FT)	F (SIGW)	NC F(SIGW) X 1800V
10.	0.	0.1368454E-04	0.
15.	0.2993697E-25	0.2563735E-05	0.1108322E-24
20.	0.3589259E-15	0.9425586E-06	0.4885378E-15
22.	0.6361527E-13	0.5841866E-06	0.5366583E-13
24.	0.3263377E-11	0.3459464E-06	0.1630275E-11
26.	0.6989357E-10	0.1957401E-06	0.1975613E-10
28.	0.7948520E-09	0.1058192E-06	0.1214607E-09
30.	0.5849825E-08	0.5465913E-07	0.4459463E-09
32.	0.2812489E-07	0.2697582E-07	0.1095596E-08
34.	0.1063578E-06	0.1272039E-07	0.1953685E-08
36.	0.3242319E-06	0.5731121E-08	0.2683369E-08
38.	0.8327842E-06	0.2467133E-08	0.2966948E-08
40.	0.1863406E-05	0.1014751E-08	0.2730561E-08
45.	0.8909196E-05	0.9020098E-10	0.1160471E-08
50.	0.2728715E-04	0.6031117E-11	0.2376517E-09
55.	0.6247506E-04	0.3033394E-12	0.2736603E-10
60.	0.1173313E-03	0.1147567E-13	0.1944361E-11
65.	0.1916566E-03	0.3265664E-15	0.9038163E-13
70.	0.2829674E-03	0.6790171E-17	0.2856417E-14
75.	0.3876062E-03	0.1125550E-18	0.6299999E-16
80.	0.5016712E-03	0.1363216E-20	0.9875717E-18

TABLE 22. EXCEEDANCES PER HOUR - CONDITION 9 (38,000 FT.)

7208 CONDITION 9 VERTICAL GUST ANALYSIS

WING ETA STATION = 0.33 STRUCTURAL ELEMENT 110

ALTITUDE 38,000 FT.

TURBULENCE PARAMETERS

P1 = 0.008300
P2 = 0.000100
B1 = 2.[illegible]50000
B2 = 9.500000

1G STRESSES (PSI)

SHEAR	SKIN	SEGMENT
-1667.0	-12830.0	-12260.0

V TRUE (FT/SEC) =802.3

G BAR = 0.4021656E-07 PER HOUR

RMS GUST VELOCITY (FT/SEC)	NC (PER FT)	F (SIGW)	NC F(SIGW) X 1800V
10.	0.	0.1200366E-04	0.
15.	0.2993697E-25	0.2420095E-05	0.1046225E-24
20.	0.3589759E-15	0.9157799E-06	0.4746581E-15
22.	0.6361527E-13	0.5750183E-06	0.5282360E-13
24.	0.3263377E-11	0.3454012E-06	0.1627706E-11
26.	0.6989357E-10	0.1984803E-06	0.2003271E-10
28.	0.7948520E-09	0.1091095E-06	0.1252373E-09
30.	0.5649825E-08	0.5737982E-07	0.4681436E-09
32.	0.2812489E-07	0.2886738E-07	0.1172419E-08
34.	0.1063578E-06	0.1389335E-07	0.2133836E-08
36.	0.3242319E-06	0.6396730E-08	0.2995013E-08
38.	0.8327842E-06	0.2817478E-08	0.3388270E-08
40.	0.1863406E-05	0.1187175E-08	0.3194532E-08
45.	0.8909196E-05	0.1127036E-09	0.1449977E-08
50.	0.2728715E-04	0.8110684E-11	0.3195954E-09
55.	0.6247506E-04	0.4424601E-12	0.3991772E-10
60.	0.1173313E-03	0.1829732E-13	0.3100176E-11
65.	0.1916566E-03	0.5735850E-15	0.1587473E-12
70.	0.2829674E-03	0.1363028E-16	0.5569628E-14
75.	0.3876062E-03	0.2455324E-18	0.1374309E-15
80.	0.5016712E-03	0.3352815E-20	0.2428922E-17

TABLE 23. EXCEEDANCES PER HOUR - CONDITION 10

7208 CONDITION 10 VERTICAL GUST ANALYSIS

WING ETA STATION = 0.33 STRUCTURAL ELEMENT 110

TURBULENCE PARAMETERS

P1 = 0.010500
P2 = 0.000090
B1 = 2.950000
B2 = 9.850000

1G STRESSES (PSI)

SHEAR	SKIN	SEGMENT
-1680.0	-12440.0	-11890.0

V TRUE (FT/SEC) =802.3

G BAR = 0.9421857E-07 PER HOUR

RMS GUST VELOCITY (FT/SEC)	NC (PER FT)	F (SIGW)	NC F(SIGW) X 1800V
10.	0.	0.1343433E-04	0.
15.	0.6825464E-24	0.2293402E-05	0.2260463E-23
20.	0.1980235E-[illegible]	0.9279008E-06	0.2653404E-14
22.	0.2562953E-12	0.6018662E-06	0.2227540E-12
24.	0.1034991E-10	0.3746223E-06	0.5599060E-11
26.	0.1839855E-09	0.2237600E-06	0.5944988E-10
28.	0.1804632E-08	0.1282526E-06	0.3342257E-09
30.	0.1138379E-07	0.7054160E-07	0.1159624E-08
32.	0.5139145E-07	0.3723226E-07	0.2763091E-08
34.	0.1792147E-06	0.1885769E-07	0.4880306E-08
36.	0.5104520E-06	0.9165430E-08	0.6756048E-08
38.	0.1237806E-05	0.4274765E-08	0.7640991E-08
40.	0.2636902E-05	0.1913228E-08	0.7285271E-08
45.	0.1145940E-04	0.2140765E-09	0.3542549E-08
50.	0.3278019E-04	0.1851253E-10	0.8763187E-09
55.	0.7135182E-04	0.1237248E-11	0.1274814E-09
60.	0.1289484E-03	0.6390609E-13	0.1189989E-10
65.	0.2044269E-03	0.2551068E-14	0.7530868E-12
70.	0.2947557E-03	0.7870392E-16	0.3349991E-13
75.	0.3961485E-03	0.1876571E-17	0.1073515E-14
80.	0.5049039E-03	0.3458024E-19	0.2521283E-16

TABLE 24. EXCEEDANCES PER HOUR - CONDITION 11

720B CONDITION 11   VERTICAL GUST ANALYSIS

WING ETA STATION = 0.33   STRUCTURAL ELEMENT 110

TURBULENCE PARAMETERS

P1 = 0.010500
P2 = 0.000090
B1 = 2.950000
B2 = 5.850000

1G STRESSES (PSI)

SHEAR	SKIN	SEGMENT
-1688.0	-12290.0	-11740.0

V TRUE (FT/SEC) =802.3

G BAR = 0.1386928E-06 PER HOUR

RMS GUST VELOCITY (FT/SEC)	NC (PER FT)	F (SIGW)	NC F(SIGW) X 1800V
10.	0.	0.1343433E-04	0.
15.	0.1018789E-22	0.2293402E-05	0.3374035E-22
20.	0.8984191E-14	0.9279008E-06	0.1203831E-13
22.	0.6878843E-12	0.6018662E-06	0.7716872E-12
24.	0.2920107E-10	0.3746223E-06	0.1579710E-10
26.	0.4424843E-09	0.2237600E-06	0.1429767E-09
28.	0.3824009E-08	0.1282526E-06	0.7082233E-09
30.	0.2178173E-07	0.7054160E-07	0.2218827E-08
32.	0.9045698E-07	0.3723226E-07	0.4863477E-08
34.	0.2943696E-06	0.1885769E-07	0.8016161E-08
36.	0.7912543E-06	0.9165430E-08	0.1047258E-07
38.	0.1826948E-05	0.4274765E-08	0.1127777E-07
40.	0.3732443E-05	0.1913228E-08	0.1031205E-07
45.	0.1495351E-04	0.2140765E-09	0.4622716E-08
50.	0.4035565E-04	0.1851253E-10	0.1078835E-08
55.	0.8413070E-04	0.1237248E-11	0.1503132E-09
60.	0.1471225E-03	0.6390609E-13	0.1357708E-10
65.	0.2273304E-03	0.2551068E-14	0.8374610E-12
70.	0.3211684E-03	0.7870397E-16	0.3650179E-13
75.	0.4246314E-03	0.1876571E-17	0.1150700E-14
80.	0.5340711E-03	0.3458024E-19	0.2666932E-16

TABLE 25. EXCEEDANCES PER HOUR - CONDITION 12

720B CONDITION 12 VERTICAL GUST ANALYSIS

WING ETA STATION = 0.33 STRUCTURAL ELEMENT 110

TURBULENCE PARAMETERS

P1 = 0.100000
P2 = 0.000600
B1 = 3.550000
B2 = 9.700000

1G STRESSES (PSI)

SHEAR	SKIN	SEGMENT
-2322.0	-10730.0	-10250.0

V TRUE (FT/SEC) =523.6

G BAR = 0.7597590E-06 PER HOUR

RMS GUST VELOCITY (FT/SEC)	NC (PER FT)	F (SIGW)	NC F(SIGW) X 1800V
10.	0.	0.4542770E-03	0.
15.	0.1561897E-22	0.1791400E-04	0.2636922E-21
20.	0.1380613E-13	0.5893658E-05	0.7668476E-13
22.	0.1371655E-11	0.3769846E-05	0.4873272E-11
24.	0.4532674E-10	0.2312003E-05	0.9876321E-10
26.	0.6896673E-09	0.1358943E-05	0.8832697E-09
28.	0.5981280E-08	0.7655112E-06	0.4315169E-08
30.	0.3417333E-07	0.4132748E-06	0.1331001E-07
32.	0.1422918E-06	0.2138274E-06	0.2867447E-07
34.	0.4641149E-06	0.1060290E-06	0.4637700E-07
36.	0.1250027E-05	0.5038757E-07	0.5936015E-07
38.	0.2891313E-05	0.2294875E-07	0.6253258E-07
40.	0.5916142E-05	0.1001686E-07	0.5584792E-07
45.	0.2377751E-04	0.1046859E-08	0.2345884E-07
50.	0.6432291E-04	0.8387859E-10	0.5086743E-08
55.	0.1343430E-03	0.5152532E-11	0.6523609E-09
60.	0.2352751E-03	0.2426593E-12	0.5380531E-10
65.	0.3640106E-03	0.8761528E-14	0.3005703E-11
70.	0.5149513E-03	0.2425321E-15	0.1177030E-12
75.	0.6819313E-03	0.5147134E-17	0.3307945E-14
80.	0.8594628E-03	0.8374681E-19	0.6783402E-16

TABLE 26 (a)

EXCEEDANCES OF LIMIT STRENGTH PER AVERAGE FLIGHT HOUR FOR TOTAL AIRPLANE USAGE, N_p - VERTICAL ANALYSIS, WING

Component	Station	Structural Element	Np
Wing	Eta .33	0	$2.5x10^{-8}$
		1	$1.0x10^{-8}$
		7	$1.1x10^{-6}$
		9	$2.1x10^{-6}$
		17	$1.5x10^{-7}$
		99	$9.1x10^{-9}$
		100	$3.5x10^{-11}$
		101	$6.7x10^{-10}$
		110	$1.1x10^{-6}$
		117	$2.3x10^{-5}$
		122	$6.5x10^{-6}$
		199	$9.1x10^{-8}$

R

TABLE 26 (b)

EXCEEDANCES OF LIMIT STRENGTH PER AVERAGE FLIGHT HOUR FOR TOTAL AIRPLANE USAGE, N_p - VERTICAL ANALYSIS, FUSELAGE

Component	Station	Structural Element	N_p
Fuselage	Body 540	100	$1.2(10^{-11})$
		2	$1.7(10^{-11})$
		3	$2.3(10^{-11})$
		4	$9.1(10^{-11})$
		8	$9.0(10^{-10})$
		9	$2.0(10^{-9})$
		16	$6.9(10^{-13})$
		20	$5.1(10^{-12})$
		23	$3.0(10^{-13})$
		2700	$2.9(10^{-11})$
		28	$3.1(10^{-16})$
		29	$2.9(10^{-14})$
		30	$1.1(10^{-10})$
	Body 1040	100	$3.0(10^{-15})$
		2	$2.1(10^{-14})$
		3	$8.0(10^{-14})$
		4	$9.3(10^{-14})$
		8	$3.5(10^{-15})$
		16	$3.5(10^{-11})$
		20	$10.0(10^{-15})$
		23	$3.3(10^{-27})$
		27	$5.4(10^{-21})$
		28	$1.8(10^{-11})$
	Body 1360	100	$1.02(10^{-14})$
		2	$2.6(10^{-14})$
		3	$1.1(10^{-14})$
		4	$3.4(10^{-15})$
		8	$5.6(10^{-21})$
		1200	$2.0(10^{-48})$
		14	$8.2(10^{-31})$
		16	$2.2(10^{-20})$
		23	$7.8(10^{-17})$
		27	$1.8(10^{-15})$
		28	$1.6(10^{-15})$
		29	$1.9(10^{-16})$
		31	$2.7(10^{-12})$

TABLE 26 (c)
EXCEEDANCES OF LIMIT STRENGTH PER AVERAGE FLIGHT HOUR FOR TOTAL AIRPLANE USAGE, N_p - LATERAL ANALYSIS

Component	Station	Structural Element	Np Yaw Damper On	Np Yaw Damper Off
Fuselage	Body 1040	100	$9.1(10^{-13})$	$3.4(10^{-10})$
		2	$1.2(10^{-12})$	$4.0(10^{-10})$
		3	$9.5(10^{-13})$	$7.1(10^{-10})$
		4	$8.5(10^{-14})$	$1.5(10^{-10})$
		8	$9.9(10^{-13})$	$5.4(10^{-10})$
		16	$8.1(10^{-13})$	$3.7(10^{-10})$
		20	$3.5(10^{-12})$	$6.3(10^{-11})$
		23	$1.6(10^{-27})$	$1.7(10^{-19})$
		27	$6.4(10^{-32})$	$3.2(10^{-22})$
		28	$2.3(10^{-23})$	$1.0(10^{-16})$
	Body 1360	100	$4.8(10^{-19})$	$2.2(10^{-13})$
		2	$2.0(10^{-19})$	$1.8(10^{-13})$
		3	$4.8(10^{-16})$	$1.6(10^{-11})$
		4	$1.2(10^{-13})$	$6.8(10^{-10})$
		8	$6.9(10^{-11})$	$7.5(10^{-8})$
		1200	$4.3(10^{-10})$	$2.1(10^{-7})$
		14	$5.5(10^{-9})$	$1.4(10^{-6})$
		16	$2.1(10^{-8})$	$3.5(10^{-6})$
		23	$9.6(10^{-9})$	$1.1(10^{-6})$
		27	$3.0(10^{-10})$	$3.2(10^{-7})$
		28	$2.1(10^{-9})$	$4.4(10^{-7})$
		29	$1.1(10^{-10})$	$6.0(10^{-8})$
		3100	$3.1(10^{-11})$	$9.8(10^{-8})$
Fin	Elastic Axis 158	0	$2.6(10^{-9})$	$8.0(10^{-6})$
		1	$4.7(10^{-9})$	$1.3(10^{-6})$
		5	$1.0(10^{-12})$	$7.6(10^{-9})$
		10	$9.8(10^{-15})$	$5.2(10^{-10})$
		110	$2.4(10^{-16})$	$3.9(10^{-11})$
		100	$4.7(10^{-9})$	$1.7(10^{-6})$

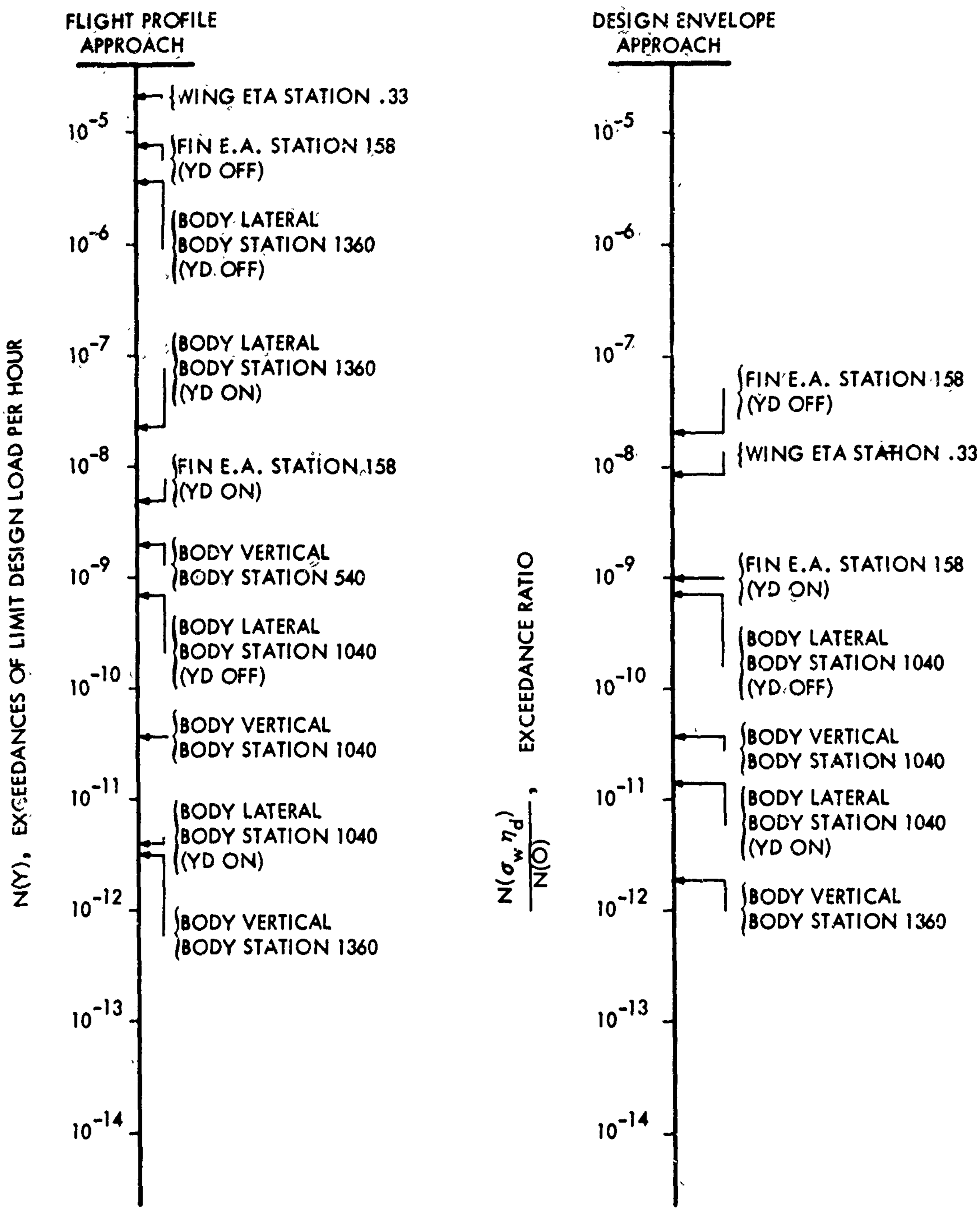

FIGURE 84. SUMMARY OF DESIGN VALUES OF EXCEEDANCE RATIOS AND FREQUENCY OF EXCEEDANCES BASED ON JOINT PROBABILITY

CONCLUSIONS

General

The use of power spectral techniques to assess the strength capability of airplanes subjected to continuous turbulence appears to be the most rational approach to the airplane gust design problem. The statistical methods which were developed basically in the communications field are well founded and understood; however, their application to complex aircraft structure in dynamic loads analyses has only been pursued in recent years.

There are two rather general problems associated with a detailed gust power spectral analyses. The first is the "long chain" of calculations that must be conducted to arrive at the solution, and the second is the interpretation of the statistical result in terms that are meaningful to the design engineer. In the foregoing analysis, the first problem was partially overcome by proper linking of the individual digital computer programs required to calculate the dynamic responses in the flexible modes, the rms loads and stresses, and finally the statistical results into a chain program. This allowed for orderly flow of data by the use of tape storage from one program to another. This enables an engineer to analyze many conditions in a relatively short period of time. The results of this study will serve as a guide to the solution of the second problem.

Dynamic analyses leading up to an assessment of the strength of structural elements or components is complex and can be very sensitive to the mathematical description of the airplane being analyzed. Even when the analysis is conducted for an airplane that is currently in service, a vehicle for which a great deal of information is available, the analysis is still difficult to accomplish. Experienced personnel who are capable of exercising good judgment on estimates of sensitive airplane parameters are needed to use this approach in the preliminary design stage.

Certainly, power spectral gust analyses should be conducted early in the design stages to "raise-the-flag" on possible problem areas. Furthermore, these analyses should include parametric variations of sensitive parameters, which need better definition. The analyses may become more complex as the design nears the final stages, but the analysis should be assessed in each stage by comparing reduced solutions of the basic equations with separate maneuver and flutter solutions.

One Parameter Versus Joint Probability Approaches

If the structure being analyzed is sensitive primarily to an axial stress which results predominantly from bending, the bending moment approach and the joint probability approach should lead to nearly the same result. This is true, because the other load quantities contribute only slightly to the margin of safety in the more critical structural elements. Since the effort involved in a single parameter bending moment approach is about one-half of that of the full joint probability stress analysis, it is advantageous to use a bending moment criteria when suitable.

The bending moment analysis is useful in the design envelope approach to help locate the critical flight condition. The selection of critical conditions for vertical analyses in this program required 20 separate analyses. If all of these analyses had been carried through the joint probability solution, the analyses time would have been extended several months. Since all of the load quantities tended to increase as the critical condition was approached, the bending moment served as a good measure of the criticalness of the condition.

The success of using the bending moment to locate the critical structure is dependent again upon whether or not the structural element is more likely to reach limit load under an axial stress condition or a combined stress condition. If it is a stress condition which results from combined loadings then the bending moment alone will lead to erroneous results.

The joint probability method, while more rational in considering combined loading, has some drawbacks in regards to its use in a design sense. One of these problems is in obtaining the detailed stress coefficients, another is the definition of the strength envelope.

Model 720B Analysis Results

Limit-strength values of $\sigma_w \eta_d$ and of hours to exceed limit design strength, for the model 720B, are summarized in Figures 85 and 86. Results based on both the bending moment analyses and the more exact joint probability analyses are shown.

Recommendations for Design

Specifically, the following recommendations are offered concerning the use of gust power spectral techniques in airplane design:

1. Gust power spectral analysis techniques appear to be the most rational approach to the gust loads design problem. However, they should be used in such a manner that they can truly assure timely design information, and hence a properly designed airplane from the standpoint of gust loading. This can be

accomplished by a continual study during the airplane design stages using the best available data at each stage to eliminate the possibility of unpleasant surprises after the airplane is in service.

2. Initially, the aerodynamic, structural, and stability augmentation data used in the analyses will be rough; therefore, these initial analyses should be simple and should include parametric variations on the more significant input data.

3. Then, the more sensitive parameters should be isolated and studied further through separate test and analysis programs.

4. Later studies will be used to evaluate the limit bending moments, shears, and torsions for the major components. Also, the phasing or correlation between these loads should be obtained and used as a guide in the design.

5. Joint probability techniques to properly account for the phasing of the loads or stresses should be employed only for the more critical components of the airplane when the margin of safety is highly dependent on combined loading and the statistical correlation between the loads or the stresses is poor.

6. All of the studies should be subjected to a set of checks with separate maneuver and flutter analyses or test results in order to keep the studies in perspective and to provide confidence in the results as the analyses become more complex during the later design stages.

7. Stability augmentation systems and control dynamic effects should be incorporated in the early studies and developed along with the basic airframe in coupled dynamic loads gust analyses.

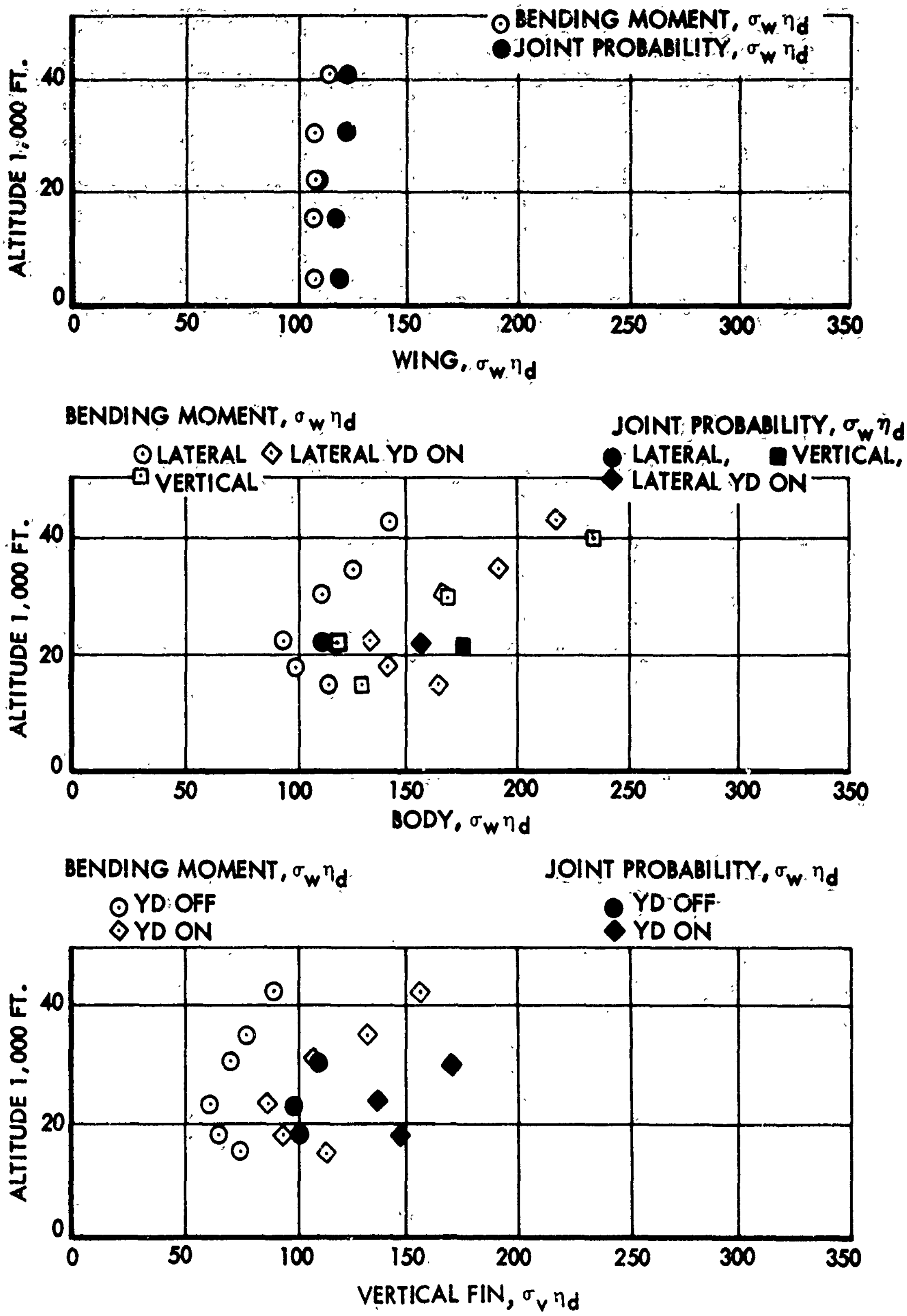

FIGURE 85. SUMMARY OF CRITICAL VALUES OF $\sigma_w \eta_d$

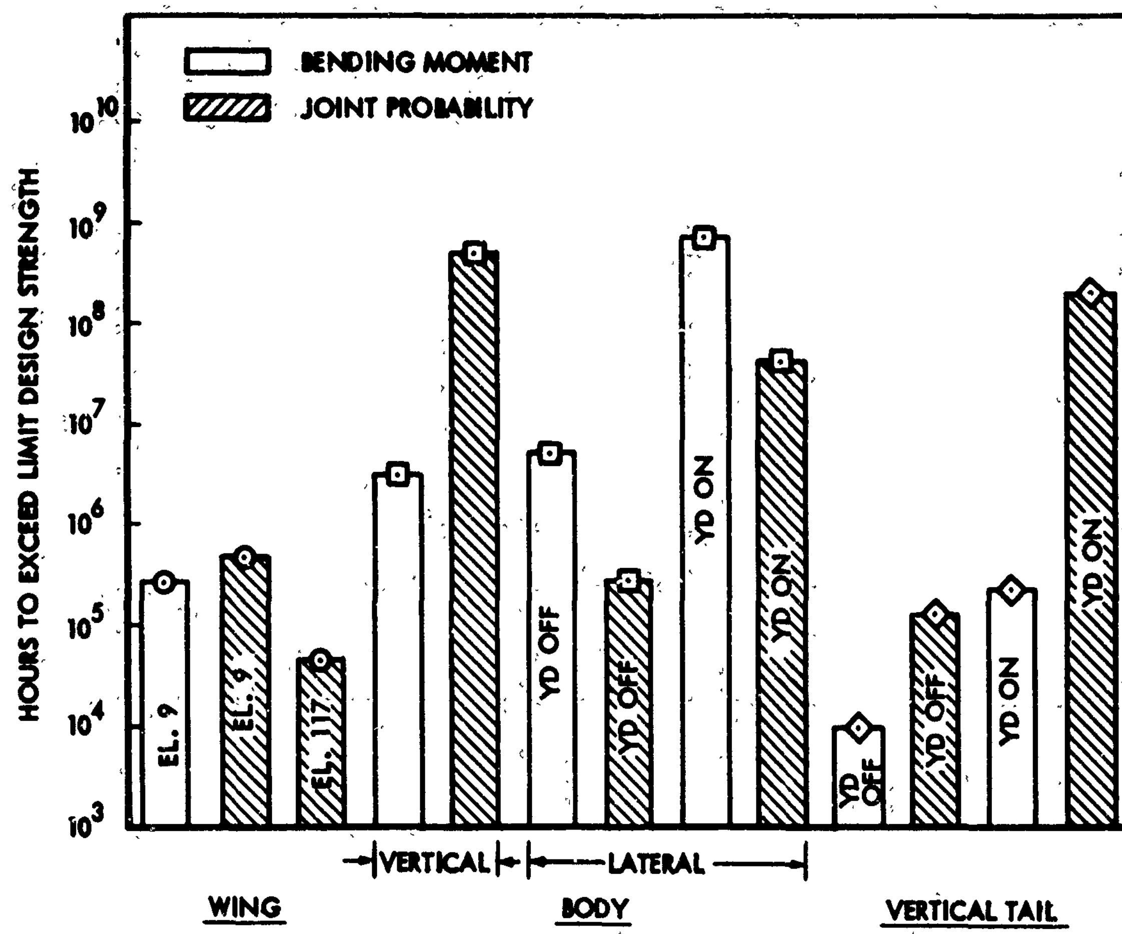

FIGURE 86. SUMMARY OF FLIGHT PROFILE RESULTS

APPENDIX A

EQUATIONS OF MOTION

APPENDIX A

EQUATIONS OF MOTION

General Comments

The degree of success in evaluating the strength capability of a complex airplane structure subjected to flight in atmospheric turbulence relies almost entirely upon the ability to construct a mathematical model of the physical system. An airplane in flight is considered to be an elastic-dynamic system which when acted upon by external aerodynamic gust velocities undergoes motions necessary to maintain an energy balance. The analysis procedure generally used is referred to as the Energy Method and is applicable to a system where the total change in kinetic energy is equal to the summation of the work done by all forces acting during a slight deflection from the equilibrium position. In other words the application of the energy method is contingent on the principle of virtual work which may be stated as follows:

> If a body is in equilibrium under the action of prescribed external forces, the work done by these forces in a small additional displacement compatible with the constraints is equal to the change in strain energy.

The above statement can be expressed as Eq. (A1)

$$\delta W_e + \delta W_{in} = \delta V \qquad \text{(A1)}$$

where

δW_e = the external work done

δW_{in} = the internal work done

δV = the change in strain energy

The airplane motions, as given by Eq. (A2), are expressed as the summation over a set of independent generalized coordinates which are defined explicitly in terms of space and time.

$$\delta_i = \sum_{j=1}^{n} \phi_{ij} q_j \qquad \text{(A2)}$$

where

ϕ_{ij} = the jth normalized mode shape which is a function of geometry only.

q_j = the jth generalized coordinate which is a function of time only.

Using the above coordinate definition and Lagrange's specialized form of the energy equation, the equations of motion for the physical system are formed using Eq. (A3).

$$\left[\frac{d}{dt}\left(\frac{\partial T}{\partial \dot{q}_j}\right) - \frac{\partial T}{\partial q_j} + \frac{\partial V}{\partial q_j}\right] \delta q_j + Q_j \delta q_j = \bar{Q}_j \phi \alpha_g \tag{A3}$$

where

T = the kinetic energy of the system.

V = the strain energy of the system.

Q_j = generalized external force due to the system's response.

$\bar{Q}_j$ = generalized external force due to the gust velocity.

q_j = the jth generalized coordinate displacement.

$\dot{q}_j$ = the jth generalized coordinate velocity.

For a linear elastic system such as the airplane structure the elastic forces are given by $\partial V / \partial q_j$ and the kinetic energy is not dependent upon the displacement, q_j, thus $\partial T / \partial q_j = 0$, leaving the Lagrangian equation as Eq. (A4) below.

$$\left[\frac{d}{dt}\left(\frac{\partial T}{\partial \dot{q}_j}\right) \quad \frac{\partial V}{\partial q_j} + Q_j\right] \delta q_j = \bar{Q}_j \phi \alpha_g \tag{A4}$$

VERTICAL ANALYSES

<u>Generalized Inertia</u>

The kinetic energy, T, in the above equation is obtained by multiplying the individual lumped masses by their respective velocities squared and then summing over the generalized coordinates. This can be expressed in matrix form as Eq. (A5).

$$\lfloor \dot{q}_j \rfloor \left[\phi_{ij}\right] \left[a_{ri}\right] \left[M_{rr}\right] \left[a_{ri}\right] \left[\phi_{ij}\right] \left\{\dot{q}_j\right\} = 2\,T \tag{A5}$$

where

$\left[M_{rr}\right]$ = the mass and inertia properties described about the principle axis at the lumped mass center of gravity.

$\left[a_{ri}\right]$ = the transformation matrix transforming lumped mass center of gravity displacements to elastic axis displacements.

$\left[\phi_{ij}\right]$ = the normalized mode shapes.

When this kinetic energy matrix, T, is substituted into Lagrange's equation and the appropriate differentiations carried out the following inertia matrix is generated:

$$\frac{d}{dt}\left[\frac{\partial T}{\partial \dot{q}_j}\right] = \left[M_3\right]\left\{\ddot{q}_j\right\} \tag{A6}$$

where

$\left[M_3\right] = \left[\phi_{ij}\right]' \left[J_{ii}\right] \left[\phi_{ij}\right]$

$\ddot{q}_j$ = generalized coordinate acceleration

$\left[J_{ii}\right] = \left[a_{ri}\right]' \left[M_{rr}\right] \left[a_{ri}\right]$

as described above.

Generalized Stiffness

The second portion of equations of motion by the Lagrangian approach are the strain energy terms. The strain energy associated with a deflection in the generalized coordinates could be generated by considering the elastic axis as a series of springs having stiffnesses of k_i. Then the strain energy would be given by Eq. (A7).

$$2V = \lfloor q_j \rfloor \left[\phi_{ij}\right]' \left[k_{ii}\right] \left[\phi_{ij}\right] \left\{q_j\right\} \tag{A7}$$

and when substituted in Lagrange's equation would result as Eq. (A8)

$$\frac{\partial V}{\partial q} = \left[K_{jj} \right] \left\{ q_j \right\} \quad \text{(A8)}$$

where

$$\left[K \right] = \left[\phi_{ij} \right]' \left[k_{ii} \right] \left[\phi_{ij} \right]$$

However, it is more convenient to use the natural frequency of the jth normal mode to represent the generalized stiffness as expressed by Eq. (A9):

$$\left[M_3 \right]_{jj} \omega_{n_j}^2 = \left[K_{jj} \right] \quad \text{(A9)}$$

A tabulation of the natural frequencies used in the analysis are given in Tables 6 and 7 in the Analysis Section.

Generalized Response Aerodynamics

The generalized external forces which result from the motion of the system, Q_j, are the aerodynamic lift and moments. These force expressions are based upon a modified strip theory (8) which incorporates the aerodynamic induction between the individual aerodynamic panels. The transmittal time associated with this aerodynamic induction is also incorporated as a phase lag between the resultant force vector and the originating panel motion. The strip theory coefficients which give the aerodynamic forces on a panel due to its own motion are used as they were originally expressed by Theodorsen (9) and Küssner (10) with two exceptions. These exceptions are the two dimensional lift and moment expressions, 2π, and $(1/2+a)$ are changed to values more representative of the aerodynamic surface being examined. The adjusted values are obtained by reducing the oscillatory lift and moment coefficients to their steady state values and using the static induction matrix (7) to solve for the lift and moment coefficients that give the proper steady state lift and moment distributions. These values are then used with the dynamic induction matrix and oscillatory lift and moment coefficients to give the generalized external aerodynamic force due to system response. A representative equation for this generalized external force is given below in matrix form as Eq. (A10):

$$\left\{ Q_j \right\}_{\substack{\text{wing}\\ \text{tail}}} = 2\rho b_r^2 \omega^2 \left[\phi_{ij} \right]' \begin{bmatrix} \left[S_1^{-1} f(t) \right] \Delta x_i & 0 \\ T \left[S_1^{-1} f(t) \right] \Delta x_i & \left[S_1^{-1} f(t) \right] \Delta x_i \end{bmatrix} \begin{bmatrix} A_{Lh} & A_{L\alpha} \\ A_{mh} & A_{m\alpha} \end{bmatrix} \left[\phi_{ij} \right] \left\{ q_j \right\} \quad \text{(A10)}$$

where

ρ = atmospheric density - lb.sec.^{2} per in.^{4}

b_r = reference semi-chord - in.

ω = response frequency - rad. per sec.

Δx_i = span of the ith aerodynamic panel - in.

T = distance from panel quarter chord to panel rotation axis - in.

$\left[S_1^{-1} f(t) \right]$ = dynamic induction matrix - in.

A_{Lh} = oscillatory panel lift coefficient due to the translation motion of the panel rotation axis.

$A_{L\alpha}$ = oscillatory panel lift coefficient due to angular motion about the panel rotation axis.

A_{mh} = oscillatory panel moment coefficient due to translation motion of the panel rotation axis.

$A_{m\alpha}$ = oscillatory panel moment coefficient due to rotation motion about the panel rotation axis.

Selecting a frequence, ω, the evaluation of the above generalized external force expression results in an aerodynamic matrix with complex coefficients. Since this expression is for a discrete harmonic frequency these complex coefficients can be expressed by Eq. (A11).

$$\left[a+ib \right] q_j = \left[a \right] q_j + \frac{1}{\omega} \left[b \right] \dot{q}_j \quad \text{(A11)}$$

where

$$q_j = q_{o_j} e^{si\omega t}$$

$$\dot{q}_j = i\omega q_j$$

$$\ddot{q}_j = -\omega^2 q_j$$

Applying this to $\left[Q_j \right]_{W\&T}$ in Eq. (A10) gives a set of aerodynamic coefficients for the generalized coordinate displacements and velocities as shown in Eq. (A12).

$$\left[Q_j\right]_{W\&T} = \frac{1}{\omega}\left[A_1\right]_{W\&T} \dot{q}_j + \left[A_2\right]_{W\&T} q_j \qquad (A12)$$

The aerodynamic forces acting upon the body panels are treated separately. Quasi-steady expressions are used which account for apparent angles of attack due to translation velocities, rotation displacements and rotational velocities of each body panel. The expression for these forces are given below in Eq. (A13).

$$\left[Q_j\right]_B = 2\rho b_r^3 \omega^2 \left[\phi_{ij}\right] \begin{bmatrix} \bar{A}_{Lh} & \bar{A}_{L\alpha} \\ \bar{A}_{mh} & \bar{A}_{m\alpha} \end{bmatrix} \left[\phi_{ij}\right]' q_j \qquad (A13)$$

where

$\bar{A}_{Lh}$ = quasi static lift coefficient due to translation

$\bar{A}_{L\alpha}$ = quasi static lift coefficient due to rotation

$\bar{A}_{mh}$ = quasi static moment coefficient due to translation

$\bar{A}_{m\alpha}$ = quasi static moment coefficient due to rotation

These are calculated for each frequency and converted to displacement and velocity coefficients and added the generalized forces calculated for the wing and horizontal tail to give total generalized external force due to system response.

Generalized Excitation Aerodynamics

The remaining external force arises from the turbulence velocities, U. The expressions used to describe this generalized force are similar to those used to describe the aerodynamic forces due to response. The only essential difference is that these forces arise from gust angles of attack. When employing the power spectral density approach, it is necessary to obtain the response of the airplane to discrete gust frequencies. These gust angle inputs are expressed by Eq. (A14).

$$\alpha_g = \frac{U}{V_T} e^{i\omega t} \qquad (A14)$$

U = gust velocity, usually taken as 1 ft. per sec.

V_T = true airplane velocity, ft. per sec.

ω = gust excitation frequency, rad. per sec.

As the airplane penetrates the gust the excitation force is felt progressively along the direction of flight. The gradual penetration effect is represented as a phase lag by Eq. (A15).

$$\alpha_g = \frac{U}{V_T} e^{i(\omega t+\theta)} \tag{A15}$$

where

$$\theta = \omega \frac{\lambda_i + b_i}{V_T}$$

$\lambda_i + b_i$ = the distance from the leading edge of the foremost panel to the mid-chord of panel i.

Substituting the expression for θ into Eq. (A15) gives Eq. (A16).

$$\alpha_g = \frac{U}{V_T} e^{i\omega t} e^{\frac{i\omega(\lambda_i+b_i)}{V_T}} \tag{A16}$$

The end expression for the generalized external force due to a sinusoidal gust velocity is given by Eq. (A17).

$$\left\{\bar{Q}_j\right\} = 2\rho b_r^3 \omega^2 \left[\phi_{ij}\right]' \left[a_{ij}\right] \left[S_1^{-1} f(t)\Delta x\right] \left[\bar{A}_{L\alpha_g}\right] \frac{W}{V} e^{i\omega t} e^{\frac{i\omega(\lambda+b)}{V_T}} \tag{A17}$$

where

$\left[\bar{A}_{L\alpha_g}\right]$ = modified two dimensional lift coefficient due to gust angle of attack.

Structural Damping

The final item that may be included and is not shown in Lagrange's equation is the structural damping force. This force is assumed to be proportional to the generalized stiffness but in phase with the generalized coordinate velocity. An expression for this is shown below:

$$\text{structural damping} = i\, g_j\, k_j\, q_j \tag{A18}$$

where

g_j = damping coefficient approximately equal to twice the damping ratio c/c_c.

i = phasing operator which shifts the force vector 90 degrees ahead of the displacement q_j.

k_j = generalized stiffness for the jth mode.

The expression used in the equations of motion is given by the following form:

$$i\, g_j\, k_j\, q_j = \frac{g_j M_{3jj} \omega_{N_j}^2}{\omega} \dot{q}_j \qquad \text{(A19)}$$

The equations of motion for the mathematical model of the airplane system are formed by collecting all of the above expressions into a matrix equation as follows:

$$\left[M_3\right] \ddot{q}_j + \frac{1}{\omega}\left\{\left[A_1\right]_{W\&T} + \left[A_1\right]_B + \left[g_j\, M_{3jj}\, \omega_{N_j}^2\right]\right\} \dot{q}_j + \left\{\left[A_2\right]_{W\&T} + \left[A_2\right]_B + \left[M_{3jj}\omega_{N_j}^2\right]\right\} q_j = \frac{W}{V}\left[A_g\right] e^{\frac{i\omega(\lambda+b_i)}{V_T}} e^{i\omega t} \qquad \text{(A20)}$$

or simplified

$$\left[M_3\right] \ddot{q} + \left[M_2\right] \dot{q} + \left[M_1\right] q = \frac{W}{V}\left\{C_3\right\} e^{\frac{i\omega(\lambda+b_i)}{V_T}} e^{i\omega t} \qquad \text{(A21)}$$

Substituting for $\ddot{q}$ and q under the assumption of harmonic motion as shown in Eq. (A11) we obtain

$$\left\{-\omega^2\left[M_3\right] + \left[M_1\right] + i\omega\left[M_2\right]\right\} q_{oj} = \frac{W}{V}\left\{C_3\right\} e^{\frac{i\omega(\lambda+b)}{V_T}} \qquad \text{(A22)}$$

Solution of Equations of Motion

The final step is the solving of the equations of motion to obtain the response of the generalized coordinate, q_{oj}. This solution, obtained for each discrete frequency, ω as shown by Eq. (A23), results in the vector magnitude and phase angle relative to the gust input of each of the generalized coordinates.

$$q_{oj} = \left\{ \left[-\omega^2 \left[M_3 \right] + \left[M_1 \right] \right] + i\omega \left[M_2 \right] \right\}^{-1} \frac{W}{V} \left\{ C_3 \right\} e^{\frac{i\omega(\lambda+b)}{V_T}} \quad \text{(A23)}$$

Representative frequency response curves are shown in Fig. 27 of the Results section.

LATERAL ANALYSES

Areas of Similarity between Vertical and Lateral Analyses

The equations of motion for the lateral analyses are also formed using the Lagrangian approach. The formulation of the generalized inertia and stiffness matrices for the lateral equations of motion follow the same procedure as outlined for the vertical analyses. The generalized coordinates used in these lateral equations are the antisymmetric body and vertical tail cantilevered modes as listed in Table 8 of the Analyses Section.

Generalized Aerodynamics

The aerodynamic response and excitation forces, however, are based on quasi-steady expressions which are convoluted with the Wagner and Küssner lift growth functions. The Wagner and Küssner lift growth effects were represented by the step response functions (recommended on Page 344, Ref. 18) for an aspect ratio of three. The frequency domain analysis requires that lift growth effects be represented by the impulse function which is obtained by writing the Laplace transform of the first time derivative of the step function.

Yaw Damper Simulation

The yaw damper is designed to reduce the yaw response to disturbances and, in doing so, increases the Dutch roll stability. The yaw damper system is best defined as a electromechanical and composed of a rate gyro which provides an output signal proportional to yaw rate. The signal from the rate gyro is applied to a bandpass filter which removes the low frequency components resulting from steady state turns and the higher frequency components associated with the structural vibrations. After filtering, the signal is amplified and applied to a servo-motor which results in a hydraulically actuated rudder deflection to oppose the yawing motion.

The method of simulating the yaw damper is illustrated by the simplified block diagram below:

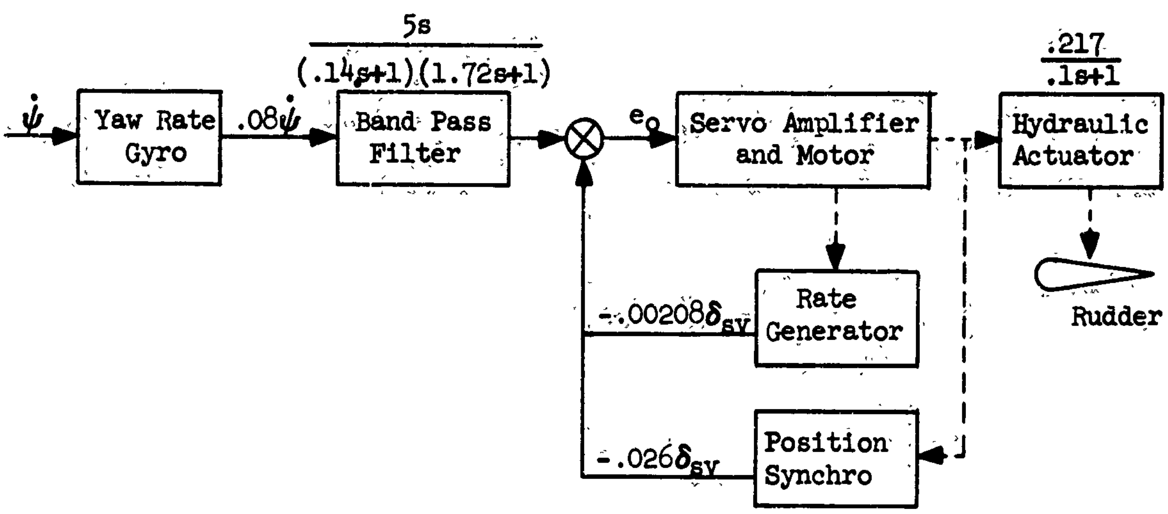

where:

$\dot{\psi}$ = yaw rate, deg/sec.

e_o = input to summation point from filter.

δ_{sv} = servo output-drum rotation, deg.

δ_r = rudder rotation, deg.

The transfer function of the servo amplifier and motor combination is approximated by

$$\frac{1}{0.01s^2 + .14s + 1}$$

The response time of the servo is assumed to be negligibly small and the expression for e_o can be expressed by the following equation.

$$e_o = \frac{.4s}{(.143s + 1)(1.72s + 1)}\dot{\psi} + (.026 + .00208s)\,\delta_{sv} = 0$$

$$\delta_r = -\frac{.217}{(.1s + 1)}\;\delta_{sv}$$

$$\delta_r = \frac{3.3\;\dot{\psi}\;s}{(.143s + 1)(1.72s + 1)(.1s + 1)(.08s + 1)} = \dot{\psi}T(s)$$

where

$T_{(s)}$ = yaw damper transfer function

Solution of Equations of Motion

The input format for the digital computer program requires that coefficient matrices be formed as indicated.

$$\left[M_1\right] q_j + \left[M_2\right] \dot{q}_j + \left[M_3\right] \ddot{q}_j + \left[M_4\right] * q_j + \left[M_5\right] * \dot{q}_j = \left[C_3\right] * \alpha_g$$

where:

$\left[M_1\right]$ = generalized stiffness matrix.

$\left[M_2\right]$ = non-circulatory response aerodynamic damping matrix.

$\left[M_3\right]$ = generalized inertia matrix.

$\left[M_4\right]$ = circulatory response aerodynamic stiffness matrix.

$\left[M_5\right]$ = circulatory response aerodynamic damping matrix.

$\left[C_3\right]$ = generalized exc'tation aerodynamic matrix.

α_g = instantaneous gust angle.

$*$ = indicates the application of Duhamel's integral to include Wagner or Küssner effects.

The generalized force coefficients associated with rudder deflection due to the yaw damper are formed into a set of matrices defined as $\left[S_i T(s)\right]$ in the digital computation operation format. The coefficient matrices for the equations of motion are then modified from the above form to include the yaw damper effects as shown by the following expression:

$$\left[\tilde{M}_i\right] = \left[M_i + S_i\ T(s)\right]_{i = 1 \text{ through } 5}$$

where

$\left[\tilde{M}_i\right]$ = the new coefficient matrices of q_j, $\dot{q}_j$ and $\ddot{q}_j$

$\left[M_i\right]$ = the original coefficient matrices of q_j, $\dot{q}_j$ and $\ddot{q}_j$

The digital program used for the lateral solution solves for the responses by using the Laplace transformed equations of motion with the Laplace transform variable set equal to $i\omega$. The solution then proceeds as follows:

$$\left\{q_j\right\} = \left[\left[\tilde{M}_1\right] + i\omega\left[\tilde{M}_2\right] - \omega^2\left[\tilde{M}_3\right] + \left[\tilde{M}_4\right] * g + i\omega\left[\tilde{M}_5\right] * g\right]^{-1}\left[C_3 * f\right]\alpha_g$$

g = Laplace transform of 1st time derivative of Wagner

f = Laplace transform of 1st time derivative of Küssner

This procedure yields a set of complex generalized responses for the frequency under consideration. The complex generalized responses are then used to compute the load responses. A set of representation solutions for for lateral Conditions 10 and 10YD are given in Fig. 28 of the Analyses Section.

APPENDIX B

STATISTICAL ANALYSIS FOR COMBINED RANDOM STRESSES

STATISTICAL ANALYSIS FOR COMBINED RANDOM STRESSES

Design Envelope Analysis Stress Relationships

The cumulative probability function, $P(MS \leq 0)$, is derived from the strength envelope for the structural element in question, the Gaussian joint probability density distribution for the incremental axial and shear stresses on the structural element, and the one-factor level flight stresses. Consider the diagram in Fig. B1 where the joint probability density function for axial and shear stress is shown in relation to the strength envelope defined by the appropriate interaction curves. The probability, $P(MS > 0, \sigma_w)$, that the combined axial and shear stresses will not exceed the limit strength for a given root-mean-square gust intensity is equal to the volume of the probability function within the region, R, bounded by the appropriate limit strength envelope.

$$P(MS > 0) = \iint_R p(f,\xi)\,df\,d\xi \qquad \text{(B1)}$$

Of course, the probability that the margin will be less than zero, that is, that the margin will be negative is,

$$P(MS \leq 0,\sigma_w) = 1 - P(MS > 0,\sigma_w) \qquad \text{(B2)}$$

The probability function, $P(MS \leq 0,\sigma_w)$, can be obtained by several integrations for various σ_w and plotted as illustrated in Fig. B2.

The joint Gaussian probability density function illustrated in Fig. B1 can be expressed as follows:

$$p(f,\xi) = \frac{1}{2\pi\sigma_f\sigma_\xi\sqrt{1-\rho^2}}\, e^{-G/2} \qquad \text{(B3a)}$$

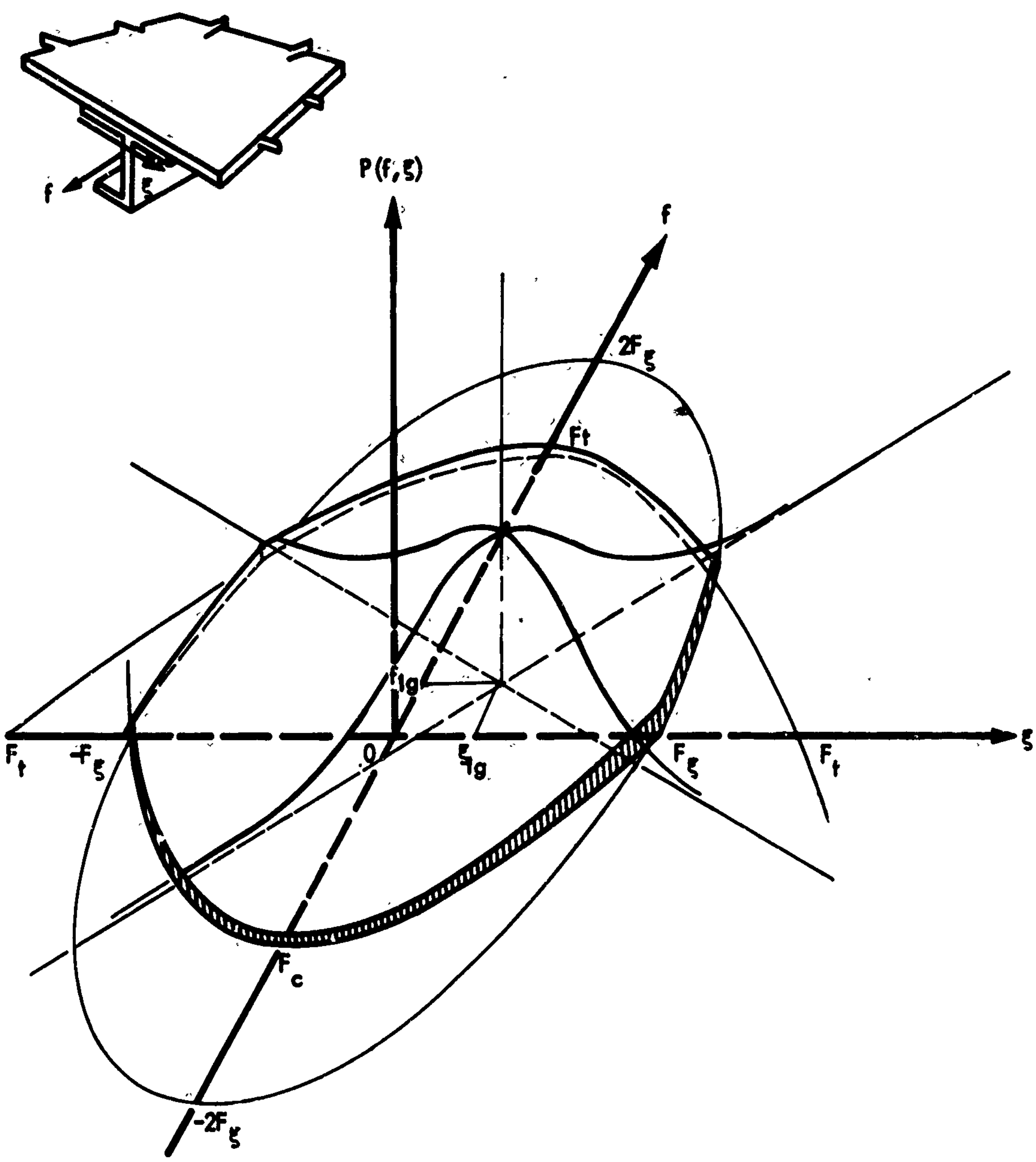

FIGURE B1. JOINT GAUSSIAN PROBABILITY DENSITY FUNCTION

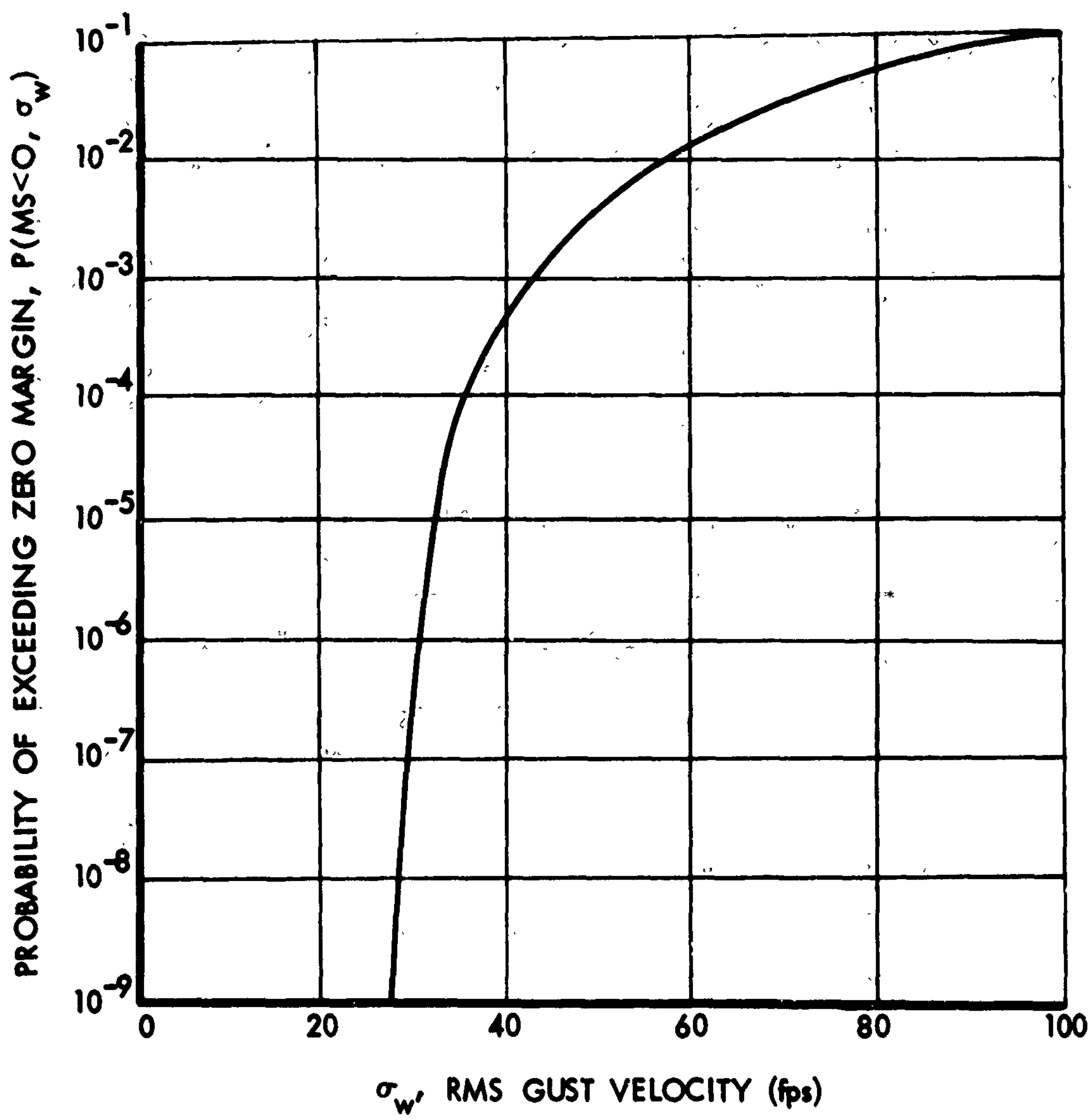

FIGURE B2. PROBABILITY OF EXCEEDING LIMIT DESIGN STRENGTH FOR VARIOUS RMS GUST VELOCITIES

where

$$G = \frac{1}{(1-\rho^2)}\left[\frac{(f-\bar{f})^2}{\sigma_f^2} - \frac{2\rho(f-\bar{f})(\xi-\bar{\xi})}{\sigma_f\sigma_\xi} + \frac{(\xi-\bar{\xi})^2}{\sigma_\xi^2}\right] \qquad \text{(B3B)}$$

The parameter, ρ, is the correlation coefficient expressing the statistical correlation between the axial and shear stresses. It can be defined from the cross-power spectrum between the axial and shear stresses as follows:

$$\rho\sigma_f\sigma_\xi = \int_0^\infty \phi_{f\xi}(\omega)d\omega = \text{ave}\left\{f(t)\xi(t)\right\} \qquad \text{(B4)}$$

Eq. (B4) is derived as follows: Assume that $h_f(t)$ and $h_\xi(t)$ are impulse response functions for the axial and shear stresses. Then, the time histories of axial and shear stresses for an arbitrary gust loading, $w(t)$, can be determined by convolution.

$$f(t) = \int_0^\infty h_f(\tau_1)w(t-\tau_1)d\tau_1 \qquad \text{(B5a)}$$

$$\xi(t-\tau) = \int_0^\infty h_\xi(\tau_2)w(t-\tau-\tau_2)d\tau_2 \qquad \text{(B5b)}$$

By definition the cross-correlation function for the axial and shear stresses is,

$$R_{f\xi}(\tau) = \lim_{T\to\infty}\frac{1}{2T}\int_{-T}^{T} f(t)\xi(t-\tau)dt. \qquad \text{(B6a)}$$

$$R_{f\xi}(\tau) = \lim_{T\to\infty} \frac{1}{2T} \int_{-T}^{T} \left[\int_0^{\infty} h_f(\tau_1) w(t-\tau_1) d\tau_1\right]\left[\int_0^{\infty} h_\xi(\tau_2) w(t-\tau-\tau_2) d\tau_2\right] \quad \text{(B6b)}$$

If we assume that the gust loading has been acting prior to time zero, the lower limits on the convolution integrals can be extended to minus infinity. Also, the order of integration can be changed.

$$R_{f\xi}(\tau) = \int_{-\infty}^{\infty}\int_{-\infty}^{\infty} h_f(\tau_1) h_\xi(\tau_2)\left[\lim_{T\to\infty} \int_{-T}^{T} w(t-\tau_1) w(t-\tau-\tau_2) dt\right] d\tau_1 d\tau_2 \quad \text{(B7a)}$$

$$R_{f\xi}(\tau) = \int_{-\infty}^{\infty}\int_{-\infty}^{\infty} h_f(\tau_1) h_\xi(\tau_2) R_w(\tau-\tau_1+\tau_2) d\tau_1 d\tau_2 \quad \text{(B7b)}$$

The cross-power spectral density function is,

$$\phi_{f\xi}(\omega) = \frac{1}{\pi} \int_{-\infty}^{\infty} R_{f\xi}(\tau) e^{-i\omega\tau} d\tau \quad \text{(B8a)}$$

$$\phi_{f\xi}(\omega) = \frac{1}{\pi} \int_{-\infty}^{\infty}\int_{-\infty}^{\infty} h_f(\tau_1) h_\xi(\tau_2)\left[\int_{-\infty}^{\infty} R_w(\tau-\tau_1+\tau_2) e^{-i\omega\tau} d\tau\right] d\tau_1 d\tau_2 \quad \text{(B8b)}$$

If we set $\tau-\tau_1+\tau_2 = \tau_3$ and rewrite the interior integral we obtain,

$$\phi_{f\xi}(\omega) = \frac{1}{\pi} \int_{-\infty}^{\infty}\int_{-\infty}^{\infty} h_f(\tau_1) h_\xi(\tau_2)\left[\int_{-\infty}^{\infty} R_w(\tau_3) e^{-i\omega(\tau_3+\tau_1-\tau_2)} d\tau_3\right] d\tau_1 d\tau_2 \quad \text{(B8c)}$$

Rearranging again, we obtain

$$\phi_{f\xi}(\omega) = \frac{1}{\pi}\int_{-\infty}^{\infty} h_f(\tau_1)e^{-i\omega\tau_1}d\tau_1 \int_{-\infty}^{\infty} h_\xi(\tau_2)e^{-i\omega\tau_2}d\tau_2 \int_{-\infty}^{\infty} R_w(\tau_3)e^{-i\omega\tau_3}d\tau_3 \tag{B8d}$$

However, we note that

$$\phi_w(\omega) = \frac{1}{\pi}\int_{-\infty}^{\infty} R_w(\tau_3)e^{-i\omega\tau_3}d\tau_3 = \frac{2}{\pi}\int_{0}^{\infty} R_w(\tau_3)\cos\omega\tau_3 d\tau_3 \tag{B9a}$$

$$H_f(\omega) = \int_{-\infty}^{\infty} h_f(\tau_1)e^{-i\omega\tau_1}d\tau_1 \tag{B9b}$$

$$H_\xi^*(\omega) = \int_{-\infty}^{\infty} h_\xi(\tau_3)e^{-i\omega\tau_3}d\tau_3 \tag{B9c}$$

where,

$\phi_w(\omega)$	gust power spectral density function
$H_f(\omega)$	complex frequency response function for axial stress in the structural element
$H_\xi^*(\omega)$	complex conjugate frequency response function for shear stress in the element.

Therefore,

$$\phi_{f\xi}(\omega) = \phi_w(\omega)H_f(\omega)H_\xi^*(\omega) \tag{B10}$$

Obviously, the cross-power spectral density function is complex, that is

$$\phi_{f\xi}(\omega) = C_{f\xi}(\omega) + iq_{f\xi}(\omega) \tag{B11}$$

where,

$C_{f\xi}(\omega)$ real part, cospectrum

$q_{f\xi}(\omega)$ imaginary part, quadrature spectrum

Also we note that,

$$C_{f\xi}(\omega) = C_{\xi f}(\omega) = C_{f\xi}(-\omega) \tag{B12a}$$

$$q_{f\xi}(\omega) = -q_{\xi f}(\omega) = -q_{f\xi}(-\omega) \tag{B12b}$$

Therefore,

$$\text{ave}\left\{f(t)\xi(t)\right\} = \rho\sigma_f\sigma_\xi = \frac{1}{2}\int_{-\infty}^{\infty}\phi_{f\xi}(\omega)d\omega = \int_0^{\infty} C_{f\xi}(\omega)d\omega \tag{B4}$$

and

$$\rho = \frac{\frac{1}{2}\int_{-\infty}^{\infty}\phi_w(\omega)H_f(\omega)H_\xi^*(\omega)d\omega}{\left[\int_0^{\infty}\phi_w(\omega)\left|H_f(\omega)\right|^2 d\omega\right]^{1/2}\left[\int_0^{\infty}\phi_w(\omega)\left|H_\xi(\omega)\right|^2 d\omega\right]^{1/2}} \tag{B13}$$

where,

$$\rho\sigma_f\sigma_\xi = \frac{1}{2}\int_{-\infty}^{\infty}\phi_w(\omega)H_f(\omega)H_\xi^*(\omega)d\omega \tag{B14a}$$

$$\sigma_f = \left[\int_0^{\infty} \phi_w(\omega)\left|H_f(\omega)\right|^2 d\omega\right]^{1/2} \tag{B14b}$$

$$\sigma_\xi = \left[\int_0^{\infty} \phi_w(\omega)\left|H_\xi(\omega)\right|^2 d\omega\right]^{1/2} \tag{B14c}$$

It will be noted that the correlation coefficient, ρ, can vary from minus one to plus one.

The strength envelope can be obtained from the expressions for the margin of safety

$$M.S._{SHEAR} = \frac{F_\xi}{\left[\left(\frac{f}{2}\right)^2 + \xi^2\right]^{1/2}} - 1 \tag{B15}$$

$$M.S._{TENSION} = \frac{F_t}{\frac{f}{2} + \left[\left(\frac{f}{2}\right)^2 + (\xi)^2\right]^{1/2}} - 1 \tag{B16}$$

$$M.S._{COMPRESSION} = \frac{2}{\frac{f}{F_c} + \left[\left(\frac{f}{F_c}\right)^2 + \left(2\frac{\xi}{F_\xi}\right)^2\right]^{1/2}} - 1 \tag{B17}$$

where,

F_ξ	Allowable in shear
F_t	Allowable in tension
F_c	Allowable in compression
f	Applied normal stress

ξ Applied shear stress

MS Margin of safety

Setting the margin of safety equal to zero and solving for the normal stress in terms of the shearing stress one obtains

$$\text{Shear} \qquad f = 2\left\{F_{\xi}^2 - \xi^2\right\}^{1/2} \tag{B18}$$

$$\text{Tension} \qquad f = F_t - \frac{\xi^2}{F_t} \tag{B19}$$

$$\text{Compression} \qquad f = F_c\left(1 - \frac{\xi^2}{F_{\xi}^2}\right) \tag{B20}$$

The resulting envelope is shown in Fig. B3.

<u>Flight Profile Analysis Stress Relationships</u>

The number of times per hour that zero or negative strength margin will occur on a structural element for a given flight condition can be expressed as follows:

$$\overline{G}(MS \leq 0) = \frac{3600}{2}\int_0^{\infty} N_c(\sigma_w)\hat{f}(\sigma_w)d\sigma_w \tag{B21}$$

where,

$\hat{f}(\sigma_w)$ the probability density distribution of rms gust velocity for the appropriate altitude is given by Eq. (2), and is repeated below

$$\hat{f}(\sigma_w) = \frac{P_1}{b_1}\sqrt{\frac{2}{\pi}}\, e^{-\sigma_w^2/2b_1^2} + \frac{P_2}{b_2}\sqrt{\frac{2}{\pi}}\, e^{-\sigma_w^2/2b_2^2} \tag{B22}$$

The constants P_1, P_2, b_1, and b_2 are those given in Figs. 5 and 6.

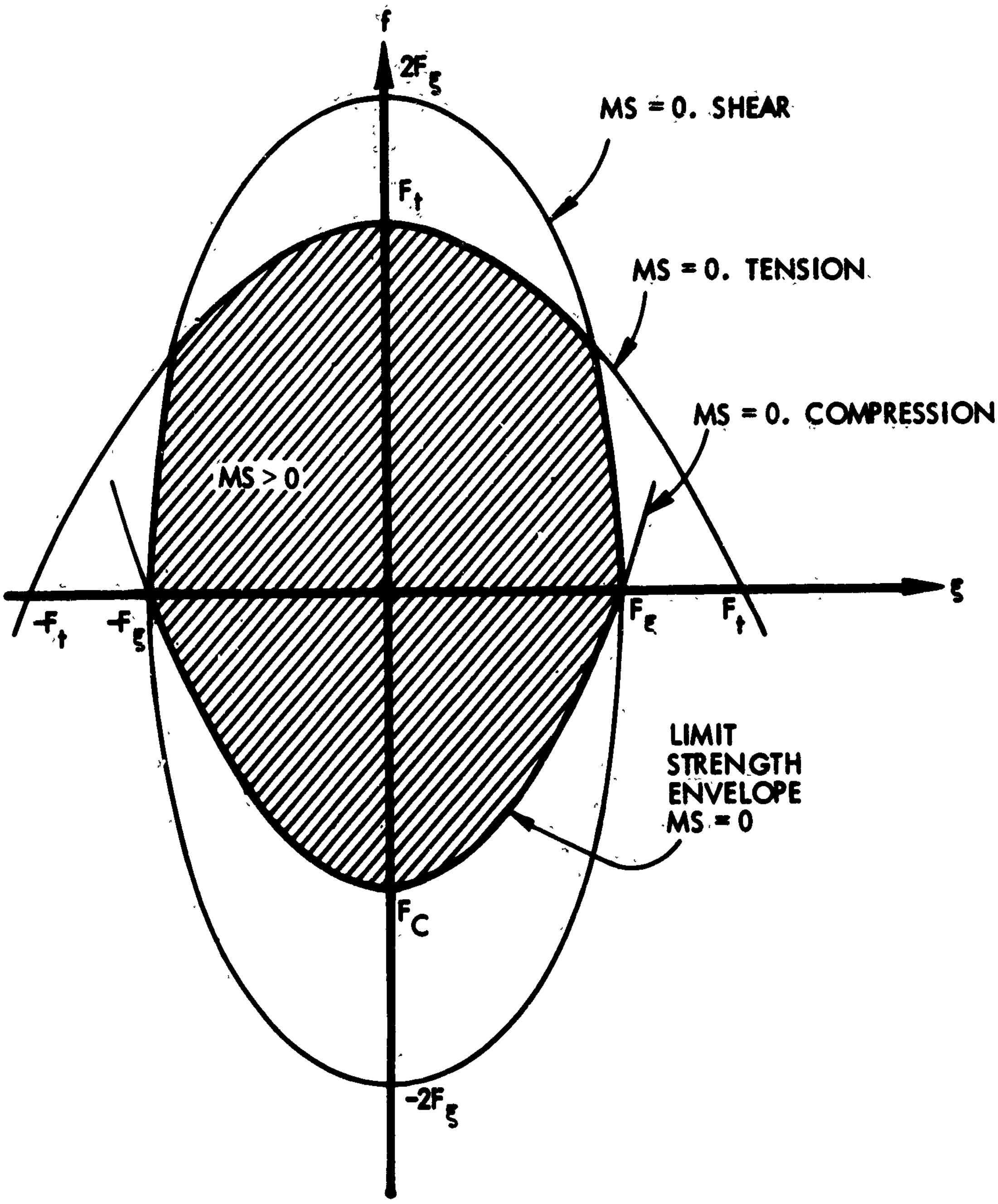

FIGURE B3. LIMIT STRENGTH ENVELOPE

$N_c(\sigma_w)$ Number of crossings of the strength envelope per second for two correlated random stress time histories. The derivation of $N_c(\sigma_w)$ is given in the following discussion.

Crossings of an Arbitrary Strength Envelope

Consider a probability density function

$$p(x,\alpha,y,\beta)\,dx\,d\alpha\,dy\,d\beta = \text{Prob}\,[x<\xi\leq x+dx,\ \alpha<\dot{\xi}\leq\alpha+d\alpha,\ y<f\leq y+dy,\ \beta<\dot{f}\leq\beta+d\beta]$$

where,

f axial stress, psi

$\beta = \dot{f}$ time rate of change of axial stress, psi per sec.

ξ shear stress, psi

$\alpha = \dot{\xi}$ time rate of change of shear stress, psi per sec.

For a given period of time, the above expression represents the fraction of time per unit time that the stress vector $\overline{z}(t) = \overline{x}(t)i + \overline{y}(t)j$ spends in the interval $(x, x+dx;\ y, y+dy)$ with velocities in the intervals $(\alpha, \alpha+d\alpha;\ \beta, \beta+d\beta)$.

The expected number of times per unit time that the stress vector, $\overline{z}(t)$, passes through the interaction boundary interval $(z_C(x,y),\ z_C(x,y+d\eta))$ is equal to the time spent in the interval divided by the time required to cross the interval.

The time required to cross the interval, $d\eta$, is equal to $d\eta$ divided by the velocity component of $\overline{z}$ normal to C, the interaction boundary curve indicated in Fig. B4.

A unit vector normal to C is,

$$\overline{N} = \frac{\text{grad } C}{|\text{grad } C|} \tag{B24}$$

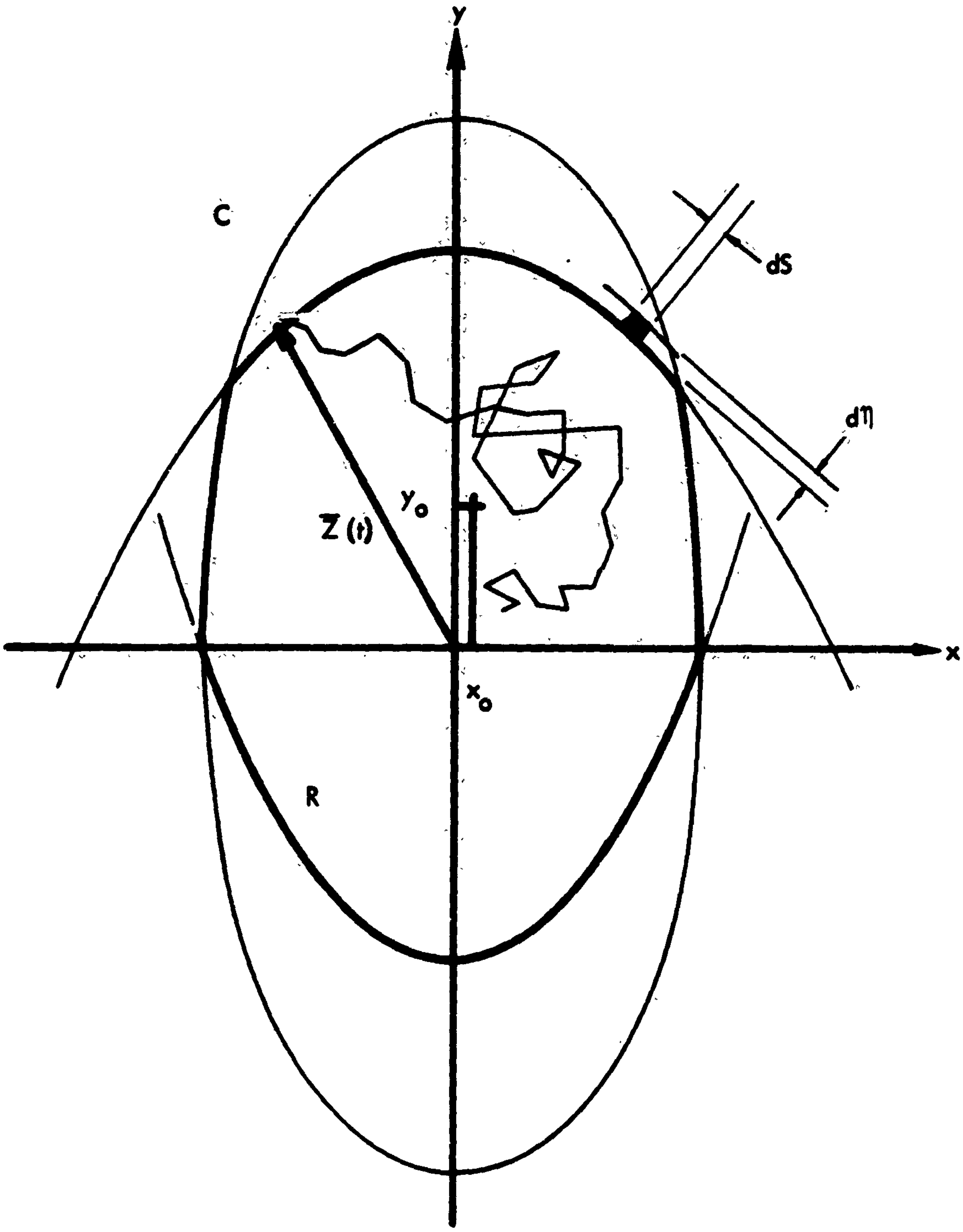

FIGURE B4. COMBINED STRESS VECTOR

If C is a function of x and y, such as

$$y = F_t - \frac{x^2}{F_t}$$

where this function represents an interaction curve for shear and tension,

$$C = y - F_t + \frac{x^2}{F_t} = 0$$

The gradient of C, denoted, grad C, is

$$\frac{\partial C}{\partial x}i + \frac{\partial C}{\partial y}j = \frac{2x}{F_t}i + j$$

The length of the gradient vector is,

$$\sqrt{\left(\frac{\partial C}{\partial x}\right)^2 + \left(\frac{\partial C}{\partial y}\right)^2} = \sqrt{\frac{4x^2}{F_t^2} - 1} = \frac{1}{F_t}\sqrt{4x^2 + F_t^2}$$

Therefore, the unit normal vector on C is

$$\overline{N} = \frac{2x}{\sqrt{4x^2 + F_t^2}}i + \frac{F_t}{\sqrt{4x^2 + F_t^2}}j \qquad \text{(B25)}$$

The velocity vector, $\dot{z}$, is

$$\dot{z}(t) = \alpha(t)i + \beta(t)j$$

Then, the rate at which the interval $d\eta$ is traversed is equal to the dot product of the unit normal vector with the velocity vector.

$$\frac{\text{grad } C}{|\text{grad } C|} \cdot \dot{\bar{z}}(t) = \frac{2\alpha x}{\sqrt{4x^2 + F_t^2}} + \frac{\beta F_t}{\sqrt{4x^2 + F_t^2}}$$

If the time required to cross the interval $d\eta$ is τ, then,

$$\tau = \frac{d\eta}{\left| \frac{\text{grad } C}{|\text{grad } C|} \cdot \dot{\bar{z}} \right|} \qquad (\tau > 0) \tag{B26}$$

The expected number of times per unit time that the curve C is crossed by $\bar{z}$ with velocities α and β is equal to the time spent in the interval $d\eta$ divided by the time required to cross the interval.

$$N_{C_{\alpha\beta}} = \int_C \frac{\frac{[P(x,\alpha,y,\beta)\, d\alpha\, d\beta]\, d\eta}{d\eta}}{\left| \frac{\text{grad } C}{|\text{grad } C|} \cdot \dot{\bar{z}} \right|}\, dS \tag{B27}$$

The total number of passages both into the interval $d\eta$ from the region R and into the interval toward the region R is obtained by integrating for all possible velocities α and β. Therefore, the total number of passages, N_C is,

$$N_C = \int_{\beta=-\infty}^{\infty} \int_{\alpha=-\infty}^{\infty} \left\{ \int_C \left[P(x,\alpha,y,\beta) \right] \left| \frac{\text{grad } C}{|\text{grad } C|} \cdot \dot{\bar{z}} \right| dS \right\} d\alpha\, d\beta \tag{B28}$$

Now, if the process is Gaussian, the probability density can be written as follows:

$$P(x_1, x_2, x_3, x_4, \cdots, x_N) = [2\pi]^{-N/2} |M|^{-1/2} \exp\left\{\frac{-1}{2|M|} \sum_{i=1}^{N} \sum_{j=1}^{N} M_{ij} x_i x_j\right\}, \tag{B29}$$

where $|M|$ is the determinate of the time averages of the products and cross products of $x_1, x_2, x_3, \cdots, x_N$, and M_{ij} is the co-factor of the ij element of $|M|$.

If we let

$$x_1 = x(t)$$
$$x_2 = \alpha(t) = \dot{x}(t)$$
$$x_3 = y(t)$$
$$x_4 = \beta(t) = \dot{y}(t)$$

then $|M|$ can be expressed as,

$$|M| = \left| \lim_{T \to \infty} \frac{1}{2T} \int_{-T}^{T} \begin{bmatrix} x(t) \\ \alpha(t) \\ y(t) \\ \beta(t) \end{bmatrix} \lfloor x(t) \; \alpha(t) \; y(t) \; \beta(t) \rfloor \, dt \right| \tag{B30a}$$

or

$$|M| = \left| \lim_{T \to \infty} \frac{1}{2T} \int_{-T}^{T} \begin{bmatrix} x^2 & x\alpha & xy & x\beta \\ \alpha x & \alpha^2 & \alpha y & \alpha\beta \\ yx & y\alpha & y^2 & y\beta \\ \beta x & \beta\alpha & \beta y & \beta^2 \end{bmatrix} dt \right| \tag{B30b}$$

The elements of $|M|$ are determined by carrying out the integration over-time to obtain the following for the (i,i) elements.

$$\overline{x^2} = \sigma_x^2 = \lim_{T\to\infty} \frac{1}{2T} \int_{-T}^{T} x^2(t)dt = \int_0^\infty \phi_x(\omega)d\omega$$

$$\overline{\alpha^2} = \sigma_\alpha^2 = \lim_{T\to\infty} \frac{1}{2T} \int_{-T}^{T} \alpha^2(t)dt = \int_0^\infty \omega^2\phi_x(\omega)d\omega$$

$$\overline{y^2} = \sigma_y^2 = \lim_{T\to\infty} \frac{1}{2T} \int_{-T}^{T} y^2(t)dt = \int_0^\infty \phi_y(\omega)d\omega \qquad \text{(B30c)}$$

$$\overline{\beta^2} = \sigma_\beta^2 = \lim_{T\to\infty} \frac{1}{2T} \int_{-T}^{T} \beta^2(t)dt = \int_0^\infty \omega^2\phi_y(\omega)d\omega$$

For the (1,2) and (2,1) elements we obtain,

$$\lim_{T\to\infty} \frac{1}{2T} \int_{-T}^{T} x(t)\dot{x}(t)dt = 0$$

This is determined by integrating by parts and by taking the limit,

$$\lim_{T\to\infty} \frac{1}{2T} \int_{-T}^{T} x(t)\dot{x}(t)dt = \lim_{T\to\infty} \frac{1}{2T} \left\{ \Big[x(t)\dot{x}(t)\Big]_{-T}^{T} - \int_{-T}^{T} x(t)\dot{x}(t)dt \right\} . \qquad \text{(B31)}$$

Then,

$$\lim_{T\to\infty} \frac{1}{2T} \int_{-T}^{T} x(t)\dot{x}(t)dt = \lim_{T\to\infty} \frac{1}{4T} \Big[x(T) - x(-T)\Big] = 0$$

This integral is identically equal to zero, since the respective values of x(T) and x(-T) are always finite and they are divided by T which is arbitrarily large.

Therefore, the (1,2) and (2,1) elements of |M| are zero.

The (1,3) and (3,1) elements are by definition of the cross correlation between x(t) and y(t) and are

$$\overline{xy} = \rho\sigma_x\sigma_y = \lim_{T\to\infty}\frac{1}{2T}\int_{-T}^{T} x(t)y(t)dt = \frac{1}{2}\int_{-\infty}^{\infty}\phi_{xy}(\omega)d\omega \qquad \text{(B32)}$$

where ρ is the correlation coefficient which varies in the interval (1,-1).

All other elements are more obscure will be assumed equal to zero.

Therefore,

$$|M| = \begin{vmatrix} \sigma_x^2 & 0 & \rho\sigma_x\sigma_y & 0 \\ 0 & \sigma_\alpha^2 & 0 & 0 \\ \rho\sigma_x\sigma_y & 0 & \sigma_y^2 & 0 \\ 0 & 0 & 0 & \sigma_\beta^2 \end{vmatrix} \qquad \text{(B33)}$$

The frequency density is now expressed as follows:

$$P(x,\alpha,y,\beta) = \frac{1}{(2\pi)^2}\,\frac{1}{\sigma_x\sigma_\alpha\sigma_y\sigma_\beta(1-\rho^2)^{1/2}}\exp\left\{\frac{-1}{2(1-\rho^2)}\left[\frac{x^2}{\sigma_x^2}-\frac{2\rho xy}{\sigma_x\sigma_y}+\frac{y^2}{\sigma_y^2}\right]\right\} \qquad \text{(B34)}$$

$$\exp\left\{-\frac{1}{2}\left[\frac{\alpha^2}{\sigma_\alpha^2}+\frac{\beta^2}{\sigma_\beta^2}\right]\right\}$$

If we assume that x and y shown in Eq. (B34) are incremental or time variant values varying from the mean or one-factor flight values, then, x is replaced by $(x-x_0)$ and y by $(y-y_0)$.

$$p(x,\alpha,y,\beta) = \frac{1}{(2\pi)^2} \frac{1}{\sigma_x\sigma_\alpha\sigma_y\sigma_\beta(1-\rho^2)^{1/2}} \exp\left\{\frac{-1}{2(1-\rho^2)}\left[\frac{(x-x_0)^2}{\sigma_x^2} - 2\rho\frac{(x-x_0)(y-y_0)}{\sigma_x\sigma_y} + \frac{(y-y_0)^2}{\sigma_y^2}\right]\right\} \exp\left\{-\frac{1}{2}\left[\frac{\alpha^2}{\sigma_\alpha^2} + \frac{\beta^2}{\sigma_\beta^2}\right]\right\} \tag{B35}$$

Substituting Eq. (B35) into Eq. (B27), we obtain

$$N_{C_{\alpha\beta}} = \frac{1}{(2\pi)^2} \frac{1}{\sigma_x\sigma_\alpha\sigma_y\sigma_\beta(1-\rho^2)^{1/2}} \exp\left\{-\frac{1}{2}\left[\frac{\alpha^2}{\sigma_\alpha^2} + \frac{\beta^2}{\sigma_\beta^2}\right]\right\} \int_C \left|\frac{\text{grad } C}{|\text{grad } C|} \cdot \dot{\bar{z}}\right| \exp\left\{\frac{-1}{2(1-\rho^2)}\left[\frac{(x-x_0)^2}{\sigma_x^2} - 2\rho\frac{(x-x_0)(y-y_0)}{\sigma_x\sigma_y} + \frac{(y-y_0)^2}{\sigma_y^2}\right]\right\} dS d\alpha d\beta \tag{B36}$$

The number of crossings per unit time is obtained from Eqs. (B28) and (B35).

$$N_C = \frac{1}{(2\pi)^2} \frac{1}{\sigma_x\sigma_\alpha\sigma_y\sigma_\beta(1-\rho^2)^{1/2}} \int_{\alpha=-\infty}^{\infty} \int_{\beta=-\infty}^{\infty} \int_C \left|\frac{\text{grad } C}{|\text{grad } C|} \cdot \dot{\bar{z}}\right| \exp\left\{\frac{-1}{2(1-\rho^2)}\left[\frac{(x-x_0)^2}{\sigma_x^2} - 2\rho\frac{(x-x_0)(y-y_0)}{\sigma_x\sigma_y} + \frac{(y-y_0)^2}{\sigma_y^2}\right]\right\} \exp\left\{-\frac{1}{2}\left[\frac{\alpha^2}{\sigma_\alpha^2} + \frac{\beta^2}{\sigma_\beta^2}\right]\right\} dS d\alpha d\beta \tag{B37}$$

If we assume zero mean values for $x(t)$ and $y(t)$, we can easily obtain the familiar expression for the number of times per unit time that $\bar{z}(t) = x(t)i + y(t)j$ crosses a constant level, $y = a$.

The general equation for the number of crossings per unit time is obtained in Eq. (B37). If we assume that

$$C = y - a; \qquad \frac{\partial C}{\partial x} = 0; \qquad \frac{\partial C}{\partial y} = 1$$

and the grad C = 0i + 1j. Then, $|\text{grad } C| = 1$. The velocity vector component of $\alpha i + \beta j$ normal to C is,

$$\beta = (0i + 1\beta j) \cdot (\alpha i + \beta j)$$

Then,

$$\left| \frac{\text{grad } C}{|\text{grad } C|} \cdot \dot{z} \right| = |\beta|$$

If Eq. (B37) is rewritten for this example, we obtain,

$$N_C = \frac{1}{2\pi} \frac{1}{\sigma_\alpha \sigma_\beta} \int_{\alpha=-\infty}^{\infty} \int_{\beta=-\infty}^{\infty} |\beta| \exp\left\{ -\frac{1}{2}\left[\frac{\alpha^2}{\sigma_\alpha^2} + \frac{\beta^2}{\sigma_\beta^2}\right]\right\} d\alpha d\beta$$

$$\int_{x=-\infty}^{\infty} \frac{1}{2\pi} \frac{1}{\sigma_x \sigma_y (1-\rho^2)^{1/2}} \exp\left\{\frac{-1}{2(1-\rho^2)}\left[\frac{x^2}{\sigma_x^2} - \frac{2\rho xy}{\sigma_x \sigma_y} + \frac{y^2}{\sigma_y^2}\right]\right\} dx \qquad \text{(B38)}$$

We note that integral over x is identically equal to

$$\int_{x=-\infty}^{\infty} = \frac{1}{\sqrt{2\pi}\sigma_y} e^{-y^2/2\sigma_y^2} \qquad \text{(B39a)}$$

and the double integral can be rewritten in simpler form after the following integrations are made:

$$\int_{\alpha=-\infty}^{\infty} e^{-\alpha^2/2\sigma_\alpha^2}\, d\alpha = \sqrt{2\pi}\;\sigma_\alpha \quad \text{since,} \tag{B39b}$$

$$\frac{1}{\sqrt{2\pi}\,\sigma_\alpha}\int_{-\infty}^{\infty} e^{-\alpha^2/2\sigma_\alpha^2}\, d\alpha = 1 \tag{B39c}$$

The integral over β can be written as,

$$\int_{\beta=-\infty}^{\infty} |\beta|\, e^{-\beta^2/2\sigma_\beta^2}\, d\beta = 2\int_0^{\infty} \beta\, e^{-\beta^2/2\sigma_\beta^2}\, d\beta = 2\sigma_\beta^2 \tag{B39d}$$

The double integral over α and β is equal to

$$\int_\alpha \int_\beta = 2\sqrt{2\pi}\,\sigma_\alpha\,\sigma_\beta^2 \tag{B39e}$$

Substituting Eqs. (B39a) and (B39b) into Eq. (B38) gives,

$$N_C = \frac{1}{2\pi}\frac{1}{\sigma_\alpha\sigma_\beta}\left(2\sqrt{2\pi}\,\sigma_\alpha\sigma_\beta^2\right)\frac{1}{\sqrt{2\pi}\,\sigma_y}\, e^{-y^2/2\sigma_y^2} \tag{B39f}$$

Reducing Eq. (B39f) gives,

$$N_C = \frac{1}{\pi}\frac{\sigma_\beta}{\sigma_y}\, e^{-y^2/2\sigma_y^2} \tag{B40}$$

This is the well known expression for the total number of crossings of a level $y = a$, where a is arbitrary in magnitude and in sign.(14)

The preceding derivation treated a continuous envelope C; however, the algebra is simpler if the envelope is defined by a series of straight line segments. In the following development, an expression for the value of N_C is determined for one of these line segments. Through a cycling process the N_C for any envelope can be determined.

Consider the number of crossings per unit time of an arbitrary straight line segment from (x_1, y_1) to (x_2, y_2). The equation of the line through the point is,

$$y = \left(\frac{y_1 - y_2}{x_1 - x_2}\right)(x - x_1) + y_1 \qquad \text{(B41a)}$$

or

$$y = m(x - x_1) + y_1$$

where m is the slope.

Therefore,

$$C = y - m(x - x_1) - y_1 = 0$$

$$\frac{\partial C}{\partial x} = -m; \qquad \frac{\partial C}{\partial y} = 1; \qquad \text{grad } C = -mi + j \qquad \text{(B42)}$$

The absolute value of the grad C is,

$$|\text{grad } C| = \left|\sqrt{m^2 + 1}\right|$$

Then,

$$\left|\frac{\text{grad } C}{|\text{grad } C|} \cdot \dot{z}\right| = \left|\frac{(-mi + j) \cdot (\alpha i + \beta j)}{\sqrt{m^2 + 1}}\right|$$

$$\bar{N} = \left|\frac{-m\alpha + \beta}{\sqrt{m^2 + 1}}\right| \qquad (B43)$$

Assuming $x_0 = y_0 = 0$, we can rewrite Eq. (B37) as,

$$N_C = \frac{1}{(2\pi)^2} \frac{}{\sigma_x \sigma_\alpha \sigma_y \sigma_\beta (1-\rho^2)^{1/2}}$$

$$\int_{\alpha=-\infty}^{\infty} \int_{\beta=-\infty}^{\infty} \int_C \left|\frac{-m\alpha+\beta}{\sqrt{m^2+1}}\right| \exp\left\{\frac{-1}{2(1-\rho^2)}\left[\frac{x^2}{\sigma_x^2} - \frac{2\rho xy}{\sigma_x \sigma_y} + \frac{y^2}{\sigma_y^2}\right]\right\} dS \qquad (B44)$$

$$\exp\left\{-\frac{1}{2}\left[\frac{\alpha^2}{\sigma_\alpha^2} + \frac{\beta^2}{\sigma_\beta^2}\right]\right\} d\alpha d\beta$$

Eq. (B44) can be rearranged and applied to the k-th segment of the strength envelope:

$$N_{C_k} = \frac{1}{2\pi} \frac{1}{\sigma_\alpha \sigma_\beta} \int_{-\infty}^{\infty} \int_{-\infty}^{\infty} \left|\frac{-m\alpha+\beta}{\left[m^2+1\right]^{1/2}}\right| \exp\left\{-\frac{1}{2}\left[\frac{\alpha^2}{\sigma_\alpha^2} + \frac{\beta^2}{\sigma_\beta^2}\right]\right\} d\alpha d\beta$$

$$\frac{1}{2\pi} \frac{1}{\sigma_x \sigma_y (1-\rho^2)^{1/2}} \int_{x_1, y_1}^{x_2, y_2} \exp\left\{\frac{-1}{2(1-\rho^2)}\left[\frac{x^2}{\sigma_x^2} - \frac{2\rho xy}{\sigma_x \sigma_y} + \frac{y^2}{\sigma_y^2}\right]\right\} dS \qquad (B45)$$

Eq. (B45) shows that N_{C_k} is the product of a slope-velocity function, which is constant for a given line segment, and a line integral over the joint probability function, $P(x,y)$. While it is possible to express both functions in series form, it has been found to be advantageous to evaluate the slope-velocity term by an infinite series and to evaluate the second function directly.

The suggested method of solution is to numerically evaluate the crossing density, dN_{c_k}/dS, at a sufficient number of points along the various line segments around the strength envelope.

$$\frac{dN_{c_k}}{dS} = \left\{ \sqrt{\frac{2}{\pi}} \left[\frac{\sigma_\beta^2}{\left[m^2\sigma_\alpha^2+\sigma_\beta^2\right]^{1/2}} + \frac{\sigma_\alpha^2}{\sigma_\beta} \sum_{n=0}^{\infty} \frac{(-1)^n m^{(2n+2)} (2n)!}{(n!)^2} \left(\frac{\sigma_\alpha}{2\sigma_\beta}\right)^{2n} \right] \right\}$$

$$\left\{ \frac{1}{2\pi} \frac{1}{\sigma_x \sigma_y (1-\rho^2)^{1/2}} \exp\left[\frac{-1}{2(1-\rho^2)} \left[\frac{x^2}{\sigma_x^2} - \frac{2\rho xy}{\sigma_x \sigma_y} + \frac{y^2}{\sigma_y^2} \right] \right] \right\} \qquad \text{(B46)}$$

The crossings of the k-th segment of the strength envelope can be determined as follows:

$$N_{c_k} = \left\{ \sqrt{\frac{2}{\pi}} \left[\frac{\sigma_\beta^2}{\left[m^2\sigma_\alpha^2+\sigma_\beta^2\right]^{1/2}} + \frac{\sigma_\alpha^2}{\sigma_\beta} \sum_{n=0}^{\infty} \frac{(-1)^n m^{(2n+2)} (2n)!}{(n!)^2} \left(\frac{\sigma_\alpha}{2\sigma_\beta}\right)^{2n} \right] \right\} \qquad \text{(B47)}$$

$$\left\{ \int_{c_k} p(x,y)\, dS_k \right\}$$

Eq. (B47) can be properly evaluated if the series converges and if the second term, the line integral, is carefully evaluated over each line segment. The convergence of the series in less than 30 terms can be assured if (1) the ratio $\sigma_\alpha/\sigma_\beta$ is normalized to unity, and if the line segment slopes are restricted to the interval (-1,1).

The ratio $\sigma_\alpha/\sigma_\beta$ can be made equal to unity by stretching the strength envelope and all x-dependent parameters by the ratio $\sigma_\alpha/\sigma_\beta$. The stretching, of course, will change the slopes of the line segments. N_{c_k} can be evaluated directly after transformation for all line segments with slopes in the interval (-1,1). Segments with slopes outside the interval (-1,1) can be handled by exchanging the coordinates in Eq. (B47).

Combined Stresses for Vertical and Lateral Gusts

Calculations to estimate airplane loads and stresses resulting from flight in continuous atmospheric turbulence are nearly always carried out under the assumption that the vertical and lateral motions of the airplane are not coupled. As a result, two separate analyses are usually conducted; one for the vertical component of the turbulent gust velocity field and a separate analysis for the lateral. However, certain parts of the airplane, particularly the fuselage and empennage, are stressed significantly by the simultaneous action of both the vertical and lateral gust components. It is shown in the following development, that stresses derived separately from vertical and lateral power spectral gust analyses can be combined in a simple manner if the turbulent gust velocity field is isotropic.

Consider two stress components in a structural element in the fuselage. Let $f_V(t)$ be the axial stress time-history that results from the vertical component of turbulence, and let $\xi_L(t)$ be the shear stress resulting from the lateral component of turbulence. The cross correlation between these two stress components can be expressed as follows:

$$R_{f_V \xi_L}(\tau) = \lim_{T \to \infty} \frac{1}{2T} \int_{-T}^{T} f_V(t)\xi_L(t-\tau)dt \qquad \text{(B48)}$$

Expressions for the time-histories of $f_V(t)$ and $\xi_L(t)$ can be written in terms of the stress impulse response functions $h_{f_V}(\tau)$ and $h_{\xi_L}(\tau)$ and the gust time-histories using summation integrals.

$$f_V(t) = \int_{-\infty}^{\infty} h_{f_V}(\tau_1)w(t-\tau_1)d\tau_1 \qquad \text{(B49a)}$$

$$\xi_L(t-\tau) = \int_{-\infty}^{\infty} h_{\xi_L}(\tau_2)v(t-\tau-\tau_2)d\tau_2 \qquad \text{(B49b)}$$

Eq. (B48) can now be rewritten as follows:

$$R_{f_v \xi_L}(\tau) = \lim_{T \to \infty} \frac{1}{2T} \int_{-T}^{T} \left[\int_{-\infty}^{\infty} h_{f_v}(\tau_1) w(t-\tau_1) d\tau_1 \right] \left[\int_{-\infty}^{\infty} h_{\xi_L}(\tau_2) v(t-\tau-\tau_2) d\tau_2 \right] dt \qquad \text{(B50a)}$$

Rearranging the order of integration, we obtain,

$$R_{f_v \xi_L}(\tau) = \int_{-\infty}^{\infty}\int_{-\infty}^{\infty} h_{f_v}(\tau_1) h_{\xi_L}(\tau_2) \left[\lim_{T \to \infty} \frac{1}{2T} \int_{-T}^{T} w(t-\tau_1) v(t-\tau-\tau_2) dt \right] d\tau_1 d\tau_2 \qquad \text{(B50b)}$$

It will be noted that the term in brackets in Eq. (B50b) is the cross-correlation function for the vertical and lateral gust velocity components.

$$R_{wv}(\tau-\tau_1+\tau_2) = \lim_{T \to \infty} \frac{1}{2T} \int_{-T}^{T} w(t-\tau_1) v(t-\tau-\tau_2) dt \qquad \text{(B51)}$$

The cross-power spectral density function for the two stress components is,

$$\Phi_{f_v \xi_L}(\omega) = \frac{1}{\pi} \int_{-\infty}^{\infty} R_{wv}(\tau_3)\, e^{-i\omega\tau_3}\, d\tau_3 \qquad \text{(B52)}$$

where,

$$\tau_3 = \tau - \tau_1 + \tau_2 \qquad \text{(B53)}$$

After substituting Eqs. (B53) and (B51) into (B50b) and rewriting Eq. (B52), we have,

$$\phi_{f_v\xi_L}(\omega) = \frac{1}{\pi}\int_{-\infty}^{\infty}\int_{-\infty}^{\infty} h_{f_v}(\tau_1) h_{\xi_L}(\tau_2) \left[\int_{-\infty}^{\infty} R_{wv}(\tau_3)\, e^{-i\omega(\tau_3+\tau_1-\tau_2)}\, d\tau_3\right] d\tau_1 d\tau_2 \qquad \text{(B54)}$$

Rearranging the order of integration in Eq. (B54) gives,

$$\phi_{f_v\xi_L}(\omega) = \frac{1}{\pi}\int_{-\infty}^{\infty} h_{f_v}(\tau_1)e^{-i\omega\tau_1}d\tau_1 \int_{-\infty}^{\infty} h_{\xi_L}(\tau_2)e^{i\omega\tau_2}d\tau_2 \int_{-\infty}^{\infty} R_{wv}(\tau_3)e^{-i\omega\tau_3}d\tau_3 \qquad \text{(B55)}$$

$$\phi_{f_v\xi_L}(\omega) = H_{f_v}(\omega)\, H^*_{\xi_L}(\omega)\, \phi_{wv}(\omega)$$

where,

$H_{f_v}(\omega)$ complex frequency response function for axial stress on the element resulting from the vertical component of atmospheric turbulence

$H_{\xi_L}(\omega)$ complex conjugate frequency response function for shear stress on the element resulting from the lateral component of turbulence.

$\phi_{wv}(\omega)$ cross-power spectral density function for the vertical and lateral gust velocity components.

The integral of the cross-power spectrum in Eq. (B55) gives

$$\rho_{f_v\xi_L}\sigma_{f_v}\sigma_{\xi_L} = \frac{1}{2}\int_{-\infty}^{\infty} H_{f_v}(\omega)\, H^*_{\xi_L}(\omega)\, \phi_{wv}(\omega)\, d\omega \qquad \text{(B56)}$$

where $\rho_{f_v\xi_L}$ is the correlation coefficient.

Eq. (B56) provides the same result as the following integral:

$$\rho_{f_V \xi_L} \sigma_{f_V} \sigma_{\xi_L} = \lim_{T \to \infty} \frac{1}{2T} \int_{-T}^{T} f_V(t) \xi_L(t) dt \tag{B57}$$

The axial and shear stresses at a point in the airplane structure resulting from the vertical component and the lateral component of atmospheric turbulence are as follows:

$$\begin{aligned} f(t) &= f_V(t) + f_L(t) \\ \xi(t) &= \xi_V(t) + \xi_L(t) \end{aligned} \tag{B58}$$

The matrix of mean squared stresses used to define the joint probability distribution is,

$$[M] = \lim_{T \to \infty} \frac{1}{2T} \int_{-T}^{T} \begin{bmatrix} f_V + f_L \\ \xi_V + \xi_L \end{bmatrix} \lfloor (f_V + f_L) \quad (\xi_V + \xi_L) \rfloor dt$$

$$[M] = \lim_{T \to \infty} \frac{1}{2T} \int_{-T}^{T} \begin{bmatrix} (f_V + f_L)^2 & (f_V + f_L)(\xi_V + \xi_L) \\ (f_V + f_L)(\xi_V + \xi_L) & (\xi_V + \xi_L)^2 \end{bmatrix} dt \tag{B59}$$

$$[M] = \lim_{T \to \infty} \frac{1}{2T} \int_{-T}^{T} \begin{bmatrix} (f_V^2 + 2f_V f_L + f_L^2) & (f_V \xi_V + f_V \xi_L + f_L \xi_V + f_L \xi_L) \\ (f_V \xi_V + f_V \xi_L + f_L \xi_V + f_L \xi_L) & (f_V^2 + 2\xi_V \xi_L + \xi_L^2) \end{bmatrix} dt$$

If it is assumed that the turbulence is isotropic, the time averaged product of two gust velocities $w(x_1,t)$ and $v(x_2,t)$ at two points x_1 and x_2 along the airplane fuselage is,

$$\rho_{w_{x_1} v_{x_2}} \sigma_w \sigma_v = \lim_{T \to \infty} \frac{1}{2T} \int_{-T}^{T} w(x_1,t) v(x_2,t) dt$$

$$= \overline{wv} \tag{B60}$$

$$= R_{wv}(|x_1 - x_2|)$$

It would be expected that the above space correlation would be sensitive to the absolute value of x_1 minus x_2. However, in the same manner as von Karman and Howarth[15], it can be shown that this correlation is always identically zero for isotropic turbulence for any x_1 and x_2.

If we rotate the coordinate axis system about either the y or z-axis by 180°, and denote the transformed velocities $\tilde{w}$ and $\tilde{v}$, respectively, we observe that

$$\overline{wv} = -\overline{\tilde{w}\tilde{v}} \tag{B61a}$$

But by the isotropic property,

$$\overline{wv} \equiv \overline{\tilde{w}\tilde{v}} \tag{B61b}$$

Therefore,

$$\overline{wv} \equiv 0 \tag{B61c}$$

Since,

$$\sigma_w \neq 0, \qquad \sigma_v \neq 0 \tag{B62a}$$

then,

$$\rho_{wv} = 0 \tag{B62b}$$

Therefore, the vertical and lateral components of isotropic turbulence are not correlated, and the cross power spectral density function for the vertical and lateral components of gust velocity is identically zero for all frequencies. Now, by Eq. (B56) we see that all of the correlation coefficients relating stress components arising separately from the vertical and lateral components of isotropic turbulence are also equal to zero.

The matrix of mean squared stresses used to define the joint probability distribution is obtained by integrating the remaining terms in Eq. (B59).

$$[M] = \begin{bmatrix} \sigma_{f_V}^2 + \sigma_{f_L}^2 & \rho_x \sigma_{f_V} \sigma_{\xi_V} + \rho_L \sigma_{f_L} \sigma_{\xi_L} \\ \rho_V \sigma_{f_V} \sigma_{\xi_V} + \rho_L \sigma_{f_L} \sigma_{\xi_L} & \sigma_{\xi_V}^2 + \sigma_{\xi_L}^2 \end{bmatrix} \tag{B63}$$

Now, the total mean squared stresses from the vertical and lateral analysis results are,

$$\begin{aligned} \sigma_f^2 &= \sigma_{f_V}^2 + \sigma_{f_L}^2 \\ \sigma_\xi^2 &= \sigma_{\xi_V}^2 + \sigma_{\xi_L}^2 \end{aligned} \tag{B64}$$

and the correlation coefficient relating the total axial and total shear stresses is,

$$\rho = \frac{\rho_V \sigma_{f_V} \sigma_{\xi_V} + \rho_L \sigma_{f_L} \sigma_{\xi_L}}{\sigma_f \sigma_\xi} \tag{B65}$$

The power spectral density function for the total axial stress can be obtained from the total autocorrelation function

$$R_f(\tau) = \lim_{T \to \infty} \frac{1}{2T} \int_{-T}^{T} \left[f_V(t) + f_L(t)\right]\left[f_V(t+\tau) + f_L(t+\tau)\right] dt \tag{B66}$$

Then,

$$\phi_f(\omega) = \frac{2}{\pi}\int_0^\infty R_f(\tau)\, e^{-i\omega\tau}\, d\tau \qquad \text{(B67a)}$$

$$= \frac{2}{\pi}\int_0^\infty \left[\lim_{T\to\infty}\frac{1}{2T}\int_{-T}^{T} f_V(t)f_V(t+\tau)d\right.$$

$$\left. + \lim_{T\to\infty}\frac{1}{2T}\int_{-T}^{T} f_L(t)f_L(t+\tau)d\tau\right] e^{-i\omega\tau}\, d\tau \qquad \text{(B67b)}$$

$$\phi_f(\omega) = \frac{2}{\pi}\int_{-0}^\infty \left[R_{f_V}(\tau) + R_{f_L}(\tau)\right] e^{-i\omega\tau}\, d\tau \qquad \text{(B68)}$$

The total number of level crossings per second with both positive and negative slope for one stress component can be obtained from Rice's expression (14).

$$N_{0_f} = \frac{1}{\pi}\left[\frac{\int_0^\infty \omega^2\phi_f(\omega)\, d\omega}{\int_0^\infty \phi_f(\omega)\, d\omega}\right]^{1/2} \qquad \text{(B69)}$$

Substituting Eq. (B68) into Eq. (B69), we have

$$N_{0_f} = \frac{1}{\pi}\left[\frac{\int_0^\infty \omega^2\phi_{f_V}(\omega)d\omega + \int_0^\infty \omega^2\phi_{f_L}(\omega)d\omega}{\int_0^\infty \phi_{f_V}(\omega)d\omega + \int_0^\infty \phi_{f_L}(\omega)d\omega}\right]^{1/2} \qquad \text{(B70)}$$

Then,

$$N_{0_f} = \frac{1}{\pi}\left[\frac{\sigma^2_{\beta_{f_V}} + \sigma^2_{\beta_{f_L}}}{\sigma^2_{f_V} + \sigma^2_{f_L}}\right]^{1/2} \doteq \frac{1}{\pi}\left[\frac{\sigma_{\beta_f}}{\sigma_f}\right] \qquad \text{(B71a)}$$

$$N_{0_\xi} = \frac{1}{\pi}\left[\frac{\sigma^2_{\alpha_{\xi_V}} + \sigma^2_{\alpha_{\xi_L}}}{\sigma^2_{\xi_V} + \sigma^2_{\xi_L}}\right]^{1/2} = \frac{1}{\pi}\left[\frac{\sigma_{\alpha_\xi}}{\sigma_\xi}\right] \qquad \text{(B71b)}$$

The values σ_ξ, σ_{α_ξ}, σ_f, $\sigma_{\alpha f}$ and ρ derived from Eq. (B65), (B71a) and (B71b) can be used in the joint probability statistical analysis described previously.

APPENDIX C

NUMERICAL RESULTS

APPENDIX C

NUMERICAL RESULTS

The wing, body and vertical tail loads resulting from a one foot per second rms gust, $\bar{A}$, and corresponding number of crossings per second, N_o, are tabulated on the following pages. The condition numbers correspond with those shown in Tables 2 through 5 in the Analysis Conditions section.

CONDITION 1
VERTICAL ANALYSIS

GW 181,600 LB.
ALT. 5,000 FT.
CG 18.6 PERCENT MAC

SPEED
V_i 290 KT.
V_e 269 KT.
M .45

CG ACCELERATION:
$\bar{A}$ .01642 g
N_o 1.609 PER SEC.

WING

WING STATION	η	BEAM BENDING MOMENT 10^3 IN. LB. $\bar{A}$	BEAM BENDING MOMENT 10^3 IN. LB. 1g	BEAM BENDING MOMENT N_o, PER SEC.	BEAM SHEAR LB. $\bar{A}$	BEAM SHEAR LB. 1g	BEAM SHEAR N_o, PER SEC.	TORSION 10^3 IN. LB. $\bar{A}$	TORSION 10^3 IN. LB. 1g	TORSION N_o, PER SEC.
0	0	213.6	14,900	1.088	586.8	48,600	1.381	69.28	-2,600	1.573
94.4	.12	183.3	12,000	.9646	447.4	37,200	1.701	31.58	-1,530	2.993
157.3	.20	161.0	10,400	.8986	417.7	31,200	1.726	30.39	-900	3.001
259.6	.33	123.2	7,500	.9981	374.1	22,300	1.685	31.07	-550	2.769
322.5	.41	93.54	5,800	.9945	379.6	26,000	.9870	17.99	-250	2.201
432.7	.55	52.54	3,150	1.201	295.2	16,600	1.157	17.92	-380	2.154
503.5	.64	34.20	2,150	1.319	246.2	9,750	1.430	18.55	-400	2.068
550.7	.70	21.42	1,500	1.352	179.6	12,200	1.118	2.937	-50	2.270
645.1	.82	6.613	450	1.512	95.82	6,000	1.421	1.686	-30	2.129
715.9	.91	1.450	100	1.999	40.10	2,700	1.476	.8031	-10	2.571

FUSELAGE

BODY BALANCE STATION	BENDING MOMENT 10^3 IN. LB. $\bar{A}$	BENDING MOMENT 10^3 IN. LB. 1g	BENDING MOMENT N_o, PER SEC.	SHEAR LB. $\bar{A}$	SHEAR LB. 1g	SHEAR N_o, PER SEC.
300	15.04	-740	3.907	170.3	-10,090	3.418
480	65.00	-3,950	3.096	374.7	-25,650	2.641
620	122.9	-8,226	2.767	466.3	-34,900	2.232
720	170.5	—	2.581	520.1	—	1.960
890	182.7	-18,050	2.388	568.2	-53,890	1.323
1000	132.2	-13,160	2.762	484.6	-39,010	1.610
1160	79.39	-7,624	3.197	321.6	-28,970	2.290
1320	45.11	-3,802	3.259	190.3	-23,940	3.153
1400	31.22	-2,043	3.252	172.8	-30,520	3.165
1636	0	0	—	0	0	0

CONDITION 1
VERTICAL ANALYSIS

C-4

CONDITION 2
VERTICAL ANALYSIS

GW 178,800 LB.
ALT. 15,000 FT.
CG 17.0 PERCENT MAC

SPEED
V_T 370 KT.
V_E 295 KT.
M .59

CG ACCELERATION:
$\bar{A}$ .01694 g
N_o 1.860 PER SEC.

WING

WING STATION	η	BEAM BENDING MOMENT 10^3 IN. LB. $\bar{A}$	BEAM BENDING MOMENT 10^3 IN. LB. 1g	BEAM BENDING MOMENT N_o, PER SEC.	BEAM SHEAR LB. $\bar{A}$	BEAM SHEAR LB. 1g	BEAM SHEAR N_o, PER SEC.	TORSION 10^3 IN. LB. $\bar{A}$	TORSION 10^3 IN. LB. 1g	TORSION N_o, PER SEC.
0	0	217.0	15,700	1.212	604.0	54,500	1.431	69.50	-2,900	1.779
94.4	.12	183.5	12,500	1.075	461.2	40,100	1.786	37.81	-1,900	2.997
157.3	.20	160.2	10,600	.9927	435.6	33,400	1.897	37.53	-1,300	2.945
259.6	.33	122.0	7,700	1.093	393.5	23,000	1.932	37.73	- 940	2.754
322.5	.41	91.15	6,000	1.041	383.7	26,000	1.096	21.41	- 550	2.375
432.7	.55	56.26	3,300	1.248	295.4	16,600	1.235	21.20	- 630	2.296
503.5	.64	33.18	2,200	1.426	243.9	9,800	1.566	21.62	- 600	2.208
550.7	.70	20.26	1,600	1.448	170.6	12,000	1.068	3.522	- 100	3.151
645.1	.82	6.566	500	2.052	88.58	6,000	1.429	1.886	- 50	3.142
715.9	.91	1.563	100	2.816	39.66	2,500	2.107	.8604	- 10	3.534

FUSELAGE

BODY BALANCE STATION	BENDING MOMENT 10^3 IN. LB. $\bar{A}$	BENDING MOMENT 10^3 IN. LB. 1g	BENDING MOMENT N_o, PER SEC.	SHEAR LB. $\bar{A}$	SHEAR LB. 1g	SHEAR N_o, PER SEC.
300	14.79	- 740	4.274	167.9	-10,090	3.662
480	64.38	-3,950	3.231	374.7	-25,650	2.709
620	122.6	- 8,226	2.836	472.0	-34,900	2.255
720	170.9	—	2.625	531.4	—	1.983
890	174.0	-19,770	2.293	580.4	-56,520	1.391
1000	121.8	-14,590	2.725	489.2	-41,640	1.646
1160	69.94	- 8,628	3.337	309.8	-31,600	2.223
1320	40.36	- 4,385	3.499	162.6	-26,570	3.302
1400	29.09	- 2,416	3.489	145.7	-39,100	3.463
1636	0	0	—	0	0	—

CONDITION 2
VERTICAL ANALYSIS

CONDITION 3
VERTICAL ANALYSIS

GW 178,800 LB.
ALT. 25,000 FT.
CG 17.0 PERCENT MAC

SPEED
V_T 432 KT.
V_e 290 KT.
M .72

CG ACCELERATION:
$\bar{A}$ .01630 g
N_o 1.975 PER SEC.

WING

WING STATION	η	BEAM BENDING MOMENT 10^3 IN. LB. $\bar{A}$	BEAM BENDING MOMENT 10^3 IN. LB. 1g	BEAM BENDING MOMENT N_o, PER SEC.	BEAM SHEAR LB. $\bar{A}$	BEAM SHEAR LB. 1g	BEAM SHEAR N_o, PER SEC.	TORSION 10^3 IN. LB. $\bar{A}$	TORSION 10^3 IN. LB. 1g	TORSION N_o, PER SEC.
0	0	208.2	16,900	1.209	576.5	58,000	1.395	69.46	-3,270	1.900
94.4	.12	176.2	13,300	1.097	439.0	43,400	1.747	40.24	-2,100	2.969
157.3	.20	153.7	11,800	1.031	415.3	36,400	1.872	39.40	-1,470	2.917
259.6	.33	117.1	8,100	1.131	376.6	25,000	1.923	39.12	-1,100	2.746
322.5	.41	87.03	6,250	1.069	369.2	27,600	1.137	21.59	-650	2.398
432.7	.55	47.92	3,400	1.289	283.8	17,400	1.234	21.23	-700	2.307
503.5	.64	31.66	2,250	1.492	235.0	10,200	1.496	21.52	-690	2.215
550.7	.70	19.18	1,550	1.511	161.2	13,300	1.126	3.610	-150	3.256
645.1	.82	6.253	500	2.155	83.70	6,000	1.515	1.901	-80	3.314
715.9	.91	1.511	100	2.939	37.67	2,500	2.265	.8225	-50	3.718

FUSELAGE

BODY BALANCE STATION	BENDING MOMENT 10^3 IN. LB. $\bar{A}$	BENDING MOMENT 10^3 IN. LB. 1g	BENDING MOMENT N_o, PER SEC.	SHEAR LB. $\bar{A}$	SHEAR LB. 1g	SHEAR N_o, PER SEC.
300	13.45	- 740	4.505	153.3	-10,090	3.803
480	58.95	- 3,950	3.291	345.6	-25,650	2.688
620	112.8	- 8,226	2.833	439.7	-34,900	2.195
720	157.9	—	2.594	498.5	—	1.916
890	167.2	-19,920	2.264	558.6	-56,750	1.402
1000	116.6	-14,710	2.709	470.4	-41,870	1.649
1160	66.21	- 8,716	3.388	298.2	-31,830	2.205
1320	38.02	- 4,436	3.624	153.0	-26,800	3.370
1400	27.82	- 2,449	3.598	134.2	-36,590	3.665
1636	0	0	—	0	0	—

CONDITION 3
VERTICAL ANALYSIS

CONDITION 4
VERTICAL ANALYSIS

GW 166,000 LB.
ALT. 15,000 FT.
CG 18.1 PERCENT MAC

SPEED
V_T 370 KT.
V_e 295 KT.
M .59

CG ACCELERATION:
$\bar{A}$ .01785 g
N_o 1.791 PER SEC.

WING

WING STATION	η	BEAM BENDING MOMENT 10^3 IN. LB. $\bar{A}$	BEAM BENDING MOMENT 10^3 IN. LB. 1g	BEAM BENDING MOMENT N_o, PER SEC.	BEAM SHEAR LB. $\bar{A}$	BEAM SHEAR LB. 1g	BEAM SHEAR N_o, PER SEC.	TORSION 10^3 IN. LB. $\bar{A}$	TORSION 10^3 IN. LB. 1g	TORSION N_o, PER SEC.
0	0	221.0	15,300	1.161	639.7	54,400	1.366	70.18	-3,000	1.706
94.4	.12	184.4	11,700	1.019	496.1	41,700	1.638	58.27	-1,830	3.037
157.3	.20	158.7	9,300	.9552	464.7	34,400	1.682	38.13	-1,290	2.969
259.6	.33	119.1	6,850	1.110	390.7	22,700	1.842	38.44	-980	2.763
322.5	.41	88.24	5,150	1.080	377.7	25,800	1.020	21.27	-550	2.355
432.7	.55	48.57	2,700	1.321	2860	13,800	1.255	21.40	-620	2.270
503.5	.64	32.38	1,800	1.504	237.3	7,400	1.551	21.90	-600	2.191
550.7	.70	19.63	1,350	1.462	164.1	10,400	1.105	3.530	-140	3.195
645.1	.82	6.417	400	2.054	85.66	4,950	1.422	1.875	-70	3.211
715.9	.91	1.551	100	2.830	38.62	2,100	2.084	.8717	-40	3.604

FUSELAGE

BODY BALANCE STATION	BENDING MOMENT 10^3 IN. LB. $\bar{A}$	BENDING MOMENT 10^3 IN. LB. 1g	BENDING MOMENT N_o, PER SEC.	SHEAR LB. $\bar{A}$	SHEAR LB. 1g	SHEAR N_o, PER SEC.
300	15.87	- 740	4.163	180.7	-10,090	3.599
480	69.23	- 3,950	3.203	401.7	-25,650	2.693
620	131.6	- 8,226	2.824	504.4	-34,900	2.236
720	183.2	—	2.614	566.6	—	1.952
890	189.1	-19,670	2.374	609.1	-56,370	1.313
1000	133.9	-14,510	2.802	516.0	-41,490	1.630
1160	77.17	- 8,571	3.375	334.6	-31,450	2.309
1320	43.17	- 4,352	3.535	179.7	-26,430	3.359
1400	30.65	- 2,395	3.518	156.7	-35,780	3.525
1636	0	0	—	0	0	—

CONDITION 4
VERTICAL ANALYSIS

CONDITION 5
VERTICAL ANALYSIS

GW 191,800 LB.
ALT. 15,000 FT.
CG 19.6 PERCENT MAC

SPEED
V_t 370 KT.
V_e 295 KT.
M .59

CG ACCELERATION:
$\bar{A}$ .01610 g
N_o 1.440 PER SEC.

WING

WING STATION	η	BEAM BENDING MOMENT 10^3 IN. LB. $\bar{A}$	BEAM BENDING MOMENT 10^3 IN. LB. 1g	BEAM BENDING MOMENT N_o, PER SEC.	BEAM SHEAR LB. $\bar{A}$	BEAM SHEAR LB. 1g	BEAM SHEAR N_o, PER SEC.	TORSION 10^3 IN. LB. $\bar{A}$	TORSION 10^3 IN. LB. 1g	TORSION N_o, PER SEC.
0	0	209.3	15,400	1.075	579.6	53,500	1.478	70.74	-2,600	1.704
94.4	.12	181.6	12,200	.9697	431.9	38,600	1.846	30.31	-1,690	2.983
157.3	.20	161.1	10,300	.8982	401.3	32,200	1.805	27.11	-1,200	3.063
259.6	.33	123.7	7,600	.9632	364.2	24,100	1.549	27.54	-850	2.853
322.5	.41	94.28	5,850	.9908	381.2	27,400	.9631	16.09	-450	2.195
432.7	.55	53.78	3,000	1.213	293.6	16,300	1.099	15.77	-550	2.105
503.5	.64	34.04	2,000	1.311	250.5	9,000	1.377	16.49	-550	1.993
550.7	.70	22.28	1,300	1.503	179.8	10,900	1.166	3.611	-110	2.422
645.1	.82	6.927	450	1.801	100.8	5,400	1.608	2.003	-60	2.514
715.9	.91	1.401	100	2.020	42.27	2,450	1.933	1.038	-40	2.878

FUSELAGE

BODY BALANCE STATION	BENDING MOMENT 10^3 IN. LB. $\bar{A}$	BENDING MOMENT 10^3 IN. LB. 1g	BENDING MOMENT N_o, PER SEC.	SHEAR LB. $\bar{A}$	SHEAR LB. 1g	SHEAR N_o, PER SEC.
300	13.96	-740	4.267	159.1	-10,090	3.616
480	60.90	-3,950	3.171	355.8	-25,650	2.677
620	116.1	-8,226	2.791	447.5	-34,900	2.236
720	161.9	—	2.591	503.0	—	1.955
890	182.5	-19,250	2.508	567.8	-55,730	1.542
1000	131.2	-14,160	2.823	4870	-40,850	1.878
1160	77.10	-8,327	3.183	324.3	-30,810	2.473
1320	42.85	-4,210	3.213	185.4	-25,780	3.180
1400	29.38	-2,304	3.176	166.6	-34,420	3.244
1636	0	0	—	0	0	—

CONDITION 5
VERTICAL ANALYSIS

CONDITION 6
VERTICAL ANALYSIS

GW 211,600 LB.
ALT. 15,000 FT.
CG 20.6 PERCENT MAC

SPEED
V_T 370 KT.
V_e 295 KT.
M .59

CG ACCELERATION:
$\bar{A}$ .01632 g
N_0 2.191 PER SEC.

WING

WING STATION	η	BEAM BENDING MOMENT 10^3 IN. LB. $\bar{A}$	BEAM BENDING MOMENT 10^3 IN. LB. 1g	BEAM BENDING MOMENT N_0, PER SEC.	BEAM SHEAR LB. $\bar{A}$	BEAM SHEAR LB. 1g	BEAM SHEAR N_0, PER SEC.	TORSION 10^3 IN. LB. $\bar{A}$	TORSION 10^3 IN. LB. 1g	TORSION N_0, PER SEC.
0	0	199.4	15,000	1.214	537.8	54,000	1.426	67.40	-2,430	1.719
94.4	.12	173.1	11,000	1.112	393.1	36,400	1.869	33.73	-1,650	2.848
157.3	.20	154.2	10,400	1.024	378.2	29,400	2.039	31.76	-1,240	2.914
259.6	.33	119.9	7,700	1.022	371.0	22,400	2.037	31.74	-800	2.754
322.5	.41	91.22	6,200	.9858	372.1	26,000	1.285	18.75	-420	2.351
432.7	.55	51.89	3,500	1.216	296.6	16,300	1.181	18.26	-540	2.327
503.5	.64	34.62	2,400	1.375	244.8	10,900	1.442	18.62	-550	2.231
550.7	.70	21.93	1,700	1.581	182.5	14,200	1.203	3.252	-100	2.562
645.1	.82	6.892	550	1.327	98.08	6,700	1.691	1.805	-50	2.501
715.9	.91	1.515	200	2.491	42.16	3,000	1.987	.8542	-20	3.006

FUSELAGE

BODY BALANCE STATION	BENDING MOMENT 10^3 IN. LB. $\bar{A}$	BENDING MOMENT 10^3 IN. LB. 1g	BENDING MOMENT N_0, PER SEC.	SHEAR LB. $\bar{A}$	SHEAR LB. 1g	SHEAR N_0, PER SEC.
300	14.53	- 740	4.462	161.5	-10,090	3.877
480	61.06	- 3,950	3.445	345.4	-25,650	2.874
620	113.8	- 8,226	3.022	426.5	-34,900	2.340
720	156.9	—	2.78:	476.5	—	2.012
890	159.4	-18,660	2.475	521.4	-54,830	1.405
1000	115.6	-13,670	2.931	439.5	-39,950	1.694
1160	72.11	- 7,983	3.426	282.8	-29,910	2.389
1320	43.70	- 4,010	3.458	170.2	-24,880	3.368
1400	31.13	- 2,176	3.446	161.4	-32,520	3.379
1636	0	0	—	0	0	—

CONDITION 6
VERTICAL ANALYSIS

CONDITION 7
VERTICAL ANALYSIS

GW 163,800 LB
ALT. 30,000 FT.
CG 16.4 PERCENT MAC

SPEED
V_T 480 KT.
V_E 294 KT.
M .82

CG ACCELERATION:
$\bar{A}$ .01767 g
N_o 1.872 PER SEC.

WING

WING STATION	η	BEAM BENDING MOMENT 10^3 IN. LB. $\bar{A}$	BEAM BENDING MOMENT 10^3 IN. LB. 1g	BEAM BENDING MOMENT N_o, PER SEC.	BEAM SHEAR LB. $\bar{A}$	BEAM SHEAR LB. 1g	BEAM SHEAR N_o, PER SEC.	TORSION 10^3 IN. LB. $\bar{A}$	TORSION 10^3 IN. LB. 1g	TORSION N_o, PER SEC.
0	0	219.7	18,100	1.224	6479	63,400	1.391	76.09	-3,530	1.864
94.4	.12	182.4	13,150	1.089	502.7	18,000	1.686	46.14	-2,490	2.982
157.3	.20	156.0	10,700	1.039	470.6	39,400	1.769	45.22	-1,900	2.945
259.6	.33	117.1	7,550	1.231	394.9	25,500	1.949	44.41	-1,580	2.796
322.5	.41	85.19	5,450	1.166	371.7	27,300	1.086	23.32	-940	2.468
432.7	.55	46.72	3,000	1.427	281.1	14,500	1.304	23.01	-940	2.380
503.5	.64	31.03	2,000	1.634	236.7	7,750	1.609	23.31	-900	2.298
550.7	.70	18.23	1,350	1.531	153.8	11,300	1.186	4.337	-410	3.375
645.1	.82	6.013	400	2.200	79.49	5,000	1.488	2.203	-100	3.512
715.9	.91	1.506	100	3.091	36.00	2,000	2.272	1.069	- 50	3.879

FUSELAGE

BODY BALANCE STATION	BENDING MOMENT 10^3 IN. LB. $\bar{A}$	BENDING MOMENT 10^3 IN. LB. 1g	BENDING MOMENT N_o, PER SEC.	SHEAR LB. $\bar{A}$	SHEAR LB. 1g	SHEAR N_o, PER SEC.
300	15.36	- 739	4.336	176.2	-10,540	3.673
480	67.72	- 3,948	3.238	395.1	-24,920	2.669
620	129.5	- 7,968	2.815	500.1	-31,540	2.206
720	180.8	—	2.590	564.3	—	1.933
890	195.2	-20,150	2.288	624.4	-55,200	1.375
1000	137.1	-15,040	2.690	529.6	-41,790	1.658
1160	76.54	- 8,949	3.322	345.5	- 32,440	2.259
1320	41.48	- 4,572	3.645	117.2	-27,410	3.333
1400	29.98	- 2,536	3.624	147.1	-37,880	3.752
1636	0	0	—	0	0	—

CONDITION 7
VERTICAL ANALYSIS

CONDITION 8
VERTICAL ANALYSIS

GW 163,800 LB.
ALT. 35,000 FT.
CG 16.4 PERCENT MAC

SPEED
V_T 475 KT.
V_E 263 KT.
M .82

CG ACCELERATION:
$\bar{A}$ .01573 g
N_o 1.807 PER SEC.

WING

WING STATION	η	BEAM BENDING MOMENT 10³ IN. LB. $\bar{A}$	BEAM BENDING MOMENT 10³ IN. LB. 1g	BEAM BENDING MOMENT N_o, PER SEC.	BEAM SHEAR LB. $\bar{A}$	BEAM SHEAR LB. 1g	BEAM SHEAR N_o, PER SEC.	TORSION 10³ IN. LB. $\bar{A}$	TORSION 10³ IN. LB. 1g	TORSION N_o, PER SEC.
0	0	202.8	17,200	1.119	570.0	60,300	1.248	74.23	-3,700	1.790
94.4	.12	171.1	13,400	1.029	443.3	46,400	1.501	43.47	-2,460	2.869
157.3	.20	147.3	11,200	1.012	417.8	38,400	1.569	41.94	-1,740	2.872
259.6	.33	110.6	7,950	1.188	355.1	25,500	1.739	41.13	-1,360	2.732
322.5	.41	81.19	5,900	1.145	348.1	28,000	1.054	21.97	- 750	2.362
432.7	.55	44.93	3,200	1.396	265.8	15,800	1.236	21.47	- 800	2.285
503.5	.64	30.02	2,200	1.615	222.8	9,000	1.497	21.62	- 750	2.207
550.7	.70	17.75	1,500	1.500	148.3	12,300	1.162	3.923	- 120	3.125
645.1	.82	5.861	400	2.073	77.57	5,600	1.446	2.000	- 80	3.210
715.9	.91	1.449	200	2.864	35.26	2,200	2.105	.9757	- 40	3.550

FUSELAGE

BODY BALANCE STATION	BENDING MOMENT 10³ IN. LB. $\bar{A}$	BENDING MOMENT 10³ IN. LB. 1g	BENDING MOMENT N_o, PER SEC.	SHEAR LB. $\bar{A}$	SHEAR LB. 1g	SHEAR N_o, PER SEC.
300	12.66	- 706	4.325	145.4	-10,140	3.659
480	56.09	- 3,852	3.211	330.4	-24,690	2.598
620	107.9	- 7,858	2.759	422.4	-31,550	2.101
720	151.3	—	2.517	480.2	—	1.813
890	176.1	-19,190	2.154	563.3	-53,950	1.248
1000	123.4	-14,220	2.563	477.3	-40,390	1.517
1160	68.34	- 8,376	3.221	310.9	-30,940	2.121
1320	36.60	- 4,239	3.582	159.1	-25,910	3.230
1400	26.34	- 2,323	3.567	131.4	-34,700	3.651
1636	0	0	—	0	0	—

CONDITION 8
VERTICAL ANALYSIS

CONDITION 9
VERTICAL ANALYSIS

GW 163,800 LB.
ALT. 40,000 FT.
CG 16.4 PERCENT MAC

SPEED
V_t 475 KT.
V_e 234 KT.
M .82

CG ACCELERATION:
$\bar{A}$ .01377 g
N_o 1.725 PER SEC.

WING

WING STATION	η	BEAM BENDING MOMENT 10^3 IN. LB. $\bar{A}$	BEAM BENDING MOMENT 10^3 IN. LB. 1g	BEAM BENDING MOMENT N_o, PER SEC.	BEAM SHEAR LB. $\bar{A}$	BEAM SHEAR LB. 1g	BEAM SHEAR N_o, PER SEC.	TORSION 10^3 IN. LB. $\bar{A}$	TORSION 10^3 IN. LB. 1g	TORSION N_o, PER SEC.
0	0	184.9	17,200	1.053	497.9	56,100	1.146	68.77	-3,880	1.664
94.4	.12	158.0	13,600	.9911	390.1	44,300	1.367	37.62	-2,380	2.802
157.3	.20	136.5	11,400	.9886	370.5	37,200	1.420	35.99	-1,680	2.800
259.6	.33	102.6	8,250	1.144	318.9	25,800	1.577	35.59	-1,160	2.653
322.5	.41	75.89	6,200	1.123	319.6	28,500	1.019	19.86	-560	2.259
432.7	.55	42.42	3,400	1.365	246.7	16,600	1.183	19.39	-670	2.192
503.5	.64	28.65	2,400	1.613	206.5	10,000	1.413	19.50	-700	2.119
550.7	.70	16.92	1,550	1.469	140.3	13,000	1.149	3.456	-90	2.895
645.1	.82	5.585	500	1.957	74.09	6,000	1.412	1.766	-40	2.927
715.9	.91	1.361	100	2.657	33.75	2,450	1.963	.8686	-10	3.244

FUSELAGE

BODY BALANCE STATION	BENDING MOMENT 10^3 IN. LB. $\bar{A}$	BENDING MOMENT 10^3 IN. LB. 1g	BENDING MOMENT N_o, PER SEC.	SHEAR LB. $\bar{A}$	SHEAR LB. 1g	SHEAR N_o, PER SEC.
300	10.44	-676	4.264	120.2	-9,782	3.613
480	46.54	-3,767	3.168	276.3	-24,470	2.533
620	89.97	-7,757	2.704	356.3	-31,530	2.019
720	126.7	—	2.452	407.5	—	1.721
890	157.3	-18,370	2.041	502.5	-52,890	1.158
1000	109.9	-13,530	2.445	426.0	-39,180	1.412
1160	60.24	-7,887	3.115	277.9	-29,660	2.007
1320	31.79	-3,955	3.509	142.2	-24,630	3.113
1400	22.85	-2,141	3.499	116.7	-31,990	3.527
1636	0	0	—	0	0	—

CONDITION 9
VERTICAL ANALYSIS

CONDITION 10
VERTICAL ANALYSIS

GW	204,200 LB	SPEED	CG ACCELERATION:
ALT.	35,000 FT.	V_T 475 KT.	$\bar{A}$ .01476 g
CG	21.5 PERCENT MAC	V_e 263 KT.	N_o 2.256 PER SEC.
		M .82	

WING

WING STATION	η	BEAM BENDING MOMENT 10³ IN. LB.			BEAM SHEAR LB.			TORSION 10³ IN. LB.		
		$\bar{A}$	1g	N_o, PER SEC.	$\bar{A}$	1g	N_o, PER SEC.	$\bar{A}$	1g	N_o, PER SEC.
0	0	184.5	16,100	1.113	485.0	57,300	1.129	68.59	-2,760	1.677
94.4	.12	160.9	12,700	1.089	353.9	41,300	1.465	34.64	-1,880	2.716
157.3	.20	142.1	10,900	1.050	339.7	33,600	1.689	32.05	-1,490	2.774
259.6	.33	108.3	8,000	1.039	329.6	23,500	1.863	31.97	-1,140	2.639
322.5	.41	81.92	6,300	1.016	338.8	26,400	1.311	19.28	- 580	2.295
432.7	.55	46.24	3,600	1.246	272.0	16,500	1.148	18.61	- 700	2.276
503.5	.64	31.14	2,400	1.482	226.3	10,800	1.571	18.57	- 700	2.191
550.7	.70	19.33	1,630	1.630	163.2	14,300	1.269	3.474	- 90	2.589
645.1	.82	6.039	500	1.983	87.07	6,900	1.731	1.828	- 50	2.620
715.9	.91	1.309	100	2.607	37.24	3,000	2.081	.9204	- 40	3.087

FUSELAGE

BODY BALANCE STATION	BENDING MOMENT 10³ IN. LB.			SHEAR LB.		
	$\bar{A}$	1g	N_o, PER SEC.	$\bar{A}$	1g	N_o, PER SEC.
300	10.96	- 666	4.905	122.9	- 9,766	4.135
480	46.87	- 3,739	3.578	271.9	-24,230	2.741
620	88.80	- 7,665	2.972	346.7	-30,760	2.038
720	124.0	—	2.630	396.6	—	1.649
890	149.8	-17,520	2.194	490.1	-51,220	1.226
1000	106.4	-12,840	2.693	412.7	-37,780	1.476
1160	62.30	- 7,402	3.411	266.8	-28,390	2.150
1320	35.77	- 3,673	3.688	147.8	-23,360	3.365
1400	25.78	- 1,961	3.664	131.2	-29,300	3.668
1636	0	[illegible]	—	0	0	—

CONDITION 10
VERTICAL ANALYSIS

CONDITION 11
VERTICAL ANALYSIS

GW 183,000 LB.
ALT. 35,000 FT.
CG 19.4 PERCENT MAC

SPEED
V_T 280 KT.
V_E 263 KT.
M .82

CG ACCELERATION:
$\bar{A}$ .01467 g
N_o 1.599 PER SEC.

WING

WING STATION	η.	BEAM BENDING MOMENT 10^3 IN. LB. $\bar{A}$	BEAM BENDING MOMENT 10^3 IN. LB. 1g	BEAM BENDING MOMENT N_o, PER SEC.	BEAM SHEAR LB. $\bar{A}$	BEAM SHEAR LB. 1g	BEAM SHEAR N_o, PER SEC.	TORSION 10^3 IN. LB. $\bar{A}$	TORSION 10^3 IN. LB. 1g	TORSION N_o, PER SEC.
0	0	196.1	16,600	1.034	527.7	57,500	1.195	69.60	-3,180	1.530
94.4	.12	169.5	13,000	.978	396.4	43,300	1.470	30.79	-2,170	2.772
157.3	.20	148.2	10,900	.9457	371.1	35,800	1.514	28.71	-1,560	2.809
259.6	.33	112.3	7,900	1.013	335.9	24,600	1.504	29.47	-1,250	2.592
322.5	.41	84.91	6,000	1.038	348.0	27,500	1.014	18.35	- 640	2.138
432.7	.55	48.07	3,200	1.267	274.4	16,700	1.124	17.96	- 730	2.077
503.5	.64	31.18	2,450	1.485	236.2	9,000	1.347	16.38	- 720	1.992
550.7	.70	19.39	1,600	1.496	163.0	11,500	1.263	3.160	- 100	2.531
645.1	.82	5.772	440	1.686	88.4	5,500	1.554	1.679	- 50	2.556
715.9	.91	1.166	100	2.023	35.00	2,500	1.840	.8861	- 40	3.002

FUSELAGE

BODY BALANCE STATION	BENDING MOMENT 10^3 IN. LB. $\bar{A}$	BENDING MOMENT 10^3 IN. LB. 1g	BENDING MOMENT N_o, PER SEC.	SHEAR LB. $\bar{A}$	SHEAR LB. 1g	SHEAR N_o, PER SEC.
300	10.39	- 690	4.667	120.7	- 9,900	3.770
480	47.04	- 3,808	3.181	285.7	-24,510	2.463
620	92.17	- 7,782	2.636	373.2	-31,240	1.934
720	130.8	—	2.366	429.8	—	1.646
890	162.1	-17,430	2.076	529.7	-51,190	1.260
1000	112.4	-12,760	2.450	448.3	-37,680	1.551
1160	61.15	- 7,349	3.073	288.4	-28,250	2.070
1320	32.34	- 3,642	3.424	145.1	-23,220	3.081
1400	22.65	- 1,941	3.418	122.5	-29,000	3.493
1636	0	0	—	0	0	—

CONDITION 11
VERTICAL ANALYSIS

CONDITION 12
VERTICAL ANALYSIS

GW 159,000 LB
ALT. 10,000 FT.
CG 17.0 PERCENT MAC

SPEED
V_T 310 KT.
V_E 264 KT.
M .48

CG ACCELERATION:
$\bar{A}$ .01673 g
N_0 1.770 PER SEC.

WING

WING STATION	η	BEAM BENDING MOMENT 10^3 IN. LB. $\bar{A}$	1g	N_0, PER SEC.	BEAM SHEAR LB. $\bar{A}$	1g	N_0, PER SEC.	TORSION 10^3 IN. LB. $\bar{A}$	1g	N_0, PER SEC.
0	0	213.5	15,000	1.113	597.7	51,500	1.318	68.90	-3,750	1.568
94.4	.12	180.2	11,700	.9828	467.9	40,400	1.574	34.63	-2,500	2.995
157.3	.20	155.7	9,800	.9256	440.7	34,100	1.606	34.36	-1,850	2.953
259.6	.33	117.1	6,900	1.064	374.1	23,500	1.752	34.97	-1,500	2.737
322.5	.41	87.35	5,000	1.040	367.8	23,700	.9960	19.82	- 700	2.257
432.7	.55	48.36	2,800	1.260	280.8	13,100	1.217	19.96	- 790	2.193
503.5	.64	32.19	2,000	1.430	231.9	7,000	1.492	20.46	- 800	2.123
550.7	.70	19.73	1,300	1.413	164.2	10,000	1.034	3.151	- 70	2.818
645.1	.82	6.435	400	1.941	86.46	5,000	1.367	1.706	- 40	2.719
715.9	.91	1.526	200	2.631	38.96	2,500	1.929	.7868	- 10	3.097

FUSELAGE

BODY BALANCE STATION	BENDING MOMENT 10^3 IN. LB. $\bar{A}$	1g	N_0, PER SEC.	SHEAR LB. $\bar{A}$	1g	N_0, PER SEC.
300	15.16	- 740	3.958	172.0	-10,090	3.474
480	65.70	- 3,950	3.151	378.4	-25,650	2.665
620	124.3	- 8,226	2.803	471.8	-34,900	2.226
720	172.4	—	2.602	527.7	—	1.939
890	184.2	-19,260	2.324	575.3	-55,740	1.232
1000	132.4	-14,170	2.743	468.9	-40,860	1.521
1160	78.11	- 8,330	3.285	322.6	-30,820	2.233
1320	43.75	- 4,212	3.448	183.8	-25,790	3.254
1400	30.62	- 2,366	3.458	162.2	-34,450	3.353
1636	0	0	—	0	0	—

CONDITION 12
VERTICAL ANALYSIS

CONDITION 13
VERTICAL ANALYSIS

GW 159,000 LB
ALT. 20,000 FT.
CG 17.0 PERCENT MAC

SPEED
V_T 380 KT.
V_e 277 KT.
M .62

CG ACCELERATION:
$\bar{A}$ .01658g
N_o 1.784 PER SEC.

WING

WING STATION	η	BEAM BENDING MOMENT 10^3 IN. LB.			BEAM SHEAR LB.			TORSION 10^3 IN. LB.		
		$\bar{A}$	1g	N_o, PER SEC.	$\bar{A}$	1g	N_o, PER SEC.	$\bar{A}$	1g	N_o, PER SEC.
0	0	209.5	15,400	1.134	592.9	54,900	1.327	68.11	-3,720	1.680
94.4	.12	176.0	11,900	1.008	461.7	42,300	1.586	36.92	-2,560	2.956
157.3	.20	151.8	9,900	.9579	434.3	35,700	1.624	36.54	-1,980	2.937
259.6	.33	114.2	7,000	1.108	361.7	24,400	1.775	36.79	-1,600	2.737
322.5	.41	84.75	5,000	1.082	359.4	24,400	1.014	20.36	- 800	2.302
432.7	.55	46.91	2,600	1.320	273.7	13,000	1.230	20.42	- 850	2.221
503.5	.64	31.30	1,800	1.508	227.2	9,400	1.509	20.84	- 850	2.146
550.7	.70	18.93	1,200	1.448	157.6	10,000	1.105	3.317	- 100	3.094
645.1	.82	6.191	400	2.006	82.65	4,600	1.411	1.764	- 50	3.092
715.9	.91	1.491	100	2.739	37.32	2,000	2.036	.8200	- 10	3.478

FUSELAGE

BODY BALANCE STATION	BENDING MOMENT 10^3 IN. LB.			SHEAR LB.		
	$\bar{A}$	1g	N_o, PER SEC.	$\bar{A}$	1g	N_o, PER SEC.
300	14.40	- 740	4.149	164.2	-10,090	3.597
480	62.94	- 3,950	3.200	365.8	-25,650	2.679
620	113.8	- 8,226	2.815	460.5	-34,900	2.212
720	167.0	—	2.600	518.5	—	1.922
890	177.3	-19,910	2.331	570.5	-56,830	1.277
1000	125.4	-14,760	2.761	483.3	-41,950	1.589
1160	71.82	- 8,747	3.352	313.9	-31,910	2.267
1320	39.87	- 4,454	3.540	167.8	-26,880	3.340
1400	28.29	- 2,460	3.523	145.2	-36,760	3.536
1636	0	0	—	0	0	—

CONDITION 13
VERTICAL ANALYSIS

CONDITION 14
VERTICAL ANALYSIS

GW 119,700 LB.
ALT. 22,000 FT.
CG 20.6 PERCENT MAC

SPEED
V_T 532 KT.
V_e 375 KT.
M .87

CG ACCELERATION:
$\bar{A}$ .027876 g
N_o 2.283 PER SEC.

WING

WING STATION	η	BEAM BENDING MOMENT 10^3 IN. LB. $\bar{A}$	BEAM BENDING MOMENT 10^3 IN. LB. 1g	BEAM BENDING MOMENT N_o, PER SEC.	BEAM SHEAR LB. $\bar{A}$	BEAM SHEAR LB. 1g	BEAM SHEAR N_o, PER SEC.	TORSION 10^3 IN.-LB. $\bar{A}$	TORSION 10^3 IN.-LB. 1g	TORSION N_o, PER SEC.
℄	0	181.637	12,500	1.937	672.087		1.883	72.753		2.143
94.4	.12	143.173	9,250	1.537	513.521		2.293	54.550		3.029
157.3	.20	119.079	7,220	1.337	478.915		2.396	54.036		2.975
259.6	.33	89.448	4,520	1.604	375.232		2.836	52.099		2.980
322.5	.41	61.317	3,000	1.589	287.855		1.341	24.419		3.115
432.7	.55	34.130	1,300	2.066	189.621		1.873	25.214		2.917
503.5	.64	27.157	950	2.127	174.021		2.404	25.888		2.763
550.7	.70	14.400	650	2.140	124.696		1.788	6.583		4.031
645.1	.82	5.043	200	3.363	62.791		2.070	3.452		4.336
715.9	.91	1.557	0	4.623	29.241		3.366	1.796		4.674

FUSELAGE

BODY BALANCE STATION	BENDING MOMENT 10^3 IN. LB. $\bar{A}$	BENDING MOMENT 10^3 IN. LB. 1g	BENDING MOMENT N_o, PER SEC.	SHEAR LB. $\bar{A}$	SHEAR LB. 1g	SHEAR N_o, PER SEC.
300	25.399		4.302	292.246		3.695
480	100.376		3.402	502.224		3.011
620	174.424		3.130	569.260		2.686
720	232.757		2.972	630.928		2.392
890	238.288		2.789	615.492		1.898
1000	178.705		3.061	548.800		2.232
1160	106.712		3.541	439.511		2.599
1320	66.998		3.957	260.164		3.419
1400	40.285		4.001	203.496		4.024
1636	0	0	—	0	0	—

CONDITION 14
VERTICAL ANALYSIS

CONDITION 15
VERTICAL ANALYSIS

GW 156,000 LB.
ALT. 22,000 FT.
CG 15.6 PERCENT MAC

SPEED
V_T 532 KT.
V_E 375 KT.
M .87

CG ACCELERATION:
$\bar{A}$ .023326 g
N_o 2.189 PER SEC.

WING

WING STATION	η	BEAM BENDING MOMENT 10^3 IN. LB. $\bar{A}$	BEAM BENDING MOMENT 10^3 IN. LB. 1g	BEAM BENDING MOMENT N_o, PER SEC.	BEAM SHEAR LB. $\bar{A}$	BEAM SHEAR LB. 1g	BEAM SHEAR N_o, PER SEC.	TORSION 10^3 IN. LB. $\bar{A}$	TORSION 10^3 IN. LB. 1g	TORSION N_o, PER SEC.
0	0	261.938	17,850	1.434	898.432		1.502	93.563		1.607
94.4	.12	207.491	13,400	1.264	700.419		1.776	48.812		2.934
157.3	.20	168.747	10,550	1.149	634.453		1.889	47.982		2.959
259.6	.33	119.022	6,440	1.810	487.608		2.233	47.502		2.831
322.5	.41	83.103	4,200	1.308	407.799		1.141	28.762		2.820
432.7	.55	44.313	2,020	1.658	287.603		1.489	20.834		2.733
503.5	.64	29.737	1,350	1.933	252.246		1.890	29.099		2.636
550.7	.70	16.479	820	1.732	144.478		1.518	6.593		4.020
645.1	.82	5.550	300	2.908	71.839		1.645	3.473		4.312
715.9	.91	1.619	100	4.360	32.481		2.861	1.806		4.653

FUSELAGE

BODY BALANCE STATION	BENDING MOMENT 10^3 IN. LB. $\bar{A}$	BENDING MOMENT 10^3 IN. LB. 1g	BENDING MOMENT N_o, PER SEC.	SHEAR LB. $\bar{A}$	SHEAR LB. 1g	SHEAR N_o, PER SEC.
300	21.771	-768	4.787	244.906	-10,874	2.189
480	92.581	-3,961	3.683	524.154	-25,322	4.068
620	173.465	-8,079	3.118	657.896	-32,561	2.981
720	240.648	—	2.854	750.836	—	2.431
890	262.595	-25,529	2.590	808.619	-57,655	2.077
1000	185.006	-19,478	3.033	720.233	-52,473	1.542
1160	106.487	-11,973	3.594	464.084	-41,026	1.904
1320	59.853	-6,294	3.790	247.939	-31,010	2.624
1400	43.031	-3,900	3.747	211.297	-55,958	3.608
1636	0	0	—	0	0	—

CONDITION 15
VERTICAL ANALYSIS

CONDITION 16
VERTICAL ANALYSIS

GW 186,000 LB.
ALT. 22,000 FT.
CG 16.3 PERCENT MAC

SPEED
V_T 532 KT.
V_E 375 KT.
M .87

CG ACCELERATION:
$\bar{\Sigma}$ .02206 g
N_o 2.496 PER SEC.

WING

WING STATION	η	BEAM BENDING MOMENT 10³ IN. LB. Σ̄	1g	N_o, PER SEC.	BEAM SHEAR LB. Σ̄	1g	N_o, PER SEC.	TORSION 10³ IN. LB. Σ̄	1g	N_o, PER SEC.
0	0	261.8		1.599	843.8		1.830	99.36		2.079
94.4	.12	213.5	14,100	1.425	655.9	57,500	2.258	56.14	-4,500	3.044
157.3	.20	179.3	11,400	1.260	607.2	44,500	2.421	53.61	-3,400	3.044
259.6	.33	130.8	7,500	1.296	515.1	27,000	2.474	52.09	-2,500	2.919
322.5	.41	93.35	5,600	1.207	435.1	27,600	1.378	29.96	-1,750	2.789
432.7	.55	49.33	2,600	1.499	324.6	13,600	1.440	28.61	-1,300	2.697
503.5	.64	31.36	1,700	1.735	279.2	6,560	1.826	28.53	-1,040	2.587
550.7	.70	18.87	1,100	1.977	165.6	9,000	1.571	6.427	- 480	3.935
645.1	.82	6.209	300	3.003	83.95	3,100	2.028	3.373	- 250	4.213
715.9	.91	1.637	100	4.296	37.91	500	3.119	1.724	- 100	4.578

FUSELAGE

BODY BALANCE STATION	BENDING MOMENT 10³ IN. LB. Σ̄	1g	N_o, PER SEC.	SHEAR LB. Σ̄	1g	N_o, PER SEC.
300	23.17	- 728	4.722	256.9	-10,480	4.097
480	95.95	- 3,843	3.683	524.9	-24,860	3.171
620	175.7	- 7,884	3.288	636.4	-31,790	2.683
720	239.8	—	3.061	709.9	—	2.352
890	271.6	-25,270	2.806	829.8	-57,020	1.901
1000	198.2	-19,280	3.156	708.1	-52,040	2.203
1160	119.6	-11,830	3.572	480.5	-40,660	2.818
1320	67.91	- 6,212	3.725	283.3	-30,640	3.560
1400	48.29	- 3,854	3.719	246.6	-55,170	3.828
1636	0	0	—	0	0	—

CONDITION 16
VERTICAL ANALYSIS

CONDITION 17
VERTICAL ANALYSIS

GW 221,600 LB.
ALT. 22,000 FT.
CG 16.5 PERCENT MAC

SPEED
V_T 532 KT.
V_E 375 KT.
M .87

CG ACCELERATION:
$\bar{A}$ .020111 g
N_o 2.180 PER SEC.

WING

WING STATION	η	BEAM BENDING MOMENT 10³ IN. LB.			BEAM SHEAR LB.			TORSION 10³ IN. LB.		
		$\bar{A}$	1g	N_o, PER SEC.	$\bar{A}$	1g	N_o, PER SEC.	$\bar{A}$	1g	N_o, PER SEC.
0	0	232.815	17,350	1.176	693.894		1.244	91.608		1.896
94.4	.12	201.777	13,800	1.164	471.989		1.598	40.973		2.639
157.3	.20	176.932	11,250	1.127	433.524		1.793	35.755		2.911
259.6	.33	133.600	7,350	1.121	413.132		1.932	35.283		2.708
322.5	.41	99.004	5,300	1.112	425.316		1.361	22.033		2.347
432.7	.55	55.643	2,680	1.355	332.056		1.235	20.455		2.343
503.5	.64	34.961	1,800	1.563	282.020		1.444	20.630		2.223
550.7	.70	22.369	1,100	1.961	185.953		1.366	6.665		3.036
665.1	.82	7.018	470	2.579	102.678		2.118	3.607		3.342
715.9	.91	1.368	200	3.089	44.526		2.833	2.003		3.680

FUSELAGE

BODY BALANCE STATION	BENDING MOMENT 10³ IN. LB.			SHEAR LB.		
	$\bar{A}$	1g	N_o, PER SEC.	$\bar{A}$	1g	N_o, PER SEC.
300	15.080	-697	6.019	163.464	-19,184	4.941
480	61.403	-3,752	4.135	349.476	-24,507	3.164
620	114.571	-7,733	3.365	450.232	-31,205	2.285
720	159.917	—	2.937	530.661	—	1.790
890	194.168	-24,133	2.372	696.732	-55,092	1.461
1000	135.241	-18,341	2.881	573.583	-50,276	1.819
1160	82.229	-11,175	3.495	347.247	-38,936	2.487
1320	50.901	-5,830	3.624	197.083	-28,920	3.513
1400	36.410	-3,609	3.568	192.305	-61,528	3.859
1636	0	0	—	0	0	—

CONDITION 17
VERTICAL ANALYSIS

CONDITION 18
VERTICAL ANALYSIS

GW 186,000 LB.
ALT. 5,000 FT.
CG 16.3 PERCENT MAC

SPEED
V_T 403 KT.
V_E 375 KT.
M .62

CG ACCELERATION:
$\bar{A}$ .021532 g
N_o 1.995 PER SEC.

WING

WING STATION	η	BEAM BENDING MOMENT 10^3 IN. LB. $\bar{A}$	BEAM BENDING MOMENT 10^3 IN. LB. 1g	BEAM BENDING MOMENT N_o, PER SEC.	BEAM SHEAR LB. $\bar{A}$	BEAM SHEAR LB. 1g	BEAM SHEAR N_o, PER SEC.	TORSION 10^3 IN. LB. $\bar{A}$	TORSION 10^3 IN. LB. 1g	TORSION N_o, PER SEC.
0	0	269.404	16,000	1.390	891.600		1.579	76.721		1.971
94.4	.12	218.921	12,000	1.223	636.080		1.986	[illegible]		3.131
157.3	.20	197.099	9,800	1.071	587.748		2.152	42.284		3.016
259.6	.33	199.491	7,000	1.127	504.837		2.218	42.933		2.793
322.5	.41	102.472	6000	1.061	455.489		1.146	27.055		2.666
432.7	.55	54.950	2,700	1.294	330.936		1.322	26.632		2.650
503.5	.64	35.829		1.481	282.669		1.688	27.086		2.434
550.7	.70	21.511		1.569	186.029		1.195	4.723		3.811
645.1	.82	6.945		2.426	93.615		1.594	2.464		3.970
715.9	.91	1.702		3.451	41.556		2.606	1.138		4.406

FUSELAGE

BODY BALANCE STATION	BENDING MOMENT 10^3 IN. LB. $\bar{A}$	BENDING MOMENT 10^3 IN. LB. 1g	BENDING MOMENT N_o, PER SEC.	SHEAR LB. $\bar{A}$	SHEAR LB. 1g	SHEAR N_o, PER SEC.
300	20.082		4.653	237.343		3.900
480	87.217		3.364	509.650		2.817
620	166.790		2.920	651.641		2.327
720	234.101		2.686	748.174		2.031
830	216.535		2.623	761.318		1.642
1000	149.579		2.963	630.168		1.950
1160	87.483		3.481	384.163		2.525
1320	52.589		3.526	203.905		3.444
1400	38.202		3.508	188.451		3.576
1636	0	0	—	0	0	—

CONDITION 18
VERTICAL ANALYSIS

CONDITION 19
VERTICAL ANALYSIS

GW 186,000 LB.
ALT. 15,000 FT.
CG 16.3 PERCENT MAC

SPEED
V_T 472 KT.
V_e 375 KT.
M .76

CG ACCELERATION:
$\bar{A}$ .021650 g
N_o 2.234 PER SEC.

WING

WING STATION	η	BEAM BENDING MOMENT 10^3 IN. LB. $\bar{A}$	BEAM BENDING MOMENT 10^3 IN. LB. 1g	BEAM BENDING MOMENT N_o, PER SEC.	BEAM SHEAR LB. $\bar{A}$	BEAM SHEAR LB. 1g	BEAM SHEAR N_o, PER SEC.	TORSION 10^3 IN. LB. $\bar{A}$	TORSION 10^3 IN. LB. 1g	TORSION N_o, PER SEC.
0	0	265.584	17,950	1.506	851.978		1.223	76.982		2.199
94.4	.12	213.497	13,800	1.333	652.334		2.144	44.620		3.153
157.3	.20	190.912	10,120	1.152	601.776		2.307	44.922		3.040
259.6	.33	133.991	7,400	1.169	509.425		2.361	44.711		2.831
322.5	.41	97.652	5,300	1.095	442.326		1.224	29.390		2.777
432.7	.55	52.032	2,300	1.355	328.921		1.368	27.706		2.647
503.5	.64	33.856		1.576	277.112		1.764	27.930		2.627
550.7	.70	20.225		1.725	175.077		1.324	5.386		3.968
645.1	.82	6.576		2.659	87.967		1.808	2.600		4.199
715.9	.91	1.645		3.728	39.302		2.933	1.208		4.668

FUSELAGE

BODY BALANCE STATION	BENDING MOMENT 10^3 IN. LB. $\bar{A}$	BENDING MOMENT 10^3 IN. LB. 1g	BENDING MOMENT N_o, PER SEC.	SHEAR LB. $\bar{A}$	SHEAR LB. 1g	SHEAR N_o, PER SEC.
300	21.655		4.652	244.956		3.935
480	93.218		3.448	533.431		2.909
620	175.946		3.023	670.373		2.430
720	244.763		2.791	761.426		2.130
890	233.081		2.731	774.641		1.828
1000	169.981		3.119	650.765		2.132
1160	101.240		3.570	421.497		2.734
1320	58.571		3.677	237.919		3.545
1400	42.067		3.668	210.144		3.746
1636	0	0	—	0	0	—

CONDITION 19
VERTICAL ANALYSIS

CONDITION 20
VERTICAL ANALYSIS

GW 186,000 LB.
ALT. 30,000 FT.
CG 16.5 PERCENT MAC

SPEED
V_T 530 KT.
V_e 327 KT.
M .90

CG ACCELERATION:
$\bar{A}$ .019130 g
N_o 2.262 PER SEC.

WING

WING STATION	η	BEAM BENDING MOMENT 10^3 IN. LB. $\bar{A}$	BEAM BENDING MOMENT 10^3 IN. LB. 1g	BEAM BENDING MOMENT N_o, PER SEC.	BEAM SHEAR LB. $\bar{A}$	BEAM SHEAR LB. 1g	BEAM SHEAR N_o, PER SEC.	TORSION 10^3 IN. LB. $\bar{A}$	TORSION 10^3 IN. LB. 1g	TORSION N_o, PER SEC.
0	0	230.360	18,900	1.287	662.219		1.482	102.246		1.931
94.4	.12	196.496	14,600	1.204	505.191		1.800	60.894		2.867
157.3	.20	169.147	12,000	1.173	472.620		1.938	54.382		2.918
259.6	.33	125.966	8,300	1.311	422.337		2.010	53.868		2.839
322.5	.41	90.451	6,000	1.210	405.731		1.316	26.686		2.505
432.7	.55	45.537	3,190	1.436	307.803		1.325	25.447		2.423
503.5	.64	30.891		1.667	258.766		1.563	25.202		2.337
550.7	.70	18.369		1.698	159.016		1.354	5.875		3.476
645.1	.82	6.010		2.594	81.474		1.665	3.188		3.631
715.9	.91	1.579		3.786	36.790		2.559	1.659		3.892

FUSELAGE

BODY BALANCE STATION	BENDING MOMENT 10^3 IN. LB. $\bar{A}$	BENDING MOMENT 10^3 IN. LB. 1g	BENDING MOMENT N_o, PER SEC.	SHEAR LB. $\bar{A}$	SHEAR LB. 1g	SHEAR N_o, PER SEC.
300	15.624		5.031	171.165		4.278
480	64.114		3.777	355.324		3.116
620	119.201		3.273	443.277		2.527
720	162.805		2.986	508.775		2.153
880	211.164		2.455	690.535		1.531
1000	142.726		2.895	579.152		1.914
1160	89.026		3.424	372.279		2.461
1320	52.005		3.580	209.364		3.430
1400	37.745		3.539	187.008		3.710
1636	0	0	—	0	0	—

CONDITION 20
VERTICAL ANALYSIS

CONDITION 21
VERTICAL ANALYSIS

GW 186,000 LB.
ALT. 40,000 FT.
CG 16.3 PERCENT MAC

SPEED
V_T 516 KT.
V_E 260 KT.
M .90

CG ACCELERATION:
$\bar{A}$ .01380g
N_o 1.943 PER SEC.

WING

WING STATION	η	BEAM BENDING MOMENT 10^3 IN. LB. $\bar{A}$	BEAM BENDING MOMENT 10^3 IN. LB. 1g	BEAM BENDING MOMENT N_o, PER SEC.	BEAM SHEAR LB. $\bar{A}$	BEAM SHEAR LB. 1g	BEAM SHEAR N_o, PER SEC.	TORSION 10^3 IN. LB. $\bar{A}$	TORSION 10^3 IN. LB. 1g	TORSION N_o, PER SEC.
0	0	195.4		1.085	503.4		1.188	8615		1.651
94.4	.12	170.9	15,800	1.061	392.3	48,200	1.419	4550	-3,940	2.654
157.3	.20	148.6	13,200	1.067	372.7	40,000	1.514	41.26	-2,570	2.743
259.6	.33	111.0	9,400	1.175	343.8	28,600	1.580	40.00	-1,510	2.651
322.5	.41	81.66	7,300	1.134	349.5	31,200	1.155	22.38	— 700	2.286
432.7	.55	44.81	3,900	1.344	271.8	19,700	1.179	21.41	— 600	2.229
503.5	.64	29.67	2,500	1.644	227.1	12,100	1.360	21.19	— 580	2.159
550.7	.70	17.56	1,800	1.526	148.6	14,400	1.186	4.533	— 50	2.920
645.1	.82	5.730	400	2.149	77.76	7,000	1.446	2.472	— 30	2.964
715.5	.91	1.425	100	3.077	35.28	2,800	2.053	1.284	— 20	3.180

FUSELAGE

BODY BALANCE STATION	BENDING MOMENT 10^3 IN. LB. $\bar{A}$	BENDING MOMENT 10^3 IN. LB. 1g	BENDING MOMENT N_o, PER SEC.	SHEAR LB. $\bar{A}$	SHEAR LB. 1g	SHEAR N_o, PER SEC.
300	10.03		4.929	110.6		4.188
480	41.58		3.668	237.1		2.923
620	78.01		3.110	306.6		2.260
720	109.2		2.782	361.5		1.855
890	164.1		2.109	550.9		1.268
1000	113.6		2.549	460.3		1.505
1160	64.21		3.184	291.4		2.112
1320	36.52		3.418	156.5		3.154
1400	26.71		3.374	137.3		3.441
1636	0	0	—	0	0	—

CONDITION 21
VERTICAL ANALYSIS

CONDITION 22
VERTICAL ANALYSIS

GW 186,000 LB.
ALT. 22,000 FT.
CG 16.3 PERCENT MAC

SPEED
V_T 359 KT.
V_e 253 KT.
M .59

CG ACCELERATION:
$\bar{A}$ .013830 g
N_o 1.763 PER SEC.

WING

WING STATION	η	BEAM BENDING MOMENT 10³ IN. LB. $\bar{A}$	BEAM BENDING MOMENT 10³ IN. LB. 1g	BEAM BENDING MOMENT N_o, PER SEC.	BEAM SHEAR LB. $\bar{A}$	BEAM SHEAR LB. 1g	BEAM SHEAR N_o, PER SEC.	TORSION 10³ IN LB. $\bar{A}$	TORSION 10³ IN LB. 1g	TORSION N_o, PER SEC.
0	0	201.036	17,750	1.117	533.178		1.298	66.697		1.619
94.4	.12	171.576	14,000	1.012	415.023		1.595	33.096		2.908
157.3	.20	149.401	11,850	0.954	393.650		1.685	32.496		2.881
259.6	.33	113.113	8,800	1.044	358.853		1.714	32.991		2.684
322.5	.41	84.902	6,800	1.006	353.825		1.043	19.382		2.240
432.7	.55	47.076	3,700	1.195	275.682		1.167	19.124		2.188
503.5	.64	30.807	2,420	1.384	227.715		1.398	19.422		2.116
550.7	.70	18.962		1.363	158.438		1.018	2.960		2.831
645.1	.82	6.142		1.862	83.111		1.338	1.613		2.740
715.9	.91	1.440		2.517	37.248		1.889	0.741		3.108

FUSELAGE

BODY BALANCE STATION	BENDING MOMENT 10³ IN. LB. $\bar{A}$	BENDING MOMENT 10³ IN. LB. 1g	BENDING MOMENT N_o, PER SEC.	SHEAR LB. $\bar{A}$	SHEAR LB. 1g	SHEAR N_o, PER SEC.
300	11.963		4.161	135.045		3.633
480	51.820		3.244	301.651		2.731
620	98.827		2.858	396.140		2.233
720	138.586		2.625	445.156		1.902
890	153.389		2.211	516.083		1.276
1000	106.807		2.665	438.908		1.533
1160	61.663		3.246	268.088		2.177
1320	35.374		3.396	145.853		3.210
1400	25.232		3.387	139.666		3.341
1636	0	0	—	0	0	—

CONDITION 22
VERTICAL ANALYSIS

CONDITION 23
VERTICAL ANALYSIS

GW 186,000 LB.
ALT. 22,000 FT.
CG 16.5 PERCENT MAC

SPEED
V_T 425 KT.
V_e 300 KT.
M .70

CG ACCELERATION:
$\bar{A}$ .016643 g
N_o 1.945 PER SEC.

WING

WING STATION	η	BEAM BENDING MOMENT 10³ IN. LB. $\bar{A}$	BEAM BENDING MOMENT 10³ IN. LB. 1g	BEAM BENDING MOMENT N_o, PER SEC.	BEAM SHEAR LB. $\bar{A}$	BEAM SHEAR LB. 1g	BEAM SHEAR N_o, PER SEC.	TORSION 10³ IN LB $\bar{A}$	TORSION 10³ IN LB 1g	TORSION N_o, PER SEC.
0	0	226.145	18,080	1.216	639.404		1.397	73.260		1.853
94.4	.12	189.489	13,900	1.095	490.131		1.736	41.116		2.992
157.3	.20	163.972	11,620	1.021	460.182		1.864	40.357		2.936
259.6	.33	133.736	8,400	1.123	411.092		1.919	40.409		2.767
322.5	.41	91.609	6,150	1.057	373.673		1.119	22.700		2.410
432.7	.55	50.095	3,250	1.270	301.634		1.235	22.314		2.328
503.5	.64	32.541	2,250	1.467	249.934		1.507	22.610		2.239
550.7	.70	19.799		1.483	167.188		1.116	3.750		3.331
645.1	.82	6.430		2.139	86.337		1.989	1.976		3.399
715.9	.91	1.551		2.946	38.693		2.255	0.916		3.804

FUSELAGE

BODY BALANCE STATION	BENDING MOMENT 10³ IN. LB. $\bar{A}$	BENDING MOMENT 10³ IN. LB. 1g	BENDING MOMENT N_o, PER SEC.	SHEAR LB. $\bar{A}$	SHEAR LB. 1g	SHEAR N_o, PER SEC.
300	14.361		4.438	162.831		3.841
480	62.639		3.336	366.698		2.761
620	120.025		2.887	472.279		2.244
720	168.827		2.635	545.899		1.926
890	175.160		2.230	602.147		1.421
1000	120.941		2.760	498.982		1.693
1160	69.249		3.407	308.016		2.288
1320	40.298		3.584	161.441		3.389
1400	29.354		3.666	142.847		3.643
1636	0	0	—	0	0	—

CONDITION 23
VERTICAL ANALYSIS

CONDITION 24
VERTICAL ANALYSIS

GW 186,000 LB.
ALT. 22,000 FT.
CG 16.3 PERCENT MAC

SPEED
V_T 480 KT.
V_e 340 KT.
M .78

CG ACCELERATION:
$\bar{A}$ .01942g
N_o 2.174 PER SEC.

WING

WING STATION	η	BEAM BENDING MOMENT 10^3 IN. LB. $\bar{A}$	BEAM BENDING MOMENT 10^3 IN. LB. 1g	BEAM BENDING MOMENT N_o, PER SEC.	BEAM SHEAR LB. $\bar{A}$	BEAM SHEAR LB. 1g	BEAM SHEAR N_o, PER SEC.	TORSION 10^3 IN. LB. $\bar{A}$	TORSION 10^3 IN. LB. 1g	TORSION N_o, PER SEC.
0	0	248.8		1.397	760.8		1.609	78.09		2.140
94.4	.12	203.2	13,900	1.242	584.4	52,800	2.003	48.39	-2,390	3093
157.3	.20	173.8	11,400	1.116	542.7	42,000	2.156	47.89	-1,850	3016
259.6	.33	130.2	8,100	1.201	469.8	28,000	2.211	47.10	-1,560	2.649
322.5	.41	95.00	5,990	1.108	422.4	29,000	1.208	26.36	-1,040	2.613
432.7	.55	51.18	3,200	1.349	318.3	16,200	1.341	25.82	-1,010	2.576
503.5	.64	33.19	2,080	1.561	267.2	8,500	1.679	26.07	- 940	2.433
550.7	.70	19.82	1,200	1.638	169.7	11,100	1.241	4.608	- 270	3.723
645.1	.82	6.451	410	2.460	86.16	5,000	1.673	2.386	- 150	3895
715.9	.91	1.601	10	3.414	38.60	700	2.658	1.112	- 60	1.336

FUSELAGE

BODY BALANCE STATION	BENDING MOMENT 10^3 IN. LB. $\bar{A}$	BENDING MOMENT 10^3 IN. LB. 1g	BENDING MOMENT N_o, PER SEC.	SHEAR LB. $\bar{A}$	SHEAR LB. 1g	SHEAR N_o, PER SEC.
300	18.88		4.536	213.9		3.854
480	81.58		3.410	467.9		2.866
620	154.3		2.988	590.2		2.376
720	214.9		2.752	672.3		2.068
890	216.5		2.615	701.1		1.681
1000	154.3		3.024	588.0		1.973
1160	91.28		3.523	380.8		2.613
1320	52.48		3.671	213.4		3.506
1400	31.89		3.656	186.0		3.744
1636	0	0	—	0	0	—

CONDITION 24
VERTICAL ANALYSIS

CONDITION 24C
VERTICAL ANALYSIS

GW 186,000 LB.
ALT. 22,000 FT.
CG 16.3 PERCENT MAC

SPEED
V_T 480 KT.
V_e 340 KT.
M .78

CG ACCELERATION:
$\bar{A}$ .019773 g
N_o 1.900 PER SEC.

WING

WING STATION	η	BEAM BENDING MOMENT 10^3 IN. LB. $\bar{A}$	BEAM BENDING MOMENT 10^3 IN. LB. 1g	BEAM BENDING MOMENT N_o, PER SEC.	BEAM SHEAR LB. $\bar{A}$	BEAM SHEAR LB. 1g	BEAM SHEAR N_o, PER SEC.	TORSION 10^3 IN. LB. $\bar{A}$	TORSION 10^3 IN. LB. 1g	TORSION N_o, PER SEC.
0	0	253.966	18,200	1.342	771.998		1.482	80.438		2.110
94.4	.12	208.027	13,400	1.190	585.099		1.899	51.251		3.091
157.3	.20	178.548	11,050	1.071	544.696		2.076	50.579		3.030
259.6	.33	133.882	7,750	1.172	475.075		2.168	49.572		2.872
322.5	.41	97.691	5,600	1.064	433.566		1.156	25.742		2.611
432.7	.55	52.481	3,000	1.295	321.958		1.289	25.335		2.494
503.5	.64	34.406		1.490	266.489		1.638	25.697		2.383
550.7	.70	20.473		1.511	176.474		1.163	4.705		3.676
645.1	.82	6.604		2.300	89.069		1.540	2.449		3.821
715.9	.91	1.618		3.270	39.492		2.493	1.139		4.250

FUSELAGE

BODY BALANCE STATION	BENDING MOMENT 10^3 IN. LB. $\bar{A}$	BENDING MOMENT 10^3 IN. LB. 1g	BENDING MOMENT N_o, PER SEC.	SHEAR LB. $\bar{A}$	SHEAR LB. 1g	SHEAR N_o, PER SEC.
300	20.596		4.228	237.286		3.661
480	80.956		3.387	406.786		3.036
620	140.957		3.141	458.204		2.755
720	188.144		3.002	502.833		2.487
890	187.559		2.802	644.903		1.689
1000	133.358		3.242	532.266		2.047
1160	81.632		3.653	333.370		2.794
1320	49.549		3.623	192.282		3.647
1400	36.247		3.557	176.625		3.789
1636	0	0	—	0	0	—

CONDITION 24C
VERTICAL ANALYSIS

CONDITION 25
VERTICAL ANALYSIS

GW 186,000 LB.
ALT. 22,000 FT.
CG 16.3 PERCENT MAC

SPEED
V_T 676 KT.
V_E 406 KT.
M .96

CG ACCELERATION:
$\bar{A}$ .02174 g
N_0 2.459 PER SEC.

WING

WING STATION	η	BEAM BENDING MOMENT 10^3 IN. LB. $\bar{A}$	BEAM BENDING MOMENT 10^3 IN. LB. 1g	BEAM BENDING MOMENT N_0, PER SEC.	BEAM SHEAR LB. $\bar{A}$	BEAM SHEAR LB. 1g	BEAM SHEAR N_0, PER SEC.	TORSION 10^3 IN LB. $\bar{A}$	TORSION 10^3 IN LB. 1g	TORSION N_0, PER SEC.
0	0	262.251	17,300	1.524	799.063		1.816	121.008		1.962
94.4	.12	220.597	13,160	1.363	630.955		2.174	71.984		2.885
157.3	.20	187.372	10,550	1.279	580.058		2.271	66.068		2.996
259.6	.33	138.313	7,000	1.419	511.413		2.303	62.280		2.918
322.5	.41	96.624	4,720	1.279	453.220		1.469	29.099		2.633
432.7	.55	50.495	2,050	1.495	337.197		1.482	28.269		2.531
503.5	.64	30.357	1,320	1.738	288.878		1.769	28.062		2.457
550.7	.70	17.985		1.910	160.587		1.683	7.552		3.918
645.1	.82	5.784		3.095	91.045		1.999	4.442		4.129
715.9	.91	1.671		4.564	36.218		3.052	2.376		4.383

FUSELAGE

BODY BALANCE STATION	BENDING MOMENT 10^3 IN. LB. $\bar{A}$	BENDING MOMENT 10^3 IN. LB. 1g	BENDING MOMENT N_0, PER SEC.	SHEAR LB. $\bar{A}$	SHEAR LB. 1g	SHEAR N_0, PER SEC.
300	20.614		5.060	246.797		4.308
480	90.775		3.815	484.940		3.321
620	163.543		3.400	578.316		2.848
720	220.988		3.183	640.784		2.526
890	270.997		2.745	836.631		1.839
1000	196.603		3.097	715.131		2.188
1160	117.753		3.522	481.749		2.798
1320	66.542		3.696	286.213		3.516
1400	47.197		3.680	255.334		3.768
1636	0	0	—	0	0	—

CONDITION 25
VERTICAL ANALYSIS

1400	47.197		3.680	255.334		3.769
1636	0	0	—	0	0	—

CONDITION 26
VERTICAL ANALYSIS

GW 221,600 LB.
ALT. 5,000 FT.
CG 21.2 PERCENT MAC

SPEED
V_T 403 KT.
V_E 375 KT.
M .62

CG ACCELERATION:
$\bar{A}$ .02066g
N_o 2.039 PER SEC.

WING

WING STATION	η	BEAM BENDING MOMENT 10^3 IN. LB. $\bar{A}$	BEAM BENDING MOMENT 10^3 IN. LB. 1g	BEAM BENDING MOMENT N_o, PER SEC.	BEAM SHEAR LB. $\bar{A}$	BEAM SHEAR LB. 1g	BEAM SHEAR N_o, PER SEC.	TORSION 10^3 IN. LB. $\bar{A}$	TORSION 10^3 IN. LB. 1g	TORSION N_o, PER SEC.
0	0	241.2		1.229	739.9		1.416	75.18		1.813
94.4	.12	203.5	12,200	1.140	517.8	43,900	1.878	35.95	-1,600	2.868
157.3	.20	179.7	10,100	1.043	477.1	35,100	2.056	32.82	-1,450	2.970
259.6	.33	138.4	7,200	1.042	441.3	24,000	2.068	32.40	-1,100	2.812
322.5	.41	104.7	5,600	1.023	436.2	26,500	1.278	19.85	- 700	2.471
432.7	.55	59.63	2,900	1.283	337.9	14,500	1.215	19.04	- 680	2.428
503.5	.64	38.77	1,900	1.410	283.7	8,600	1.513	19.75	- 620	2.277
550.7	.70	25.20	1,400	1.808	205.1	11,000	1.257	4.984	- 220	2.856
645.1	.82	8.052	400	2.338	114.3	5,000	1.982	2.705	- 160	3.050
715.9	.91	1.678	200	2.681	49.90	2,000	2.584	1.374	- 90	3.466

FUSELAGE

BODY BALANCE STATION	BENDING MOMENT 10^3 IN. LB. $\bar{A}$	BENDING MOMENT 10^3 IN. LB. 1g	BENDING MOMENT N_o, PER SEC.	SHEAR LB. $\bar{A}$	SHEAR LB. 1g	SHEAR N_o, PER SEC.
300	18.14		4.979	201.8		4.150
480	76.99		3.534	446.6		2.878
620	146.0		3.006	570.0		2.268
720	204.3	—	2.717	657.3	—	1.896
830	189.2		2.661	670.1		1.567
1000	135.5		3.112	551.9		1.978
1160	86.93		3.450	336.8		2.686
1320	54.88		3.346	207.9		3.406
1400	39.07		3.299	206.4		3.389
1636	0	0	—	0	0	—

CONDITION 26
VERTICAL ANALYSIS

CONDITION 27
VERTICAL ANALYSIS

GW 221,600 LB.
ALT. 15,000 FT.
CG 21.2 PERCENT MAC

SPEED
V_T 472 KT.
V_E 375 KT.
M .76

CG ACCELERATION:
$\bar{A}$ .02027g
N_o 2,098 PER SEC.

WING

WING STATION	η	BEAM BENDING MOMENT 10^3 IN. LB. $\bar{A}$	BEAM BENDING MOMENT 10^3 IN. LB. 1g	BEAM BENDING MOMENT N_o, PER SEC.	BEAM SHEAR LB. $\bar{A}$	BEAM SHEAR LB. 1g	BEAM SHEAR N_o, PER SEC.	TORSION 10^3 IN. LB. $\bar{A}$	TORSION 10^3 IN. LB. 1g	TORSION N_o, PER SEC.
0	0	235.1		1,186	718.5		1,301	74.72		1,817
94.4	.12	198.5	13,600	1,133	492.8	47,800	1,717	37.38	−1,940	2,818
157.3	.20	175.1	11,200	1,062	453.3	41,200	1,911	34.08	−1,640	2,904
259.6	.33	134.3	7,800	1,058	425.7	27,800	2,003	33.60	−1,300	2,750
322.5	.41	101.1	5,700	1,037	427.6	27,800	1,295	20.27	− 850	2,435
432.7	.55	57.00	3,000	1,284	331.2	15,200	1,215	19.51	− 820	2,372
503.5	.64	36.89	2,000	1,452	278.3	8,600	1,475	20.14	− 750	2,227
550.7	.70	23.78	1,300	1,837	194.9	11,100	1,293	5,196	− 300	3,015
645.1	.82	7.547	400	2,413	107.7	5,000	2,040	2,795	− 160	3,270
715.9	.91	1.573	100	2,852	46.68	1,700	2,747	1.436	− 70	3,701

FUSELAGE

BODY BALANCE STATION	BENDING MOMENT 10^3 IN. LB. $\bar{A}$	BENDING MOMENT 10^3 IN. LB. 1g	BENDING MOMENT N_o, PER SEC.	SHEAR LB. $\bar{A}$	SHEAR LB. 1g	SHEAR N_o, PER SEC.
300	16.19		5.509	181.1		4.452
480	69.56		3.683	410.7		2,846
620	133.4		3.014	534.6		2,148
720	188.4		2.662	625.4		1,752
890	176.5		2.562	650.9		1,498
1000	123.6		3.096	531.8		1,895
1160	77.54		3.587	316.6		2,625
1320	49.41		3.530	184.1		3.566
1400	35.64		3.459	182.9		3,664
1636	0	0	—	0	0	—

CONDITION 27
VERTICAL ANALYSIS

CONDITION 28
VERTICAL ANALYSIS

GW 221,600 LB.
ALT. 30,000 FT.
CG 21.2 PERCENT MAC

SPEED
V_T 530 KT.
V_E 327 KT.
M .90

CG ACCELERATION:
$\bar{A}$ .01670g
N_0 2.062 PER SEC.

WING

WING STATION	η	BEAM BENDING MOMENT 10^3 IN. LB. $\bar{A}$	BEAM BENDING MOMENT 10^3 IN. LB. 1g	BEAM BENDING MOMENT N_0, PER SEC.	BEAM SHEAR LB. $\bar{A}$	BEAM SHEAR LB. 1g	BEAM SHEAR N_0, PER SEC.	TORSION 10^3 IN. LB. $\bar{A}$	TORSION 10^3 IN. LB. 1g	TORSION N_0, PER SEC.
0	0	214.0		1.130	582.0		1.261	90.08		1.363
94.4	.12	189.5	14,300	1.097	414.2	48,500	1.555	35.83	-4,700	2.357
157.3	.20	166.7	11,800	1.060	390.5	38,800	1.695	29.14	-3,500	2.694
259.6	.33	126.0	8,400	1.051	379.8	26,800	1.746	28.76	-2,200	2.62[illegible]
322.5	.41	94.54	6,200	1.019	393.3	28,400	1.266	18.95	-1,250	2.236
432.7	.55	59.22	3,400	1.247	315.2	15,700	1.164	17.85	- 900	2.255
503.5	.64	33.21	2,200	1.446	267.6	9,500	1.333	17.95	- 850	2.147
550.7	.70	21.44	1,400	1.740	178.9	12,000	1.256	5.598	- 200	2.771
645.1	.82	6.588	400	2.258	98.40	5,400	1.854	3.150	- 110	2.988
715.9	.91	1.238	200	2.774	41.91	2,300	2.386	1.755	- 50	3.286

FUSELAGE

BODY BALANCE STATION	BENDING MOMENT 10^3 IN. LB. $\bar{A}$	BENDING MOMENT 10^3 IN. LB. 1g	BENDING MOMENT N_0, PER SEC.	SHEAR LB. $\bar{A}$	SHEAR LB. 1g	SHEAR N_0, PER SEC.
300	12.27		5.737	132.0		4.747
480	49.20		4.056	275.8		3.154
620	90.89		3.361	352.7		2.366
720	126.2	—	2.971	415.4	—	1.897
890	175.7		2.165	618.5		1.363
1000	122.0		2.620	511.3		1.650
1160	72.85		3.233	312.0		2.228
1320	44.23		3.409	175.8		3.234
1400	31.35		3.374	169.6		3.546
1636	0	0	—	0	0	—

CONDITION 28
VERTICAL ANALYSIS

CONDITION 29
VERTICAL ANALYSIS

GW 221,600 LB.
ALT. 40,000 FT.
CG 21.2 PERCENT MAC

SPEED
V_T 516 KT.
V_E 260 KT.
M .90

CG ACCELERATION:
$\bar{A}$ .012642 g
N_0 1.827 PER SEC.

WING

WING STATION	η	BEAM BENDING MOMENT 10^3 IN. LB. $\bar{A}$	BEAM BENDING MOMENT 10^3 IN. LB. 1g	BEAM BENDING MOMENT N_0, PER SEC.	BEAM SHEAR LB. $\bar{A}$	BEAM SHEAR LB. 1g	BEAM SHEAR N_0, PER SEC.	TORSION 10^3 IN. LB. $\bar{A}$	TORSION 10^3 IN. LB. 1g	TORSION N_0, PER SEC.
0	0	182.832	19,050	1.061	455.480		1.194	77.707		1.178
94.4	.12	164.258	15,000	1.014	338.392		1.473	27.001		2.118
157.3	.20	145.000	12,820	0.972	327.445		1.572	20.034		2.689
259.6	.33	110.239	9,320	0.965	325.434		1.563	20.136		2.667
322.5	.41	83.626	6,900	0.959	337.580		1.144	14.175		2.072
432.7	.55	47.260	2,900	1.103	277.373		1.091	13.364		2.105
503.5	.64	29.193	2,650	1.248	235.271		1.234	13.528		2.033
550.7	.70	19.250		1.467	160.777		1.092	4.144		2.271
645.1	.82	5.867		1.850	88.368		1.551	2.371		2.403
715.9	.91	1.077		2.268	37.438		1.907	1.306		2.693

FUSELAGE

BODY BALANCE STATION	BENDING MOMENT 10^3 IN. LB. $\bar{A}$	BENDING MOMENT 10^3 IN. LB. 1g	BENDING MOMENT N_0, PER SEC.	SHEAR LB. $\bar{A}$	SHEAR LB. 1g	SHEAR N_0, PER SEC.
300	8.945		5.182	97.200		4.360
480	36.412		3.796	206.187		3.012
620	67.830		3.206	265.686		2.308
720	94.592		2.862	313.809		1.868
890	144.434		1.921	497.994		1.210
1000	97.386		2.338	413.226		1.434
1160	56.842		2.948	254.486		1.952
1320	32.953		3.181	138.157		2.932
1400	22.997		3.180	128.436		3.218
1636	0	0	—	0	0	—

CONDITION 29
VERTICAL ANALYSIS

CONDITION 30
VERTICAL ANALYSIS

GW 221,600 LB.
ALT. 15,000 FT.
CG 21.2 PERCENT MAC

SPEED
V_T 319 KT.
V_e 253 KT.
M .51

CG ACCELERATION:
$\bar{A}$ .013200 g
N_o 1.734 PER SEC.

WING

WING STATION	η	BEAM BENDING MOMENT 10^3 IN. LB. $\bar{A}$	BEAM BENDING MOMENT 10^3 IN. LB. 1g	BEAM BENDING MOMENT N_o, PER SEC.	BEAM SHEAR LB. $\bar{A}$	BEAM SHEAR LB. 1g	BEAM SHEAR N_o, PER SEC.	TORSION 10^3 IN. LB. $\bar{A}$	TORSION 10^3 IN. LB. 1g	TORSION N_o, PER SEC.
0	0	196.554	16,550	1.134	502.339		1.476	64.109		1.432
94.4	.12	163.043	12,800	1.009	379.497		1.880	24.327		2.638
157.3	.20	144.947	11,200	0.914	369.511		1.955	20.883		2.946
259.6	.33	112.546	8,330	0.925	337.822		1.809	21.082		2.766
322.5	.41	86.721	6,500	0.907	338.797		1.092	13.960		2.321
432.7	.55	50.166	3,750	1.092	273.667		1.091	13.310		2.344
503.5	.64	32.246		1.153	289.884		1.354	13.687		2.236
550.7	.70	21.326		1.431	172.893		1.089	3.123		1.982
645.1	.82	6.768		1.741	96.381		1.545	1.779		1.966
715.9	.91	1.396		1.896	41.925		1.826	0.878		2.358

FUSELAGE

BODY BALANCE STATION	BENDING MOMENT 10^3 IN. LB. $\bar{A}$	BENDING MOMENT 10^3 IN. LB. 1g	BENDING MOMENT N_o, PER SEC.	SHEAR LB. $\bar{A}$	SHEAR LB. 1g	SHEAR N_o, PER SEC.
300	12.753		4.017	142.845		3.543
480	54.261		3.231	308.904		2.796
620	101.864		2.909	385.092		2.360
720	141.129		2.713	435.427		2.043
830	152.762		2.416	485.001		1.449
1000	110.849		2.769	407.521		1.727
1160	68.696		3.104	265.308		2.373
1320	40.225		3.109	166.328		3.054
1400	27.770		3.109	155.579		3.011
1636	0	0	—	0	0	—

CONDITION 30
VERTICAL ANALYSIS

CONDITION 31
VERTICAL ANALYSIS

GW 221,600 LB.
ALT. 16,000 FT.
CG 21.2 PERCENT MAC

SPEED
V_T 378 KT.
V_e 300 KT.
M .60

CG ACCELERATION:
$\bar{A}$ .015780 g
N_o 1.914 PER SEC.

WING

WING STATION	η	BEAM BENDING MOMENT 10^3 IN. LB. $\bar{A}$	BEAM BENDING MOMENT 10^3 IN. LB. 1g	BEAM BENDING MOMENT N_o, PER SEC.	BEAM SHEAR LB. $\bar{A}$	BEAM SHEAR LB. 1g	BEAM SHEAR N_o, PER SEC.	TORSION 10^3 IN. LB. $\bar{A}$	TORSION 10^3 IN. LB. 1g	TORSION N_o, PER SEC.
0	0	209.347	16,550	1.162	591.001		1.415	69.702		1.562
94.4	.12	180.321	12,500	1.065	425.964		1.835	28.562		2.727
157.3	.20	159.871	10,750	0.975	401.303		1.958	25.206		2.935
259.6	.33	123.644	7,900	0.973	378.470		1.891	25.342		2.755
322.5	.41	94.591	6,000	0.956	379.056		1.180	16.376		2.357
432.7	.55	54.419	3,400	1.172	301.998		1.141	15.684		2.349
503.5	.64	35.141		1.286	253.564		1.387	16.154		2.227
550.7	.70	22.990		1.594	186.535		1.127	3.768		2.400
645.1	.82	7.303		1.998	104.095		1.734	2.091		2.488
715.9	.91	1.509		2.234	45.179		2.151	1.050		2.703

FUSELAGE

BODY BALANCE STATION	BENDING MOMENT 10^3 IN. LB. $\bar{A}$	BENDING MOMENT 10^3 IN. LB. 1g	BENDING MOMENT N_o, PER SEC.	SHEAR LB. $\bar{A}$	SHEAR LB. 1g	SHEAR N_o, PER SEC.
300	14.180		4.488	158.383		3.954
480	60.285		3.393	346.525		2.841
620	113.745		2.966	437.956		2.301
720	158.462		2.713	501.443		1.943
890	164.747		2.466	550.869		1.462
1000	118.189		2.875	458.361		1.795
1160	73.367		3.261	289.267		2.456
1320	44.123		3.254	176.225		3.214
1400	30.963		3.236	167.474		3.217
1636	0	0	—	0	0	—

CONDITION 31
VERTICAL ANALYSIS

CONDITION 32
VERTICAL ANALYSIS

GW 221,600 LB.
ALT. 15,000 FT.
CG 21.2 PERCENT MAC

SPEED
V_T 561 KT.
V_e 445 KT.
M .90

CG ACCELERATION:
$\bar{A}$ .024033 g
N_o 2.402 PER SEC.

WING

WING STATION	η	BEAM BENDING MOMENT 10^3 IN LB. $\bar{A}$	BEAM BENDING MOMENT 10^3 IN LB. 1g	BEAM BENDING MOMENT N_o, PER SEC.	BEAM SHEAR LB. $\bar{A}$	BEAM SHEAR LB. 1g	BEAM SHEAR N_o, PER SEC.	TORSION 10^3 IN. LB. $\bar{A}$	TORSION 10^3 IN. LB. 1g	TORSION N_o, PER SEC.
0	0	244.511	16,550	1.281	796.928		1.428	103.222		1.780
94.4	.12	209.496	10,750	1.276	524.232		1.758	51.851		2.695
157.3	.20	182.699	8,450	1.248	469.860		1.964	45.702		2.825
259.6	.33	136.502	5,050	1.249	437.748		2.144	44.017		2.768
322.5	.41	99.073	3,150	1.225	448.818		1.546	25.270		2.533
432.7	.55	54.576	1,350	1.500	340.241		1.372	23.615		2.469
503.5	.61	33.562		1.734	292.277		1.587	23.620		2.330
550.7	.70	21.924		2.292	181.411		1.620	8.862		3.445
645.1	.82	7.032		3.078	101.474		2.476	4.954		3.746
715.9	.91	1.396		3.733	46.187		3.362	2.784		4.034

FUSELAGE

BODY BALANCE STATION	BENDING MOMENT 10^3 IN. LB. $\bar{A}$	BENDING MOMENT 10^3 IN. LB. 1g	BENDING MOMENT N_o, PER SEC.	SHEAR LB. $\bar{A}$	SHEAR LB. 1g	SHEAR N_o, PER SEC.
300	18.877		6.621	200.133		5.389
480	73.987		4.602	407.656		3.435
620	134.882		3.654	514.934		2.535
720	185.818		3.201	603,698		2.030
890	221.279		2.613	805.829		1.690
1000	156.525		3.110	663,073		2.118
1160	100.012		3.648	399.579		2.783
1320	64.522		3.731	239.643		3.713
1400	46.470		3.632	244.081		4.097
1636	0	0	—	0	0	—

CONDITION 32
VERTICAL ANALYSIS

CONDITION 24A
VERTICAL ANALYSIS

GW 186,000 LB.
ALT. 22,000 FT.
CG 16.3 PERCENT MAC

SPEED
V_T 480 KT.
V_E 340 KT.
M .78

CG ACCELERATION:
$\bar{A}$ .019205 g
N_o 2.202 PER SEC.

WING

WING STATION	η	BEAM BENDING MOMENT 10^3 IN. LB. $\bar{A}$	1g	N_o, PER SEC.	BEAM SHEAR LB. $\bar{A}$	1g	N_o, PER SEC.	TORSION 10^3 IN. LB. $\bar{A}$	1g	N_o, PER SEC.
0	0			1.386	747.176		1.601	71.115		2.147
94.4	.12			1.215	571.399		2.002	45.326		3.071
157.3	.20			1.067	529.425		2.158	45.564		2.156
259.6	.33			1.157	452.958		2.208	45.461		2.780
322.5	.41			1.062	396.785		1.153	27.127		2.623
432.7	.55			1.317	301.095		1.322	26.706		2.491
503.5	.64			1.584	259.330		1.685	26.990		2.385
550.7	.70			1.672	150.639		1.287	4.602		3.702
645.1	.82			2.563	75.784		1.737	2.364		3.925
715.9	.91			3.508	34.281		2.922	1.109		4.338

FUSELAGE

BODY BALANCE STATION	BENDING MOMENT 10^3 IN. LB. $\bar{A}$	1g	N_o, PER SEC.	SHEAR LB. $\bar{A}$	1g	N_o, PER SEC.
300	18.607		4.572	211.050		3.863
480	80.597		3.406	463.631		2.841
620	152.699		2.969	585.979		2.343
720	212.969		2.726	668.218		2.034
890	209.228		2.666	676.822		1.688
1000	150.071		3.078	566.734		1.997
1160	90.307		3.549	367.140		2.664
1320	52.740		3.660	209.898		3.539
1400	38.234		3.630	185.168		3.755
1636	0	0	—	0	0	—

CONDITION 24A
VERTICAL ANALYSIS

CONDITION 24B
VERTICAL ANALYSIS

GW 186,000 LB.
ALT. 22,000 FT.
CG 16.3 PERCENT MAC

SPEED
V_T 480 KT.
V_E 340 KT.
M .78

CG ACCELERATION:
$\bar{A}$ .019584 g
N_0 2.236 PER SEC.

WING

WING STATION	η	BEAM BENDING MOMENT 10^3 IN. LB. $\bar{A}$	BEAM BENDING MOMENT 10^3 IN. LB. 1g	BEAM BENDING MOMENT N_0, PER SEC.	BEAM SHEAR LB. $\bar{A}$	BEAM SHEAR LB. 1g	BEAM SHEAR N_0, PER SEC.	TORSION 10^3 IN. LB. $\bar{A}$	TORSION 10^3 IN. LB. 1g	TORSION N_0, PER SEC.
0	0	248.417		1.456	773.053		1.666	78.300		2.133
94.4	.12	201.653		1.285	598.607		2.065	49.899		2.974
157.3	.20	172.067		1.134	557.093		2.224	48.979		2.921
259.6	.33	129.094		1.203	480.056		2.288	47.054		2.786
322.5	.41	94.058		1.094	417.933		1.239	24.443		2.596
432.7	.55	50.620		1.338	310.689		1.332	23.852		2.497
503.5	.64	32.610		1.516	258.220		1.686	24.094		2.396
550.7	.70	19.810		1.676	169.736		1.254	4.683		3.678
645.1	.82	6.440		2.513	86.336		1.720	2.424		3.852
715.9	.91	1.589		3.479	38.643		2.714	1.125		4.296

FUSELAGE

BODY BALANCE STATION	BENDING MOMENT 10^3 IN. LB. $\bar{A}$	BENDING MOMENT 10^3 IN. LB. 1g	BENDING MOMENT N_0, PER SEC.	SHEAR LB. $\bar{A}$	SHEAR LB. 1g	SHEAR N_0, PER SEC.
300	19.900		4.423	225.336		3.790
480	85.763		3.381	488.704		2.873
620	161.565		2.989	611.970		2.410
720	224.361		2.767	693.013		2.114
890	222.709		2.663	708.189		1.724
1000	159.969		3.047	595.869		2.011
1160	95.450		3.519	390.925		2.645
1320	54.687		3.666	223.878		3.496
1400	39.318		3.655	194.860		3.716
1636	0	0	—	0	0	—

CONDITION 24B
VERTICAL ANALYSIS

CONDITION 24C
VERTICAL ANALYSIS

GW 186,000 LB.
ALT. 22,000 FT.
CG 16.3 PERCENT MAC

SPEED
V_T 480 KT.
V_e 340 KT.
M .78

CG ACCELERATION:
$\bar{A}$ .019773 g
N_o 1.900 PER SEC.

WING

WING STATION	η	BEAM BENDING MOMENT 10^3 IN LB. $\bar{A}$	BEAM BENDING MOMENT 10^3 IN LB. 1g	BEAM BENDING MOMENT N_o, PER SEC.	BEAM SHEAR LB. $\bar{A}$	BEAM SHEAR LB. 1g	BEAM SHEAR N_o, PER SEC.	TORSION 10^3 IN LB. $\bar{A}$	TORSION 10^3 IN LB. 1g	TORSION N_o, PER SEC.
0	0	253.966	18,200	1.342	771.998		1.482	80.438		2.110
94.4	.12	208.027	13,400	1.190	585.099		1.899	51.251		3.091
157.3	.20	178.548	11,050	1.071	544.696		2.076	50.579		3.030
259.6	.33	133.882	7,750	1.172	475.075		2.168	49.572		2.872
322.5	.41	97.691	5,600	1.064	433.566		1.156	25.742		2.611
432.7	.55	52.481	3,000	1.295	321.958		1.289	35.335		2.494
503.5	.64	34.406		1.490	266.489		1.638	25.697		2.383
550.7	.70	20.473		1.511	176.474		1.163	4.705		3.676
645.1	.82	6.604		2.300	89.069		1.540	2.447		3.821
715.9	.91	1.618		3.270	39.492		2.497	1.139		4.250

FUSELAGE

BODY BALANCE STATION	BENDING MOMENT 10^3 IN. LB. $\bar{A}$	BENDING MOMENT 10^3 IN. LB. 1g	BENDING MOMENT N_o, PER SEC.	SHEAR LB. $\bar{A}$	SHEAR LB. 1g	SHEAR N_o, PER SEC.
300	20.596		4.228	237.236		3.661
480	80.956		3.387	406.786		3.036
620	140.957		3.141	458.204		2.755
720	188.144		3.002	502.835		2.487
890	187.559		2.802	644.903		1.689
1000	133.358		3.242	532.266		2.047
1160	81.632		3.653	333.370		2.794
1320	49.549		3.623	192.282		3.647
1400	36.247		3.557	176.625		3.789
1636	0	0	—	0	0	—

CONDITION 24C
VERTICAL ANALYSIS

CONDITION 24D
VERTICAL ANALYSIS

GW 186,000 LB.
ALT. 22,000 FT.
CG 16.3 PERCENT MAC

SPEED
V_T 480 KT.
V_e 340 KT.
M .78

CG ACCELERATION:
$\bar{A}$ .020410 g
N_o 2.408 PER SEC.

WING

WING STATION	η	BEAM BENDING MOMENT 10^3 IN. LB. $\bar{A}$	BEAM BENDING MOMENT 10^3 IN. LB. 1g	BEAM BENDING MOMENT N_o, PER SEC.	BEAM SHEAR LB. $\bar{A}$	BEAM SHEAR LB. 1g	BEAM SHEAR N_o, PER SEC.	TORSION 10^3 IN. LB. $\bar{A}$	TORSION 10^3 IN. LB. 1g	TORSION N_o, PER SEC.
0	0	278.678		1.731	877.654		2.107	88.003		2.235
94.4	.12	221.153		1.449	726.089		2.481	59.172		3.098
157.3	.20	185.281		1.210	682.242		2.573	60.064		3.036
259.6	.33	140.719		1.350	584.503		2.646	59.020		2.896
322.5	.41	101.473		1.214	452.564		1.329	34.442		2.804
432.7	.55	55.082		1.484	359.509		1.535	33.559		2.721
503.5	.64	35.419		1.782	317.179		1.900	33.468		2.644
550.7	.70	20.887		1.897	174.405		1.350	5.022		3.632
645.1	.82	7.005		2.713	90.696		1.924	2.576		3.797
715.9	.91	1.791		3.539	41.867		2.873	1.208		4.186

FUSELAGE

BODY BALANCE STATION	BENDING MOMENT 10^3 IN. LB. $\bar{A}$	BENDING MOMENT 10^3 IN. LB. 1g	BENDING MOMENT N_o, PER SEC.	SHEAR LB. $\bar{A}$	SHEAR LB. 1g	SHEAR N_o, PER SEC.
300	29.129		3.900	326.929		3.573
480	122.515		3.368	664.966		3.091
620	224.007		3.161	786.466		2.797
720	303.656		3.033	849.166		2.565
890	297.911		2.928	800.575		2.100
1000	224.826		3.168	701.617		2.383
1160	139.255		3.430	512.549		2.914
1320	77.810		3.532	323.129		3.421
1400	54.851		3.539	274.556		3.552
1636	0	0	—	0	0	—

CONDITION 24D
VERTICAL ANALYSIS

CONDITION 24E
VERTICAL ANALYSIS

GW 186,000 LB.
ALT. 22,000 FT.
CG 16.5 PERCENT MAC

SPEED
V_T 480 KT.
V_e 340 KT.
M .78

CG ACCELERATION:
$\bar{A}$ .017367 g
N_o 2.100 PER SEC.

WING

WING STATION	η	BEAM BENDING MOMENT 10^3 IN LB. $\bar{A}$	BEAM BENDING MOMENT 10^3 IN LB. 1g	BEAM BENDING MOMENT N_o, PER SEC.	BEAM SHEAR LB. $\bar{A}$	BEAM SHEAR LB. 1g	BEAM SHEAR N_o, PER SEC.	TORSION 10^3 IN LB. $\bar{A}$	TORSION 10^3 IN LB. 1g	TORSION N_o, PER SEC.
0	0	215.344		1.242	650.043		1.755	80.856		2.424
94.4	.12	178.918		1.170	503.443		2.031	50.729		3.137
157.3	.20	153.346		1.124	452.526		1.389	47.143		3.028
259.6	.33	114.248		1.213	379.958		1.637	45.626		2.846
322.5	.41	83.082		1.162	374.464		1.155	24.706		2.496
432.7	.55	44.652		1.371	285.606		1.280	23.641		2.336
503.5	.64	28.428		1.548	242.660		1.583	23.656		2.223
550.7	.70	16.956		1.495	146.565		1.331	-4.368		3.574
645.1	.82	5.406		1.881	74.065		1.505	2.234		3.600
715.9	.91	1.311		2.583	32.460		1.841	1.030		3.775

FUSELAGE

BODY BALANCE STATION	BENDING MOMENT 10^3 IN. LB. $\bar{A}$	BENDING MOMENT 10^3 IN. LB. 1g	BENDING MOMENT N_o, PER SEC.	SHEAR LB. $\bar{A}$	SHEAR LB. 1g	SHEAR N_o, PER SEC.
300	19.286		3.974	215.197		3.539
480	80.090		3.433	433.981		3.070
620	145.725		3.199	516.733		2.627
720	197.467		3.013	567.065		2.249
890	256.505		2.987	633.170		2.182
1000	200.883		3.185	566.334		2.422
1160	131.005		3.317	441.439		3.081
1320	74.513		3.301	318.402		3.297
1400	51.153		3.287	286.404		3.312
1636	0	0	—	0	0	—

CONDITION 24E
VERTICAL ANALYSIS

CONDITION I
LATERAL ANALYSIS

GW	[illegible],600 LB.	SPEED:		
ALT.	5,000 FT.		V_T	290. KT.
CG	18.6 PERCENT MAC		V_e	269. KT.
			M	.45

FUSELAGE

BODY BALANCE STATION	BENDING MOMENT		SHEAR		TORSION	
	$\bar{A}$, 10^3 IN LB	N_o, PER SEC.	$\bar{A}$, LB.	N_o, PER SEC.	$\bar{A}$, 10^3 IN LB.	N_o, PER SEC.
820	223.8	2.094	315.1	3.106	68.91	.8880
1020	164.2	1.771	318.0	2.746	69.86	.9193
1220	85.62	.7905	366.6	1.725	69.39	.9463
1335	48.19	.8547	381.2	1.375	68.30	.9536

VERTICAL TAIL

ELASTIC AXIS STATION	BENDING MOMENT		SHEAR		TORSION	
	$\bar{A}$, 10^3 IN LB	N_o, PER SEC.	$\bar{A}$, LB.	N_o, PER SEC.	$\bar{A}$, 10^3 IN. LB	N_o, PER SEC.
67.	38.87	1.085	314.7	.7474	5.548	1.920
104	28.50	1.211	266.2	.8272	4.143	2.193
158.	16.90	1.418	191.7	1.004	2.497	2.904
203	9.710	1.663	144.0	1.142	1.448	3.459
248.	4.669	1.974	98.96	1.335	.6323	3.896
284.	2.080	2.228	58.53	1.477	1.179	4.937
WL 239.	6.843	.8483	421.8	.6896	20.29	1.205

CONDITION I
LATERAL ANALYSIS

CONDITION 2
LATERAL ANALYSIS

GW	178,800. LB.	SPEED:		
ALT.	15,000 FT.		V_T	370. KT.
CG	17.0 PERCENT MAC		V_e	295. KT.
			M	.59

FUSELAGE

BODY BALANCE STATION	BENDING MOMENT		SHEAR		TORSION	
	$\bar{A}$, 10^3 IN. LB.	N_0, PER SEC.	$\bar{A}$, LB.	N_0, PER SEC.	$\bar{A}$, 10^3 IN LB.	N_0, PER SEC.
820.	223.9	1.975	280.2	2.559	74.07	1.026
1020	167.7	1.803	301.5	2.428	72.95	1.007
1220.	86.00	.9280	365.3	1.592	70.35	.9778
1335.	48.51	1.031	382.7	1.297	69.17	.9761

VERTICAL TAIL

ELASTIC AXIS STATION	BENDING MOMENT		SHEAR		TORSION	
	$\bar{A}$, 10^3 IN LB.	N_0, PER SEC.	$\bar{A}$, LB.	N_0, PER SEC.	$\bar{A}$, 10^3 IN. LB.	N_0, PER SEC.
67.	39.27	1.078	318.7	.7899	5.726	2.277
104.	28.78	1.189	269.3	.8455	4.288	2.576
158.	17.05	1.384	193.5	.9832	2.614	3.344
203.	9.781	1.623	145.1	1.080	1.513	3.860
248.	4.687	1.917	99.42	1.260	.6532	4.259
284.	2.174	2.491	58.68	1.369	1.331	5.520
WL239.	69.23	.8567	427.8	.7524	20.49	1.228

CONDITION 2
LATERAL ANALYSIS

CONDITION 3
LATERAL ANALYSIS

GW	178,800. LB.	SPEED:	
ALT.	25,000. FT.	V_T	432. KT.
CG	17.0 PERCENT MAC	V_E	290. KT.
		M	.72

FUSELAGE

BODY BALANCE STATION	BENDING MOMENT		SHEAR		TORSION	
	$\bar{A}$, 10^3 IN. LB.	N_0, PER SEC.	$\bar{A}$, LB.	N_0, PER SEC.	$\bar{A}$, 10^3 IN. LB.	N_0, PER SEC.
820.	205.8	2.055	251.4	2.700	69.40	1.237
1020.	154.9	1.858	279.4	2.583	68.61	1.229
1220	77.92	.9959	337.2	1.666	66.20	1.194
1335.	44.08	1.127	353.5	1.341	65.15	1.197

VERTICAL TAIL

ELASTIC AXIS STATION	BENDING MOMENT		SHEAR		TORSION	
	$\bar{A}$, 10^3 IN. LB.	N_0, PER SEC.	$\bar{A}$, LB.	N_0, PER SEC.	$\bar{A}$, 10^3 IN. LB.	N_0, PER SEC.
67.	37.32	1.361	298.6	.9054	5.546	2.398
104.	27.53	1.520	253.2	.9988	4.201	2.731
158	16.51	1.786	183.2	1.214	2.661	3.506
203.	9.633	2.094	138.2	1.355	1.612	3.992
248.	4.720	2.447	95.71	1.611	.7113	4.310
284.	2.301	3.066	56.79	1.736	1.455	5.357
WL239.	65.14	1.016	400.3	.8281	19.50	1.530

CONDITION 3
LATERAL ANALYSIS

CONDITION 4
LATERAL ANALYSIS

GW	166,000 LB.		SPEED:	
ALT.	15,000 FT.		V_T	370 KT.
CG	18.1 PERCENT MAC		V_E	295 KT.
			M	

FUSELAGE

BODY BALANCE STATION	BENDING MOMENT		SHEAR		TORSION	
	$\bar{A}$, 10^3 IN. LB.	N_0, PER SEC.	$\bar{A}$, LB.	N_0, PER SEC.	$\bar{A}$, IN. LB.	N_0, PER SEC.
820	217.5	1.944	265.2	2.513	72.64	1.071
1020	163.7	1.775	291.2	2.410	71.57	1.060
1220	83.00	.9516	357.4	1.576	68.96	1.032
1335	46.83	1.060	375.0	1.284	67.82	1.031

VERTICAL TAIL

ELASTIC AXIS STATION	BENDING MOMENT		SHEAR		TORSION	
	$\bar{A}$, 10^3 IN. LB.	N_0, PER SEC.	$\bar{A}$, LB.	N_0, PER SEC.	$\bar{A}$, 10^3 IN. LB.	N_0, PER SEC.
67	38.43	1.052	312.4	.8125	5.679	2.201
104	28.17	1.296	263.8	.8805	4.272	2.521
158	16.72	1.521	189.3	1.047	2.637	3.351
203	9.632	1.794	141.6	1.167	1.584	4.161
248	4.646	2.117	97.13	1.376	.6730	4.112
284	2.197	2.714	57.21	1.490	1.365	5.102
WL 239	67.80	.8962	420.3	.7613	20.08	1.332

CONDITION 4
LATERAL ANALYSIS

CONDITION 5
LATERAL ANALYSIS

GW	191,800 LB.	SPEED:		
ALT.	15,000 FT.		V_T	370 KT.
CG	19.6 PERCENT MAC		V_e	295. KT.
			M	.59

FUSELAGE

BODY BALANCE STATION	BENDING MOMENT		SHEAR		TORSION	
	$\bar{A}$, 10^3 IN LB	N_o, PER SEC	$\bar{A}$, LB	N_o, PER SEC.	$\bar{A}$, 10^3 IN LB	N_o, PER SEC.
820	246.2	1.825	325.3	2.267	78.60	1.084
1020	181.8	1.669	343.1	2.240	77.26	1.077
1220	92.76	.8342	397.3	1.498	74.47	1.047
1335	52.36	.9623	411.7	1.223	73.19	1.049

VERTICAL TAIL

ELASTIC AXIS STATION	BENDING MOMENT		SHEAR		TORSION	
	$\bar{A}$, 10^3 IN LB	N_o, PER SEC.	$\bar{A}$, LB	N_o, PER SEC	$\bar{A}$, 10^3 IN LB	N_o, PER SEC
67	41.93	.206	335.8	.7961	5.973	2.151
104	30.41	1.354	283.5	.8767	4.505	2.481
158	18.09	1.603	203.6	1.071	2.796	3.318
203	10.46	1.896	152.4	1.207	1.698	4.107
248	5.070	2.238	104.8	1.446	.7296	4.097
284	2.426	2.849	61.74	1.563	1.443	5.001
WL239	72.82	.8948	450.8	.7274	21.74	1.356

CONDITION 5
LATERAL ANALYSIS

CONDITION 6

LATERAL ANALYSIS

CONDITION 6
LATERAL ANALYSIS

GW	211,600 LB.	SPEED:		
ALT.	15,000 FT.		V_T	370 KT.
CG	20.6 PERCENT MAC		V_E	295 KT.
			M	.59

FUSELAGE

BODY BALANCE STATION	BENDING MOMENT		SHEAR		TORSION	
	$\bar{A}$, 10^3 IN. LB.	N_o, PER SEC.	$\bar{A}$, LB.	N_o, PER SEC.	$\bar{A}$, IN. LB.	N_o, PER SEC.
820	260.8	1.696	352.3	2.122	81.51	1.047
1020	190.8	1.544	365.9	2.098	80.00	1.042
1220	98.49	.7764	415.8	1.390	77.15	1.013
1335	55.52	.8851	428.9	1.129	75.79	1.016

VERTICAL TAIL

ELASTIC AXIS STATION	BENDING MOMENT		SHEAR		TORSION	
	$\bar{A}$, 10^3 IN. LB.	N_o, PER SEC.	$\bar{A}$, LB.	N_o, PER SEC.	$\bar{A}$, 10^3 IN. LB.	N_o, PER SEC.
67	42.88	1.185	347.8	.7717	6.076	2.104
104	31.47	1.334	293.4	.8555	4.584	2.442
158	18.71	1.585	210.8	1.050	2.833	3.292
203	10.81	1.877	157.7	1.190	1.722	4.091
248	5.238	2.220	108.4	1.430	.7477	4.104
284	2.502	2.931	63.86	1.547	1.422	5.046
WL 239	75.36	.8374	466.6	.7043	22.56	.352

CONDITION 7
LATERAL ANALYSIS

CONDITION 7
LATERAL ANALYSIS

GW	163,800. LB.	SPEED:		
ALT.	30,000. FT.		V_T	480. KT.
CG	16.4 PERCENT MAC		V_e	294. KT.
			M	.82

FUSELAGE

BODY BALANCE STATION	BENDING MOMENT		SHEAR		TORSION	
	$\bar{A}$, 10^3 IN. LB.	N_o, PER SEC.	$\bar{A}$, LB.	N_o, PER SEC.	$\bar{A}$, 10^3 IN. LB.	N_o, PER SEC.
820.	213.4	2.023	232.8	2.655	72.04	1.353
1020.	161.0	1.835	287.2	2.579	71.25	1.350
1220.	81.36	1.076	349.6	1.662	68.74	1.313
1335.	45.99	1.199	366.3	1.340	67.67	1.317

VERTICAL TAIL

ELASTIC AXIS STATION	BENDING MOMENT		SHEAR		TORSION	
	$\bar{A}$, 10^3 IN LB	N_o, PER SEC.	$\bar{A}$, LB	N_o, PER SEC.	$\bar{A}$, 10^3 IN LB	N_o, PER SEC.
67	38.90	1.305	308.6	.9648	5.774	2.506
104.	28.79	1.694	262.0	1.083	4.408	2.858
158.	17.38	1.993	190.2	1.341	2.856	3.642
203.	10.24	2.327	143.7	1.504	1.779	4.097
248.	5.080	2.698	100.1	1.795	.7956	4.372
284.	2.546	3.304	59.41	1.932	1.613	5.371
WL239.	67.46	1.103	413.6	.8658	20.39	1.685

CONDITION 8
LATERAL ANALYSIS

CONDITION 8
LATERAL ANALYSIS

GW 163,800 LB.
ALT. 35,000 FT.
CG 16.4 PERCENT MAC

SPEED:
V_T 475 KT.
V_E 263 KT.
M .82

FUSELAGE

BODY BALANCE STATION	BENDING MOMENT $\bar{A}$, 10^3 IN. LB.	BENDING MOMENT N_0, PER SEC.	SHEAR $\bar{A}$, LB.	SHEAR N_0, PER SEC.	TORSION $\bar{A}$, IN. LB.	TORSION N_0, PER SEC.
820	192.2	2.000	226.8	2.594	62.75	1.408
1020	145.4	1.819	258.4	2.520	63.15	1.336
1220	73.76	1.000	317.1	1.643	62.22	1.246
1335	41.75	1.130	332.8	1.328	61.30	1.243

VERTICAL TAIL

ELASTIC AXIS STATION	BENDING MOMENT $\bar{A}$, 10^3 IN. LB.	BENDING MOMENT N_0, PER SEC.	SHEAR $\bar{A}$, LB.	SHEAR N_0, PER SEC.	TORSION $\bar{A}$, 10^3 IN. LB.	TORSION N_0, PER SEC.
67	35.32	1.415	280.8	.9081	5.196	2.267
104	26.10	1.585	238.5	1.016	3.952	2.589
158	15.71	1.861	173.2	1.264	2.534	3.342
203	9.219	2.187	130.9	1.418	1.559	3.824
248	4.553	2.551	91.03	1.694	.6925	4.122
284	2.193	3.070	54.07	1.821	1.396	5.048
WL 239	61.34	1.037	357.9	.7997	18.56	1.621

CONDITION 9

LATERAL ANALYSIS

CONDITION 9
LATERAL ANALYSIS

GW	163,800	LB.	SPEED:		
ALT.	40,000	FT.	V_T	475	KT.
CG	16.4	PERCENT MAC	V_E	234	KT.
			M	.82	

FUSELAGE

BODY BALANCE STATION	BENDING MOMENT $\bar{A}$, 10^3 IN. LB.	BENDING MOMENT N_o, PER SEC.	SHEAR $\bar{A}$, LB.	SHEAR N_o, PER SEC.	TORSION $\bar{A}$, IN. LB.	TORSION N_o, PER SEC.
820	171.4	1.964	201.4	2.516	55.64	1.320
1020	129.8	1.794	229.3	2.443	56.07	1.256
1220	66.03	.9350	283.0	1.617	55.36	1.178
1335	37.39	1.073	297.5	1.312	54.54	1.175

VERTICAL TAIL

ELASTIC AXIS STATION	BENDING MOMENT $\bar{A}$, 10^3 IN. LB.	BENDING MOMENT N_o, PER SEC.	SHEAR $\bar{A}$, LB.	SHEAR N_o, PER SEC.	TORSION $\bar{A}$, 10^3 IN. LB.	TORSION N_o, PER SEC.
67	31.44	1.344	250.8	.8528	4.552	1.817
104	23.21	1.507	212.7	.9595	3.435	2.082
158	13.94	1.773	154.2	1.191	2.154	2.748
203	8.139	2.076	116.5	1.340	1.300	3.297
248	3.994	2.418	80.80	1.604	.5669	3.627
284	1.944	3.011	48.01	1.720	1.115	4.078
WL239	54.73	.9770	335.8	.7404	16.50	1.536

CONDITION 10
LATERAL ANALYSIS

GW 204,000 LB.
ALT. 35,000 FT.
CG 21.5 PERCENT MAC

SPEED:
V_T 475 KT.
V_E 263 KT.
M .82

FUSELAGE

BODY BALANCE STATION	BENDING MOMENT $\bar{A}$, 10^3 IN. LB.	BENDING MOMENT N_0, PER SEC.	SHEAR $\bar{A}$, LB.	SHEAR N_0, PER SEC.	TORSION $\bar{A}$, IN. LB.	TORSION N_0, PER SEC.
820	236.3	1.738	315.6	2.161	73.49	1.141
1020	172.9	1.587	333.3	2.132	72.30	1.139
1220	88.58	.8572	374.9	1.439	69.82	1.102
1335	50.13	.9764	385.5	1.170	68.62	1.105

VERTICAL TAIL

ELASTIC AXIS STATION	BENDING MOMENT $\bar{A}$, 10^3 IN. LB.	BENDING MOMENT N_0, PER SEC.	SHEAR $\bar{A}$, LB.	SHEAR N_0, PER SEC.	TORSION $\bar{A}$, 10^3 IN. LB.	TORSION N_0, PER SEC.
67	39.18	1.288	313.3	.8143	5.522	2.139
104	28.94	1.440	265.4	.9121	4.183	2.460
158	17.33	1.702	192.3	1.136	2.644	3.223
203	10.11	2.003	144.8	1.276	1.611	3.726
248	4.946	2.947	100.3	1.533	.7128	4.036
284	2.405	2.950	59.42	1.651	1.415	5.000
WL239	68.25	.9299	418.2	.7193	20.72	1.464

CONDITION 11
LATERAL ANALYSIS

GW	183,000 LB.	SPEED:		
ALT.	35,000 FT.	V_T	475	KT.
CG	19.4 PERCENT MAC	V_e	263	KT.
		M	.82	

FUSELAGE

BODY BALANCE STATION	BENDING MOMENT		SHEAR		TORSION	
	$\bar{A}$, 10^3 IN. LB.	N_o, PER SEC.	$\bar{A}$, LB.	N_o, PER SEC.	$\bar{A}$, IN. LB.	N_o, PER SEC.
820	213.7	1.836	271.2	2.353	66.25	1.361
1020	158.2	1.665	294.5	2.296	66.76	1.288
1220	81.17	.9145	344.5	1.509	65.99	1.194
1335	45.94	1.036	357.8	1.219	64.95	1.193

VERTICAL TAIL

ELASTIC AXIS STATION	BENDING MOMENT		SHEAR		TORSION	
	$\bar{A}$, 10^3 IN. LB.	N_o, PER SEC.	$\bar{A}$, LB.	N_o, PER SEC.	$\bar{A}$, 10^3 IN. LB.	N_o, PER SEC.
67	37.36	1.378	296.8	.8663	5.342	2.216
104	27.61	1.548	251.9	.9754	4.060	2.548
158	16.61	1.827	182.9	1.220	2.594	3.316
203	9.726	2.143	138.0	1.374	1.598	3.812
248	4.789	2.496	95.95	1.648	.7121	4.111
284	2.358	3.099	56.98	1.772	1.403	5.060
WL 239	64.78	.9956	39.64	.7607	19.69	1.571

CONDITION 11
LATERAL ANALYSIS

CONDITION 12
LATERAL ANALYSIS

GW	159,000. LB.	SPEED:	
ALT.	10,000. FT.	V_T	310. KT.
CG	17.0 PERCENT MAC	V_E	264. KT.
		M	.48

FUSELAGE

BODY BALANCE STATION	BENDING MOMENT $\bar{A}$, 10^3 IN LB	BENDING MOMENT N_0, PER SEC	SHEAR $\bar{A}$, LB	SHEAR N_0, PER SEC.	TORSION $\bar{A}$, 10^3 IN LB	TORSION N_0, PER SEC.
820	189.8	2.036	225.0	2.473	63.92	1.051
1020.	143.5	1.869	253.9	2.439	63.09	1.029
1220	71.84	.9623	313.7	1.677	60.88	1.001
1335	40.66	1.050	329.3	1.369	59.89	.9963

VERTICAL TAIL

ELASTIC AXIS STATION	BENDING MOMENT $\bar{A}$, 10^3 IN LB	BENDING MOMENT N_0, PER SEC.	SHEAR $\bar{A}$, LB.	SHEAR N_0, PER SEC.	TORSION $\bar{A}$, 10^3 IN LB	TORSION N_0, PER SEC.
67	34.14	1.110	276.0	.7932	5.084	2.176
104	25.05	1.226	233.6	.8455	38.21	2.465
158	14.87	1.422	168.3	.9937	2.360	3.179
203	8.555	1.665	126.3	1.085	1.384	3.679
248	4.112	1.958	86.72	1.274	.6036	4.061
284.	1.920	2.524	51.24	1.368	1.228	5.005
WL 239.	60.04	.8586	370.0	.7340	17.83	1.310

CONDITION 13
LATERAL ANALYSIS

CONDITION 13
LATERAL ANALYSIS

GW 159,000 LB.
ALT. 20,000 FT.
CG 17.0 PERCENT MAC

SPEED:
V_T 380 KT.
V_E 277 KT.
M .62

FUSELAGE

BODY BALANCE STATION	BENDING MOMENT		SHEAR		TORSION	
	$\bar{A}$, 10^3 IN. LB.	N_o, PER SEC.	$\bar{A}$, LB.	N_o, PER SEC.	$\bar{A}$, 10^3 IN. LB.	N_o, PER SEC.
820.	198.9	1.949	232.7	2.518	68.46	1.110
1020.	151.2	1.778	263.0	2.439	67.60	1.094
1220.	76.89	.9383	331.3	1.582	65.22	1.063
1335.	43.49	1.052	349.7	1.285	64.17	1.063

VERTICAL TAIL

ELASTIC AXIS STATION	BENDING MOMENT		SHEAR		TORSION	
	$\bar{A}$, 10^3 IN. LB.	N_o, PER SEC.	$\bar{A}$, LB.	N_o, PER SEC.	$\bar{A}$, 10^3 IN. LB.	N_o, PER SEC.
67.	36.61	1.210	295.3	.8234	5.386	2.203
104	26.92	1.349	249.9	.8991	4.058	2.511
158.	16.04	1.586	180.2	1.383	2.524	3.261
203.	9.279	1.867	135.5	1.205	1.500	3.771
248.	4.496	2.200	93.31	1.431	.6584	4.130
284.	2.141	2.808	55.17	1.549	1.317	5.200
WL234.	64.25	.9013	396.1	.7567	19.14	1.338

CONDITION I YD

LATERAL ANALYSIS

CONDITION I YAW DAMPER

LATERAL ANALYSIS

GW 181,600. LB.
ALT. 5,000. FT.
CG 18.6 PERCENT MAC

SPEED:
V_T 290. KT.
V_e 269. KT.
M .45

FUSELAGE

BODY BALANCE STATION	BENDING MOMENT		SHEAR		TORSION	
	$\bar{A}$, 10^3 IN.LB.	N_0, PER SEC.	$\bar{A}$, LB.	N_0, PER SEC.	$\bar{A}$, 10^3 IN.LB.	N_0, PER SEC.
820	174.3	2.737	280.6	3.689	45.13	1.407
1020	122.4	2.377	272.7	3.306	45.92	1.470
1220	55.23	1.259	271.1	2.344	45.82	1.515
1335	31.21	1.353	268.0	1.951	45.14	1.527

VERTICAL TAIL

ELASTIC AXIS STATION	BENDING MOMENT		SHEAR		TORSION	
	$\bar{A}$, 10^3 IN. LB.	N_0, PER SEC.	$\bar{A}$, LB.	N_0, PER SEC.	$\bar{A}$, 10^3 IN. LB.	N_0, PER SEC.
67	25.84	1.737	203.8	1.208	3.751	2.866
104	19.22	1.923	173.6	1.344	2.863	3.226
158	11.68	2.215	127.3	1.620	1.857	4.003
203	6.932	2.527	96.80	1.836	1.172	4.447
248	3.486	2.877	68.07	2.140	.5484	4.719
284	1.620	3.115	40.60	2.313	1.079	5.424
WL239	44.63	1.380	269.9	1.120	13.81	1.879

CONDITION 2YD

LATERAL ANALYSIS

CONDITION 2 YAW DAMPER
LATERAL ANALYSIS

GW	178,800. LB.	SPEED:		
ALT.	15,000. FT.		V_T	370. KT.
CG	17. PERCENT MAC		V_e	295. KT.
			M	.59

FUSELAGE

BODY BALANCE STATION	BENDING MOMENT $\bar{A}$, 10^3 IN. LB.	BENDING MOMENT N_o, PER SEC.	SHEAR $\bar{A}$, LB	SHEAR N_o, PER SEC.	TORSION $\bar{A}$, 10^3 IN. LB.	TORSION N_o, PER SEC.
820.	169.8	2.498	226.8	3.064	47.83	1.611
1020.	124.0	2.335	244.0	2.894	47.02	1.589
1220.	54.72	1.483	260.7	2.137	45.25	1.549
1335.	31.38	1.603	260.7	1.830	44.46	1.549

VERTICAL TAIL

ELASTIC AXIS STATION	BENDING MOMENT $\bar{A}$, 10^3 IN. LB.	BENDING MOMENT N_o, PER SEC.	SHEAR $\bar{A}$, LB.	SHEAR N_o, PER SEC.	TORSION $\bar{A}$, 10^3 IN. LB.	TORSION N_o, PER SEC.
67.	25.12	1.711	200.7	1.288	3.840	3.424
104.	18.63	1.898	170.6	1.372	2.942	3.791
158.	11.28	2.130	124.4	1.567	1.930	4.574
203.	6.663	2.429	93.95	1.712	1.197	4.943
248.	3.318	2.763	65.46	1.962	.5446	5.179
284.	1.671	3.311	38.68	2.124	1.218	6.053
WL 239.	43.80	1.391	265.9	1.244	13.57	1.885

CONDITION 3 YAW DAMPER
LATERAL ANALYSIS

GW 178,800. LB.
ALT. 25,000. FT.
CG 17. PERCENT MAC

SPEED:
V_T 432. KT.
V_e 290. KT.
M .72

FUSELAGE

BODY BALANCE STATION	BENDING MOMENT		SHEAR		TORSION	
	$\bar{A}$, 10^3 IN. LB.	N_0, PER SEC.	$\bar{A}$, LB.	N_0, PER SEC.	$\bar{A}$, 10^3 IN. LB.	N_0, PER SEC.
820.	156.9	2.513	208.6	3.080	44.14	1.946
1020.	114.2	2.339	231.0	2.947	43.52	1.944
1220.	48.42	1.622	238.8	2.191	41.85	1.898
1335.	28.01	1.768	235.8	1.874	41.17	1.905

VERTICAL TAIL

ELASTIC AXIS STATION	BENDING MOMENT		SHEAR		TORSION	
	$\bar{A}$, 10^3 IN. LB.	N_0, PER SEC.	$\bar{A}$, LB.	N_0, PER SEC.	$\bar{A}$, 10^3 IN. LB.	N_0, PER SEC.
67.	23.41	2.178	181.9	1.500	3.648	1.670
104.	17.66	2.384	156.0	1.640	2.865	3.636
158.	11.00	1.973	116.0	1.940	2.005	4.001
203.	6.724	3.027	88.75	2.137	1.322	4.656
248.	3.479	3.353	63.33	2.463	.6150	4.882
284.	1.873	3.805	37.72	2.643	1.332	5.010
WL239.	40.05	1.670	238.6	1.404	1.292	2.302

CONDITION 3 YD
LATERAL ANALYSIS

CONDITION 4 YD

LATERAL ANALYSIS

CONDITION 4 YAW DAMPER
LATERAL ANALYSIS

GW 166,600 LB.
ALT. 15,000 FT.
CG 18.1 PERCENT MAC

SPEED:
V_T 370 KT.
V_E 290 KT.
M .59

FUSELAGE

BODY BALANCE STATION	BENDING MOMENT		SHEAR		TORSION	
	$\bar{A}$, 10^3 IN. LB.	N_0, PER SEC.	$\bar{A}$, LB.	N_0, PER SEC.	$\bar{A}$, 10^3 IN. LB.	N_0, PER SEC.
820	166.4	2.417	216.6	2.963	47.55	1.653
1020	122.2	2.258	238.0	2.825	46.77	1.633
1220	53.38	1.497	257.4	2.080	44.97	1.595
1335	30.66	1.618	257.9	1.779	44.20	1.597

VERTICAL TAIL

ELASTIC AXIS STATION	BENDING MOMENT		SHEAR		TORSION	
	$\bar{A}$, 10^3 IN. LB.	N_0, PER SEC.	$\bar{A}$, LB.	N_0, PER SEC.	$\bar{A}$, 10^3 IN. LB.	N_0, PER SEC.
67	25.08	1.794	198.9	1.297	3.852	3.243
104	18.65	1.970	169.1	1.397	2.973	3.624
158	11.37	2.257	123.6	1.627	1.991	4.442
203	6.775	2.573	93.40	1.796	1.296	5.099
248	3.414	2.909	65.42	2.077	.5730	4.852
284	1.758	3.427	38.73	2.229	1.252	5.537
WL239	43.43	1.421	263.9	1.235	13.57	1.983

CONDITION 5 YD
LATERAL ANALYSIS

CONDITION 5 YAW DAMPER
LATERAL ANALYSIS

GW 191,800 LB.
ALT. 15,000 FT.
CG 19.6 PERCENT MAC

SPEED:
V_T 370 KT.
V_e 295 KT.
M .59

FUSELAGE

BODY BALANCE STATION	BENDING MOMENT $\bar{A}$, 10^3 IN. LB.	BENDING MOMENT N_o, PER SEC.	SHEAR $\bar{A}$, LB.	SHEAR N_o, PER SEC.	TORSION $\bar{A}$, 10^3 IN. LB.	TORSION N_o, PER SEC.
820	179.8	2.327	253.6	2.824	49.37	1.754
1020	129.3	2.159	268.5	2.736	48.46	1.762
1220	56.32	1.351	273.5	2.020	46.58	1.721
1335	32.36	1.478	269.8	1.720	45.77	1.729

VERTICAL TAIL

ELASTIC AXIS STATION	BENDING MOMENT $\bar{A}$, 10^3 IN. LB.	BENDING MOMENT N_o, PER SEC.	SHEAR $\bar{A}$, LB.	SHEAR N_o, PER SEC.	TORSION $\bar{A}$, 10^3 IN. LB.	TORSION N_o, PER SEC.
67	26.29	1.985	203.7	1.347	3.882	3.279
104	19.69	2.195	173.6	1.487	3.030	3.681
158	12.14	2.523	127.8	1.792	2.082	4.478
203	7.348	2.860	97.16	2.006	1.397	5.055
248	3.766	3.198	68.91	2.337	.6354	4.832
284	1.994	3.681	41.09	2.501	1.310	5.460
WL 239	44.61	1.521	269.3	1.242	14.18	2.158

CONDITION 6 YD

LATERAL ANALYSIS

CONDITION 6 YAW DAMPER
LATERAL ANALYSIS

GW	211,600 LB.		SPEED:	
ALT.	15,000 FT.		V_T	370 KT.
CG	20.6 PERCENT MAC		V_E	295 KT.
			M	.59

FUSELAGE

BODY BALANCE STATION	BENDING MOMENT		SHEAR		TORSION	
	$\bar{A}$, 10^3 IN.LB.	N_0, PER SEC.	$\bar{A}$, LB.	N_0, PER SEC.	$\bar{A}$, 10^3 IN.LB.	N_0, PER SEC.
820	188.0	2.258	270.1	2.656	49.89	1.703
1020	133.9	2.087	282.2	2.605	48.87	1.700
1220	58.57	1.306	281.7	1.951	46.99	1.660
1335	33.69	1.441	276.3	1.669	46.15	1.667

VERTICAL TAIL

ELASTIC AXIS STATION	BENDING MOMENT		SHEAR		TORSION	
	$\bar{A}$, 10^3 IN.LB.	N_0, PER SEC.	$\bar{A}$, LB.	N_0, PER SEC.	$\bar{A}$, 10^3 IN.LB.	N_0, PER SEC.
67	26.51	1.909	205.5	1.313	3.882	3.277
104	19.81	2.111	174.8	1.444	3.026	3.676
158	12.17	2.430	128.4	1.732	2.073	4.476
203	7.330	2.763	97.38	1.936	1.388	5.057
248	3.740	3.102	68.86	2.256	.6331	4.832
284	1.965	3.597	41.01	2.414	1.306	5.445
WL 239	44.96	1.475	271.8	1.217	14.34	2.123

CONDITION 7 YAW DAMPER
LATERAL ANALYSIS

GW	163,800. LB.	SPEED:		
ALT.	30,000. FT.		V_T	480. KT.
CG	16.4 PERCENT MAC		V_e	294. KT.
			M	.82

FUSELAGE

BODY BALANCE STATION	BENDING MOMENT $\bar{A}$, 10^3 IN. LB.	BENDING MOMENT N_o, PER SEC.	SHEAR $\bar{A}$, LB.	SHEAR N_o, PER SEC.	TORSION $\bar{A}$, 10^3 IN. LB.	TORSION N_o, PER SEC.
820.	157.1	2.527	201.9	3.126	45.12	2.141
1020	114.9	2.351	229.7	3.020	44.54	2.146
1220	48.86	1.798	240.1	2.225	42.79	2.100
1335	28.26	1.931	237.0	1.903	42.11	2.109

VERTICAL TAIL

ELASTIC AXIS STATION	BENDING MOMENT $\bar{A}$, 10^3 IN. LB.	BENDING MOMENT N_o, PER SEC.	SHEAR $\bar{A}$, LB.	SHEAR N_o, PER SEC.	TORSION $\bar{A}$, 10^3 IN. LB.	TORSION N_o, PER SEC.
67	24.33	2.405	183.1	1.635	3.766	3.811
104	18.51	2.624	157.8	1.809	3.006	4.164
158	11.71	2.949	118.7	2.152	2.179	4.746
203	7.280	3.265	91.47	2.367	1.483	4.893
248	3.834	3.566	66.28	2.713	.6968	4.975
284	2.120	3.959	39.72	2.892	1.477	5.812
WL239	40.62	1.863	239.4	1.503	1.343	2.546

CONDITION 8 YD
LATERAL ANALYSIS

CONDITION 8 YAW DAMPER
LATERAL ANALYSIS

GW 163,800 LB.
ALT. 35,000. FT.
CG 16.4 PERCENT MAC

SPEED:
V_T 475 KT.
V_E 263 KT.
M .82

FUSELAGE

BODY BALANCE STATION	BENDING MOMENT $\bar{A}$, 10^3 IN.LB.	BENDING MOMENT N_0, PER SEC.	SHEAR $\bar{A}$, LB.	SHEAR N_0, PER SEC.	TORSION $\bar{A}$, 10^3 IN.LB.	TORSION N_0, PER SEC.
820.	142.3	2.487	184.0	3.003	38.89	2.281
1020	103.8	2.335	209.5	2.909	38.66	2.185
1220	43.96	1.689	216.7	2.212	37.66	2.053
1335	25.51	1.832	212.7	1.910	37.08	2.048

VERTICAL TAIL

ELASTIC AXIS STATION	BENDING MOMENT $\bar{A}$, 10^3 IN. LB.	BENDING MOMENT N_0, PER SEC.	SHEAR $\bar{A}$, LB.	SHEAR N_0, PER SEC.	TORSION $\bar{A}$, 10^3 IN. LB.	TORSION N_0, PER SEC.
67	21.03	2.365	162.0	1.575	3.241	3.595
104	15.99	2.577	139.7	1.740	2.580	3.941
158	10.09	2.893	105.2	2.083	1.863	4.520
203	6.265	3.213	81.04	2.296	1.264	4.702
248	3.296	3.521	58.55	2.640	.5934	4.799
284	1.742	3.864	34.95	2.824	1.261	5.532
W.L.239	35.85	1.777	210.2	1.437	1.201	2.491

CONDITION 9 YD
LATERAL ANALYSIS

CONDITION 9 YAW DAMPER
LATERAL ANALYSIS

GW 163,800 LB.
ALT. 40,000 FT.
CG 16.4 PERCENT MAC

SPEED:
V_T 475 KT.
V_E 234 KT.
M .82

FUSELAGE

BODY BALANCE STATION	BENDING MOMENT $\bar{A}$, 10^3 IN. LB.	BENDING MOMENT N_0, PER SEC.	SHEAR $\bar{A}$, LB.	SHEAR N_0, PER SEC.	TORSION $\bar{A}$, 10^3 IN. LB.	TORSION N_0, PER SEC.
820	129.9	2.383	170.7	2.781	34.26	2.147
1020	94.13	2.263	192.2	2.720	33.98	2.068
1220	40.35	1.537	195.9	2.146	33.15	1.953
1335	23.44	1.687	191.3	1.872	32.62	1.950

VERTICAL TAIL

ELASTIC AXIS STATION	BENDING MOMENT $\bar{A}$, 10^3 IN. LB.	BENDING MOMENT N_0, PER SEC.	SHEAR $\bar{A}$, LB.	SHEAR N_0, PER SEC.	TORSION $\bar{A}$, 10^3 IN. LB.	TORSION N_0, PER SEC.
67	18.00	2.329	143.2	1.487	2.679	3.051
104	13.68	2.541	123.4	1.644	2.108	3.359
158	8.615	2.855	92.83	1.976	1.489	3.940
203	5.320	3.165	71.24	2.191	1.002	4.255
248	2.781	3.463	51.15	2.534	.4654	4.401
284	1.507	3.875	30.36	2.721	.9732	4.581
WL 239	31.57	1.691	184.6	1.348	1.062	2.365

CONDITION 10 YAW DAMPER
LATERAL ANALYSIS

GW 204,000 LB.
ALT. 35,000 FT.
CG 21.5 PERCENT MAC

SPEED:
V_T 475 KT.
V_e 263 KT.
M .82

FUSELAGE

BODY BALANCE STATION	BENDING MOMENT $\bar{A}$, 10^3 IN. LB.	BENDING MOMENT N_o, PER SEC.	SHEAR $\bar{A}$, LB.	SHEAR N_o, PER SEC.	TORSION $\bar{A}$, 10^3 IN. LB.	TORSION N_o, PER SEC.
820	163.2	2.319	236.2	2.700	41.07	2.008
1020	115.2	2.186	250.5	2.643	40.24	2.009
1220	47.74	1.566	238.9	2.078	38.66	1.964
1335	27.83	1.710	228.9	1.770	37.98	1.974

VERTICAL TAIL

ELASTIC AXIS STATION	BENDING MOMENT $\bar{A}$, 10^3 IN. LB.	BENDING MOMENT N_o, PER SEC.	SHEAR $\bar{A}$, LB.	SHEAR N_o, PER SEC.	TORSION $\bar{A}$, 10^3 IN. LB.	TORSION N_o, PER SEC.
67	21.71	2.293	164.8	1.534	3.227	3.622
104	16.48	2.505	141.7	1.698	2.572	3967
158	10.37	2.824	106.6	2.038	1.864	4.535
203	6.413	3.136	81.83	2.249	1.267	4.708
248	3.356	3.438	59.11	2.590	.5962	4.798
284	1.837	3.840	35.32	2.765	1.285	5.446
WL239	36.41	1.732	213.9	1.398	12.28	2.443

CONDITION 10YD
LATERAL ANALYSIS

CONDITION 11 YAW DAMPER
LATERAL ANALYSIS

GW	183,000 LB.	SPEED:	
ALT.	35,000 FT.	V_T	475. KT.
CG	19.4 PERCENT MAC	V_e	263. KT.
		M	.82

FUSELAGE

BODY BALANCE STATION	BENDING MOMENT		SHEAR		TORSION	
	$\bar{A}$, 10^3 IN. LB	N_0, PER SEC.	$\bar{A}$, LB.	N_0, PER SEC.	$\bar{A}$, 10^3 IN LB.	N_0, PER SEC.
820	151.8	2.386	210.8	2.850	39.23	2.288
1020	108.6	2.235	229.2	2.767	39.12	2.189
1220	45.81	1.613	226.3	2.124	38.19	2.048
1335	26.64	1.753	219.5	1.837	37.57	2.045

VERTICAL TAIL

ELASTIC AXIS STATION	BENDING MOMENT		SHEAR		TORSION	
	$\bar{A}$, 10^3 IN. LB.	N_0, PER SEC.	$\bar{A}$, LB.	N_0, PER SEC.	$\bar{A}$, 10^3 IN. LB	N_0, PER SEC.
67	21.52	2.368	163.3	1.568	3.222	3.634
104	16.38	2.585	140.7	1.740	2.575	3.981
158	10.36	2.906	106.2	2.093	1.874	4.550
203	6.428	3.218	81.75	2.312	1.281	4.717
248	3.377	3.514	59.23	2.658	.6052	4.803
284	1.860	3.902	35.44	2.836	1.274	5.510
WL239	36.14	1.779	211.7	1.473	1.222	2.509

CONDITION 11 Y. D.
LATERAL ANALYSIS

CONDITION 12. Y.D.
LATERAL ANALYSIS

CONDITION 12 YAW DAMPER
LATERAL ANALYSIS

GW 159,000 LB.
ALT. 10,000. FT.
CG 17.0 PERCENT MAC

SPEED:
V_T 310. KT.
V_E 264. KT.
M .48

FUSELAGE

BODY BALANCE STATION	BENDING MOMENT		SHEAR		TORSION	
	$\bar{A}$, 10^3 IN. LB.	N_0, PER SEC.	$\bar{A}$, LB.	N_0, PER SEC.	$\bar{A}$, 10^3 IN. LB.	N_0, PER SEC.
820.	151.2	2.429	190.3	2.787	44.10	1.513
1020.	111.6	2.283	214.6	2.747	43.43	1.499
1220.	48.72	1.434	237.0	2.112	41.84	1.454
1335	27.98	1.521	238.5	1.804	41.12	1.450

VERTICAL TAIL

ELASTIC AXIS STATION	BENDING MOMENT		SHEAR		TORSION	
	$\bar{A}$, 10^3 IN. LB.	N_0, PER SEC.	$\bar{A}$, LB.	N_0, PER SEC.	$\bar{A}$, 10^3 IN. LB.	N_0, PER SEC.
67.	23.59	1.596	185.8	1.194	3.602	3.048
104.	17.49	1.743	179.1	1.066	2.758	3.390
158.	10.57	1.986	115.3	1.460	1.809	4.111
203.	6.233	2.268	87.11	1.583	1.122	4.498
248.	3.095	2.581	60.74	1.823	.5114	4.753
284.	1.546	3.107	36.03	1.946	1.121	5.419
WL 239.	40.60	1.285	280.5	.9304	14.05	1.617

CONDITION 13 YD
LATERAL ANALYSIS

CONDITION 13 YAW DAMPER
LATERAL ANALYSIS

GW 159,000. LB.
ALT. 20,000. FT.
CG 17.0 PERCENT MAC

SPEED:
V_T 380. KT.
V_e 277. KT.
M .62

FUSELAGE

BODY BALANCE STATION	BENDING MOMENT		SHEAR		TORSION	
	$\bar{A}$, 10^3 IN. LB.	N_o, PER SEC.	$\bar{A}$, LB.	N_o, PER SEC.	$\bar{A}$, 10^3 IN. LB.	N_o, PER SEC.
820	151.3	2.426	190.3	2.950	43.88	1.730
1020	111.8	2.274	215.9	2.836	43.23	1.711
1220	48.62	1.505	235.5	2.108	41.62	1.670
1335	28.04	1.631	236.0	1.808	40.93	1.673

VERTICAL TAIL

ELASTIC AXIS STATION	BENDING MOMENT		SHEAR		TORSION	
	$\bar{A}$, 10^3 IN. LB.	N_o, PER SEC.	$\bar{A}$, LB.	N_o, PER SEC.	$\bar{A}$, 10^3 IN. LB.	N_o, PER SEC.
67	23.21	1.909	183.3	1.342	3.559	3.321
104	17.35	2.094	156.5	1.453	2.762	3.679
158	10.66	2.391	115.4	1.708	1.874	4.380
203	6.403	2.711	87.69	1.880	1.206	4.687
248	3.251	3.049	61.83	2.176	.5587	4.867
284	1.696	3.556	36.68	2.345	1.201	5.663
WL239	40.16	1.477	241.4	1.261	12.76	2.083

CONDITION 1B YAW DAMPER
LATERAL ANALYSIS

GW	214,400	LB.	SPEED:	
ALT.	43,000	FT.	V_T	516. KT.
CG	21.4	PERCENT MAC	V_e	239. KT.
			M	.9

FUSELAGE

BODY BALANCE STATION	BENDING MOMENT		SHEAR		TORSION	
	$\bar{A}$, 10^3 IN.LB.	N_o, PER SEC.	$\bar{A}$, LB.	N_o, PER SEC.	$\bar{A}$, 10^3 IN.LB.	N_o, PER SEC.
820.	163.9	2.371	240.1	2.705	37.87	2.260
1020.	115.1	2.249	252.7	2.659	37.77	2.144
1220.	47.03	1.571	237.7	2.140	37.11	2.040
1335.	27.48	1.728	226.2	1.878	36.49	1.986

VERTICAL TAIL

ELASTIC AXIS STATION	BENDING MOMENT		SHEAR		TORSION	
	$\bar{A}$, 10^3 IN.LB.	N_o, PER SEC.	$\bar{A}$, LB.	N_o, PER SEC.	$\bar{A}$, 10^3 IN.LB.	N_o, PER SEC.
67.	20.88	2.301	158.9	1.510	3.041	3.483
104.	15.82	2.519	136.4	1.679	2.412	3.837
158.	9.914	2.846	102.5	2.034	1.738	4.436
203.	6.104	3.173	78.53	2.250	1.173	4.664
248.	3.179	3.490	56.61	2.602	.5446	4.788
284.	1.727	3.920	33.82	2.775	1.212	5.293
WL239.	35.05	1.714	205.9	1.347	11.83	2.454

CONDITION 1B.Y.D.
LATERAL ANALYSIS

CONDITION 2BYD
LATERAL ANALYSIS

CONDITION 2B YAW DAMPER
LATERAL ANALYSIS

GW 214,100 LB.
ALT. 35,000 FT.
CG 21.4 PERCENT MAC

SPEED:
V_T 519 KT.
V_E 289 KT.
M .90

FUSELAGE

BODY BALANCE STATION	BENDING MOMENT		SHEAR		TORSION	
	$\bar{A}$, 10^3 IN.LB.	N_0, PER SEC.	$\bar{A}$, LB.	N_0, PER SEC.	$\bar{A}$, 10^3 IN.LB.	N_0, PER SEC.
820	185.8	2.4507	273.9	2.8578	44.50	2.5092
1020	130.7	2.3055	286.9	2.8019	44.33	2.3727
1220	53.91	1.7714	271.3	2.1883	43.38	2.1901
1335	31.30	1.9118	259.4	1.9108	42.66	2.1871

VERTICAL TAIL

ELASTIC AXIS STATION	BENDING MOMENT		SHEAR		TORSION	
	$\bar{A}$, 10^3 IN.LB.	N_0, PER SEC.	$\bar{A}$, LB.	N_0, PER SEC.	$\bar{A}$, 10^3 IN.LB.	N_0, PER SEC.
67	24.77	2.4766	184.8	1.6808	3.544	3.3505
104	18.80	2.7145	158.3	1.8629	2.797	3.6547
158	11.86	3.0663	118.5	2.2403	1.992	4.2311
203	7.370	3.4039	90.92	2.4933	1.370	4.5675
248	3.889	3.7165	65.96	2.8716	.6475	4.6927
284	2.154	4.1188	39.66	3.0503	1.283	4.4132
WL239	40.79	1.9047	242.3	1.5439	13.71	2.6927

CONDITION 3B YAW DAMPER
LATERAL ANALYSIS

GW 214,400 LB.
ALT. 50500 FT.
CG 21.4 PERCENT MAC

SPEED:
V_T 528 KT.
V_e 320. KT.
M .9

FUSELAGE

BODY BALANCE STATION	BENDING MOMENT		SHEAR		TORSION	
	$\bar{A}$, 10^3 IN. LB.	N_o, PER SEC.	$\bar{A}$, LB.	N_o, PER SEC.	$\bar{A}$, 10^3 IN. LB.	N_o, PER SEC.
820.	213.5	2.456	319.5	2.933	54.98	2.266
1020.	149.8	2.286	330.3	2.861	53.86	2.272
1220.	63.62	1.831	312.1	2.162	51.61	2.222
1335.	36.69	1.943	299.6	1.866	50.72	2.236

VERTICAL TAIL

ELASTIC AXIS STATION	BENDING MOMENT		SHEAR		TORSION	
	$\bar{A}$, 10^3 IN. LB.	N_o, PER SEC.	$\bar{A}$, LB.	N_o, PER SEC.	$\bar{A}$, 10^3 IN. LB.	N_o, PER SEC.
67.	29.59	2.509	218.5	1.767	4.497	4.359
104.	22.46	2.738	187.5	1.946	3.618	4.727
158.	14.17	3.082	140.6	2.307	2.667	5.301
203.	8.801	3.418	107.9	2.534	1.837	5.385
248.	4.635	3.738	78.29	2.935	.8771	5.424
284.	2.570	4.165	46.94	3.078	1.848	6.356
WL239.	48.35	1.975	286.7	1.644	16.19	2.754

CONDITION 4B YD
LATERAL ANALYSIS

CONDITION 4BYD
LATERAL ANALYSIS

GW 214,400. LB.
ALT. 23,500. FT.
CG 21.4 PERCENT MAC

SPEED:
V_T 544. KT.
V_e 374. KT.
M .9

FUSELAGE

BODY BALANCE STATION	BENDING MOMENT $\bar{A}$, 10^3 IN. LB.	BENDING MOMENT N_0, PER SEC.	SHEAR $\bar{A}$, LB.	SHEAR N_0, PER SEC.	TORSION $\bar{A}$, 10^3 IN. LB.	TORSION N_0, PER SEC.
820.	270.0	2.240	397.9	2.807	76.75	1.932
1020.	192.4	2.046	406.8	2.725	75.18	1.936
1220.	89.31	1.614	408.8	1.893	72.01	1.893
1335.	50.65	1.677	405.7	1.604	70.74	1.906

VERTICAL TAIL

ELASTIC AXIS STATION	BENDING MOMENT $\bar{A}$, 10^3 IN. LB.	BENDING MOMENT N_0, PER SEC.	SHEAR $\bar{A}$, LB.	SHEAR N_0, PER SEC.	TORSION $\bar{A}$, 10^3 IN. LB.	TORSION N_0, PER SEC.
67.	39.05	2.146	314.0	1.579	6.034	4.434
104.	29.13	2.350	266.2	1.699	4.742	4.883
158.	17.90	2.687	193.8	1.953	3.292	5.730
203.	10.81	3.049	145.7	2.143	2.179	5.901
248.	5.533	3.431	102.2	2.468	1.035	5.972
284.	2.962	3.986	59.93	2.691	2.180	7.348
WL239.	68.35	1.718	417.4	1.541	21.47	2.319

CONDITION 5B Y.D.
LATERAL ANALYSIS

CONDITION 5B YAW DAMPER
LATERAL ANALYSIS

GW 214,400 LB.
ALT. 18,000 FT.
CG 21.4 PERCENT MAC

SPEED:
V_T 495. KT.
V_E 374. KT.
M .8

FUSELAGE

BODY BALANCE STATION	BENDING MOMENT		SHEAR		TORSION	
	$\bar{A}$, 10^3 IN. LB.	N_0, PER SEC.	$\bar{A}$, LB.	N_0, PER SEC.	$\bar{A}$, 10^3 IN. LB.	N_0, PER SEC.
820.	260.6	2.275	375.7	2.808	69.40	2.220
1020.	185.4	2.100	392.8	2.719	69.05	2.093
1220.	85.23	1.635	391.6	1.955	67.52	1.924
1335.	48.54	1.702	385.5	1.675	66.33	1.919

VERTICAL TAIL

ELASTIC AXIS STATION	BENDING MOMENT		SHEAR		TORSION	
	$\bar{A}$, 10^3 IN. LB.	N_0, PER SEC.	$\bar{A}$, LB.	N_0, PER SEC.	$\bar{A}$, 10^3 IN. LB.	N_0, PER SEC.
67.	36.10	2.175	294.9	1.568	5.709	4.375
104.	26.96	2.380	250.7	1.682	4.495	4.806
158.	16.57	2.715	183.4	1.930	3.131	5.602
203.	10.00	3.077	138.2	2.119	2.068	5.783
248.	5.116	3.459	96.85	2.442	.9852	5.868
284.	2.736	4.003	56.62	2.672	.2067	7.133
WL239.	64.23	1.708	388.9	1.536	.2039	2.296

CONDITION 6B YD
LATERAL ANALYSIS

CONDITION 6B YAW DAMPER
LATERAL ANALYSIS

GW 214,400. LB.
ALT. 15,000. FT.
CG 21.4 PERCENT MAC

SPEED:
V_T 472.7 KT.
V_e 375. KT.
M .76

FUSELAGE

BODY BALANCE STATION	BENDING MOMENT		SHEAR		TORSION	
	$\bar{A}$, 10^3 IN. LB.	N_0, PER SEC.	$\bar{A}$, LB.	N_0, PER SEC.	$\bar{A}$, 10^3 IN. LB.	N_0, PER SEC.
820.	214.6	2.214	309.2	2.657	56.22	2.127
1020.	152.7	2.058	322.1	2.624	56.06	2.004
1220.	69.69	1.566	322.4	1.922	54.97	1.843
1335.	39.83	1.647	317.3	1.657	54.01	1.839

VERTICAL TAIL

ELASTIC AXIS STATION	BENDING MOMENT		SHEAR		TORSION	
	$\bar{A}$, 10^3 IN. LB.	N_0, PER SEC.	$\bar{A}$, LB.	N_0, PER SEC.	$\bar{A}$, 10^3 IN. LB.	N_0, PER SEC.
67.	30.12	2.068	239.9	1.495	4.596	4.107
104.	22.52	2.268	204.1	1.610	3.613	4.518
158.	13.84	2.593	149.8	1.866	2.507	5.274
203.	8.347	2.941	113.1	2.052	1.656	5.473
248.	4.265	3.306	79.62	2.369	.7900	5.565
284.	2.263	3.840	49.92	2.574	1.635	6.711
WL239.	52.35	1.634	316.2	1.449	16.71	2.238

CONDITION 1B
LATERAL ANALYSIS

GW	214,400. LB.		SPEED:		
ALT.	42,000 FT.			V_T	505 KT.
CG	21.4	PERCENT MAC		V_e	239 KT.
				M	.90

FUSELAGE

BODY BALANCE STATION	BENDING MOMENT		SHEAR		TORSION	
	$\bar{A}$, 10^3 IN LB	N_o, PER SEC.	$\bar{A}$, LB.	N_o, PER SEC.	$\bar{A}$, 10^3 IN LB	N_o, PER SEC.
820.	241.4	1.755	327.3	2.142	69.97	1.262
1020	175 8	1.610	342.4	2.123	70.57	1.187
1220.	91.13	.8507	380.8	1.458	70.07	1.094
1335	51.52	.9735	390.6	1.190	68.91	1.093

VERTICAL TAIL

ELASTIC AXIS STATION	BENDING MOMENT		SHEAR		TORSION	
	$\bar{A}$, 10^3 IN LB	N_o, PER SEC.	$\bar{A}$, LB.	N_o, PER SEC	$\bar{A}$, 10^3 IN LB	N_o, PER SEC
67.	39.42	1.263	315.3	.7944	5.435	2.015
104.	29.02	1.420	267.0	.8913	4.098	2.331
158.	17.34	1.680	193.2	1.117	2.557	3.109
203.	10.07	1.982	145.4	1.255	1.536	3.665
248.	4.900	2.331	100 5	1.510	6.690	4.008
284.	2.351	2.961	59.5	1.624	13.31	4.983
WL 239	68.62	.9097	420.3	.6895	20.80	1.446

CONDITION 1B
LATERAL ANALYSIS

CONDITION 2B
LATERAL ANALYSIS

CONDITION 2B
LATERAL ANALYSIS

GW	214,400 LB.	SPEED:		
ALT.	35,000 FT.		V_T	519 KT.
CG	21.4 PERCENT MAC		V_E	289 KT.
			M	.90

FUSELAGE

BODY BALANCE STATION	BENDING MOMENT		SHEAR		TORSION	
	$\bar{A}$, 10^3 IN LB	N_o, PER SEC.	$\bar{A}$, LB.	N_o, PER SEC.	$\bar{A}$, 10^3 IN LB	N_o, PER SEC.
820.	273.9	1.814	374.7	2.241	78.86	1.427
1020.	199.2	1.657	391.0	2.213	79.44	1.337
1220.	102.0	.9583	432.1	1.501	78.72	1.224
1335	57.43	1.077	442.4	1.225	77.39	1.222

VERTICAL TAIL

ELASTIC AXIS STATION	BENDING MOMENT		SHEAR		TORSION	
	$\bar{A}$, 10^3 IN LB	N_o, PER SEC.	$\bar{A}$, LB	N_o, PER SEC	$\bar{A}$, 10^3 IN LB	N_o, PER SEC
67.	43.84	1.418	354.3	.8898	6.176	1.954
104.	32.23	1.601	298.7	.9986	4.655	2.226
158.	19.26	1.905	214.6	1.249	2.883	2.959
203.	11.22	2.253	160.5	1.423	1.755	3.598
248.	5.508	2.642	110.7	1.723	.7756	3.946
284.	2.715	3.288	65.18	1.868	1.435	4.040
WL 239.	76.80	1.923	476.1	.7962	23.138	1.616

CONDITION 3B
LATERAL ANALYSIS

GW	214,400 LB.	SPEED:		
ALT.	30,500 FT.		V_T	528 KT.
CG	21 4 PERCENT MAC		V_e	320 KT.
			M	90

FUSELAGE

BODY BALANCE STATION	BENDING MOMENT		SHEAR		TORSION	
	$\bar{A}$, 10^3 IN LB.	N_o, PER SEC.	$\bar{A}$, LB.	N_o, PER SEC.	$\bar{A}$, 10^3 IN LB	N_o, PER SEC.
820.	308.3	1.886	426.5	2.381	93.72	1.347
1020.	223.4	1.712	443.1	2.325	92.00	1.344
1220.	114.0	1.046	483.4	1.551	88.67	1.304
1335.	64.26	1.115	493.4	1.259	87.14	1.314

VERTICAL TAIL

ELASTIC AXIS STATION	BENDING MOMENT		SHEAR		TORSION	
	$\bar{A}$, 10^3 IN LB	N_o, PER SEC.	$\bar{A}$, LB.	N_o, PER SEC.	$\bar{A}$, 10^3 IN LB	N_o, PER SEC
67.	49.53	1.512	396.3	.9812	7.134	2.781
104.	36.53	1.695	335.1	1.094	5.449	3.170
158.	21.94	2.001	242.1	1.344	3.522	4.048
203.	12.85	2.352	181.8	1.508	2.201	4.521
248.	6.334	2.745	1260	1.802	.9963	4.799
284.	3.151	3.407	74.37	1.947	1.995	5.951
WL 239.	86.196	1.113	530.6	.8936	26.19	1.717

CONDITION 3B

LATERAL ANALYSIS

CONDITION 4B
LATERAL ANALYSIS

GW	214,400. LB.	SPEED:	
ALT.	23,500. FT.	V_T	544 KT.
CG	21.4 PERCENT MAC	V_e	374. KT.
		M	9

FUSELAGE

BODY BALANCE STATION	BENDING MOMENT		SHEAR		TORSION	
	$\bar{A}$, 10^3 IN LB	N_o, PER SEC	$\bar{A}$, LB	N_o, PER SEC.	$\bar{A}$, 10^3 IN LB	N_o, PER SEC.
820.	361.9	1.903	503.5	2.449	110.1	1.327
1020	262.3	1.720	520.6	2.373	108.0	1.325
1220.	133.9	1.077	568.5	1.545	104.0	1.286
1335.	78.09	1.150	580.9	1.252	102.2	1.294

VERTICAL TAIL

ELASTIC AXIS STATION	BENDING MOMENT		SHEAR		TORSION	
	$\bar{A}$, 10^3 IN LB	N_o, PER SEC.	$\bar{A}$, LB	N_o, PER SEC.	$\bar{A}$, 10^3 IN LB	N_o, PER SEC
67.	57.47	1.451	466.7	1.026	8.478	3.184
104.	42.17	1.615	393.1	1.115	6.460	3.610
158	25.13	1.903	281.6	1.313	4.129	4.596
203.	14.60	2.245	210.0	1.456	2.547	5.066
248.	7.131	2.649	144.3	1.721	1.154	5.316
284.	3.503	3.354	84.69	1.885	2.360	6.853
WL 239.	101.1	1.128	628.6	.9885	30.20	1.630

CONDITION 5B
LATERAL ANALYSIS

CONDITION 5B
LATERAL ANALYSIS

GW	214,400	LB.	SPEED:		
ALT.	18,000	FT.	V_T	495	KT.
CG	214	PERCENT MAC	V_e	374	KT.
			M	.80	

FUSELAGE

BODY BALANCE STATION	BENDING MOMENT		SHEAR		TORSION	
	$\bar{A}$, 10^3 IN LB.	N_o, PER SEC.	$\bar{A}$, LB.	N_o, PER SEC.	$\bar{A}$, 10^3 IN LB	N_o, PER SEC.
820.	343.5	1.870	475.0	2.372	99.60	1.525
1020.	249.3	1.696	491.6	2.329	100.2	1.418
1220.	127.2	1.069	540.6	1.526	99.07	1.286
1335.	71.46	1.144	553.1	1.240	97.37	1.281

VERTICAL TAIL

ELASTIC AXIS STATION	BENDING MOMENT		SHEAR		TORSION	
	$\bar{A}$, 10^3 IN. LB.	N_o, PER SEC.	$\bar{A}$, LB.	N_o, PER SEC.	$\bar{A}$, 10^3 IN LB	N_o, PER SEC
67.	54.91	1.424	444.9	1.001	8.075	3.111
104.	40.32	1.587	375.0	1.088	6.151	3.529
158.	24.04	1.869	269.2	1.286	3.924	4.491
203.	13.96	2.204	201.1	1.429	2.418	4.968
248.	6.819	2.596	138.3	1.690	1.101	5.266
284.	3.337	3.286	81.24	1.848	2.213	6.706
WL239.	94.46	1.103	598.5	.9610	28.86	1.606

CONDITION 6B
LATERAL ANALYSIS

GW	214,400 LB.	SPEED:		
ALT.	15,000 FT.		V_T	473 KT.
CG	21.4 PERCENT MAC		V_e	375 KT.
			M	.76

FUSELAGE

BODY BALANCE STATION	BENDING MOMENT		SHEAR		TORSION	
	$\bar{A}$, 10^3 IN.LB.	N_o, PER SEC.	$\bar{A}$, LB.	N_o, PER SEC.	$\bar{A}$, 10^3 IN.LB.	N_o, PER SEC.
820.	292.6	1.763	402.6	2.200	85.00	1.394
1020.	212.8	1.608	415.5	2.186	85.61	1.299
1220.	109.4	.9831	462.0	1.449	84.79	1.182
1335.	61.58	1.065	473.7	1.186	83.32	1.179

VERTICAL TAIL

ELASTIC AXIS STATION	BENDING MOMENT		SHEAR		TORSION	
	$\bar{A}$, 10^3 IN LB	N_o, PER SEC.	$\bar{A}$, LB.	N_o, PER SEC.	$\bar{A}$, 10^3 IN LB	N_o, PER SEC
67.	47.13	1.324	380.9	.9152	6.784	2.803
104.	34.63	1.479	321.5	.9975	5.151	3.190
158.	20.63	1.746	231.2	1.190	3.282	4.094
203.	11.96	2.062	172.9	1.327	1.988	4.586
248.	5.824	2.435	119.0	1.576	.9017	4.904
284.	2.819	3.101	70.05	1.719	1.766	6.268
WL 239.	82.62	1.013	510.8	.8689	24.819	1.505

CONDITION 6B
LATERAL ANALYSIS

CONDITION 10A
LATERAL ANALYSIS

CONDITION 10A
LATERAL ANALYSIS

GW	204,000. LB.	SPEED:	
ALT.	35,000. FT.	V_T	475. KT.
CG	21.5 PERCENT MAC	V_e	280. KT.
		M	.82

FUSELAGE

BODY BALANCE STATION	BENDING MOMENT		SHEAR		TORSION	
	$\bar{A}$, 10^3 IN. LB.	N_o, PER SEC.	$\bar{A}$, LB.	N_o, PER SEC.	$\bar{A}$, 10^3 IN. LB.	N_o, PER SEC.
820.	223.2	1.824	303.2	2.242	69.52	1.201
1020.	163.5	1.668	320.6	2.209	68.42	1.199
1220.	82.66	.9097	356.7	1.507	66.08	1.164
1335	46.81	1.039	365.5	1.220	64.95	1.168

VERTICAL TAIL

ELASTIC AXIS STATION	BENDING MOMENT		SHEAR		TORSION	
	$\bar{A}$, 10^3 IN. LB.	N_o, PER SEC.	$\bar{A}$, LB.	N_o, PER SEC.	$\bar{A}$, 10^3 IN. LB.	N_o, PER SEC.
67	37.13	1.354	295.9	.8592	5.271	2.233
104.	27.43	1.519	250.9	.9619	4.001	2.561
158.	16.48	1.793	182.1	1.195	2.549	3.323
203.	9.649	2.103	137.3	1.341	1.562	3.809
248	4.746	2.455	95.32	1.608	.6887	4.101
284	2.332	3.057	56.52	1.729	1.404	5.033
WL239.	64.42	.9811	394.7	.7592	1.961	1.507

CONDITION 10B
LATERAL ANALYSIS

CONDITION 10B
LATERAL ANALYSIS

GW	204,000. LB.	SPEED:		
ALT.	35,000. FT.		V_T	475. KT.
CG	21.5 PERCENT MAC		V_e	280. KT.
			M	.82

FUSELAGE

BODY BALANCE STATION	BENDING MOMENT		SHEAR		TORSION	
	$\bar{A}$, 10^3 IN. LB.	N_o, PER SEC.	$\bar{A}$, LB.	N_o, PER SEC.	$\bar{A}$, 10^3 IN. LB.	N_o, PER SEC.
820.	239.4	1.710	322.7	2.177	75.76	1.100
1020	173.8	1.559	340.6	2.090	74.52	1.107
1220.	90.69	.8835	385.3	1.403	71.99	1.075
1335.	51.27	.9539	397.0	1.139	70.75	1.079

VERTICAL TAIL

ELASTIC AXIS STATION	BENDING MOMENT		SHEAR		TORSION	
	$\bar{A}$, 10^3 IN. LB.	N_o, PER SEC.	$\bar{A}$, LB.	N_o, PER SEC.	$\bar{A}$, 10^3 IN. LB.	N_o, PER SEC.
67	40.35	1.253	323.2	.7912	5.662	2.083
104.	29.74	1.410	273.8	.8865	4.281	2.398
158.	17.80	1.670	198.2	1.105	2.688	3.158
203	10.36	1.968	149.1	1.242	1.626	3.669
248.	5.064	2.312	103.2	1.493	.7115	3.981
284	2.454	2.919	61.08	1.609	1.421	4.982
WL239	70.29	.9041	431.6	.6984	21.28	1.396

CONDITION 10C

LATERAL ANALYSIS

CONDITION 10C
LATERAL ANALYSIS

GW 204,000. LB.
ALT. 35,000. FT.
CG 21.5 PERCENT MAC

SPEED:
V_T 475. KT.
V_e 280. KT.
M .82

FUSELAGE

BODY BALANCE STATION	BENDING MOMENT $\bar{A}$, 10^3 IN. LB.	BENDING MOMENT N_o, PER SEC.	SHEAR $\bar{A}$, LB.	SHEAR N_o, PER SEC.	TORSION $\bar{A}$, IN. LB.	TORSION N_o, PER SEC.
820.	246.0	1.667	330.6	2.070	78.29	1.076
1020.	180.8	1.518	348.7	2.043	77.01	1.074
1220.	93.94	.8062	396.9	1.346	74.40	1.043
1335.	53.08	.9226	409.8	1.105	73.11	1.046

VERTICAL TAIL

ELASTIC AXIS STATION	BENDING MOMENT $\bar{A}$, 10^3 IN. LB.	BENDING MOMENT N_o, PER SEC.	SHEAR $\bar{A}$, LB.	SHEAR N_o, PER SEC.	TORSION $\bar{A}$, 10^3 IN. LB.	TORSION N_o, PER SEC.
67.	41.66	1.216	334.9	.7667	5.823	2.026
104.	30.68	1.369	283.1	.8592	4.396	2.336
158.	18.34	1.624	204.7	1.072	2.746	3.094
203.	10.66	1.917	154.0	1.205	1.653	3.612
248.	5.195	2.258	106.4	1.450	.7210	3.933
284.	2.505	2.866	62.95	1.564	1.428	4.961
WL239.	72.68	.8760	446.7	.6765	21.96	1.355

CONDITION 10D
LATERAL ANALYSIS

GW 204,000. LB.
ALT. 35,000. FT.
CG 21.5 PERCENT MAC

SPEED:
V_T 475. KT.
V_e 280. KT.
M .82

FUSELAGE

BODY BALANCE STATION	BENDING MOMENT $\bar{A}$, 10^3 IN. LB.	BENDING MOMENT N_o, PER SEC.	SHEAR $\bar{A}$, LB.	SHEAR N_o, PER SEC.	TORSION $\bar{A}$, IN. LB.	TORSION N_o, PER SEC.
820.	249.5	1.640	332.5	2.052	80.84	1.040
1020.	184.0	1.488	351.5	2.024	79.57	1.038
1220.	96.92	.7831	405.3	1.333	76.90	1.008
1338.	59.68	.8969	420.5	1.076	75.58	1.012

VERTICAL TAIL

ELASTIC AXIS STATION	BENDING MOMENT $\bar{A}$, 10^3 IN. LB.	BENDING MOMENT N_o, PER SEC.	SHEAR $\bar{A}$, LB.	SHEAR N_o, PER SEC.	TORSION $\bar{A}$, 10^3 IN. LB.	TORSION N_o, PER SEC.
67.	43.06	1.174	346.4	.7416	6.033	1.955
104.	31.69	1.322	293.2	.8303	4.546	2.257
158.	18.91	1.571	211.8	1.035	2.823	3.006
203.	10.97	1.858	159.3	1.163	1.688	3.532
248.	5.330	2.194	109.9	1.402	.7323	3.964
284.	2.553	2.802	65.02	1.511	1.438	4.923
WL239.	75.26	.8472	463.0	.6552	22.67	1.310

CONDITION 10E
LATERAL ANALYSIS

CONDITION 10E
LATERAL ANALYSIS

GW	204,000. LB.	SPEED:		
ALT.	35,000. FT.		V_T	475. KT.
CG	21.5 PERCENT MAC		V_e	280. KT.
			M	.82

FUSELAGE

BODY BALANCE STATION	BENDING MOMENT		SHEAR		TORSION	
	$\bar{A}$, 10^3 IN. LB.	N_o, PER SEC.	$\bar{A}$, LB.	N_o, PER SEC.	$\bar{A}$, IN. LB.	N_o, PER SEC.
820.	225.7	1.600	339.2	2.012	83.67	1.007
1020.	189.0	1.450	358.4	1.984	82.37	1.004
1220.	100.5	.7575	417.2	1.296	79.62	.9747
1335.	55.63	.8672	434.1	1.044	78.26	.9779

VERTICAL TAIL

ELASTIC AXIS STATION	BENDING MOMENT		SHEAR		TORSION	
	$\bar{A}$, 10^3 IN. LB.	N_o, PER SEC.	$\bar{A}$, LB.	N_o, PER SEC.	$\bar{A}$, 10^3 IN. LB.	N_o, PER SEC.
67.	44.57	1.137	359.1	.7173	6.232	1.893
104.	32.77	1.280	303.9	.8030	4.689	2.189
158.	19.53	1.552	219.4	1.022	2.897	2.931
203.	11.41	1.804	164.9	1.126	1.722	3.463
248.	5.480	2.136	113.6	1.357	.7442	3.804
284.	2.610	2.742	67.19	1.463	1.447	4.891
WL 239.	78.00	.8191	480.3	.6338	23.44	1.268

CONDITION 10F
LATERAL ANALYSIS

GW	204,000. LB.	SPEED:	
ALT.	35,000. FT.	V_T	475. KT.
CG	21.5 PERCENT MAC	V_E	280. KT.
		M	.82

FUSELAGE

BODY BALANCE STATION	BENDING MOMENT		SHEAR		TORSION	
	$\bar{A}$, 10^3 IN. LB.	N_0, PER SEC.	$\bar{A}$, LB.	N_0, PER SEC.	$\bar{A}$, IN. LB.	N_0, PER SEC.
820	283.5	1.446	369.3	1.850	95.94	.8833
1020.	211.0	1.302	390.4	1.823	94.50	.8808
1220.	115.6	.6650	469.3	1.156	91.39	.8552
1335.	65.01	.7616	493.1	.9234	89.84	.8576

VERTICAL TAIL

ELASTIC AXIS STATION	BENDING MOMENT		SHEAR		TORSION	
	$\bar{A}$, 10^3 IN. LB.	N_0, PER SEC.	$\bar{A}$, LB.	N_0, PER SEC.	$\bar{A}$, 10^3 IN. LB.	N_0, PER SEC.
67	51.06	.9964	413.9	.6298	7.097	1.665
104.	37.45	1.124	350.0	.7039	5.313	1.945
158.	22.21	1.341	251.9	.8768	3.220	2.639
203	12.77	1.600	189.1	.9859	1.873	3.184
248	6.137	1.909	129.7	1.192	.7971	3.552
284	2.864	2.501	76.59	1.287	1.490	4.751
WL239.	89.81	.7179	554.4	.5576	26.79	1.114

CONDITION 10G
LATERAL ANALYSIS

GW	204,000. LB.	SPEED:		
ALT.	35,000. FT.		V_T	475. KT.
CG	21.5 PERCENT MAC		V_e	280. KT.
			M	.82

FUSELAGE

BODY BALANCE STATION	BENDING MOMENT		SHEAR		TORSION	
	$\bar{A}$, 10^3 IN. LB.	N_0, PER SEC.	$\bar{A}$, LB.	N_0, PER SEC.	$\bar{A}$, 10^3 IN. LB.	N_0, PER SEC.
820.	246.4	1.664	329.7	2.075	79.17	1.062
1020.	181.5	1513	348.2	2.046	77.91	1.060
1220.	94.89	.7992	399.0	1.357	75.29	1.029
1335.	53.57	.9153	412.9	1.098	73.99	1.032

VERTICAL TAIL

ELASTIC AXIS STATION	BENDING MOMENT		SHEAR		TORSION	
	$\bar{A}$, 10^3 IN. LB.	N_0, PER SEC.	$\bar{A}$, LB.	N_0, PER SEC.	$\bar{A}$, 10^3 IN. LB.	N_0, PER SEC.
67.	42.17	1.199	338.8	.7574	5.911	1.995
104.	31.05	1.350	286.8	.8480	4.459	2.302
158	18.54	1.602	207.3	1.057	2.779	3.055
203.	10.77	1.893	156.0	1.188	1.668	3.576
248	5.242	2.233	107.7	1.430	.7255	3.903
284	2.521	2.841	63.72	1.524	1.443	4.940
WL239.	73.63	.8656	45.27	.6600	22.21	1.339

CONDITION 10G
LATERAL ANALYSIS

CONDITION 10 H
LATERAL ANALYSIS

CONDITION 10 H
LATERAL ANALYSIS

GW 204,000. LB.
ALT. 35,000. FT.
CG 21.5 PERCENT MAC

SPEED:
V_T 475. KT.
V_E 280. KT.
M .82

FUSELAGE

BODY BALANCE STATION	BENDING MOMENT $\bar{A}$, 10^3 IN. LB.	BENDING MOMENT N_0, PER SEC.	SHEAR $\bar{A}$, LB.	SHEAR N_0, PER SEC.	TORSION $\bar{A}$, IN. LB.	TORSION N_0, PER SEC.
820.	254.6	1.650	338.8	2.067	82.75	1.041
1020	188.0	1.496	357.8	2.039	81.44	1.039
1220	99.37	.7827	414.4	1.340	78.72	1.009
1335.	56.05	.8966	430.3	1.080	77.37	1.012

VERTICAL TAIL

ELASTIC AXIS STATION	BENDING MOMENT $\bar{A}$, 10^3 IN. LB.	BENDING MOMENT N_0, PER SEC.	SHEAR $\bar{A}$, LB.	SHEAR N_0, PER SEC.	TORSION $\bar{A}$, 10^3 IN. LB.	TORSION N_0, PER SEC.
67.	44.06	1.178	354.8	.7437	6.159	1.964
104.	32.41	1.327	300.3	.8412	4.637	2.270
158	19.32	1.577	216.8	1.038	2.870	3.033
203.	11.19	1.869	163.0	1.168	1.709	3.577
248	5.430	2.210	112.4	1.407	.740	3.922
284	2.592	2.832	66.44	1.599	1.445	5.024
WL239	77.07	.8494	474.4	.6569	23.19	1.315